SHEAR STRENGTH OF COMPACTED MATERIALS

Thesis Submitted to

UNIVERSITY OF LONDON

(Imperial College of Science and Technology)

By

A.R.H. EL RAMLI, M.Sc.(Eng.), D.I.C.

For the Degree of

Doctor of Philosophy in the Faculty of Engineering

December, 1953

TABLE OF CONTENTS

Chapter		Page
1.	PURPOSE AND SCOPE OF RESEARCH	I
2.	STRENGTH CHARACTERISTICS OF SATURATED AND PARTIALLY SATURATED SOILS ..	5
3.	THEORETICAL CONSIDERATIONS	
	A. Shear Strength	8
	B. Pore Water Pressure	I2
4.	EXPERIMENTAL WORK	
	A. Description of Material used ..	2I
	B. Description of Apparatus and Preparation of Samples	23
	C. Types and Purpose of Tests ..	30
5.	INTERPRETATION AND DISCUSSION OF TEST RESULTS	
	A. Shear Strength	42
	B. Pore Water Pressure and Compressibility	54
6.	SUMMARY AND GENERAL CONCLUSIONS ..	76
	ACKNOWLEDGEMENTS	

Page

APPENDIX

Effect of Rubber Membrane on the Measured Strength of 4" dia. Samples 80

BIBLIOGRAPHY 83

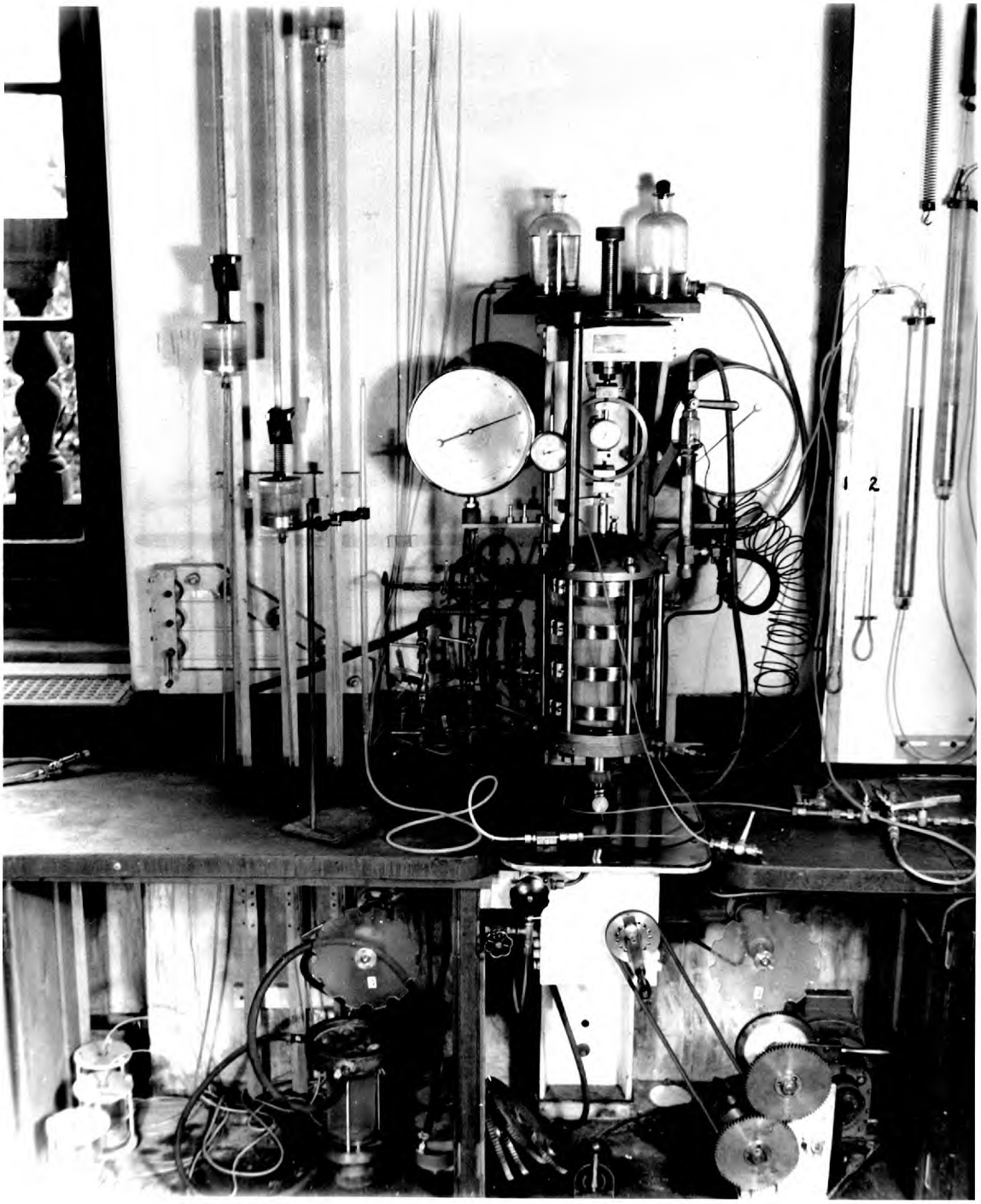


PLATE I.

Chapter 1

PURPOSE AND SCOPE OF RESEARCH

Available data on the strength characterisations of partially saturated soils is limited. A great deal of pioneering work has been done in America as well as in this country and the field data, though scanty, have confirmed the validity of some theoretical concepts, as for example, the correlation between settlements and pore pressures.

The effect of the placement conditions on the pore pressure set up inside a rolled fill dam has been studied by several authors with respect to somewhat idealized conditions. Hamilton (1939) and Bjerrum (1951) gave results of pore pressure measurements for samples tested in the triaxial machine under all round pressure; while Glynn (1948) considered as design values, the pore pressure at failure* in an undrained triaxial compression test. These two types of tests, indeed, represent two extreme conditions regarding the magnitude of the pore pressure ratio and of the principal stress ratio,

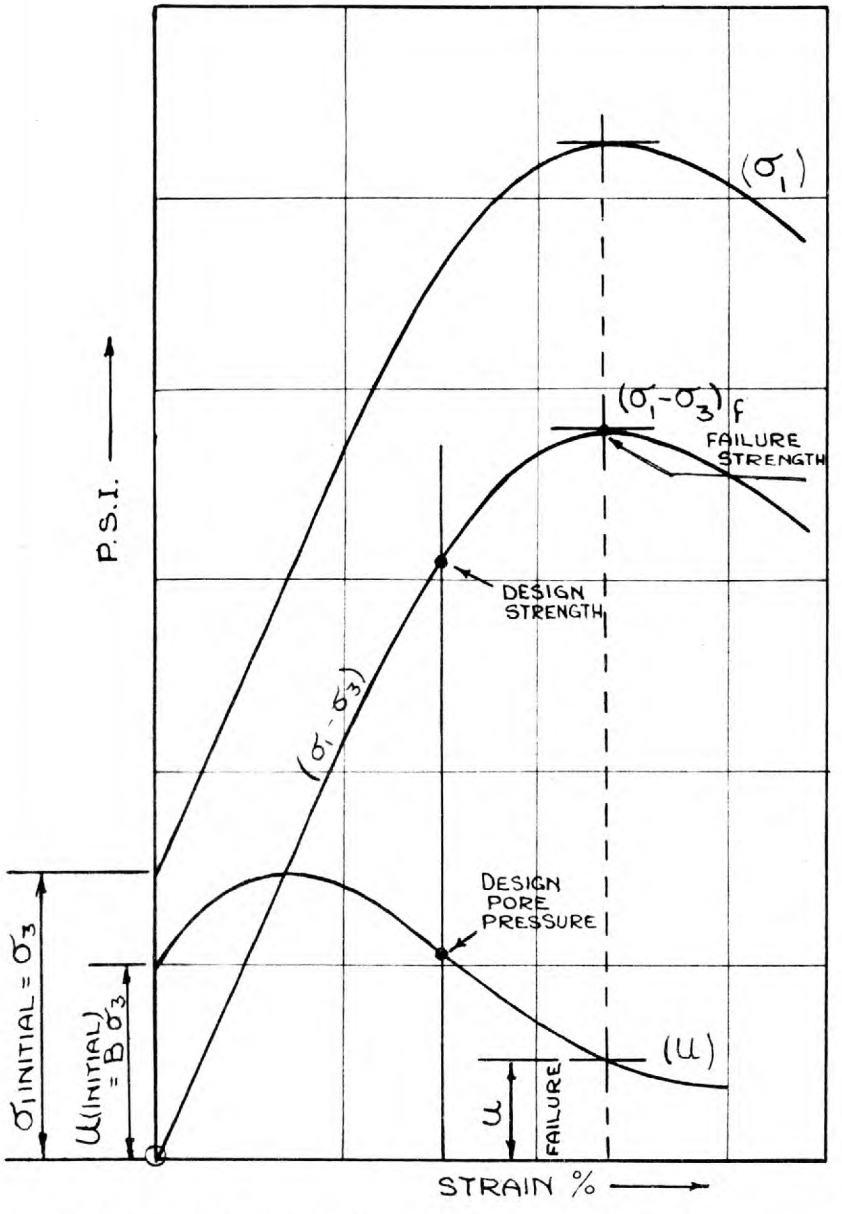
---

*Glynn considered failure to occur at maximum principal stress ratio.

Fig. (1:1), (the pore pressure ratio is that of the increment of pore pressure and the major total principal stress, and is maximum in the case of all round pressure).

The effect of the principal stress ratio was previously studied only in connection with consolidation of saturated clays and sands. Bishop (1952) showed that for clay the major effective principal stress consolidation relationship does not vary greatly with change in the principal stress ratio. The Triaxial shear report, 1947, also confirms this in the case of normally consolidated saturated clay. It quotes that the consolidation of clay depends only on the magnitude of the effective major principal stress, irrespective of the type of loading. For saturated sands, such relationship depends entirely on the principal stress ratio σ_1'/σ_3'. Two extreme cases are those for consolidation under an all round pressure ($\sigma_1'/\sigma_3' = 1$) giving maximum consolidation and the case of a drained compression test ($\sigma_1'/\sigma_3' \simeq 4.5$ for compact sand) which gives minimum consolidation. The uniaxial consolidation ($\sigma_1'/\sigma_3' \simeq 3$) shows intermediate values. This type of consolidation is referred to as the K_o condition as it makes possible an estimate of $K_o = \sigma_3'/\sigma_1'$ the coefficient of earth pressure at rest and is performed in the triaxial machine by a special technique described later.

There is no available data at present regarding the effect of intermediate values of σ_1'/σ_3' on the pore pressure



UNDRAINED TRIAXIAL COMPRESSION TEST
UNDER CELL PRESSURE = σ_3

FIG. 1:1

and compressibility of partially saturated soils. K_o undrained consolidation tests as well as others with intermediate σ'_1 / σ'_3 were therefore performed by the author and the results obtained show that pore pressures as well as consolidation depended on this ratio. (A sealed, partially saturated soil element would undergo a certain amount of consolidation under pressure, which corresponds to the change in the volume of free air it contains). The effective stress; consolidation relationship obtained by such undrained consolidation tests should be almost identical * to those obtained if drainage was allowed. But it was not possible to perform such tests with drainage successfully for reasons given later on in Chapter 4.

Investigation into the effect of the placement conditions on the shear strength parameters (cohesion and angle of shearing resistance) has been carried out by performing triaxial compression tests under conditions simulating those in an actual earth structure and it was possible to establish a relationship between the placement condition and those shear parameters.

The problem of shear strength is, in fact, a two phase

---

* drainage leads to a lower moisture content at any particular effective stress during consolidation.

one. These are the shear strength characteristics and the pore pressure. Although they are related to each other, they are treated separately in the following chapters.

Chapter 2

SHEAR STRENGTH CHARACTERISTICS OF SATURATED AND PARTIALLY SATURATED SOILS.

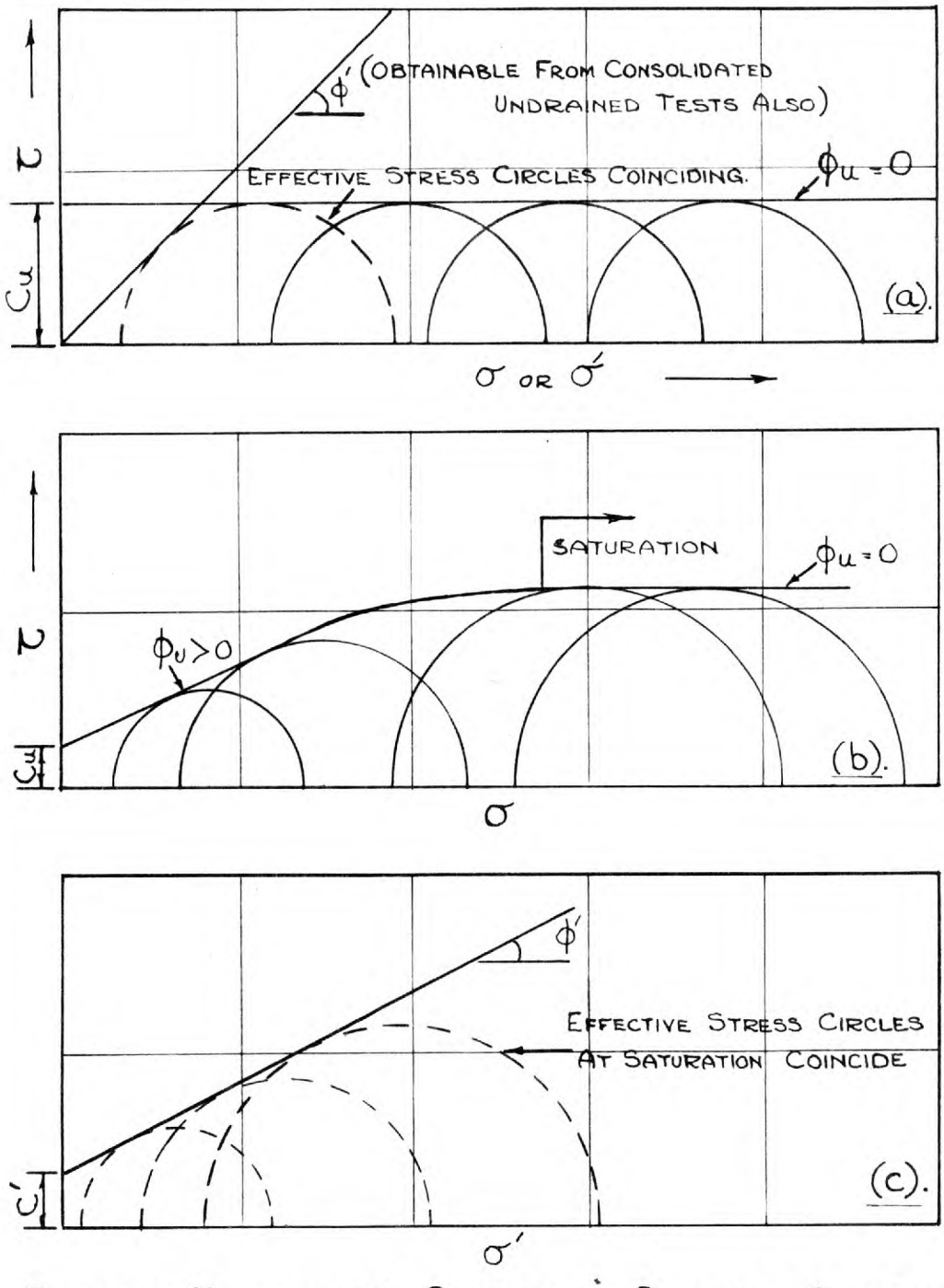
A Brief Comparison and Main Differences.

The study of the shear strength of saturated soils has shown that it depends solely on the effective stress. The principle of effective stress was established by Terzaghi in 1936 and experimental evidence was given by the shear tests carried out by Rendulic (1937). Generally speaking, the effective stress is equal to the total stress, less the corresponding pressure in the pore water. Rendulic and Hvorslev, as well as subsequent workers, showed that the strength of a saturated soil element is a function of the effective stress at failure. In all cases it is assumed that the water in the pores of a saturated sample is incompressible and consequently any change in the external loads is taken in the absence of drainage, entirely by the pore water.

It follows that a saturated soil sample will show equal strength if sheared under different external loads, provided

no drainage is allowed. This is because all external loads are taken by the water and no changes take place in the existing effective stress before shear takes place, resulting in a constant strength. In other words, the undrained Mohr's envelope touching the stress circles is a horizontal line and the angle of shearing resistance ϕ_u w.r.t. total stresses at failure is zero. Plotted in terms of effective stresses, all the circles will coincide, Fig. (2:1)a. This, however, is not the case for saturated silts and compact sands tested under low pressures where the dilatant nature of the soil structure causes the pore pressure to drop to negative values, causing cavitation, i.e., the formation of water vapour, and a departure from the conditions of complete saturation, together with a volume change. Bishop and Eldin (1950), Skempton and Golder (1948) and Eldin (1951) showed considerable values of angle of undrained shearing resistance for such soils. If the testing loads are adequately high, such that no cavitation takes place, these soils will behave like non-dilatant saturated soils and the tendency to any volume change as a result of the dilatent nature of the structure is overcome by a corresponding increase in the effective stresses (i.e. a decrease in the pore pressure).

Partially saturated soils contain free air together with water in its pores. This "pore fluid" cannot be considered incompressible, which is the main difference from saturated



STRENGTH ENVELOPES for SATURATED & PARTIALLY SATURATED SOILS UNDER CONDITIONS OF NO MOISTURE CONTENT CHANGES.

(a). SATURATED SOIL (NORMALLY CONSOLIDATED UNDER PRESSURE P. or UNDISTURBED WITH OVERBURDEN P.)

(b). & (c). PARTIALLY SATURATED SOIL.

FIG. 2:1

soils. Considering a series of undrained tests on identical samples under different loads we find that for each load the sample will undergo initially a certain amount of compression (equal to the change in volume of the free air content). Unlike saturated soils, only part of the external load will be taken by the pore water while the rest goes to the soil structure as an effective stress, the intensity of which increases with increasing loads. It follows that the strength of the soil increases accordingly, so that the angle of shearing resistance is not zero.

If the testing loads are high enough to force all the free air into solution in the pore water, the sample will subsequently behave as saturated with an angle of shearing ϕ_u w.r.t. total stresses at failure equal to zero, Fig. 2:1 (b), while the angle ϕ' w.r.t. effective stresses is always greater than zero, and is very nearly equal to the true angle of internal friction, as will be shown later, Fig. 2:1 (c).

Chapter 3

THEORETICAL CONSIDERATIONS

A. The Shear Strength

The first and most important contribution to the theories of strength of soils is Coulomb's empirical law (1776):-

$$\tau = C + \sigma_n \tan \phi \qquad 3:(1)$$

Where τ is the resistance to shear offered by the soil along the plane of incipient failure acted upon by the total normal stress σ_n. C is the cohesion and ϕ; according to Coulomb; is the angle of internal friction. Coulomb's law remained in use until the principle of effective stress was introduced.

The effective stress σ' for clays is:

$$\sigma' = \sigma - u \qquad 3:(2)$$

where u is the pore pressure.

This assumes a zero area of contact between the clay particles. This equation may be more accurately written as follows:

$$\bar{\sigma}' = \bar{\sigma} - (1 - A)\, u \qquad 3:(3)$$

Where A is the effective contact area per unit area of any plane in the soil.

Experimental evidence given by Terzaghi (1936) and Taylor (1944) proved that the value of A is almost negligible, and that for such soils the effective stress is :-

$$\bar{\sigma}' = \bar{\sigma} - u$$

Bishop (1950) studied the value of A in relation to the contact pressure between the particles, which, as he asserts, is governed by the crushing strength of the particles. He obtained theoretically a value of 0.5 per cent for A. Furthermore, he showed that the effect of A on the angle of undrained shearing resistance ϕ_u is small compared with that of the compressibility of water (the compressibility of water is here considered to be negligible, its value is 3.4×10^{-6} inches^3/ pound as compared to 570×10^{-6} inches^3/ pound for soil structure). For a well graded compacted soil it is justifiable to assume that A is negligible.

Now the validity of Coulomb's law has had to be reconsidered in the light of this principle . The result was provided by Hvorslev (1937) who showed that the law is valid for isotropic saturated clays only if modified as follows:

$$\tau = c_e + \bar{\sigma}_n \tan \phi_e \qquad 3:(4)$$

The parameters c_e and ϕ_e are the true cohesion and the true angle of internal friction and are functions of the

moisture content at failure. The experimental evidence given by Hvorslev and by Gibson (1952) showed that the variation of ϕ_e with water content is negligible, while C_e is an exclusive function of the water content.

Hvorslev's procedure to determine the true shear parameters of clay as modified by Skempton and Bishop (1950), (see also Reiner (1954)) is to perform undrained triaxial * compression tests on two samples having the same voids ratio (i.e. the same water content) but under different effective stresses, Fig. 3:1). The Mohr's envelope for effective stresses determines the parameters C_e and ϕ_e. Drained compression tests will give the same values of C_e and ϕ_e, provided the two samples have the same moisture content at failure, to which C_e and ϕ_e are related.

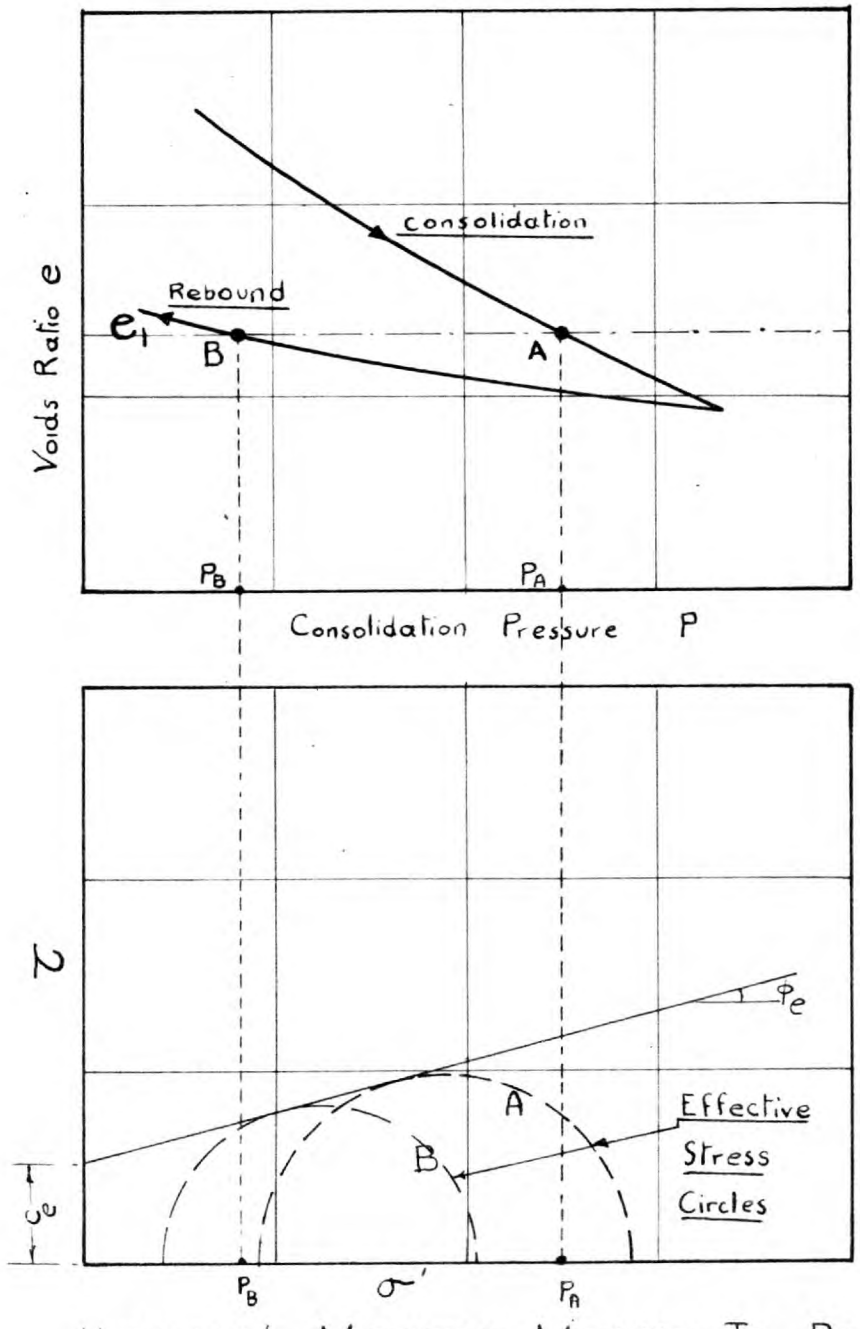
For saturated sands with no cohesion Coulomb's equation takes the form:

$$\tau = \sigma_n' \tan \phi_e$$

ϕ_e is determined experimentally by a single undrained test. The tangent to its effective stress circle through the origin determines ϕ_e which can also be obtained by carrying out a drained test and correcting the result for the energy spent by the soil structure to change its volume against the cell pressure as will be shown in Chapter 5.

---

* Hvorslev used drained direct shear tests



HVORSLEV'S MODIFIED METHOD TO DETERMINE

C_e & ϕ_e

A & B :- Two saturated samples at same voids ratio e_1 but having different effective stresses P_A & P_B

FIG 3:1

To determine the shear strength parameters for a partially saturated soil at a given placement condition, at least two identical samples are tested under two different cell pressures. This provides two samples at the same moisture content consolidated under two different effective stresses and having two different porosities. Thus Hvorslev's conditions for determining C_e and ϕ_e are only partly fulfilled in view of the difference of porosity which, in fact, is very small. It follows that the parameters C' and ϕ' obtained for effective stresses from undrained tests on a partially saturated soil are very close to C_e and ϕ_e. (They are analogous to C' and ϕ' obtained from consolidated undrained tests on clays).

It was mentioned in Chapter 3 that the angle of undrained shearing resistance ϕ_u for total stresses decreases gradually until it reaches zero. Over a certain range of stress ϕ_u and ϕ' may be taken as constant with the result that the pore pressure (U_f) at failure is a linear function of the total major principal stress at failure σ_1 and it can be shown that, Bishop (1952),

$$U_f = \sigma_1 \left(1 - \frac{1 + \operatorname{cosec} \phi'}{1 + \operatorname{cosec} \phi_u}\right) + C' \cot \phi' - C_u \cot \phi_u \times \left(\frac{1 + \operatorname{cosec} \phi'}{1 + \operatorname{cosec} \phi_u}\right) \qquad 3:(5)$$

This relationship is valid within a certain range of failure stresses, beyond which the sample approaches saturation which is reached eventually at higher stresses Fig 3:2..

B. The Pore Water Pressure

The pore pressure increment set up in a sealed partially saturated soil element is essentially less than the increment of load causing it. This means that part of the load is taken by the soil structure as an effective stress resulting in its consolidation. This consolidation, however, is equal to the change in volume of the free air content of the soil which is a function of the compressibility of the pore fluid as a whole. It follows that the relationship between the increments of load and pore pressure is a function of the compressibility of the soil structure as well as that of the pore fluid. It has been shown by Bishop (1950) that the increment $\Delta\sigma_3$ of the all round pressure required to produce an increment Δu of the pore pressure is given by the equation:

$$\Delta\sigma_3 = \Delta u \left(1 + n \frac{C_u}{C_s}\right) \qquad 3:6$$

where n is the porosity

C_u the compressibility of the pore fluid

C_s the compressibility of the soil structure.

The relationship between the pore pressure and compression of partially saturated soil has been studied by several authors (Brahtz and co-workers, 1939 , Hamilton 1939, Hilf, 1948 and Bishop, 1950). The method used is based

on Boyle's law and Henry's law of solubility of gases. Suchamethod is approximate, as it neglects the effect of the water vapour pressure which is small at ordinary temperatures and the surface tension round the air voids, and also assumes that Henry's coefficient of solubility of air in water is constant for all pressures. In fact, the change of Henry's coefficient with pressure is only 1% of its original value at 68°F and normal pressure forevery extra atmospheric pressure.

Henry's law states that at a given temperature, the weight of gas that will dissolve in a given volume of liquid is directly proportional to the pressure, and thus, by Boyle's law, the volume occupied by this gas is the same at all pressures.

Let V = total volume of a soil element

V_v = nV = volume of voids

n = porosity

Po = initial pressure of the pore fluid (absolute) and is very nearly equal to atmospheric

H = Henry's coefficient of solubility (.0205 of air per unit volume of water at ordinary pressures and temperatures)

S = Degree of saturation

volume of free air = $(1 - S)\ V_v$

volume of air in water = $SV_v \times H$

total volume of air = $(1 - S)\ V_v + SV_v \times H$

At any pressure P (absolute) the volume of free air is

$$\left\{(1 - S)\ V_v + SV_v.\ H.\right\} \frac{Po}{P} - SV_v.\ H$$

The change ir the volume of the sample V is equal to the change in the volume of free air i.e.

$$\Delta V = \left\{(1 - S)\ V_v + SV_v H\right\} \frac{Po}{P} - SV_v.H - (1-S)\ V_v$$

or $$\frac{\Delta V}{V} = \left(\frac{Po}{P} - 1\right)(1 - S + S.H)\ \frac{V_v}{V}$$

if $\Delta P = (P - Po)$ it follows that

$$\Delta P = \frac{-\frac{\Delta V}{V} \cdot Po}{\frac{\Delta V}{V} + \frac{V_v}{V}(1 - S + SH)} \qquad 3: (7)$$

where ΔP is the pore pressure (above atmospheric)

If $\frac{\Delta V}{V}$ is negative (i.e. compression)

$$\therefore \Delta P = \frac{Po.\Delta V}{V_v (1 - S + SH) - \Delta V} \qquad 3: (8)$$

$$= \frac{\text{Initial pressure x deformation}}{\text{Total volume of air - deformation}}$$

From this we obtain the compressibility of the pore fluid with respect to its initial volume i.e. $\frac{-1}{V_v} \times \frac{\Delta V}{\Delta P}$

It decreases with increasing loads and ceases to operate at saturation.

This relationship shows that the change in the pore water pressure is a function of the initial pore pressure, the

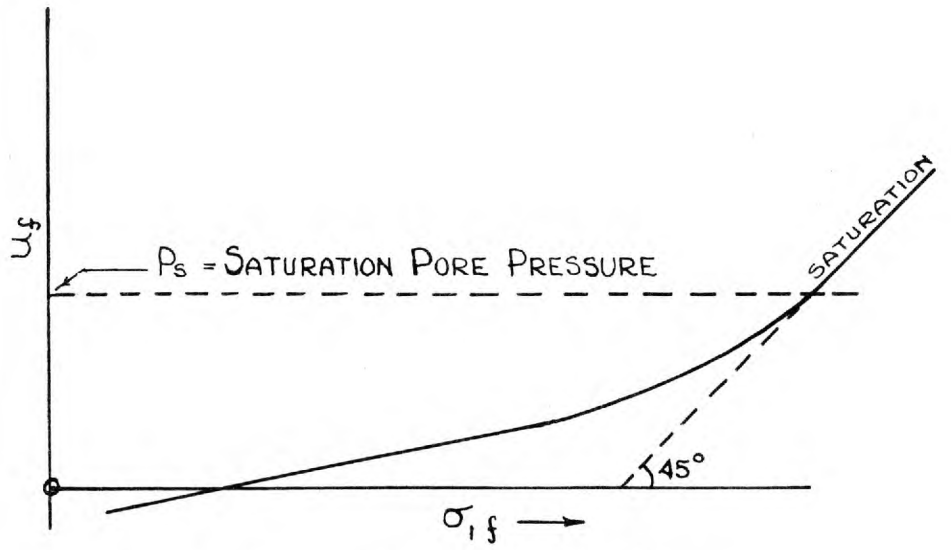
degree of saturation and the porosity. The relationship however, is valid only until all the free air has been dissolved in the water whereby the sample becomes fully saturated under external loads. No further volume change can occur without permitting drainage. Subsequent increments of load will be fully reflected on the pore pressure, Fig.3:3

The maximum deformation a soil element can undergo is equal to the volume of the free air i.e. $-(1 - S)\, V_v$ and the corresponding pore pressure is; from equation 3:8

$$P_s = Po\ \frac{(1 - S)}{S\ H} \qquad 3: (9)$$

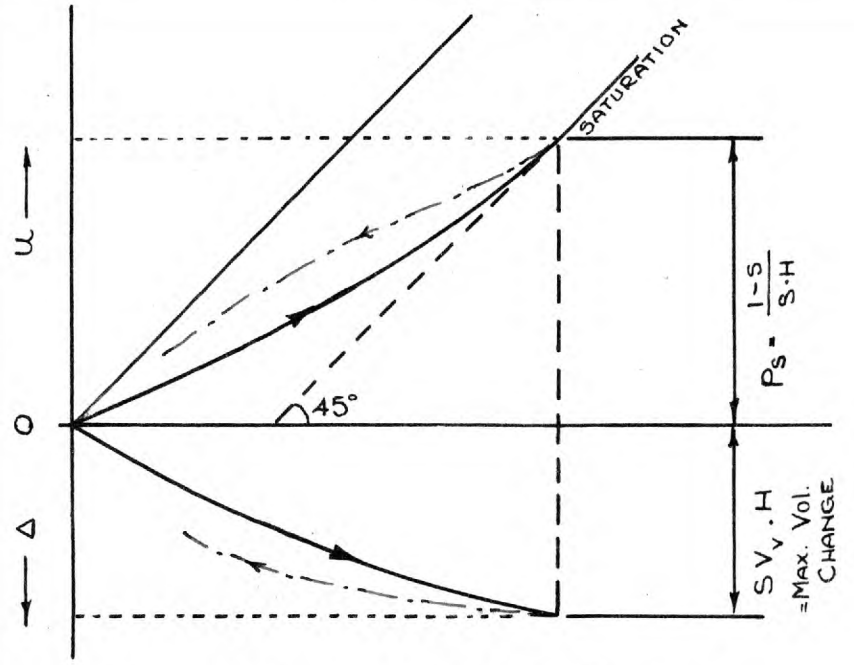
= the saturation pore pressure.

To examine the theoretical relationships established above it is necessary to carry out tests on sealed specimens in which measurements are made both of volume change (from which pore pressure can be computed) and of the pore pressure directly, Hamilton (1939). In view of the fact that properly sealed conditions are difficult to achieve (except in the triaxial machine), Hilf (1948) developed another approach to the problem. This consists of performing a drained consolidation test and determining a relation between the effective stress $\bar{\sigma}'$ and the deformation $\triangle$. From the fundamental soil properties (S, n & Po) another relationship between the pore pressure u and the deformation $\triangle$ can be computed (by using equation 3: (8)). It follows immediately that the two



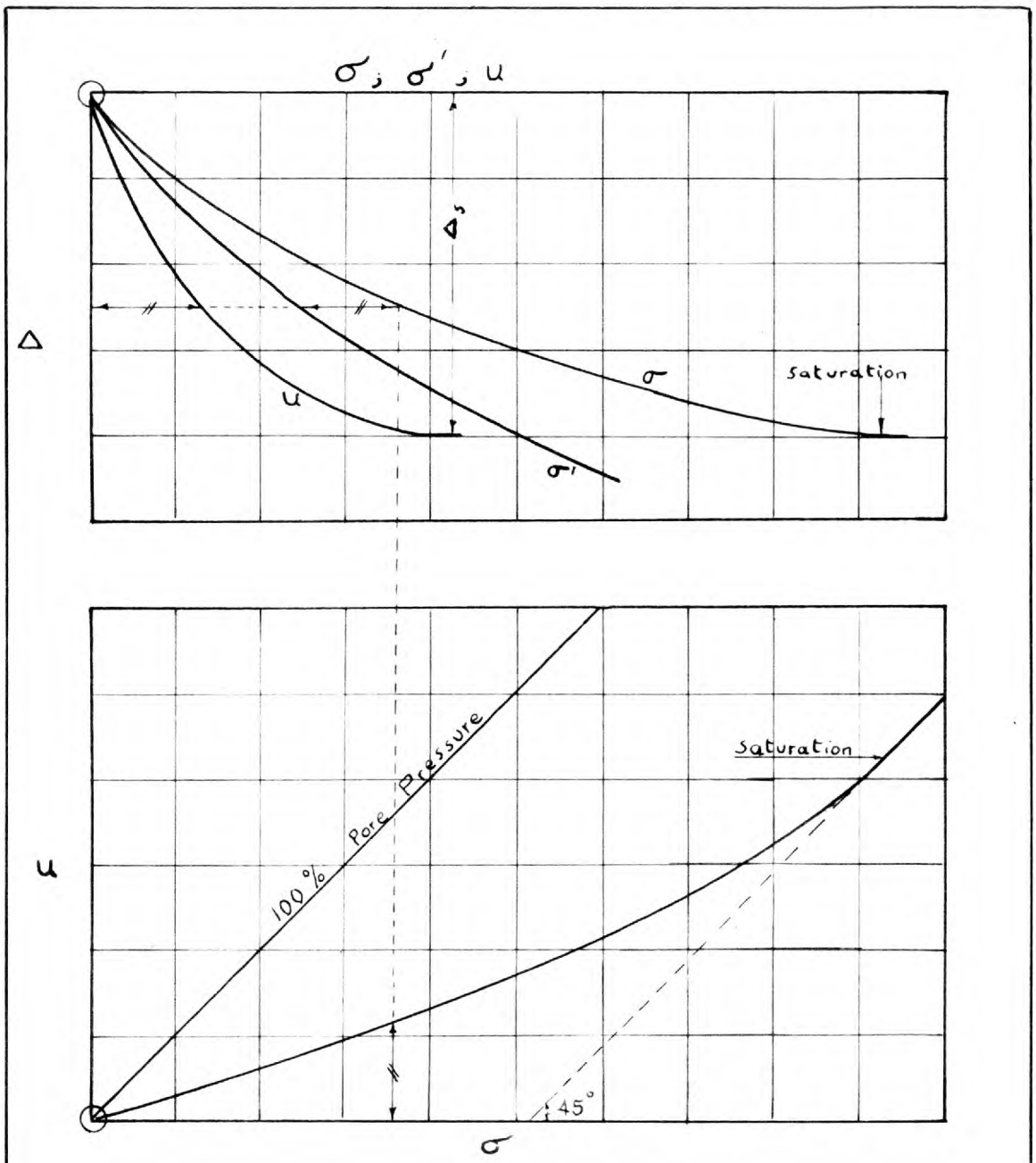
RELATION BETWEEN MAJOR PRINCIPAL STRESS & PORE PRESSURE AT FAILURE.

FIG. 3:2



RELATION BETWEEN LOAD, PORE PRESSURE & VOLUME CHANGE FOR LOADING & UNLOADING.

FIG. 3:3



Hilf's Method to Determine Load - Pore Pressure Relationship.

Δ_s = vol. change at saturation (i.e. vol. of free air) for sealed sample.

FIG. 3:4

above mentioned relationships could be combined together to give a total stress; pore pressure curve, Fig. 3:4.

Hilf's tests were carried out in an oedometer, but the method is indeed valid for any type of consolidation, although the pore pressure total load relationship will vary according to the system of stresses applied.

The validity of any experimental procedure depends largely on the accuracy by which the soil properties S, n and also the volume changes are determined, especially with a wet sample having a small air content. Furthermore, the discrepancy from the actual field conditions implied in using a certain grading of the material to suit the experimental equipment, and rejecting larger stones or cobbles, must be considered when applying the test results, but it is believed that the effect is small and on the conservative side, Gibbs (1950).

In designing an earth structure, due consideration must be given to the different phases of loading and their corresponding p.w.p. These are the construction conditions where the pore pressure is due to the consolidation of the soil under the overburden as already mentioned, the steady seepage condition where the pore pressure is estimated by a flow net and the case of a rapid draw down of the up-stream water.. The rapid draw down causes the total stresses above a soil element to decrease due to the removal of the weight of water. As a result, the soil will expand and since the expansibility

of soils is generally less than its compressibility it follows that upon unloading a soil element there will exist a certain amount of residual pore pressure, i.e. higher pore pressures under the same load during the unloading, Fig.3:3.

This is expressed by the equation:- (Bishop, 1952).

$$(\triangle u)1 = \frac{1}{1 + n \frac{Cu_1}{Cs_1}} (\triangle \bar{\sigma}3)1 \qquad 3:10$$

where $(\triangle u)1$ is the decrease in pore pressure due to expansion

$(\triangle \bar{\sigma}3)1$ is the decrement in the total all round pressure

Cu_1 is the expansibility of pore fluid = its compressibility

Cs_1 is the expansibility of soil structure and is generally less than the compressibility.

In general the pore pressure change due to a change in the state of stress for a saturated soil was given by Skempton (1948) as follows:

$$\triangle u = a(\triangle \bar{\sigma}1 - \triangle \bar{\sigma}3) + \triangle \bar{\sigma}3 \qquad 3:11$$

where $\triangle u$ = change in the pore pressure

$\triangle \bar{\sigma}1$ and $\triangle \bar{\sigma}3$ are the changes in the major and minor principal stress

"a" is a parameter depending on the shear characteristics of the soil. In triaxial tests where $\bar{\sigma}3$ is kept constant

throughout the test $a = \frac{\Delta u}{\Delta(\sigma_1 - \sigma_3)}$

For saturated soils the value of "a" at failure (af) is independent of the cell pressure σ_3 as shown in Table and in Fig. 5:91

For a partially saturated soil Δu is given as follows:

$$\Delta u = a(\Delta\sigma_1 - \Delta\sigma_3) + B.\Delta\sigma_3 \quad 3: (12)$$

where B is the pore pressure ratio under an all round pressure equal to σ_3 and is less than one. Typical values of B shown in Table 2.

It is a common practice for design purposes, to express the pore pressure ratio in terms of the change in the major principal stress σ_1 i.e.

$$\frac{\Delta u}{\Delta\sigma_1} = B + (a - B)\left(\frac{\Delta\sigma_1 - \Delta\sigma_3}{\Delta\sigma_1}\right) \quad 3: (13)$$

Since B varies with the cell pressure, it follows that (af) for partially saturated soils is not constant for different values of σ_3, Skempton and Bishop (1954). An experimental evidence in support of this criterion is given in Chapter 5, and in Fig. 5:90 and 5:91.

TABLE 1

Values of Pore Pressure Parameter a_f for saturated Soils at Failure

	Material	(a_f)
Normally consolidated clay	Haslemere Clay (Imperial College)	0.95
	Weiner Tegel (Rendulic 1937)	0.64
	Boston Clay (Taylor 1944) (Remoulded)	0.73
Over-consolidated clay	Haslemere (Imperial College) (Undisturbed)	- 0.62
Sand	Brasted Sand Loose (Imperial College)	0.08
	Dense	- 0.32

TABLE 2

Values of $B = \frac{\Delta u}{\Delta \sigma_3}$ for Partially Saturated Soils

	Opt. γ_d	Opt. M/c.	γ_d lb/cuft	M/C	S %	B	Pressure Range p.s.i
Boulder Clay (1) L.L. = 17 P.L. = 15	136	7.8	134	8.8	94	0.8	0 - 100
			136	7.8	89	0.23	
			133	6.8	71	0.05	
Moraine Clay (2) L.L. = 24 P.L. = 22	130	10.4	136	11.6	89	0.93	0 - 100
			130	10.4	88	0.62	
			129	9.6	80	0.32	
Lateritic Clay (3) L.L. = 85 P.L. = 55	70	51	68	55.0	98	0.78	0 - 40
			68	53.1	95	0.40	
			68	51.0	90	0.12	

(1) Used for present series of tests.

(2) Haefeli and Bjerrum - Private communication to Dr. A. W. Bishop

(3) Tests at Imperial College.

Chapter 4

EXPERIMENTAL WORK.

A. Properties of Material Used

The material used is a boulder clay obtained from the site of an earth dam now under construction in the Daer district. It is formed of fragments of different sizes, mainly granite, together with ground up debris.

The natural moisture content in the ground is about 8.5%.

Fragments not passing through a $\frac{3}{8}$" B.S.S. were rejected and the rest of the material (about 80%) was used for testing.

The particle size distribution is shown in Fig. 4:1 for the material finer than $\frac{3}{8}$". It shows that the material is well graded and has a clay fraction of about 5%.

Fig. 4:2 shows the compacted dry density, placement moisture content relationship for the standard Proctor compaction in the 4" dia. by 4.59" mould, together with that for the compaction in a 4" dia. by 8" mould, which is used to prepare the samples for the series of tests presented in this thesis.

Description Boulder clay

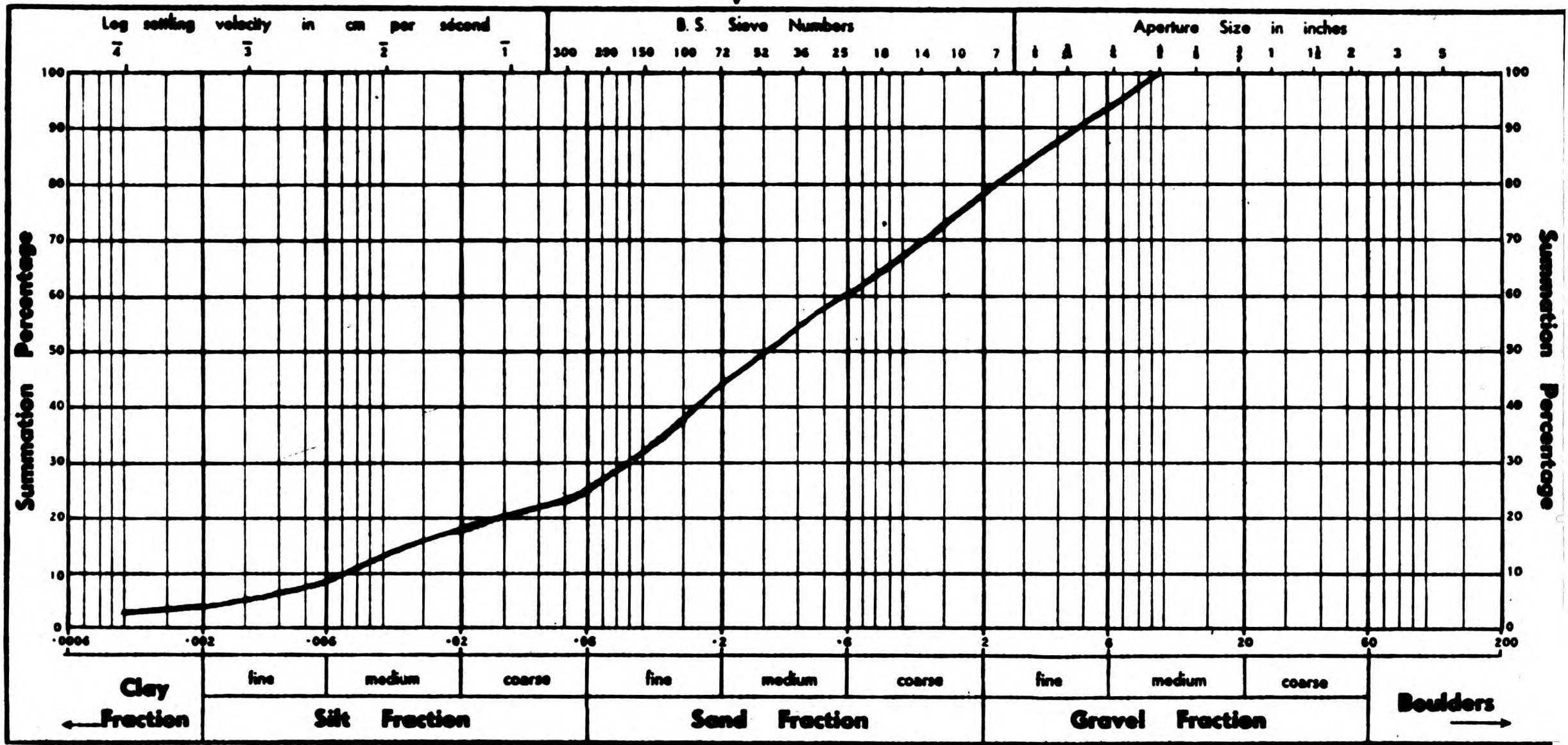
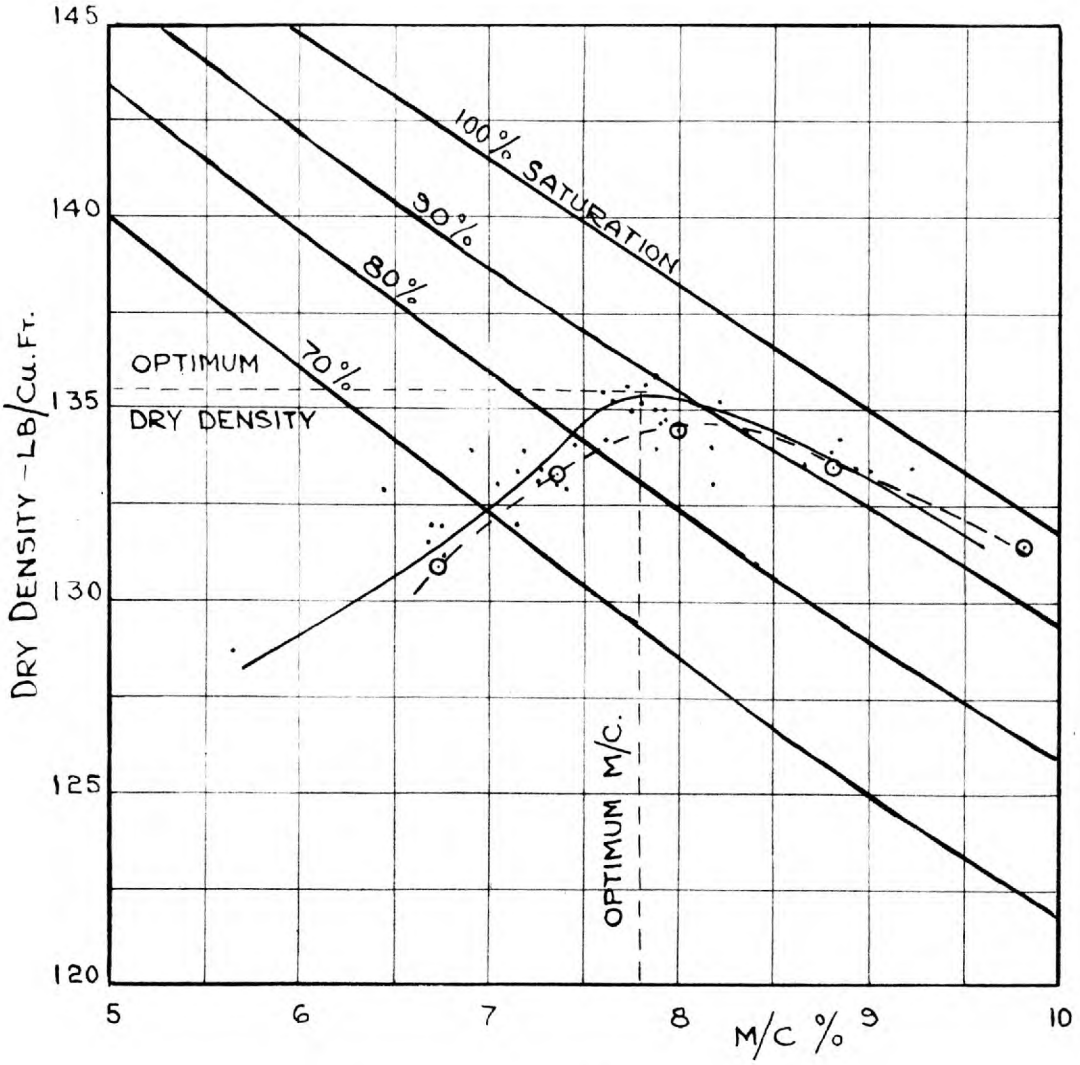


FIG. 4:1



COMPACTION CHARACTERISTICS.

· ——— COMPACTION IN SPLIT MOULD 4" DIA. x 8".

o— — — — STANDARD PROCTOR COMPACTION.

FIG. 4:2

Results of compaction in the 8" mould show that the optimum moisture content is 7.8% and the optimium dry density is 135.5 lb./cu. ft. Results of the standard compaction vary only slightly on the wetter side of the optimum while a slightly larger variation occurs with dryer samples.

Tests were carried out on samples with moisture content ranging from - 1% to + 1% of the optimum. The corresponding range of the degree of saturation is 63% to 93% approximately.

The specific gravity is 2.697.

The liquid limit for the material passing through No. 36 B.S.S. is 17% and the plastic limit is 15%.

B. Experimental Equipment and Sample Preparation

The nature of most rolled fill materials in relation to their mechanical analysis make it necessary to use samples in the triaxial compression tests larger than those of clays or sands ($1\frac{1}{2}$" dia. x 3"). By excluding the soil grains larger than $\frac{3}{8}$", it would be possible to perform triaxial tests on 4" dia. x 8" high samples, where the ratio of the size of the largest grain to the diameter of the sample is about 1:10. This ratio enables a proper compaction and a fairly smooth surface to be achieved with the size of equipment used.

Compaction is carried out in a 4" x 8" specially designed split mould, consisting of three butt jointed segments clamped together by a six piece belt tightened by a screw, and fitted on the base of the ordinary Proctor mould; Plates 2 and 4. The object of the split mould is to make possible the extraction of the sample without jacking (as with ordinary moulds), thus safeguarding against any possible changes in the density or the state of stress in the pore water before testing. The ordinary Proctor compaction was followed i.e., each layer receives 25 bumps from a $5\frac{1}{2}$ lb. hammer falling from a height of one foot. With the 8" high mould

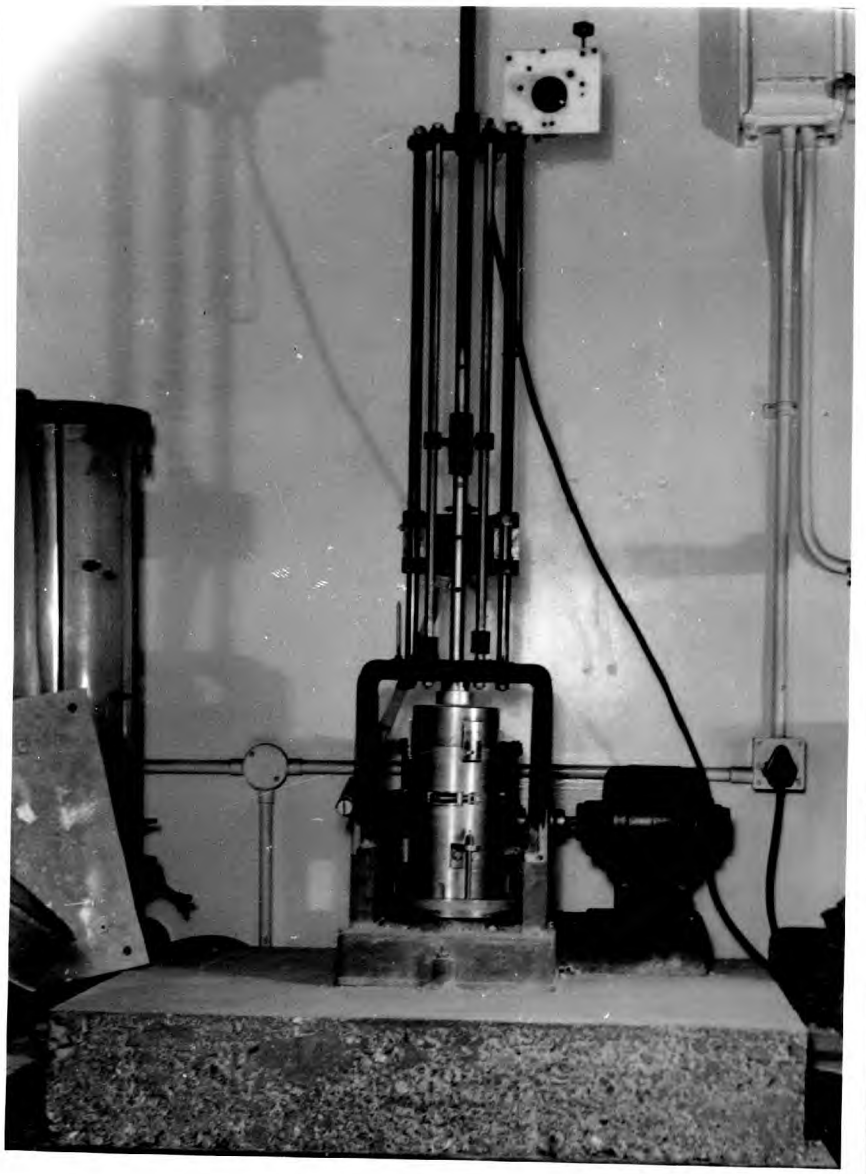


PLATE 2.

compaction was carried out on six layers, each 1½" final height, thus allowing for an extra inch of height to be trimmed off. The compacting hammer is driven mechanically, as shown in Plate 2.

In order to determine accurately the moisture content of a sample it was found necessary to use larger specimens (about 130 gms.). Non-consistent results were frequently obtained when using the ordinary sized moisture content bottles (about 50 gms. of material) where the results for the same batch varied considerably in some cases. With small specimens there is always the possibility of a variation in the quantity of larger sized soil grains in each; which becomes less relevant if larger specimens are used. It was necessary to investigate whether the moisture content of the soil batch before compaction remained constant during compaction. A comparison was made on some trial samples and the results showed insignificant change.

After compaction, the sample is trimmed level and the mould unlocked and its sides removed. The sample is then weighed, provided with two filter paper discs at its top and bottom and finally fitted on a porous plate (made of sintered bronze or sintered bauxilite) resting on the 4" dia. base of the triaxial cell. Side filter paper drains are added and tucked under a top porous plate and the loading cap. Then a 4" rubber membrane (.009" thick) is fitted around and sealed

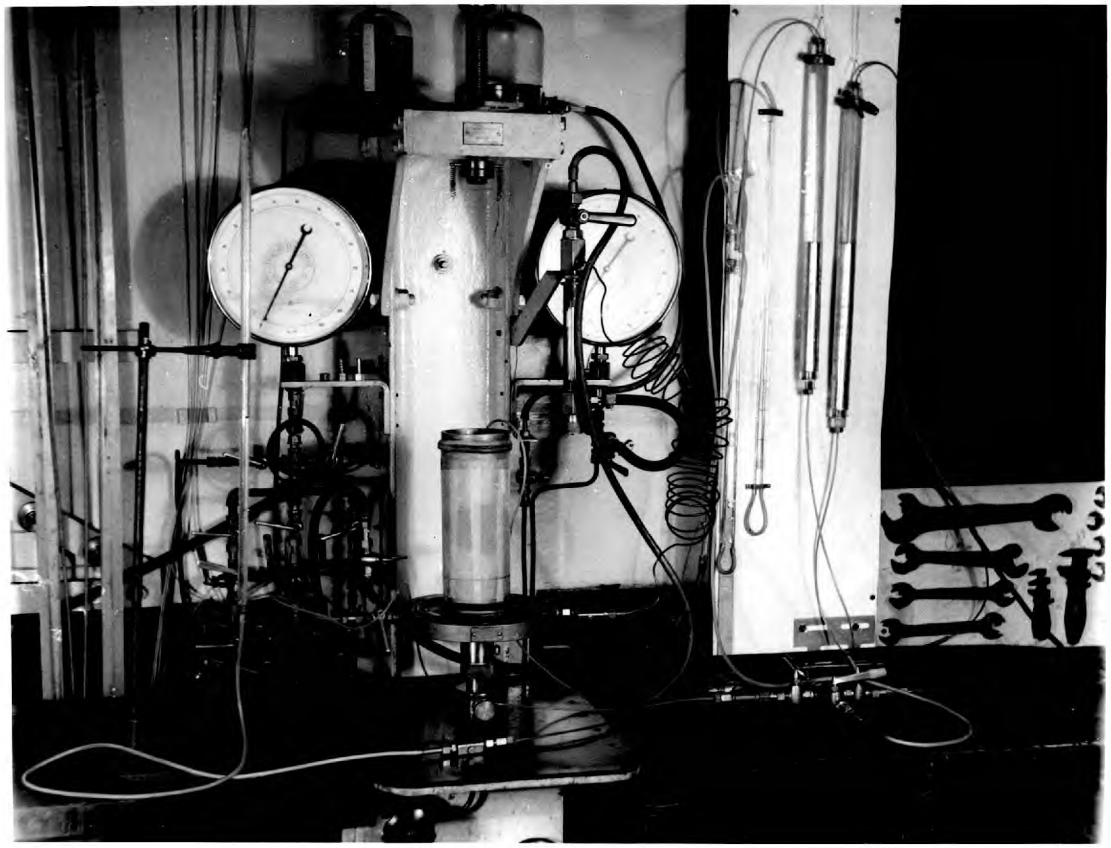


PLATE 3.

on top and bottom by Gaco sealing rings; (Plate 3).

(See Plate 4 for different accessories).

After testing, the sample is weighed and three moisture content specimens taken. The average moisture content of the specimens was found to be almost identical to that calculated from the difference of weight of the sample before and after testing (in drained and consolidated undrained tests, the moisture content of the sample changes. Such, however, is not the case for undrained tests).

It was found with samples tested to considerable strains beyond failure that the moisture content varied widely along the sample, and was maximum at the centre (especially in undrained tests). This is due to the migration of water towards the centre where maximum shear strains occur * (i.e. maximum dilatency; according to Eldin (1951)). To minimise this effect, the test has to be stopped just after reaching failure.

After setting the sample, its bottom can be connected by a lead through the base of the triaxial cell to either the pore pressure measuring unit, to a source of water under pressure used to saturate the sample, or to a pipette for drainage. In each case the connection is controlled by a leak proof valve.

---

* Shear strain is equal to $(\epsilon_1 - \epsilon_3)$ where ϵ_1 and ϵ_3 are the strains in the direction of the principal stresses $\bar{\sigma}_1$ and $\bar{\sigma}_3$.

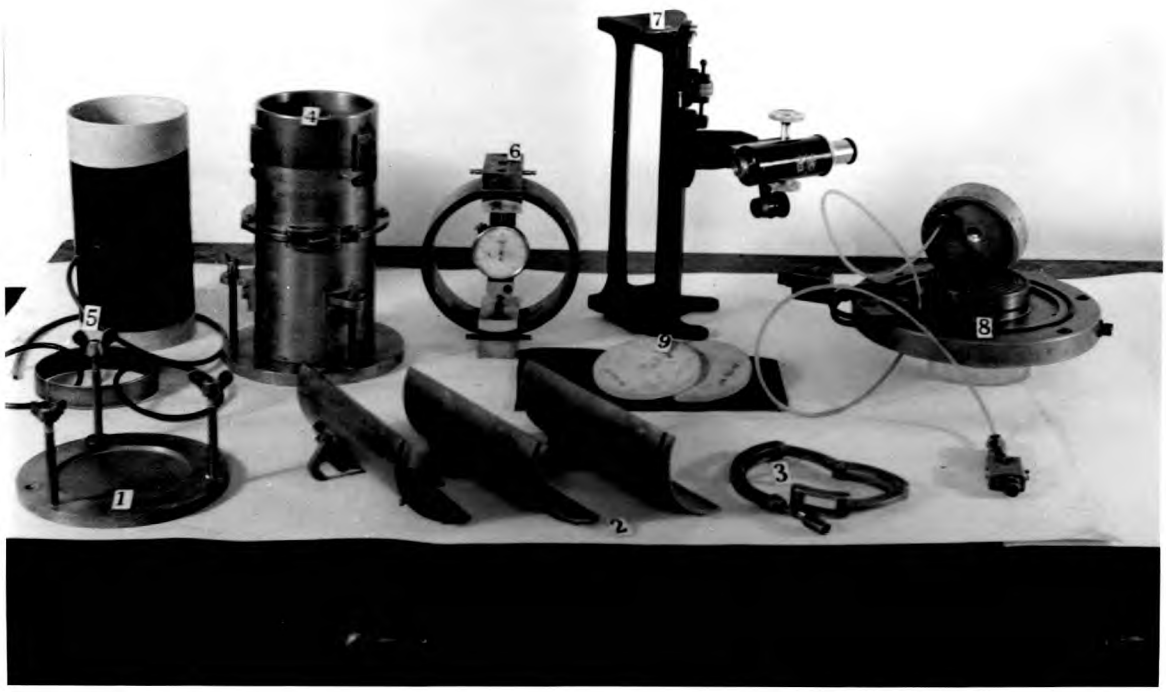


PLATE 4

1. Base of Compaction Mould
2. Segments forming Mould
3. Tightening Belt with End Screw
4. Assembled Mould with Top Cap
5. Sleeve with Membrane, Sealing Rings and Split Ring used for Fitting Sealing Rings into base.
6. Proving Ring
7. Travelling Microscope
8. Base of Triaxial Cell with Top Cap
9. Porous Plates

The top of the sample is connected to a pipette by a flexible tube with a controlling valve running through the top loading cap and through the cell base. This connection is used either to accelerate consolidation by allowing drainage from both ends or to act as an exit for the saturating water. In all undrained shear tests its valve is kept shut.

The cell is a 7" I.D. perspex cylinder capable of standing up to 150 p.s.i. of fluid pressure. The load is applied to the top cap by a $\frac{3}{4}$" stainless steel piston moving through a $1\frac{3}{4}$" dia. gland which is part of the bronze casting forming the top of the cell. This gland is fitted with a push fit perspex sleeve into which castor oil is injected when the cell is full of water. The castor oil is used to prevent any possible leakage through the gland. The function of the sleeve is to effect a leak proof system using a minimum amount of oil.

The cell pressure is applied either by an air compressor or by an adjustable column of mercury. The mercury column is provided by connecting a mercury pot resting on the floor level by a flexible tube to another movable pot. The latter is hung by a spring designed to keep the level of mercury in the pot adjusted[*] after being set, thus providing for a means to run long duration tests at constant pressures without the possibility of pressure drops due to leakage or other reasons.

[*] Bishop & Henkel; Geotechnique, December 1953.

The object of the apparatus is:

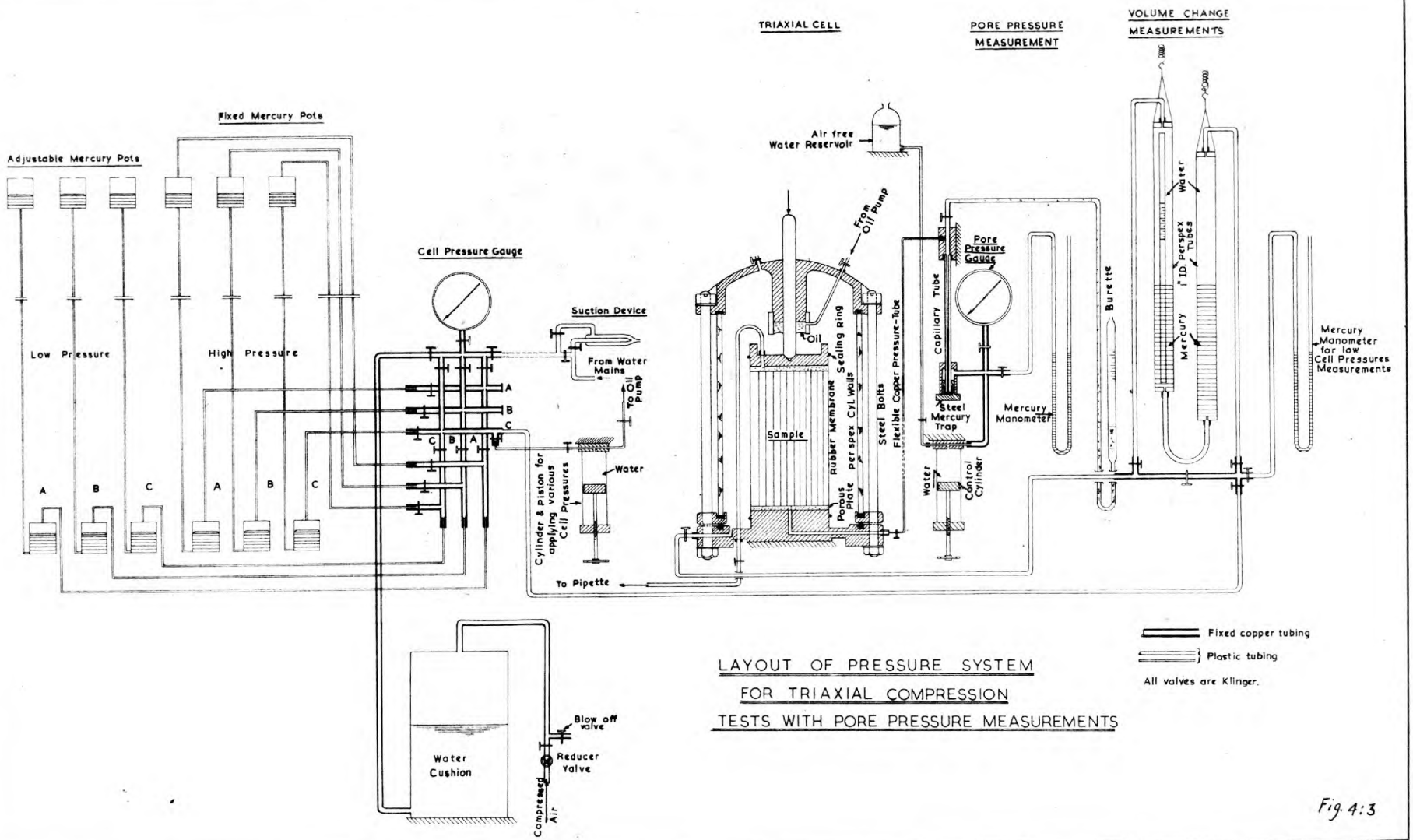
1. To apply and measure the load on the sample and to measure the strain.
2. To measure the pore pressure in the sample at any stage during the test.
3. To measure the volume changes of the sample externally.

A general layout of the apparatus is given in Fig. 4:3.\ Plate 1

1. The load is applied by a machine which gives a chosen constant rate of strain and is measured by a proving ring.

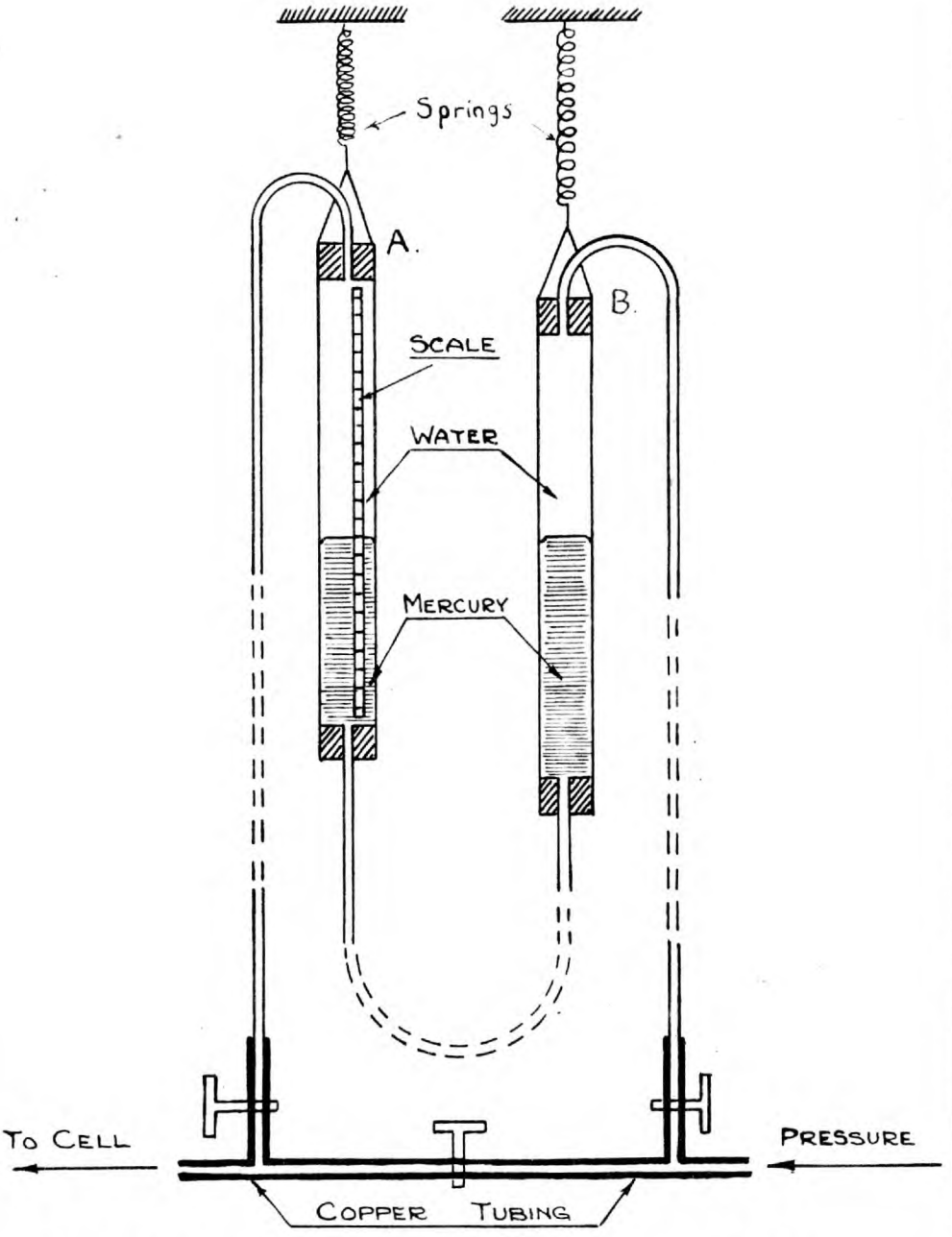
2. The pore pressure is determined by maintaining at constant level a mercury column in a capillary tube connected at the top to the bottom of the sample and at the bottom to a cylinder and piston. The piston serves to adjust the mercury column. The pressure is measured by a Bourdon gauge or by a manometer in the case of negative pore pressures.

3. The volume change measuring unit is composed of two 1" I.D. perspex tubes each 20" long connected together at the bottom by a high pressure flexible tube. One tube is connected through the top to the triaxial cell by a flexible tube, while the other is connected to the source of the cell pressure, which in this case should be the mercury column previously mentioned. The perspex tubes are half full of mercury, while the rest is full of water, Fig. 4:4, and a



LAYOUT OF PRESSURE SYSTEM FOR TRIAXIAL COMPRESSION TESTS WITH PORE PRESSURE MEASUREMENTS

Fig. 4:3



=====:— FLEXIBLE TUBES of SUFFICIENT LENGTH.

A. & B.:— PERSPEX TUBES 1" I.D. 20" LENGTH.

VOLUME CHANGE MEASURING UNIT.

FIG. 4:4

system of valves is provided to be used when re-setting the mercury level.

Any change in the combined volume of the cell and sample would cause the quantity of water in (A) to change according to the magnitude of this volume change. It follows that the mercury level in (A) and also in (B) will change, relative to the tubes, with the result that the pressure in the cell changes, unless the relative positions of the tubes are altered. If, say, (B) is moved so that the two surfaces of mercury become level again, the change in the position of the mercury surface in either (A) or (B) would be a measure of the volume change. (A) is provided with a scale graduated to determine volume changes directly. It must be mentioned that the pressure on the surface of the mercury in (B) remains constant so long as it is connected to the adjustable mercury column pressure system. In fact, the volume changes will be reflected as changes in the amount of mercury in both pots of this system.

It was found difficult to adjust (B) manually to keep the mercury surfaces in (A) and (B) level throughout the tests. An automatic adjustment was possible by hanging (A) and (B) by springs designed in such a way that their deformation is always equal to the variation in the mercury level in either tube. Thus the surface of mercury in (A) and (B) will be kept at the same horizontal level throughout the test while the tubes

move relatively.

The volume changes recorded are the algebraic sum of the change in volume of cell, and that of the sample. A third term is introduced during shear tests due to the penetration of the loading piston into the cell, and has to be accounted for. Cell deformation is determined beforehand by calibrating it when full of water.

C. Types and Purpose of Tests and Testing Procedure

The purpose of this research is to study the strength characteristics of rolled earth fill materials in relation to the design and construction of earth dams. Therefore a study of the shear parameters (cohesion and internal friction) together with a study of the pore pressures under different loading conditions, simulating those in an actual dam is needed. Consequently the types of tests fall under two main groups, i.e. tests to determine the shear strength characteristics at failure and others to study the pore pressure-stress relationship without failure.

1. Shear Tests

(i) Undrained Tests.

This type of test represents the case of an incipient failure during construction when no appreciable dissipation of water has taken place. The sample is tested to failure with the pore pressure measured at the bottom and sides.

Samples covering the range of moisture content from - 1% to + 1% from the optimum were tested under four cell pressures of 15, 40, 70 and 120 p.s.i. The sample must be left under the cell pressure for sufficient time to enable the pore pressure set up to become stable before it is sheared.

The rate of strain during shear was chosen so that a 15% strain is achieved in two hours. Holtz (1947) and Bjerrum (1951) allowed only half an hour for a 15% strain. No volume change measurements were possible in these tests.

(ii) Consolidated Undrained Tests

In these tests the sample is initially allowed to consolidate under the cell pressure. Then water under pressure (equal to a small proportion of the cell pressure) is introduced through the bottom of the sample into the top pipette, in an attempt to saturate it. This represents the softening of the soil in an embankment due to the steady seepage of the reservoir water, or due to rain fall. When the flow of water became regular (this normally takes about 24 hours) the bottom of the sample is disconnected from the source of flow and connected to the pore pressure measuring device. The connection from the top to the pipette remains open until all the residual pore pressure is dissipated and is then shut. The next step is to shear the sample without drainage, either:

(a) under the same consolidation pressure. The results of such tests are used in terms of effective stresses in the stability analysis of the embankment after consolidation. Three cell pressures of 15, 40, 70 p.s.i. were used. The range of moisture content was within - 1% to + 1% from the optimum.

(b) under various cell pressures. The results of these

tests are used to study, in terms of total stresses, the stability of an embankment after a rapid draw down of the reservoir water. This means that different values of the total stress shear parameters, C and ϕ, will have to be used for the different points on the slip circle as each point, in fact, has been consolidated under a different overburden pressure.* In terms of effective stresses, these tests should give, theoretically, the same shear parameters as those of series (a), which can be used in the case of draw down in conjunction with the appropriate values of pore pressure. Volume changes were measured during all stages of the test.

Only one moisture content was used, that at optimum, while the consolidation pressures and cell pressures were as follows:

Consolidation Pressure	Cell Pressure
15 p.s.i.	40, 70 p.s.i
40 "	70, 120 "
70 "	120 "

Test results showed that it was not possible to saturate the sample fully. It is thought that considerable time would be needed for this purpose. Prolonged flow of de-aired water might eventually achieve this, but other experiments

---

* i.e. for each consolidation pressure there will be a separate envelope for total stresses.

Casagrande* (1951), Geuze (1948) have not succeeded even in sands.

To determine the initial area of the sample before shear, the volume change due to consolidation and the axial deformation was determined. The latter was determined by using a travelling microscope. During shear, the average cross sectional area was calculated for the changes in height and volume, assuming the sample remains cylindrical. Eldin (1951) showed that this assumption is approximately accurate. He measured the actual area of the shear failure plane across a saturated sample of sand and compared it with that calculated according to the cylindrical assumption.

(iii) Drained Tests.

In these tests, the sample was allowed to consolidate under the cell pressure until the excess pore pressure had dissipated (usually in 24 hours). It was sheared under conditions of no excess pore pressure. Drainage during both phases of the test was allowed through either top or bottom of the sample, or through both. Side filter paper drains were also fitted in.

The rate of strain during shear was chosen such that all

---

* Casagrande used a flow of ammonia vapour to replace the air in the sample. Evacuation then followed to remove most of the ammonia vapour. The water was introduced to saturate the sample. Over-consolidating the sample is inevitable as a result of the evacuating pressure.

the increments of load are fully effective throughout the test and the pore pressure is zero.* This rate was found to be 0.015% per minute. It is in conformity with the theory put forward by Gibson and Henkel (1954)** which relates the rate of strain in drained tests on clays to the coefficient of consolidation C_v and the size of the sample. The average time for failure was nearly six hours (at 5% strain). A test on a wet sample was run such that failure occurred after 30 hours. Results of this test are shown in Fig. 5:42, and prove to be in accordance with the other test results obtained by using the normal rate. The following table gives measured values of $(\bar{\sigma}_1 - \bar{\sigma}_3)$ for a sample tested under a cell pressure of 15 p.s.i. The rates of strains were: 0.015% per minute, 0.015 x 5% per minute and 0.015 x $\frac{1}{5}$ % per minute:-

---

* In the present series of tests the pore pressure at the start of shear was zero (as proved by allowing the drainage from the top and measuring the pore pressure at the bottom after consolidation); but the conditions of the test are also fulfilled if the pore pressure had any value other than zero, provided it is kept constant throughout.

** The coefficient of consolidation for the material used is .008 cm^2/sec and according to Gibson and Henkel, the rate of strain for failure to occur at 5% is three hours.

Rate of strain % per minute	$(\bar{\sigma}_1 - \bar{\sigma}_3)$ p.s.i.
0.015 (Normal)	78.4
0.015 x 5	80.0
0.015 x $\frac{1}{5}$	76.4

This shows that the chosen rate represents an appropriate speed for the tests.

The cross sectional area of the sample after consolidation and during shear was determined in the same way as for the consolidated undrained tests. It may be mentioned that as the sample is partially saturated, its volume change cannot be determined by the volume change of water in the pipette as in the case of saturated samples.

The use of the results of this type of test is to analyse the condition of steady seepage of the down stream face of an embankment which has been fully consolidated under its own weight. The analysis is carried out in terms of effective stresses and the pore pressure is determined from a flow net.

Samples covering the whole range of moisture content were tested under three cell pressures:- 15, 40, and 70 p.s.i. Final moisture contents were determined. The results are expressed in terms of initial and final moisture contents.

3. Pore Pressure Tests

These tests, carried out on sealed samples, had a dual purpose; that of determining the pore pressure set up in a soil element under different conditions of loading comparable to those met with in practice, and that of determining the compressibility of the soil under such conditions. The compressibility obtained, if expressed in terms of effective stresses, should be almost identical with that obtained for similar conditions, but with complete dissipation of pore pressures (i.e. drained tests).

(i) Tests with All Round Pressure or The B Tests.

The pressure is added in increments, each is left on until the pore pressure set up becomes stable, and after the final increment becomes fully operative the pressure is reduced in stages. The relation between the increment of cell pressure $\Delta \bar{\sigma}_3$ and that of pore pressure Δu is expressed as follows:

$$\Delta u = B \cdot \Delta \bar{\sigma}_3$$

where B is essentially less than unity.

Tests were carried out for the whole range of moisture contents. The pore pressures and volume changes were measured for the unloading as well as the loading stages. A value of the coefficient B is also obtainable from the results of each of the undrained tests before shearing the sample.

(ii) Samples tested under the Condition of no Lateral Yield (The K_o tests).

A soil element lying well within the inside of an embankment deforms mainly in the direction of the overburden pressure. Lateral deformation is restricted. This condition was reproduced in the triaxial machine, resulting among other data, in an estimation of K_o, the coefficient of earth pressure at rest, which is the ratio of the minor and major effective principal stresses for zero lateral yield; Bishop (1950), Bishop and Eldin (1953).

The sample is set up under zero cell pressure. The test starts by increasing the axial load (at constant rate of strain) together with the cell pressure such that the volumetric deformation at any stage is equal to the initial cross sectional area of the sample times the vertical deformation, i.e. no lateral yield.

The testing procedure is rather complicated. This is because the increments of cell pressure which are constantly added to effect the condition of no lateral yield cause the cell to expand with the result that the volume changes recorded by the volume measuring unit will be the sum of the deformations of the cell and of the sample (and also the volume of the part of the loading piston that penetrated into the cell). While at any axial strain, the deformation the sample has to undergo is known, the cell pressure and the corresponding cell

deformation are unknown. It was therefore necessary to perform a number of trial tests until it was possible to adjust the volume changes exactly or within a difference of $\pm$0.02 cubic inches throughout the test.*

To keep the conditions of the test fulfilled throughout, the readings were taken every $\frac{5^{th}}{1000}$ of an inch to secure a continuous adjustment. The rate of strain was as low as 0.015% per minute to allow the pore pressure to adjust itself to the increments of stress.

The cell pressure is applied manually by a cylinder and piston controlled by a screw, Fig. 4:3.

The samples tested covered the whole range of moisture content.

(iii) The $\frac{1}{F}$ Tests

In these tests the sample is subjected to increases in the principal stresses applied in such a manner as to maintain a constant factor of safety throughout the test. For this purpose the factor of safety, F is used in the same sense as in the design of earth dams in terms of effective stresses, i.e. it is the factor by which C' and tan ϕ' would have to

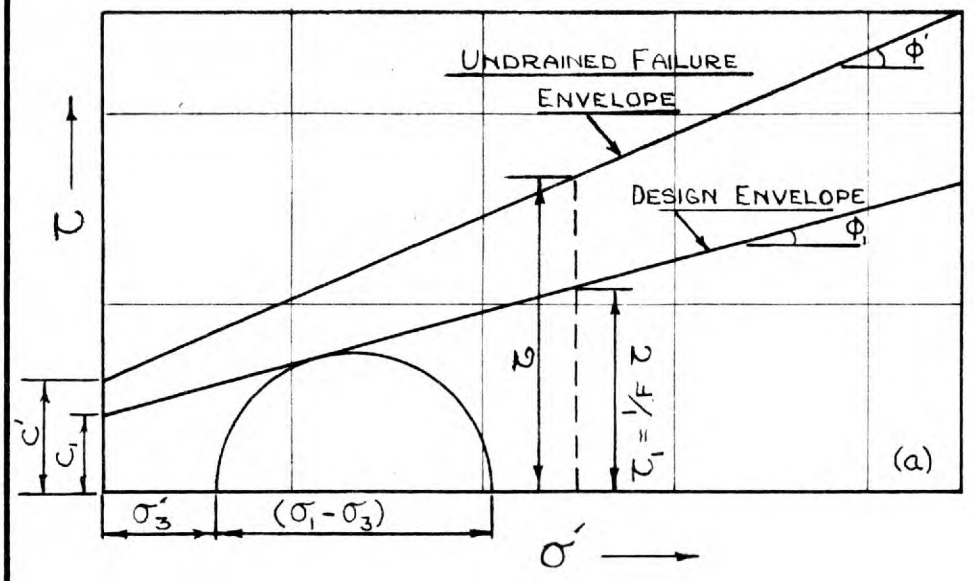
---

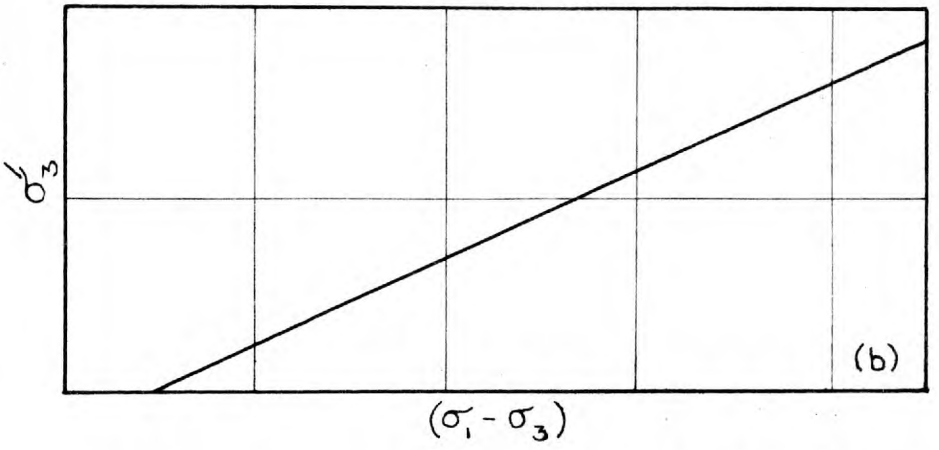
* The procedure of testing becomes a simple one if the cell is rigid enough so as not to deform under pressure and the area of the loading piston is equal to that of the sample.

be reduced for failure to occur under the applied stresses.

For a given sample the values of C' and ϕ' are taken from the undrained test results corresponding to this moisture content. The "allowable stress" envelope (C_1, ϕ_1) is then plotted by reducing C' and tan ϕ' by the factor x $\frac{1}{F}$, using a value of F = 1.5 as representing typical earth dam practice, Fig. 4:5(a). The pore pressure is measured during the test and the cell pressure adjusted to keep the effective stress circles tangential to this line i.e. to fulfil the relationship between $(\bar{\sigma}_1 - \bar{\sigma}_3)$ and $\bar{\sigma}'_3$ shown in Fig. 4:5 (b) which is derived from the (C_1, ϕ_1) envelope in Fig. 4:5 (a).

To simulate these actual conditions, the axial load on the sample as well as the cell pressure is to be increased gradually in such a way as to fulfil the graphical relationship in Fig. 4:5 (b). This is extremely difficult to achieve experimentally since both $\bar{\sigma}'_3$ and $(\bar{\sigma}_1 - \bar{\sigma}_3)$ are functions of the pore pressure which varies as the cell pressure is adjusted. A compromise solution is necessary and that is to add the cell pressure in small increments of 5 p.s.i. and to run the test very slowly to allow for the adjustment of the pore pressure. During each increment the pore pressure, as well as the deviator stress is, constantly watched until the values of $(\bar{\sigma}_1 - \bar{\sigma}_3)$ and $\bar{\sigma}'_3$ fulfil the graphical relationship in Fig. 4:5 (b) before the next increment is added. Volume changes are measured throughout. For each sample a separate relationship is required. Fig 4:5(b).





DETERMINATION OF RELATIONSHIP BETWEEN σ'_3 & $(\sigma_1 - \sigma_3)$ CORRESPONDING TO A FACTOR OF SAFETY F.

FIG. 4:5

Tests were performed on samples covering the whole range of moisture content.

The results of these tests show that for a given placement condition, the pore pressure set up in a bank with a factor of safety of 1.5 are higher than those corresponding to failure conditions.

As already mentioned, the effective stress volume change relationship obtained from these tests run under conditions of no drainage should be almost identical to those under the same conditions of loading, but allowing for complete drainage. A comparison seemed necessary, and therefore some tests were carried out. Of these tests only those under the condition of an all round pressure are presented later. Due to certain difficulties in performing the K_o tests with drainage, the results of some trial tests are not presented in this thesis.

All the undrained cases represent a soil element loaded without the possibility of dissipation of pore pressure. They represent the construction condition in an earth dam where critical pore pressure may be expected during construction if the permeability of the fill material is less than 10^{-6} cu/sec. (1 ft./year), Terzaghi and Peck (1948), Hilf (1948).

It may be worth mentioning here that in the Dam now under construction on the Usk river in South Wales, some dissipation has occurred during construction, although the permeability of

the fill material is only 2 x 10^{-7} cu/sec. However, it was found necessary to accelerate the rate of dissipation by putting in drains.

Chapter 5

INTERPRETATION AND DISCUSSION OF TEST RESULTS

A. The Shear Strength

The available shear strength τ a soil can exhibit along any plane is given by the modified Coulomb's empirical law:

$$\tau = C' + \sigma'_n \times \tan \phi'$$

where C' is the apparent cohesion

ϕ' the angle of shearing resistance

σ'_n the normal effective stress along the plane.

For any type of triaxial shear tests, C' and ϕ' are obtained by plotting the Mohr's envelope to the effective stress circles at failure.

A Failure Criterion.

There is some evidence that both C' and ϕ' vary with the failure strain. Some data in relation to cohesionless sand is given by Bishop and Eldin (1953). For practical purposes it is convenient to base the failure criterion on the state of stress corresponding to maximum deviator stress $(\sigma_1 - \sigma_3)$. With the type of soil used for the present series of tests, the difference between the values of C' and

ϕ' at maximum $(\bar{\sigma_1} - \bar{\sigma_3})$ and at maximum $\bar{\sigma_1}/\bar{\sigma_3}$ is not of practical significance.

Several points made in justifying the maximum principal stress ratio $\frac{\bar{\sigma_1}}{\bar{\sigma_3}}$ as a failure criterion deserve some comment.

Tests by Holtz (1947) on a partially saturated compacted silty clay have shown that during an undrained triaxial compression test, the maximum pore pressure (i.e. minimum lateral pressure $\bar{\sigma_3}$) coincided very closely with the maximum volume decrease and the maximum principal stress ratio. He therefore concluded that the maximum strength will correspond to maximum compression as, once the sample starts to increase in volume, rupture will occur i.e. incipient failure, despite the fact that the samples tested were still able to sustain larger shearing stresses due to the subsequent drop in pore pressure.

It is obviously incorrect to extend this reasoning to saturated soils which are known to sustain almost zero volume changes during undrained shear tests if the cell pressure is high enough, (Bishop and Eldin 1950), (Skempton and Bishop 1954). The criterion, however, is permissible for cohesionless soils where the maximum frictional resistance is mobilised at maximum principal stress ratio. For soils with cohesion the criterion may be used in the case of standard drained tests where complete dissipation of pore pressure throughout the test is maintained and also for undrained tests, where $\bar{\sigma_3}$ does not change appreciably during shear, as in

these cases the maximum principal stress ratio coincides with the maximum deviator stress and corresponds to the maximum mobilisation of the shear strength. (This represents the case of samples compacted at approximately 1% dry of the optimum in the present series of tests).

Presentation of Test Results

In all types of tests, the range of initial moisture content for the samples tested varied from about -1% to +1% of the optimum moisture content. Tests covering the whole of this range were carried out so that the average strength at any particular moisture content can be determined.

All the results of shear tests are presented as a graphical relationship between the moisture content and the corresponding maximum deviator stress for a particular cell pressure. In undrained tests as well as consolidated undrained tests, in which σ'_3 varies during shear, a second relationship is also necessary giving the change of the principal stress ratio at failure with moisture content. The object of this second plot is to determine the minor effective principal stress at failure $(\sigma'_3)_f$

where $$(\sigma'_3)_f = \frac{(\sigma_1 - \sigma_3)_f}{(\sigma'_1/\sigma'_3)_f - 1}$$

and thus plotting the corresponding Mohr's circle.

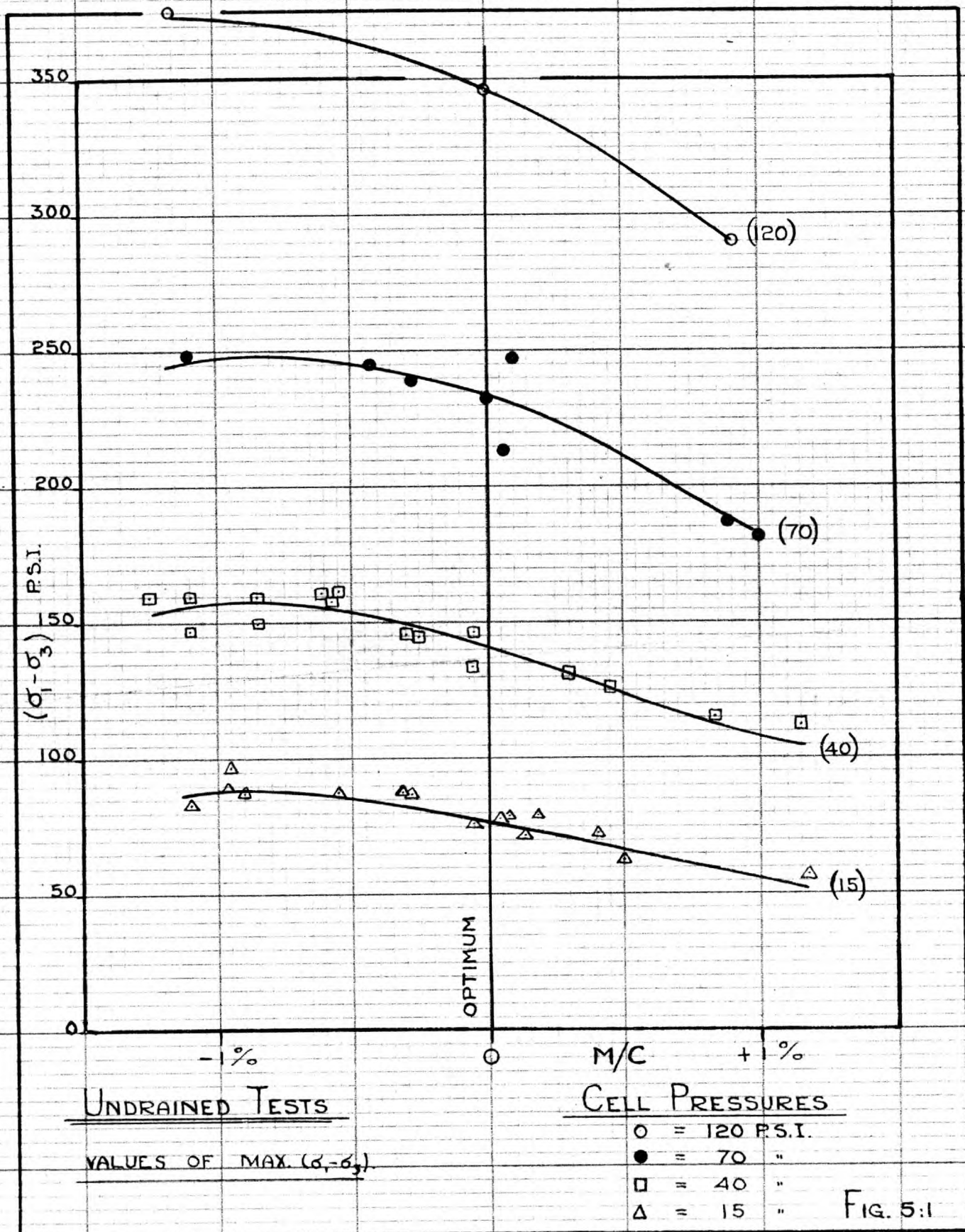
In tests in which the moisture content changes, i.e. drained and consolidated undrained tests, the data is presented in terms of initial as well as final moisture contents, Figs.

5:1 to 5:7. In these figures the axis representing the moisture content has its origin corresponding to the optimum. This is because of the change in the optimum moisture content that inevitably took place during the time taken to complete the testing programme. At the start of the work, the optimum moisture content was 7.55% and finally it was 7.8%. No changes in the optimum dry density were observed.

Typical shear test results are also presented for samples at approximately optimum - 1%, optimum and optimum +1%, for all types of tests Fig. 5:8 to Fig. 5:42*. In view of the great variations with moisture content in the values of strength and pore pressure, the results are not all plotted to the same scale and in some figures different scales are used for the pore pressure and the deviator stress, in order to present the data accurately. To obtain a qualitative picture, these typical test results are plotted on a single figure with a uniform scale for each type of shear tests, Figs. 5:43, 5:44 and 5:45. In these figures the flat portion of some of the $(\bar{\sigma}_1 - \bar{\sigma}_3)$ curves caused by bedding in the initial stages of the test, has been eliminated by correcting the origin of the curves.

---

* These figures are given at the end of this volume



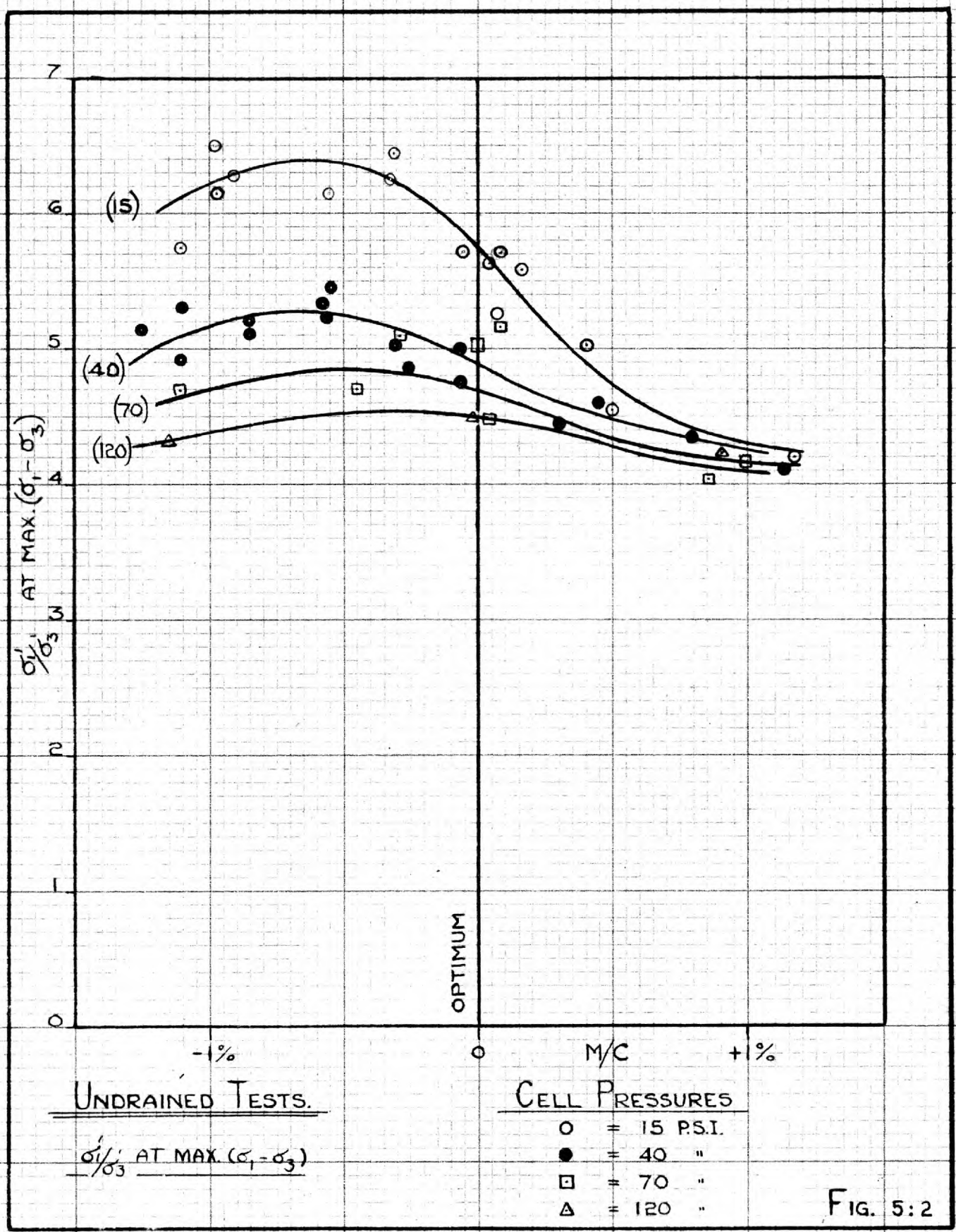
UNDRAINED TESTS

VALUES OF MAX. $(\sigma_1-\sigma_3)$.

CELL PRESSURES

○ = 120 P.S.I.
● = 70 "
□ = 40 "
△ = 15 "

FIG. 5:1



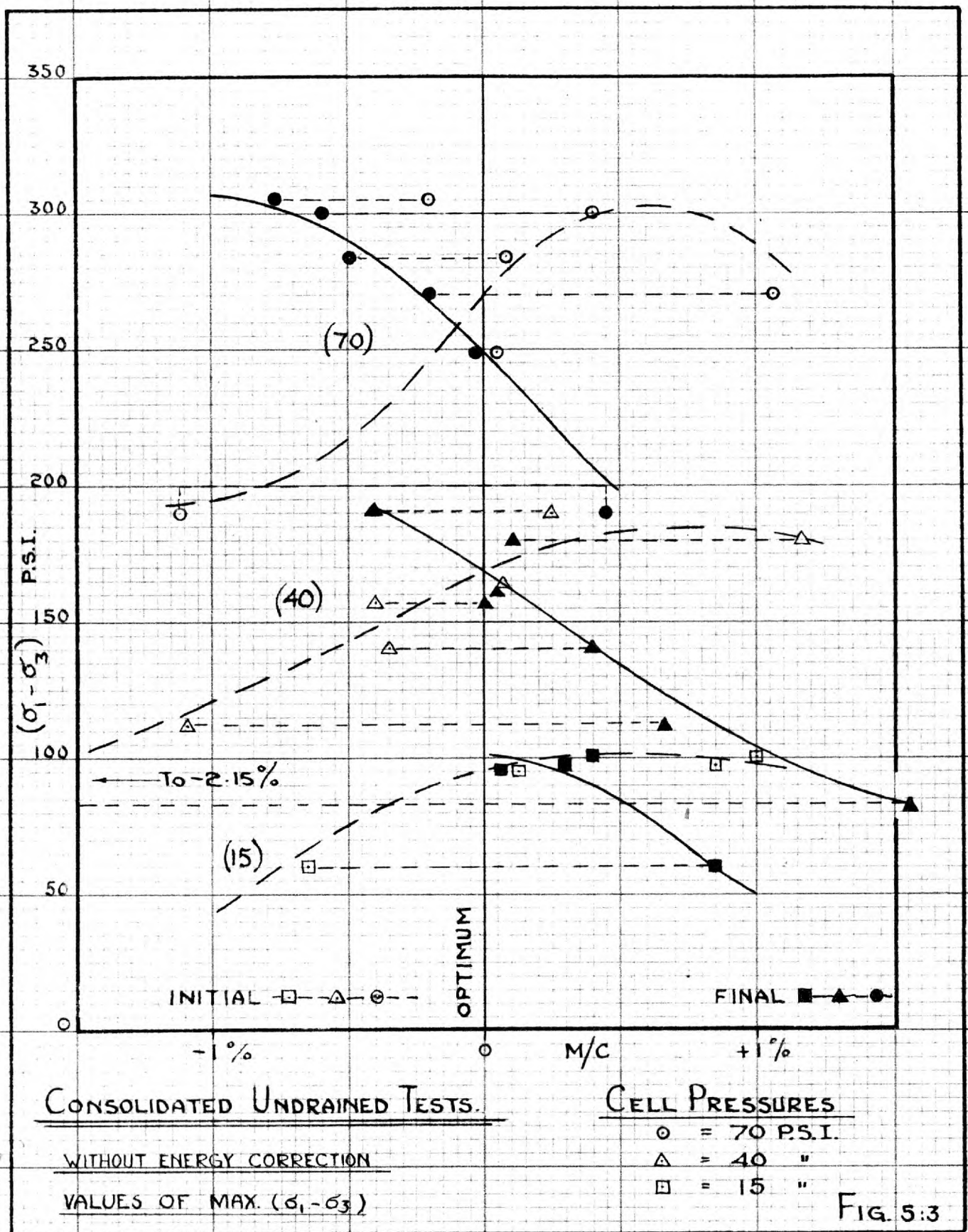
UNDRAINED TESTS.

σ_1'/σ_3' AT MAX. $(\sigma_1 - \sigma_3)$

CELL PRESSURES

- ○ = 15 P.S.I.
- ● = 40 "
- □ = 70 "
- △ = 120 "

FIG. 5:2



CONSOLIDATED UNDRAINED TESTS.

WITHOUT ENERGY CORRECTION

VALUES OF MAX. $(\sigma_1 - \sigma_3)$

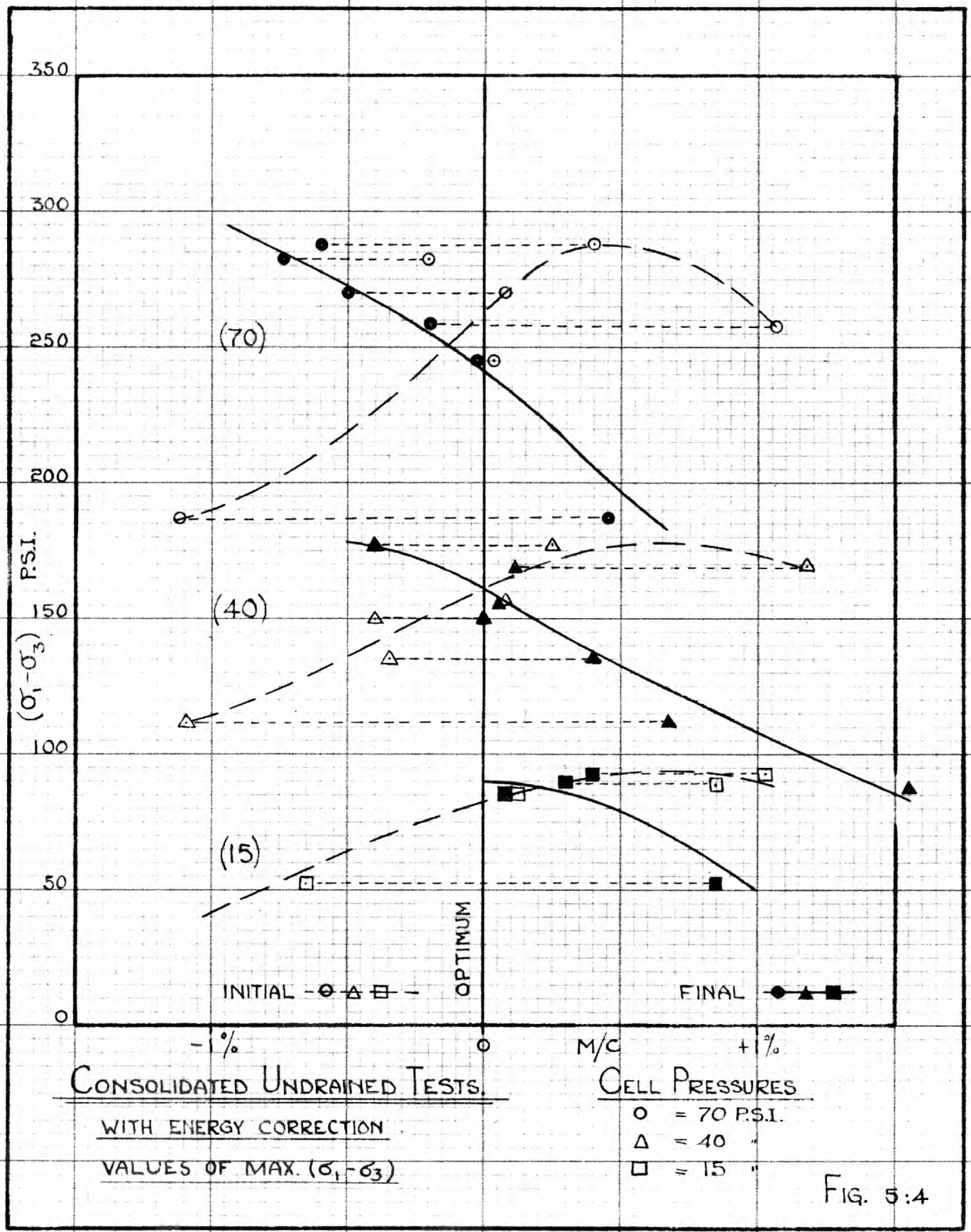
CELL PRESSURES

⊙ = 70 P.S.I.

△ = 40 "

⊡ = 15 "

FIG. 5:3



CONSOLIDATED UNDRAINED TESTS.

WITH ENERGY CORRECTION

VALUES OF MAX. $(\sigma_1-\sigma_3)$

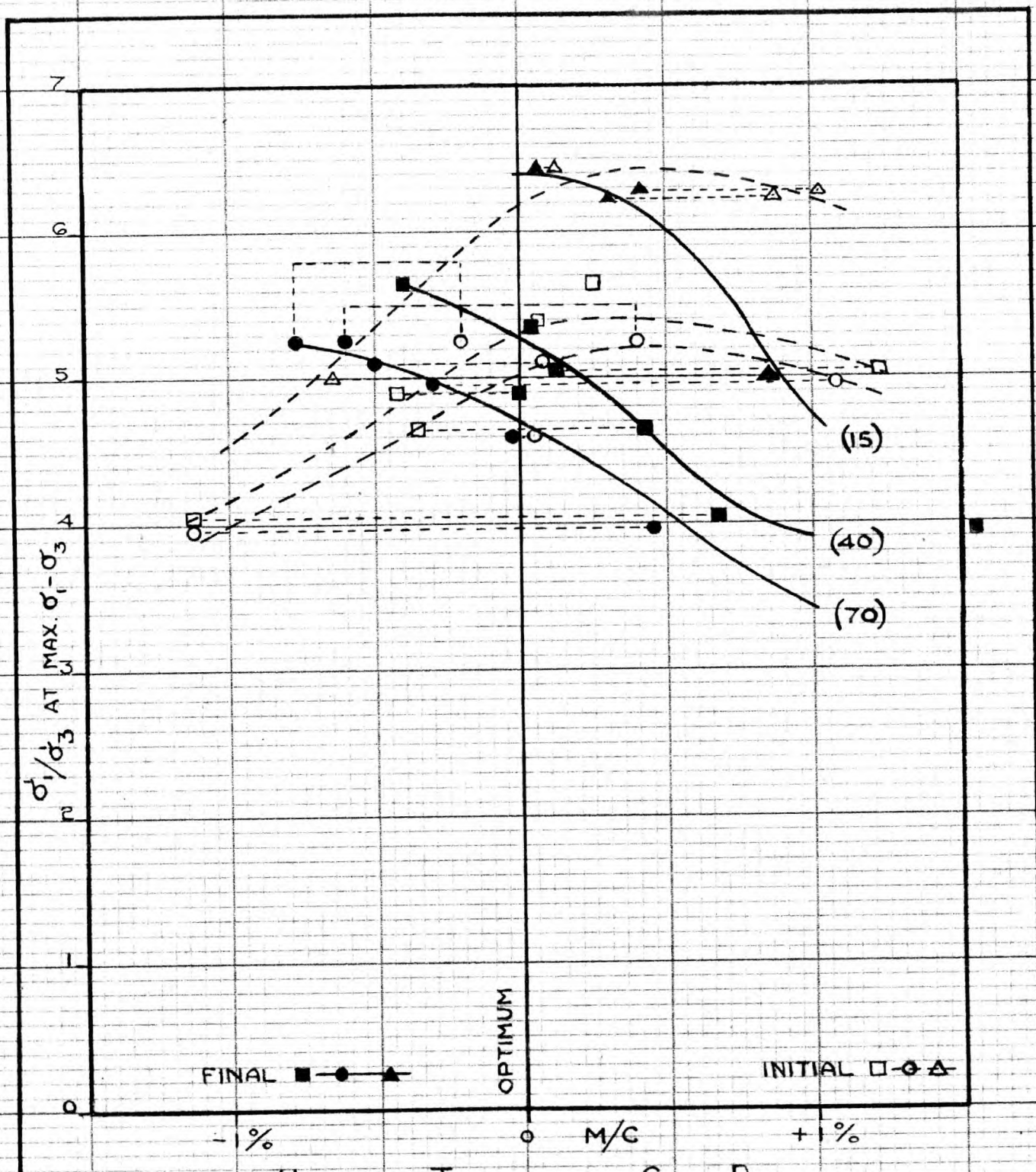
CELL PRESSURES

○ = 70 P.S.I.

△ = 40 "

□ = 15 "

FIG. 5:4



CONSOLIDATED UNDRAINED TESTS

VALUES OF σ'_1/σ'_3 AT FAILURE

WITHOUT ENERGY CORRECTION

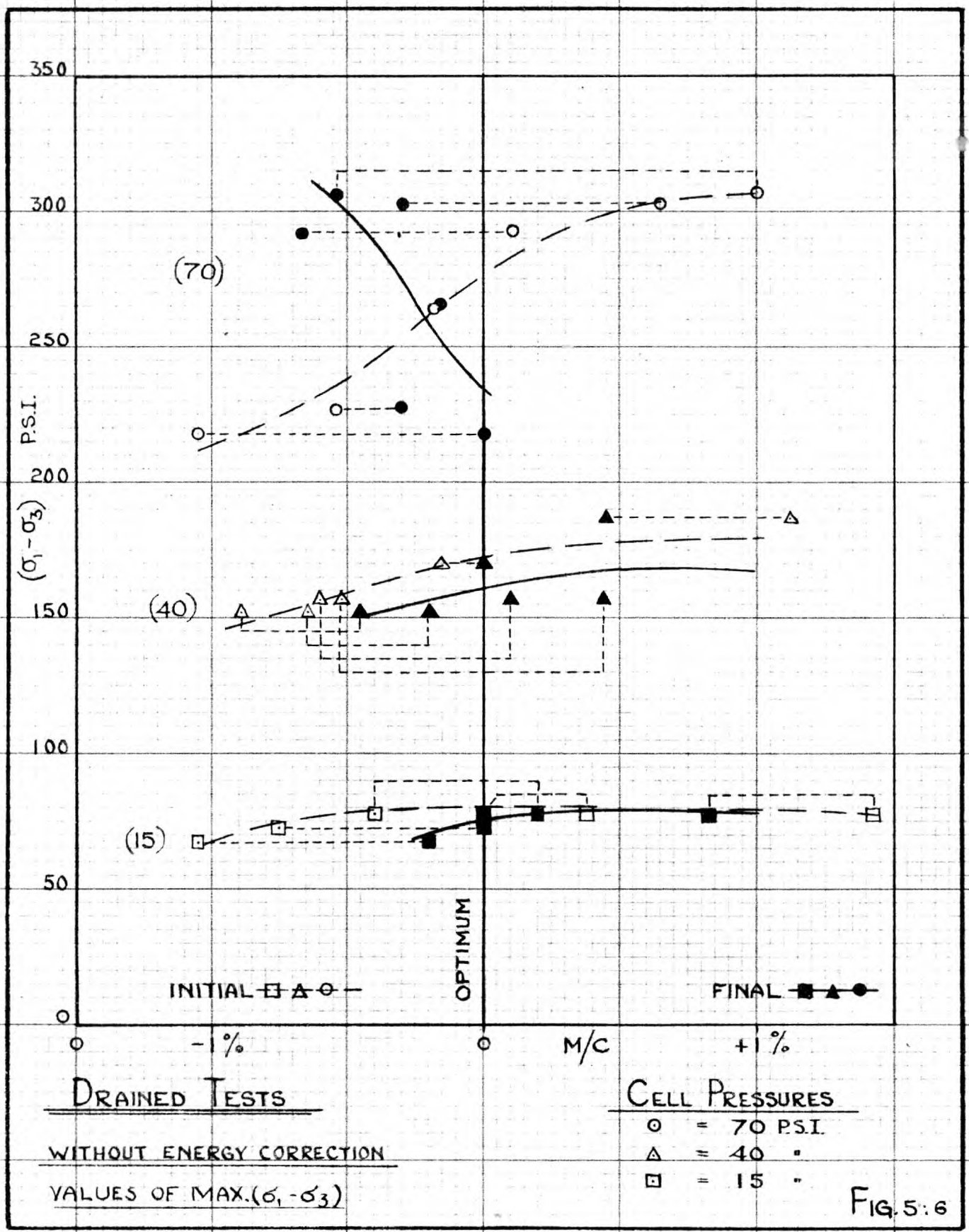
CELL PRESSURES

Δ = 15 P.S.I

□ = 40 "

O = 70 "

FIG. 5:5



DRAINED TESTS

WITHOUT ENERGY CORRECTION

VALUES OF MAX. $(\sigma_1 - \sigma_3)$

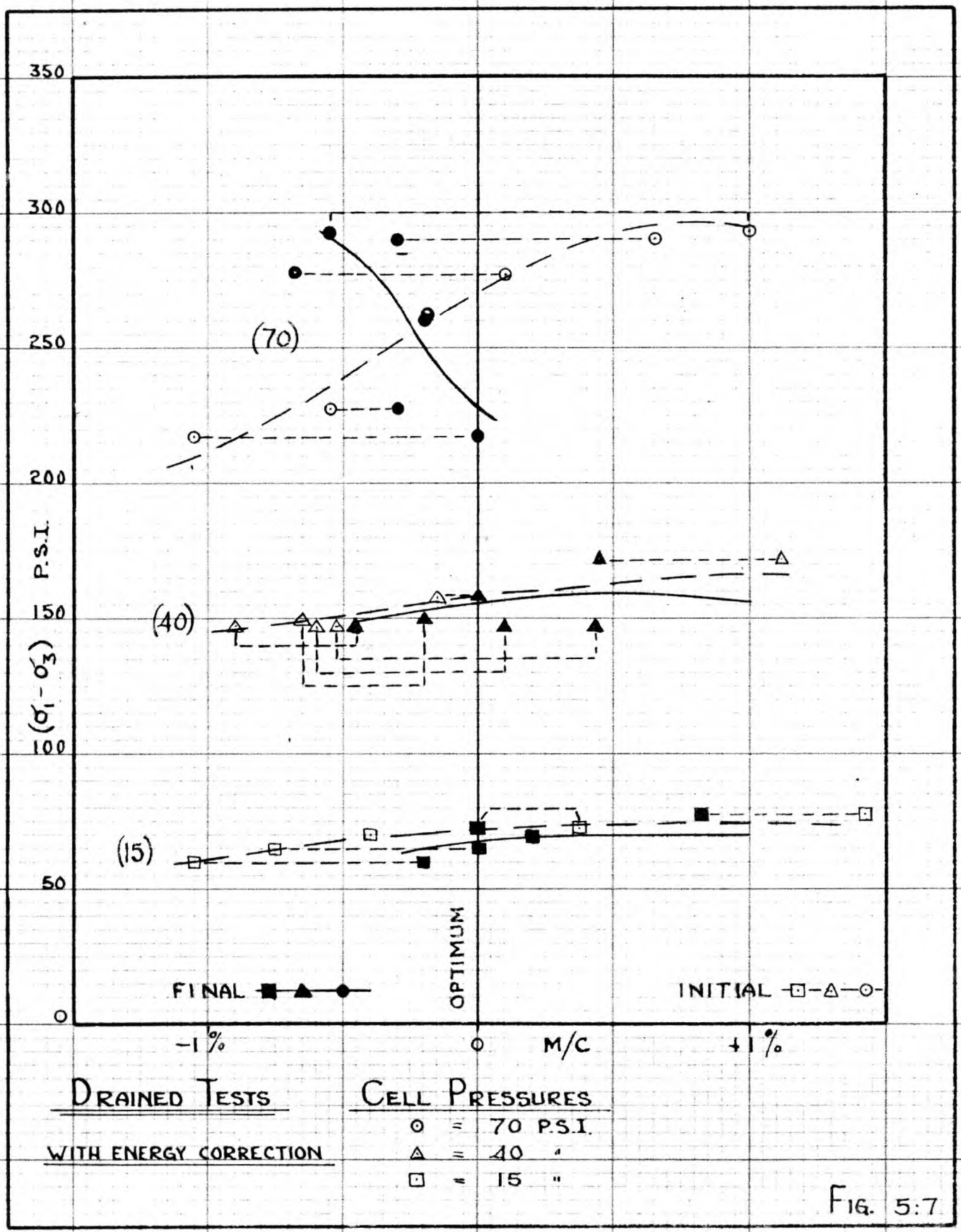
CELL PRESSURES

⊙ = 70 P.S.I.

△ = 40 "

⊡ = 15 "

FIG. 5:6



DRAINED TESTS

WITH ENERGY CORRECTION

CELL PRESSURES

⊙ = 70 P.S.I.

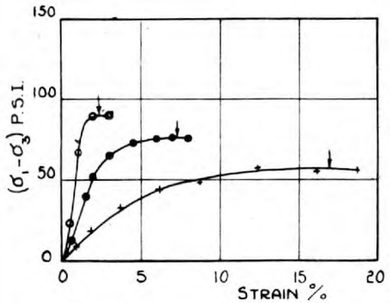
△ = 40 "

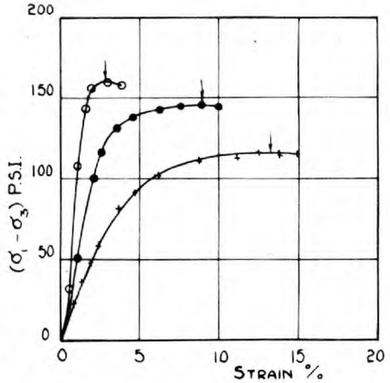
⊡ = 15 "

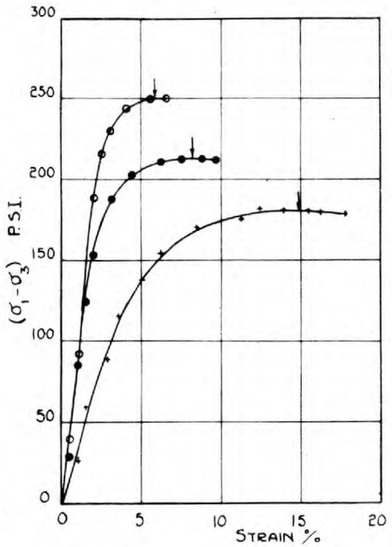
FIG. 5:7

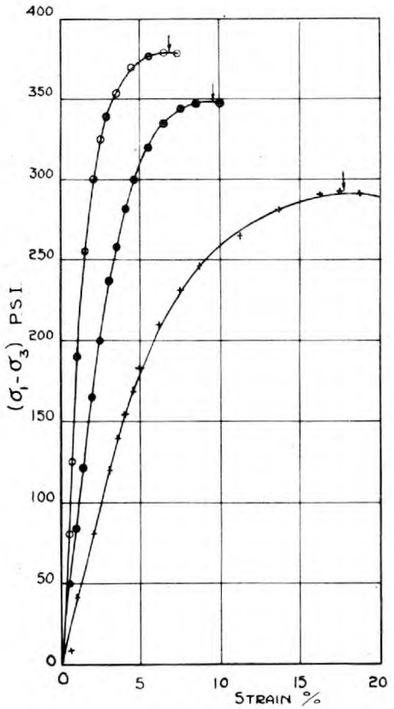
UNDRAINED TRIAXIAL COMPRESSION TESTS.

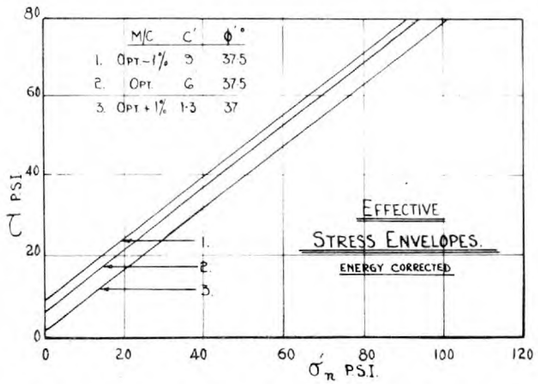
- ○ 1% DRY APPROX.
- ● OPTIMUM M/C
- \+ 1% WET APPROX.

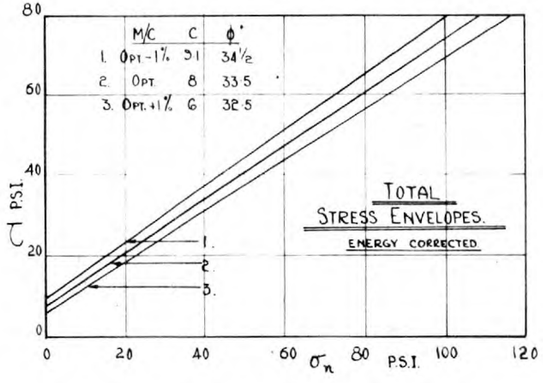


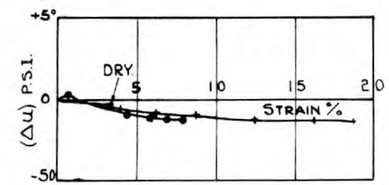


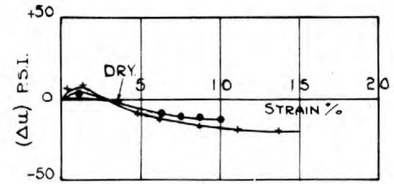


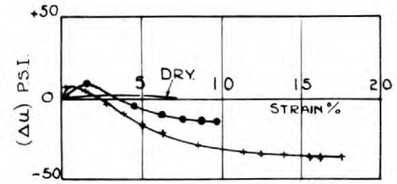


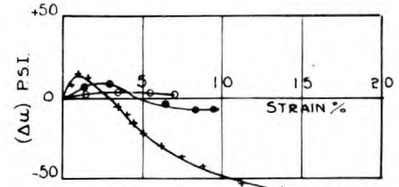


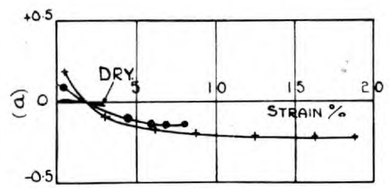


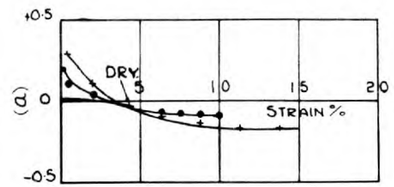


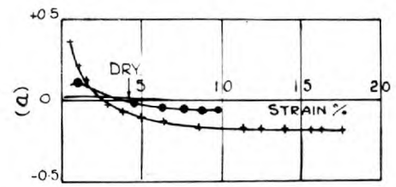


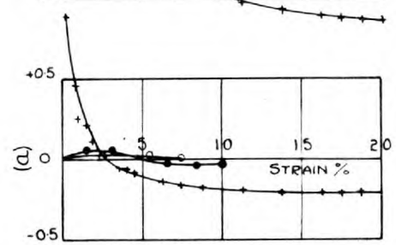












CELL PRESSURE = 15 P.S.I.

CELL PRESSURE = 40 P.S.I.

CELL PRESSURE = 70 P.S.I.

CELL PRESSURE = 120 P.S.I.

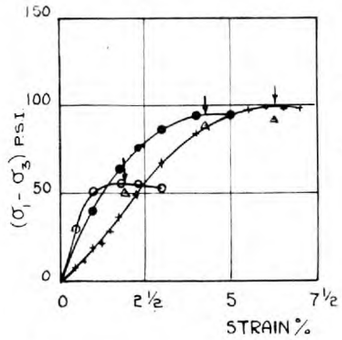
CELL PRESS. σ_3	M/C.	DRY DENSITY	S %	$B=\frac{\Delta u_0}{\Delta\sigma_3}$	
15	OPT.-1·0%	133·6	70	·05	DRY.
40	OPT.-1·1%	133	70	·078	
70	OPT.-1·1%	133·5	69	·047	
120	OPT.-1·15%	133	68	·088	
15	OPT.+0·0	136	88	·512	OPT.
40	OPT.+0·0	135·5	87	·355	
70	OPT.+0·1%	135·5	88	·337	
120	OPT.+0·0	136·2	89·2	22	
15	OPT.+1·15%	133·6	93	·77	WET.
40	OPT.+0·85%	134·4	92	·61	
70	OPT.+1·0%	134·6	94	·71	
120	OPT.+0·9%	134·7	95·4	·79	

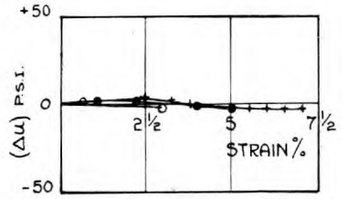
FIG. 5:43

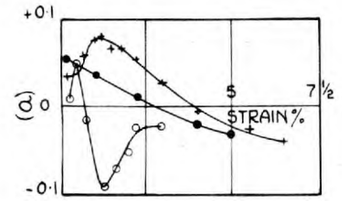
Consolidated Undrained Triaxial Tests

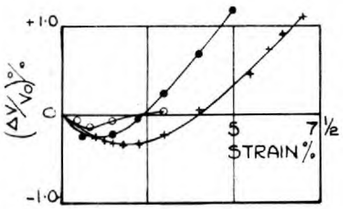
- ○ 1% Dry Approx
- ● Optimum "
- \+ 1% Wet "

Cell Pressure = 15 p.s.i.

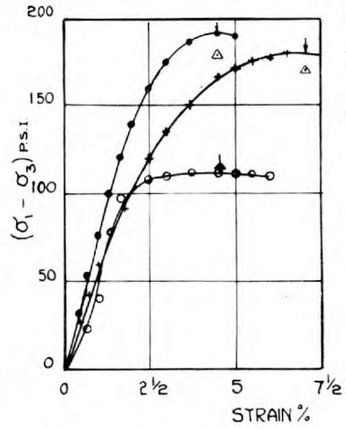


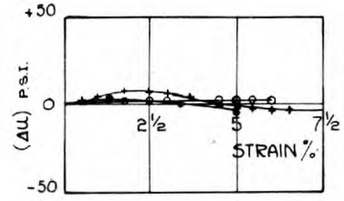


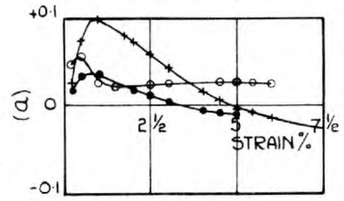


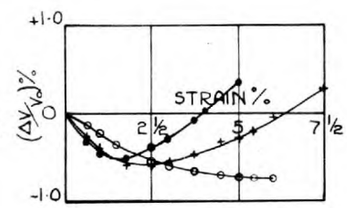


Cell Pressure = 40 p.s.i.

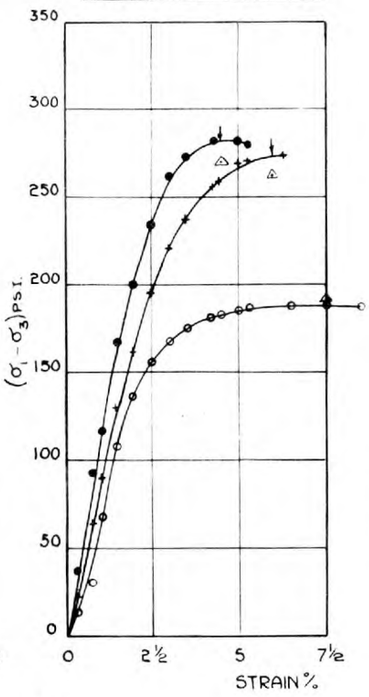


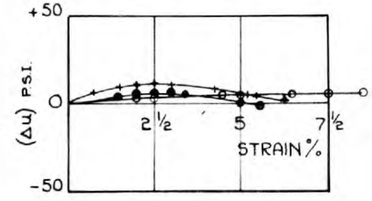


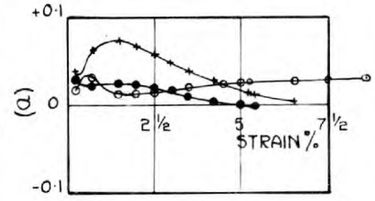


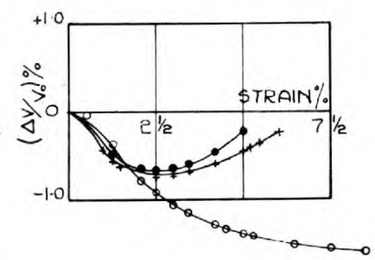


Cell Pressure = 70 p.s.i.

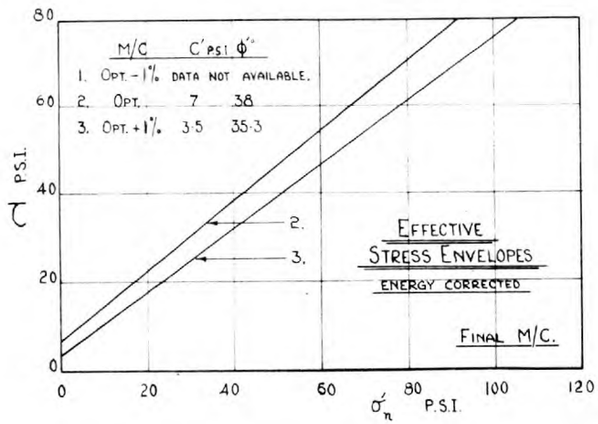


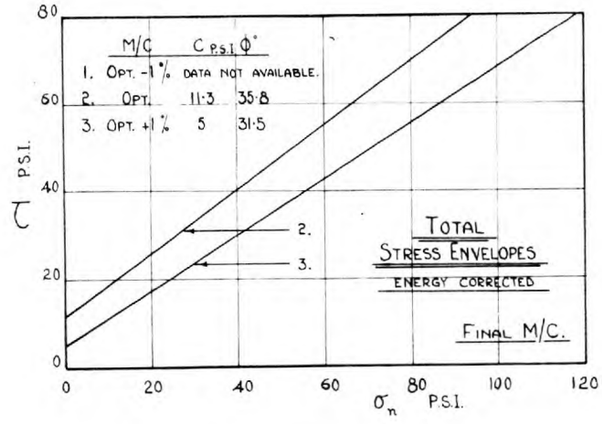






$\frac{\Delta V}{V_0}$ % ≡ Percentage Volume Change During Shear





Cell Press σ_3	M/C % Initial	M/C % Final	γ_d lbs/cu.ft. Initial	γ_d lbs/cu.ft. Final	S % Initial	S % Final	Consolidation %	
15	-0·65	+0·85	132·0	133·6	69·0	90·5	1·2	Dry
40	-1·1	+0·67	132·0	133·8	67·0	89·0	1·9	
70	-1·1	+0·45	131·6	135·3	66·5	91·5	2·6	
15	+0·1	+0·06	134·6	136·0	85·7	90·0	0·9	Opt.
40	+0·25	-0·4	135·0	138·0	86·0	91·8	1·6	
70	+0·09	-0·5	133·9	136·3	83	84·7	1·9	
15	+1·0	+0·4	134·3	136·0	94·5	94·2	1·3	Wet
40	+1·2	+0·12	133·4	136·3	94	91·8	2·1	
70	+1·07	-0·2	133·5	136·9	92·6	90·3	2·65	

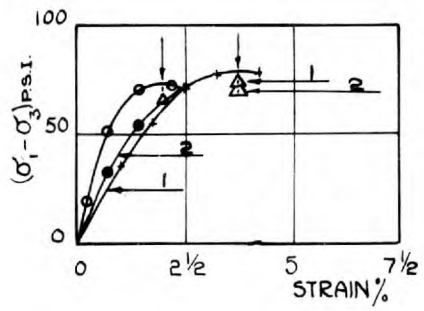
N.B. Initial & Final M/C., are expressed as a difference in percentage from Proctor Optimum M/C.

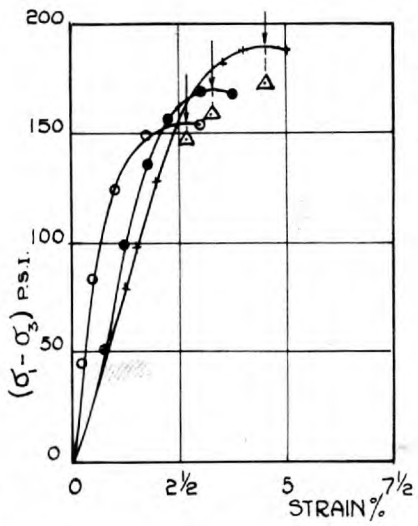
△ Peak values of $(\sigma_1 - \sigma_3)$ energy corrected.

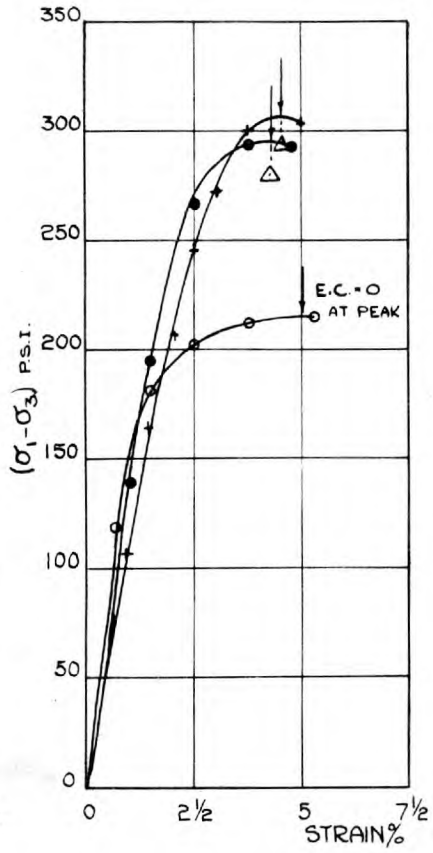
Fig. 5:44

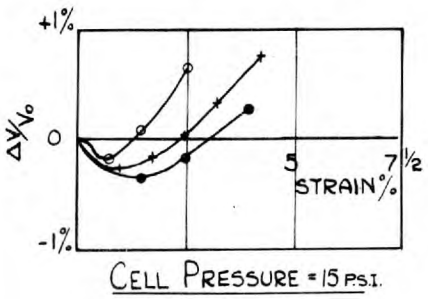
DRAINED TRIAXIAL SHEAR TESTS.

- ○ = 1% DRY APPROX.
- ● = OPT.
- \+ = 1% WET "
- △ = PEAK VALUES OF $(\sigma_1-\sigma_3)$ WITH ENERGY CORRECTIONS

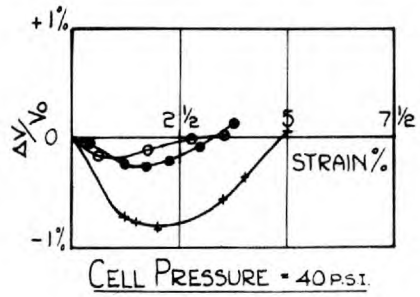




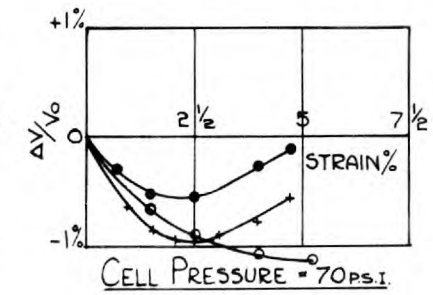




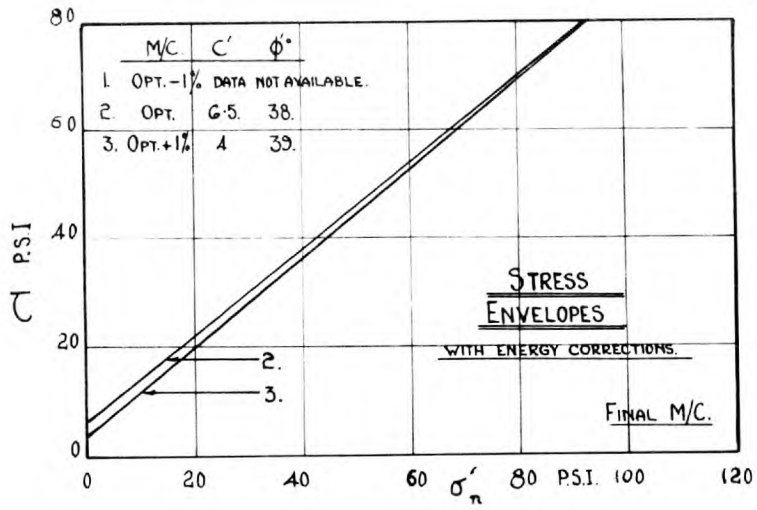
CELL PRESSURE = 15 P.S.I.

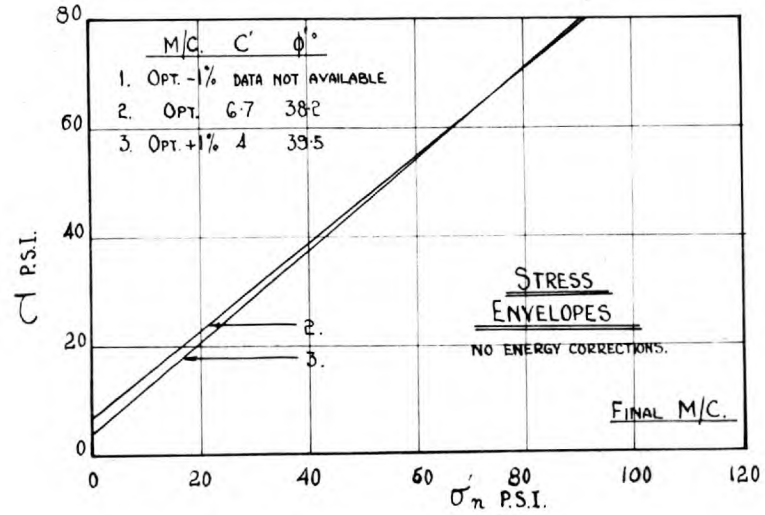


CELL PRESSURE = 40 P.S.I.



CELL PRESSURE = 70 P.S.I.





CELL PRESS	M/C % INITIAL	M/C % FINAL	γ_d INITIAL	γ_d FINAL	S % INITIAL	S % FINAL	INITIAL CONSOLID^N. %	
15	-0·8	0·00	133·6	134·8	74·0	85·0	0·18	DRY.
40	-0·9	-0·45	134	135·1	73·5	81·5	0·32	
70	-1·1	0·00	132	134·5	68·0	84·1	0·6	
15	+0·3	0·00	134·0	134·5	86·2	84·1	0·6	OPT.
40	-0·15	0·00	135·3	136·2	85·0	90·0	0·7	
70	+0·1	-0·68	134·7	136·2	86·0	82·5	1·17	
15	+1·4	+0·82	133·5	134·1	95·6	91·5	1·2	WET.
40	+1·1	+0·45	133·5	135·9	92·7	94·0	1·7	
70	+1·0	-0·55	133·9	136·8	92·5	89·3	2·1	

N.B. INITIAL & FINAL M/C. ARE EXPRESSED AS A DIFFERENCE IN PERCENTAGE FROM PROCTOR OPTIMUM M/C.

FIG. 5:45

The Principle of Energy Correction

In triaxial tests in which the volume of the sample increases during shear a part of the measured deviator stress will be required to provide the energy required to cause the sample to expand against the cell pressure. This was demonstrated by Taylor (1948) and A. W. Bishop (1950), who have shown in relation to shear box tests on sands that the measured shear strength is composed of two parts; the first part is that necessary to overcome the frictional resistance and the second part is that required to cause the sample to change its volume. In triaxial tests, this second part termed herein as $(\sigma_1 - \sigma_3)_1$ will be given at any stage of the test by the following equation:

$$(\sigma_1 - \sigma_3)_1 \, \delta e = \delta\left(\frac{\Delta V}{V_o}\right) \sigma_3$$

$$(\sigma_1 - \sigma_3)_1 = \frac{\delta\left(\frac{\Delta V}{V_o}\right)}{\delta e} \sigma_3$$

where δe is the corresponding incremental strain and $\delta\left(\frac{\Delta V}{V_o}\right)$ is the corresponding incremental volume change.

$\frac{\delta\left(\frac{\Delta V}{V_o}\right)}{\delta e}$ is the energy correction factor

$(\sigma_1 - \sigma_3)_1$ will be subtracted from the measured $(\sigma_1 - \sigma_3)$ if the sample is increasing in volume and vice versa.

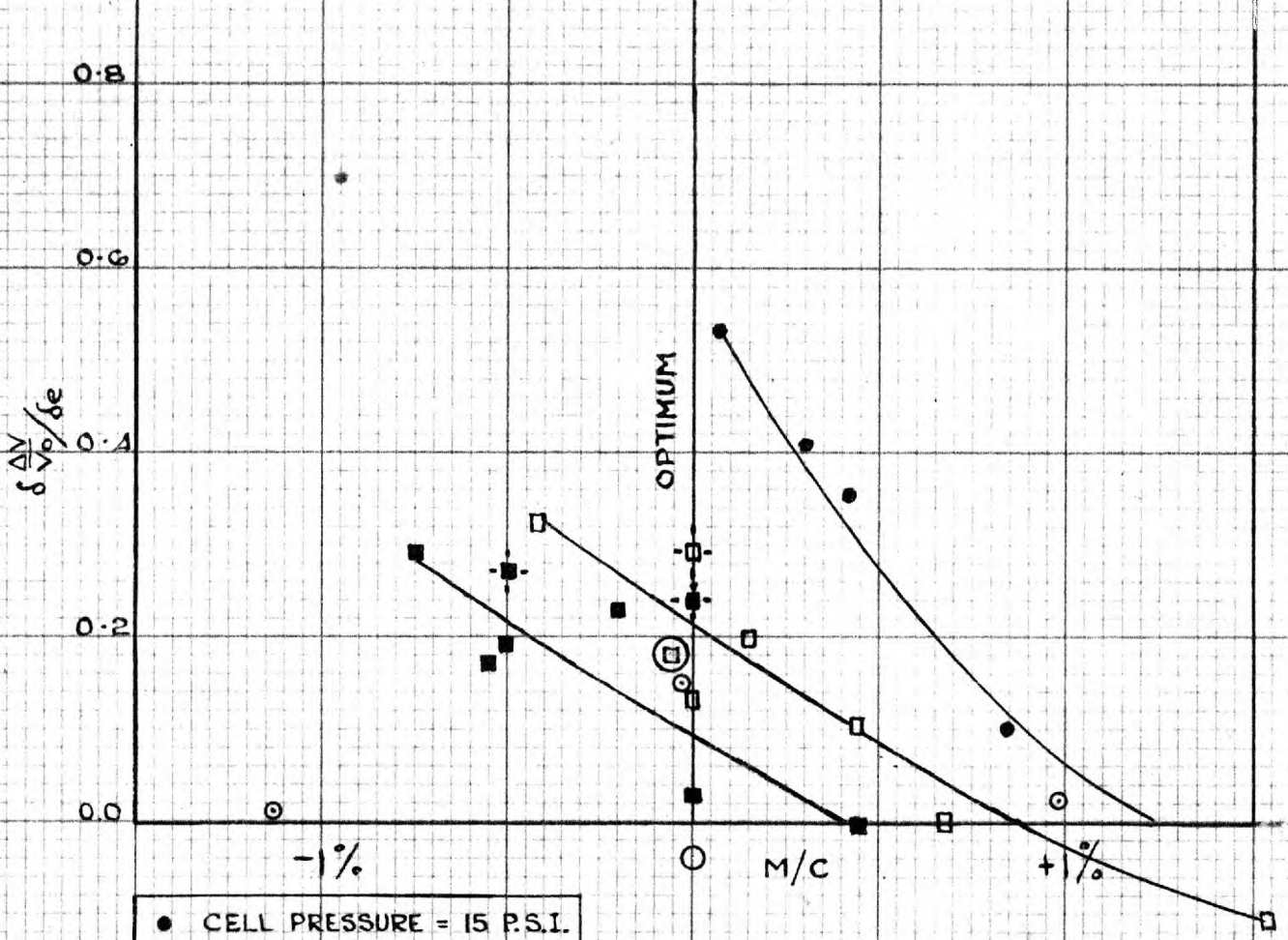
For saturated soils volume changes take place during drained shear tests only. In the case of partially saturated soils, however, volume changes during shear take place under undrained as well as under drained conditions. Unlike saturated soils, the triaxial test results under all conditions of drainage are to be corrected in order to obtain the best correlation between the frictional properties under different test conditions.

Volume changes during undrained shear were recorded only in the case of consolidated undrained tests and in the series of undrained tests under a cell pressure of 120 p.s.i.

In order to correct the results of the earlier series of undrained tests which were carried out before the volume change measuring unit was developed, the same energy correction factors were used as for the consolidated undrained tests at any particular final moisture content* and cell pressure. Such factors are obtained by plotting from the consolidated undrained test results the relationship between final moisture content and the corresponding energy correction factor at failure for the cell pressures 15, 40 and 70 p.s.i. Fig. 5:46. The lowest moisture content on this plot is approximately 0.5% less than the optimum. However, for undrained tests on

---

* This is the same as the initial moisture content for the undrained test.



Energy Correction Factor $\frac{\delta \frac{\Delta V}{V_0}}{\delta e}$ for Consolidated Undrained Tests

Fig. 5:46

samples at 1% lower of optimum, it is believed that the energy correction factor is negligible, and this is assumed in presenting the results. This seems justifiable when the corresponding C' and ϕ' are compared with those for the other moisture contents, Fig. 5:67. It must be mentioned here that the energy correction affects only the magnitude of the deviator stress, while the effective minor principal stress at failure $(\sigma_3')_f$ is the same whether or not the energy correction is applied.

Effect of the Rubber Membrane on the Measured Shear Strength

As shown in the Appendix, the effect of the rubber membrane was found to be small and is therefore omitted in computing the strength of the soil in this thesis. This is due to the large size of the samples tested. Tests on the small conventional triaxial samples ($1\frac{1}{2}$" d. x 3") should be corrected for this effect, especially if the strength is small, (Henkel and Gilbert 1952).

Determination of the Shear Parameters C' and ϕ' for the Various Types of Tests

C' and ϕ' for any type of shear test are determined from a Mohr's envelope touching the corresponding effective stress circles representing the maximum deviator stress. Typical results are given in Figs. 5:47 to 5:66 (given at the end of this volume). For a partially saturated soil, C' and ϕ' are very close to the true shear parameters C_e and ϕ_e as defined by Hvorslev (see Chapter 3 Page 9). An attempt to determine C_e and ϕ_e was made * However, the experimental results did not permit a proper evaluation of C_e and ϕ_e.

Due to the large percentage of air in the voids of such soils, they are nearly as compressible when sheared under undrained conditions as they are under drained conditions (see also Taylor, 1948). It would be expected that the shear parameters C' and ϕ' will not vary considerably under these two conditions.

---

* This is by plotting a relation between moisture content and dry density from consolidated undrained tests at two different cell pressures. If such curves intersect, the intersection will represent two samples at the same moisture content, the same dry density and, of course, the same porosity. The corresponding Mohr's circles will give C_e and ϕ_e. However, the relationship when plotted did not lead to any definite conclusion as the variation in the moisture content and the dry density were not large enough in comparison with the scatter of the results.

To study the strength of such soils in the absence of air in the voids, attempts were made to saturate the samples by allowing a steady flow of water to run through them. but were not successful in producing full saturation as shown by the table in Fig. 5:44, which gives typical results of consolidated undrained tests.

A Study of the tables in Figs. 5:43, 5:44, and 5:45, shows that the dry density does not vary very much for any particular moisture content (for consolidated undrained as well as drained tests the relevant moisture content is that at failure). Therefore the study of the shear parameters will be carried out in terms of the moisture content with which the cohesion can be closely correlated.

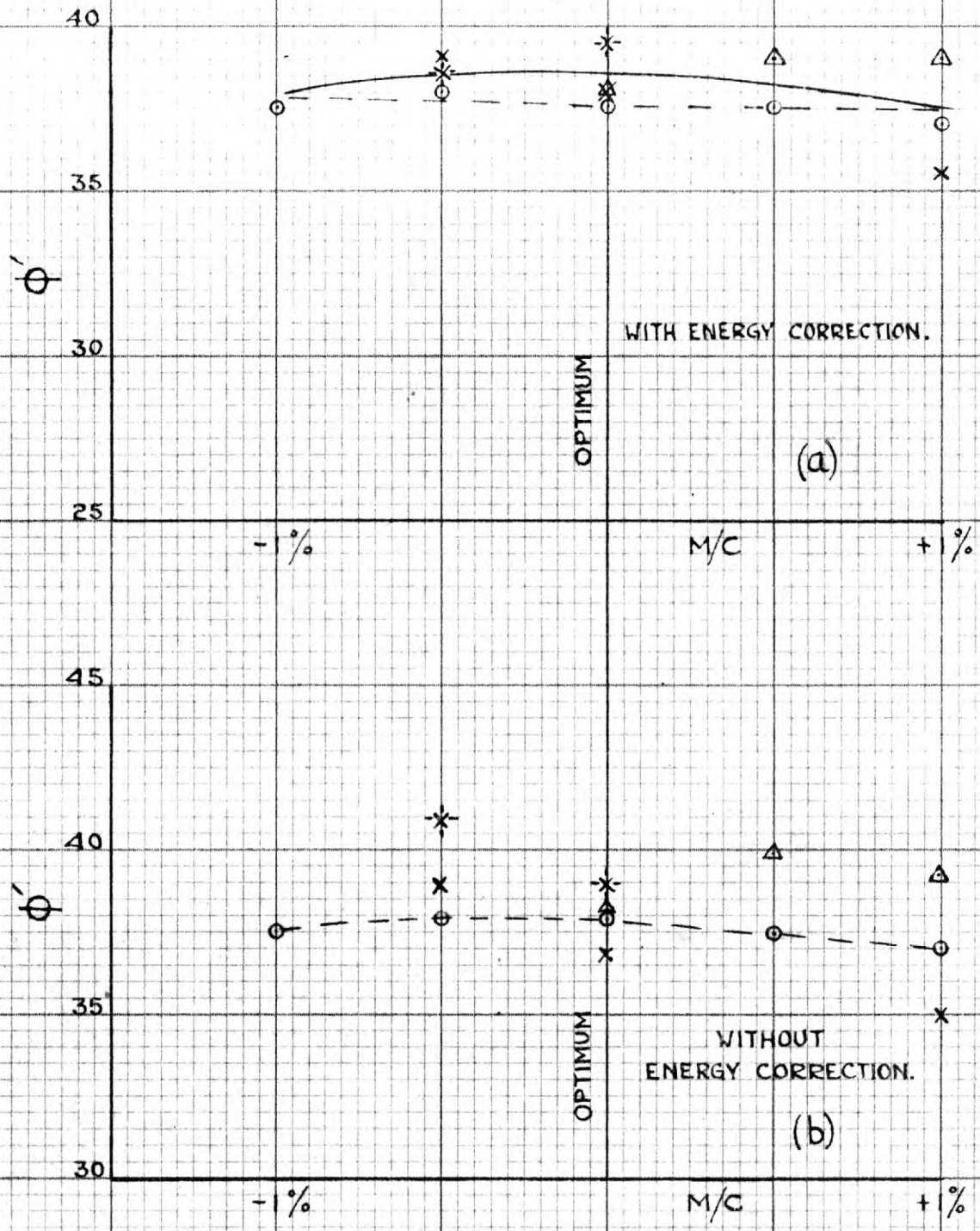
Figs. 5:67 and 5:68 show the values of ϕ' and C' respectively in relation to the moisture content at failure with and without the energy correction. Fig 5:69 . . . . contains the results obtained by plotting the Mohr's circles at failure in terms of initial moisture content with energy correction.

Fig. 5:67 (a) shows that the values of ϕ' with energy correction for any particular moisture content at failure does not vary much with the type of test except for a moisture content of optimum $\pm 1\%$. Here the most reliable value is that obtained from undrained tests, as it is a result of an envelope to four Mohr's circles while the consolidated undrained and the drained values are obtained from only two

circles since at higher cell pressures such a high moisture content at failure was not achieved. An average curve for all types of tests can be plotted (shown in solid lines). Such a curve, however, is also very close to the curve representing the results of the undrained tests alone (shown dashed). Fig. 5:67 (b) shows the results without energy correction. The scatter is large and shows that no average relationship can be established, which in fact is a justification for applying the energy correction. The curve representing the results of the undrained tests alone (shown dashed) differs only slightly from its counterpart in Fig. 5:67 (a).

Fig. 5:68 shows the values of the cohesion C' plotted in terms of the moisture contents after applying the energy correction. It is also evident that an average curve can be plotted which will show that the cohesion is a function of the moisture content at failure, irrespective of the type of shear. Fig. 5:68[b] shows the results without energy correction. Here also the scatter permits no average relationship to be established.

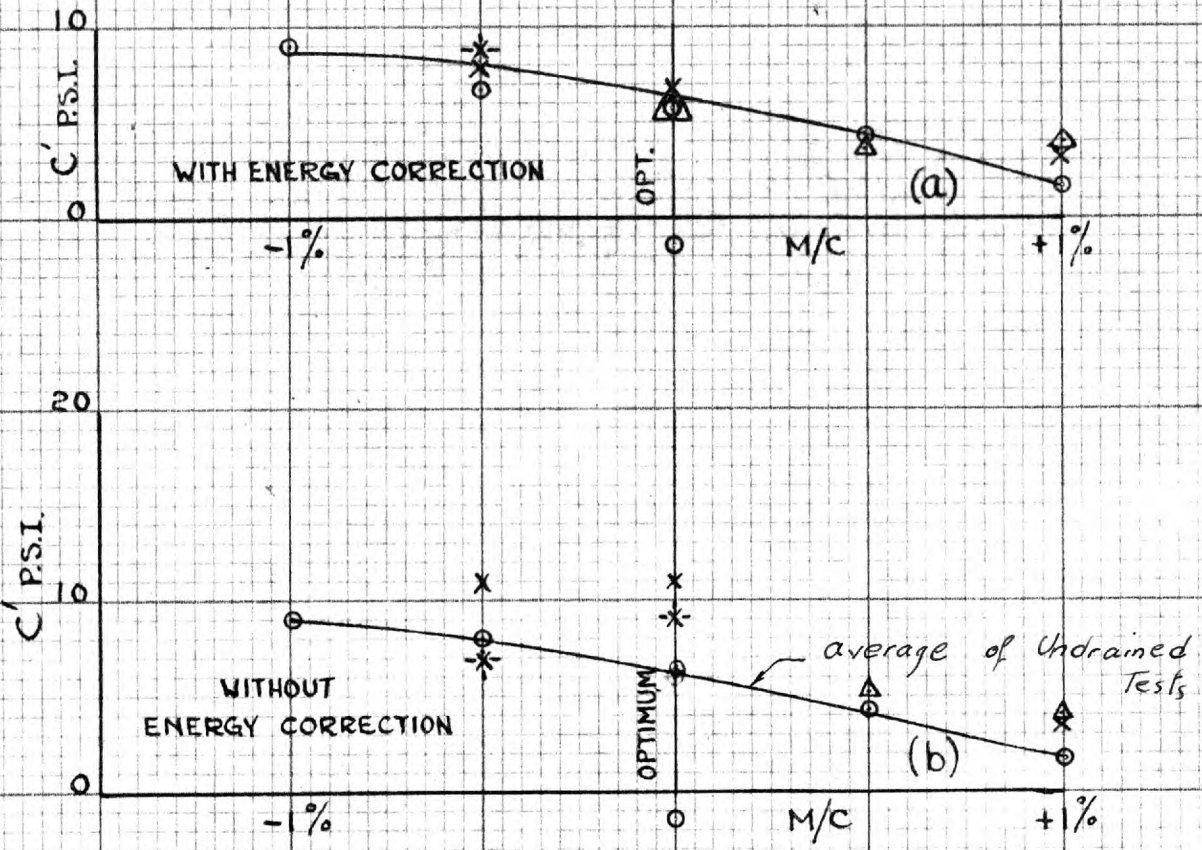
The shear strength envelopes plotted in terms of the initial moisture contents in the drained and consolidated undrained tests (in terms of effective stresses) are given in Fig. 5:69, together with the corresponding envelopes obtained from undrained tests. It will be seen that in terms of initial moisture content, samples compacted at optimum have



⊙ - UNDRAINED TESTS.
× - CONSOLIDATED UNDRAINED SERIES (a).
✳ - " " " (b).
△ - DRAINED TESTS.

ANGLE OF SHEARING RESISTANCE, ϕ'
for VARIOUS MOISTURE CONTENTS.

FIG. 5: 67



⊙ – Undrained Tests.

x – Consolidated Undrained Series (a).

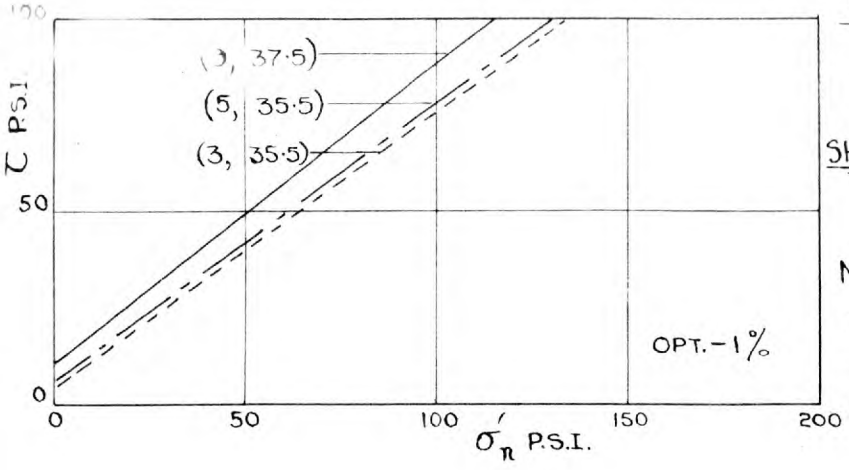
✳ – " " " (b).

△ – Drained Tests.

Apparent Cohesion C'

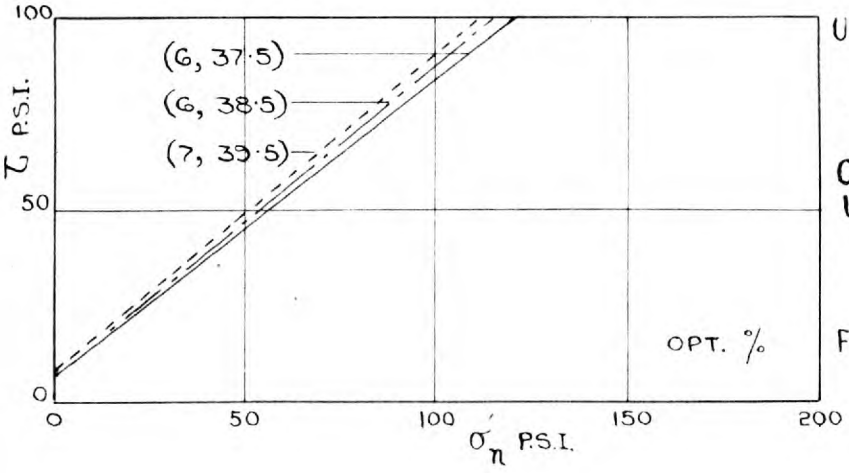
for Various Moisture Contents.

Fig. 5:68



EFFECT OF SATURATION ON SHEARING STRENGTH.

MOHR'S ENVELOPES FOR EFFECTIVE STRESSES IN TERMS OF THE INITIAL MOISTURE CONTENT.



UNDRAINED. ———

DRAINED. — · — · —

CONSOLIDATED UNDRAINED. - - - - -

FIGURES IN BRACKETS ARE c' & ϕ' RESPECTIVELY.

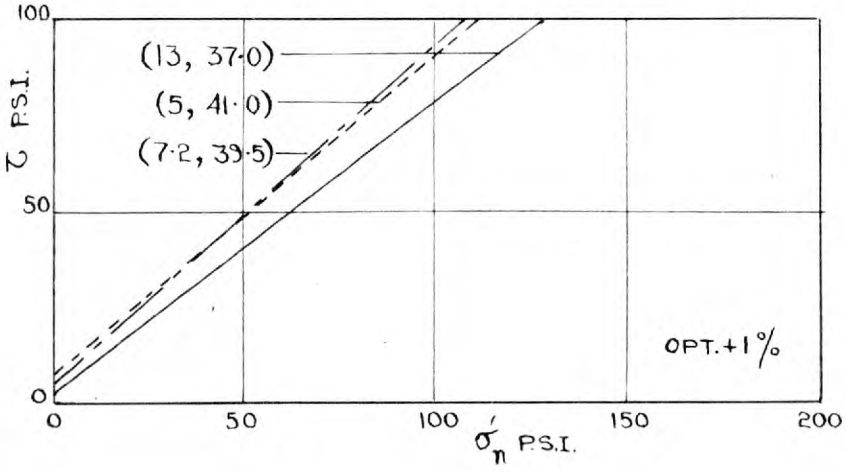


FIG. 5:69.

values of apparent cohesion and angle of shearing resistance very close to C' and ϕ' obtained from undrained tests (these are also close to C' and ϕ' obtained from other types of tests in terms of final moisture content). This shows that with respect to the shear strength, a soil compacted at optimum placement conditions is more stable and largely unaffedted by saturation. Samples compacted at 1% dryer of optimum show a considerable drop in both cohesion and angle of shearing resistance upon softening, while those compacted at 1% higher show a gain in strength above the undrained conditions. This, however, does not recommend the use of a wet fill material in a dam unless adequate provisions are made to allow for the dissipation of the comparatively high excess pore pressures normally associated with such wet soils.

From the foregoing analysis of the test results, we find that the type of shear test has only a slight effect on the angle of shearing resistance ϕ'. The results of the undrained tests can be used with a good deal of accuracy and thus avoid the elaborate procedures and time spent in other types of tests.

The change in ϕ' with moisture content is small. The range of moisture contents investigated corresponds to a range of the degree of saturation from 65% to 93% approximately. It will, therefore, be expected that at full saturation the value of ϕ' will not be far off from those determined experi-

mentally.

The cohesion varies with moisture content, but is also largely unaffected by the type of test and the values obtained from undrained tests, in fact, represent the average values obtained from all types of tests.

It is also concluded from the test results that if a fill is placed dry in a dam, the changes in its strength upon saturation are mainly changes in the cohesion which drops as the moisture content increases. The angle of shearing resistance in terms of its final moisture content remains practically unchanged.

B. Pore Water Pressure and Compressibility

The excess pore pressure set up in a soil element due to a system of applied stresses is essentially a function of the compressibility, the degree of saturation and the porosity. For a given compaction, these properties are entirely a function of the moisture content. Thus the study of the excess pore pressure due to any stress system will be carried out in terms of the placement moisture content. The stress systems are expressed in terms of their respective principal stress ratio $\bar{\sigma}_1'/\bar{\sigma}_3'$.

1. The All round Pressure System - (The "B" Tests); $\bar{\sigma}_1'/\bar{\sigma}_3' = 1$

The excess pore pressure Δu caused by an increment $\Delta\bar{\sigma}_3$ of the all round pressure is given by:

$$\Delta u = B \times \Delta\bar{\sigma}_3$$

where B is essentially less than unity due to partial saturation. For a given compaction it is a function of the moisture content for any particular load.

The relationship between Δu and $\Delta\bar{\sigma}_3$ as given by equation 3:6 is non-linear. It could, however, be approximately considered as linear over a certain range of loads beyond which the soil element approaches saturation whereby

a linear relationship is established again and is represented by a straight line at 45° i.e. at saturation each increment of load will be reflected fully on the pore pressure. The excess pore pressure ΔP_s at which a soil element becomes fully saturated under external loads is given by the equation:

$$\Delta P_s = P_o \frac{1 - S}{S \cdot H} \qquad 3:9$$

where P_o is the initial pore pressure and is normally equal to atmospheric.

H is Henry's coefficient of solubility of air in water and S is the degree of saturation.

Knowing the compressibility of the soil, the external load that will bring about saturation can be determined from equation 3:6. In the present series of tests, only samples about 1% wetter than optimum are possible to saturate. Samples at lower moisture contents need higher loads beyond the capacity of the equipment used. Fig. 5:70 shows the results of several B tests carried out at different placement conditions.

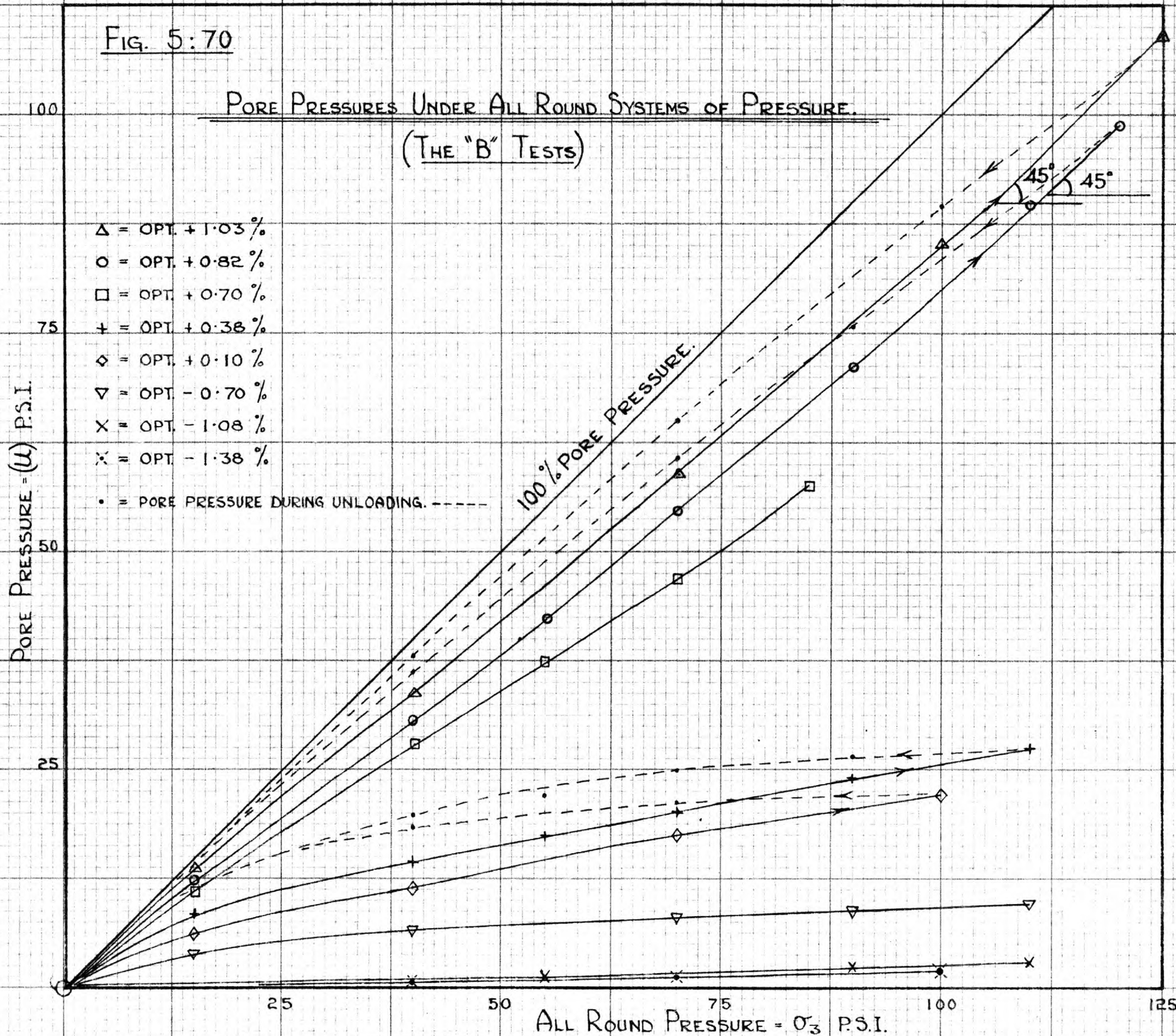
The Variation of B with Moisture Content

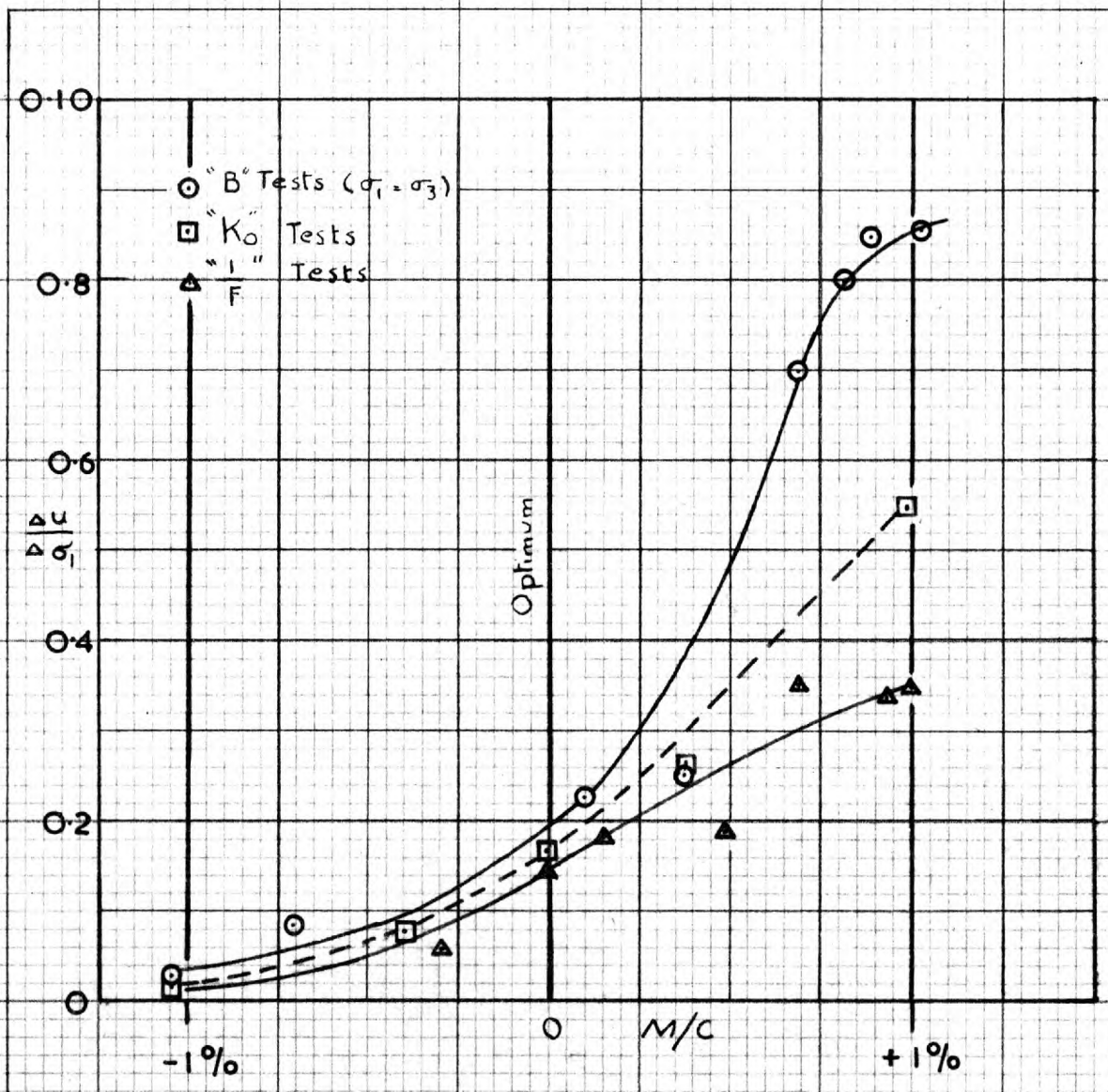
Fig. 5:71 shows the values of B plotted against moisture content for an increment of load $\Delta\bar{O}$ = 100 p.s.i. together with corresponding values from other types of tests. It shows that higher values of pore pressures are to be

FIG. 5:70

PORE PRESSURES UNDER ALL ROUND SYSTEMS OF PRESSURE.

(THE "B" TESTS)





Variation of Pore Pressure Ratio $\frac{\Delta u}{\Delta \sigma_1}$ with Moisture Content for Different Loading Conditions.

(at $\sigma_1 = 100$ p.s.i.)

FIG. 5: 71

expected if the moisture content is 1% or more higher than optimum, while at the dry side of the optimum very low values of pore pressure will be set up. But the most important fact is that the transition from these low values of pore pressures to the higher values occurs steeply around the optimum. This shows that with inadequate moisture content control of rolled fills placed at optimum, excess pore pressures may be set up due to increasing overburden pressure that may be detrimental if not allowed for in design.

Pore Pressure; Volume Change Relationship

The change in volume of a partially saturated soil element is equal to the change in the volume of the free air it contains provided no drainage is permitted. It follows that the maximum volume change a sealed soil element can undergo is equal to the volume of free air where it becomes fully saturated. The excess pore pressure ($\triangle P$) corresponding to a change in volume ($\triangle V$) is given by the following equation 3:8.

$$\triangle P = \frac{Po \ \triangle V}{V_V (1 - S + SH) - \triangle V}$$

where P_O = the initial pore pressure (normally atmospheric)

V_V = volume of voids

S = degree of saturation

H = Henry's coefficient

V_V (1 - S + SH) = the total volume of air = V_A

V_V (1 - S) = volume of free air.

When applying the volume changes recorded experimentally into the above equation, very high values of pore pressures were obtained. This large variation is clearly not the result of the simplifying assumptions involved in deriving equation 3:8 (Page 14).

A careful study of the test results showed that an extra volume of free air has been added through incomplete adhesion of the membrane especially around the side filter paper drains or by incomplete contact of the porous plates and also due to the existence of crevices on the surface of the sample. Let the volume of this extra air equal to "v". The value of "v" is determined by calculation as will be seen later. It can, however, be obtained directly from the tests only for wet samples which become fully saturated within the range of external loads available. In such cases "v" is equal to observed volume change less the free air content of the sample $\{V_V (1 - S)\}$.

It was found necessary to repeat the tests with a view to eliminating this source of experimental error. The results were successful only in reducing the value of "v" to an average of 0.9 cubic inches (about 0.9% of the volume of the sample). Therefore the results of the "B" tests,

together with other pore pressure tests were corrected in the following way:-

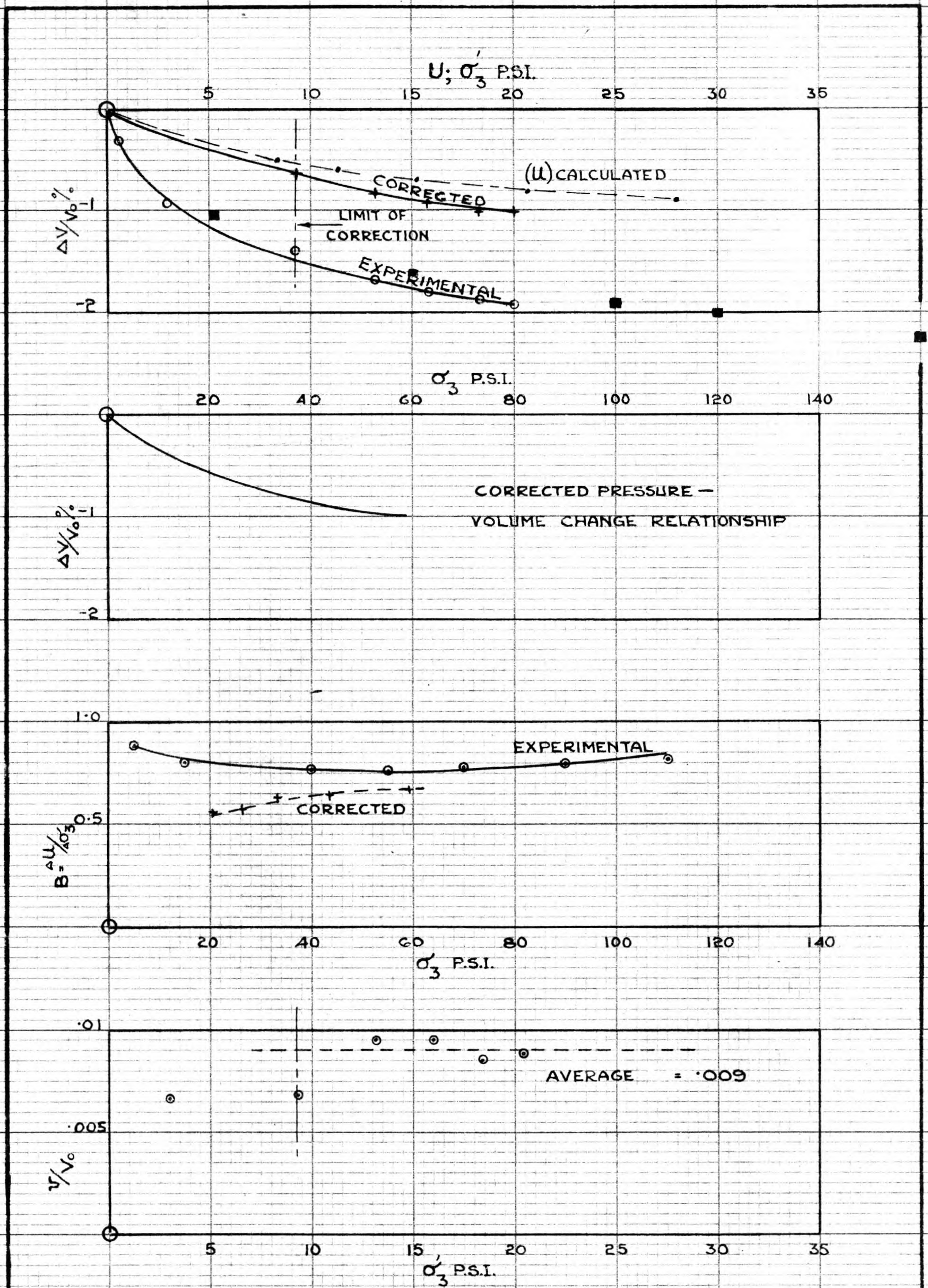
For each pressure increment insert in equation 3:8 the corresponding observed values of ΔV and ΔP to obtain a value (V_{A1}) for the total volume of air. This value is always higher than V_A the actual volume of air in the sample

$$v = V_{A1} - V_A$$

The value of "v" was not a constant at the earlier increements of pressure, but became almost so at higher pressures, thus permitting an average value to be considered over a certain range (not starting at zero). It is thought that at a certain intensity of pressure this volumetric error is eliminated through complete adhesion of membrane and plates to the sample. This means that the actual volume changes after this stage are those observed less the average value of "v", as shown in Fig. 5:72, 5:73 and 5:74 for three samples compacted at optimum + 0.82%, optimum + 0.38% and optimum - 1.1%. It is noticed that the first sample became fully saturated at an all round pressure of 112 p.s.i. thus offering an alternative means to estimate "v". Sheet I and II show typical calculations for two moisture contents.

Now we proceed to investigate the effect of this volumetric error on the value of B. Following the procedure suggested by Hilf (1948) we compute from the physical prop-

erties of the sample (S, n and M/C) a relationship between the pore pressure (u) and the compression ΔV. If we combine such relationship with the corrected effective stress volume change relationship we can ultimately obtain a relation between the total stress and the corresponding pore pressure Figs. 5:72, 5:73, and 5:74. This showed that the value of B with no trapped air is less than the corresponding experimental one which is influenced by an apparent increase in the compressibility of the soil due to the extra air trapped inside the membrane especially under small loads. The difference, however, is on the safe side. The comparison of the results of the pore pressure tests carried out herein is made in terms of the observed values. Mention must be made here to the fact that this discrepancy in the actual value of B has no effect on the values of the shear parameters C' and ϕ' obtained from undrained shear tests since the strength exhibited by a soil element at failure is a function of the effective stress i.e. any variation in the value of the initial pore pressure in a soil element results only in changing the size and position of the effective stress circle at failure due to subsequent shear. The position of the Mohr's envelope, however, remains unchanged.



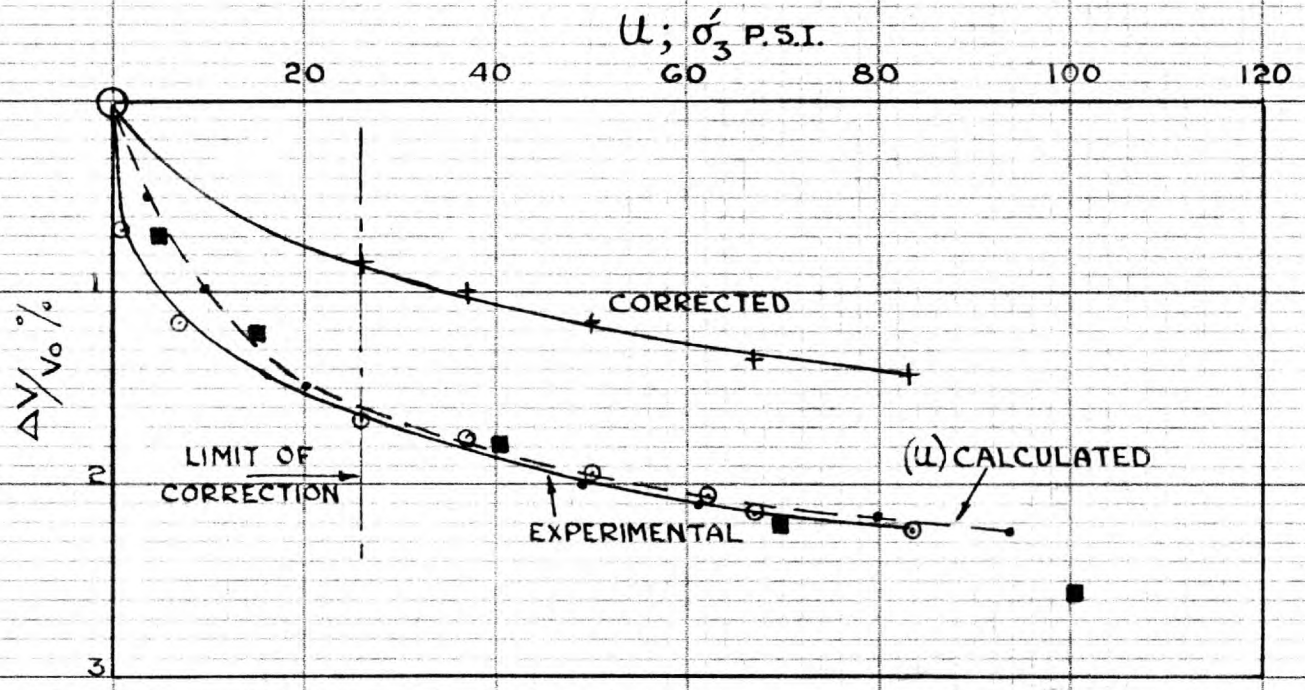
M/C = OPT. + 0·8%
S = 95%
m = ·678
K = ·00135

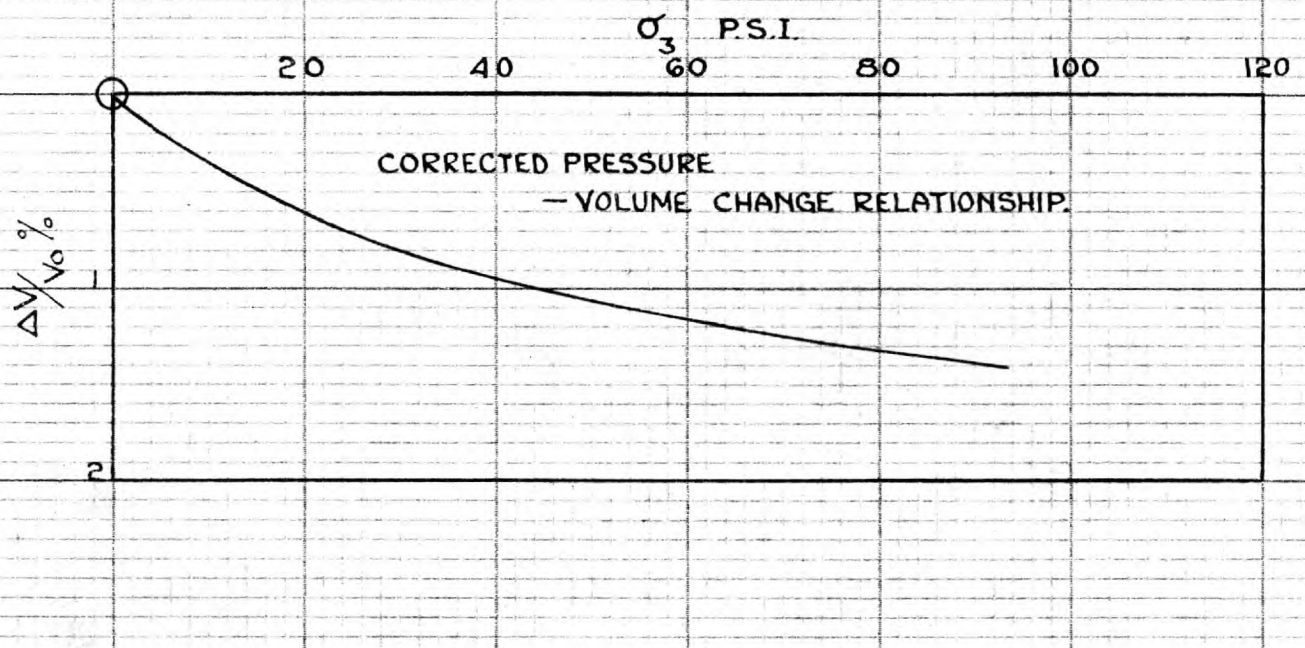
'B' Tests.

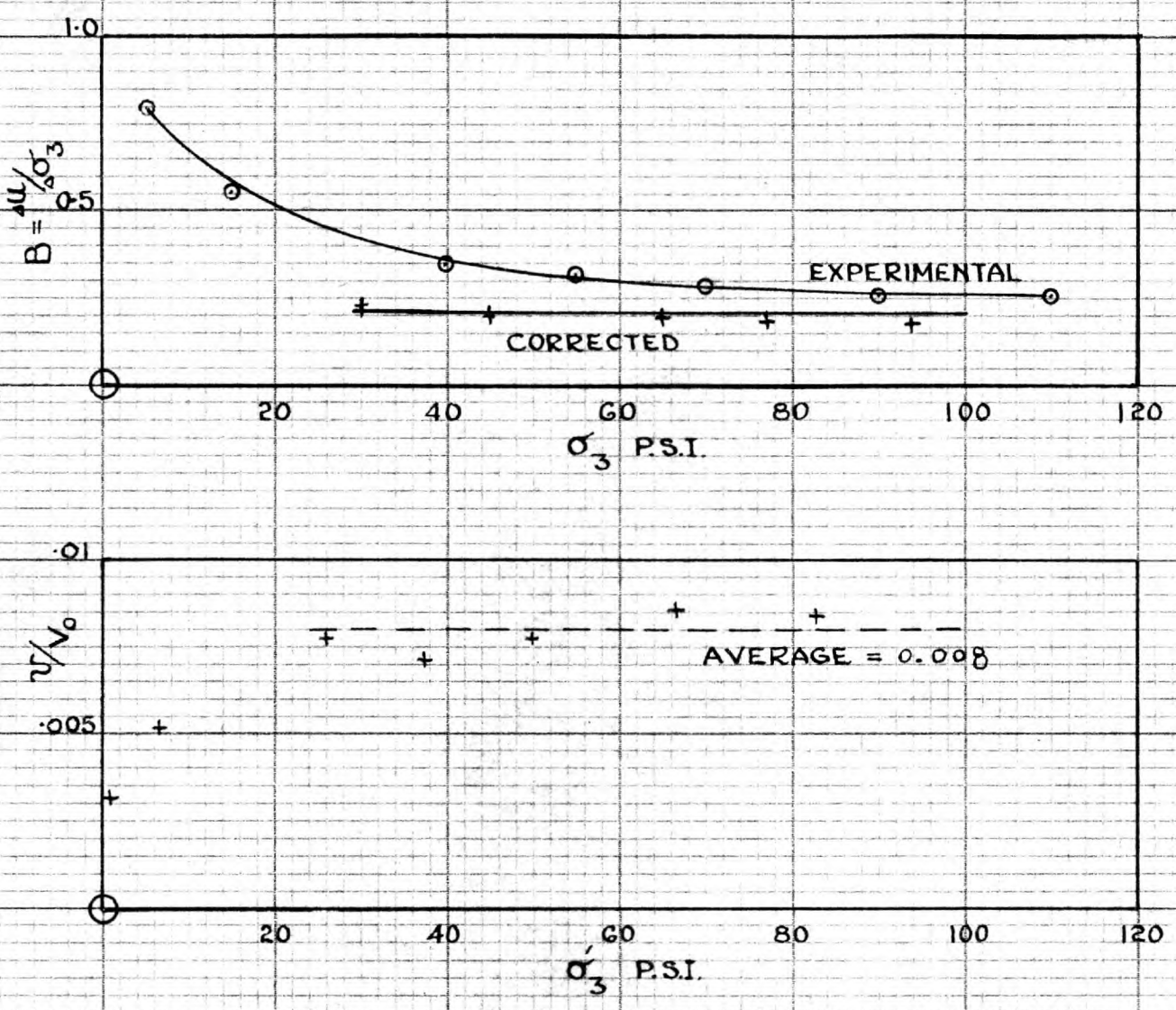
Typical Method Of Correcting Results For Free Air Trapped In Membrane

■ = Triaxial Consolidation (With Drainage)

Fig. 5:72







"B" Tests.

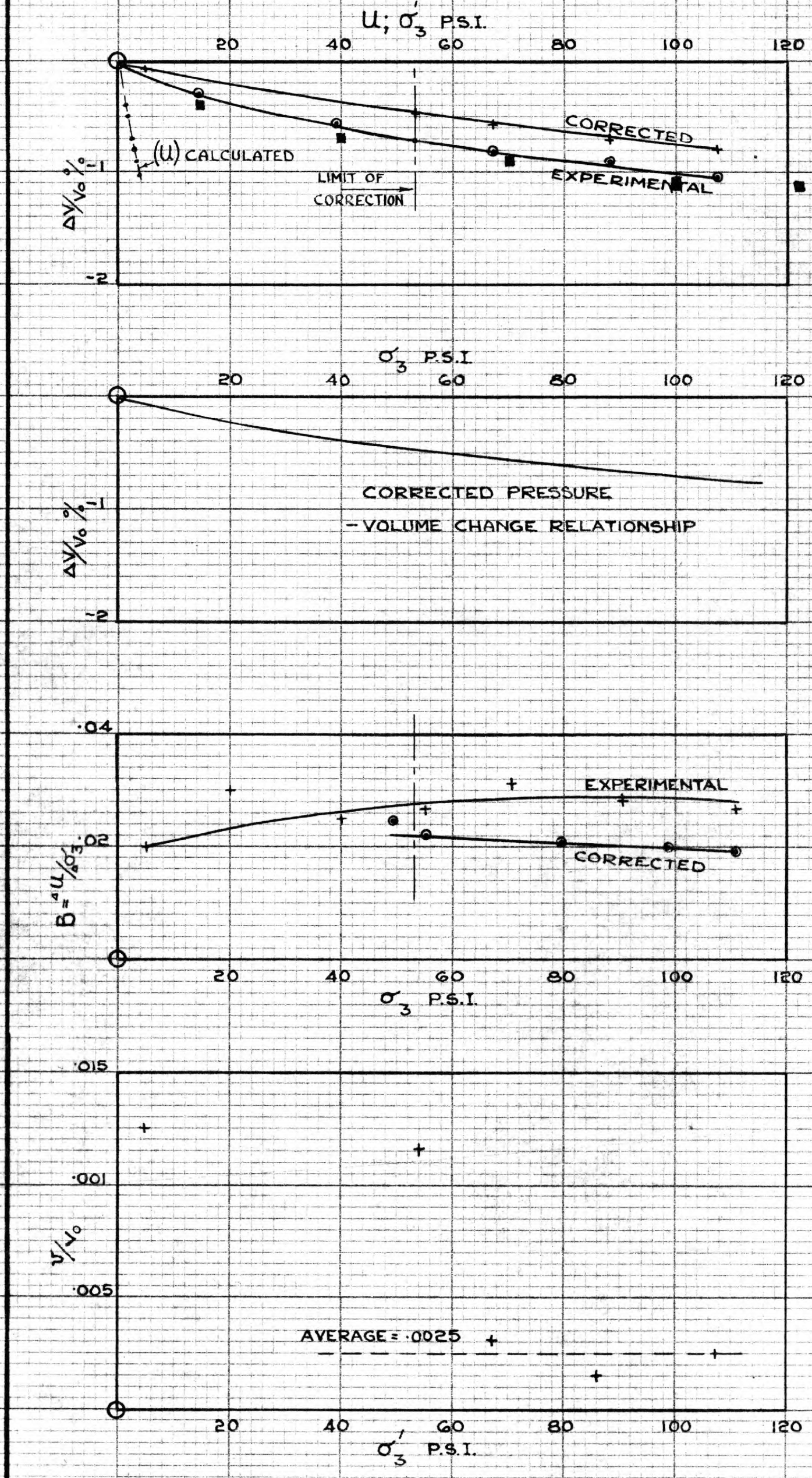
Typical Method Of Correcting Results

For Free Air Trapped In Membrane.

■ = Triaxial Consolidation (With Drainage)

M/C	= OPT. + 0.38
M	= 0·46
K	= 0·00186
S %	= 88·7

Fig. 5:73



'B' Tests.

M/C	= OPT. - 1·1 %
M	= 0·774
K	= 0·000205
S	= 72·4 %

Typical Method Of Correcting Results For Free Air Trapped In Membrane.

■ = Triaxial Consolidation (With Drainage).

Fig. 5:74

SHEET I

Typical Calculation for Correcting "B" test results

Moisture content = optimum + 0.82%

Dry density γ_d = 135.0 lb/cu. inch

Degree of saturation = 95%

Volume of Water = 18.77 cu. inch

Volume of Air :-

Dissolved in Free = 0.990 cu. inch
Water = 0.385 cu. inch
Total 1.375 cu. inch = VA

Cell Pressure p.s.i.	Compression cu. inch ΔV	Pore Pressure (u) p.s.i.	VA cu inch	VA_1 cu inch	$(VA_1 - VA) = v$ cu inch
5	0.3	4.4	1.375	1.3	-0.075
15	0.93	13.1	1.375	2.03	0.655
40	1.40	30.6	1.375	2.07	0.695
55	1.70	41.8	1.375	2.30	0.95
70	1.80	54.2	1.375	2.30	0.95
90	1.87	71.7	1.375	2.25	0.875
110	1.94	89.7	1.375	2.25	0.875
		Saturation			
120	2.00	99.6	1.375	-	-

As shown in Fig. 5:72, the average value of "v" was chosen as 0.92. The volume change $\triangle$ at saturation as observed is 1.97 and the corrected volume is 1.97 - 0.92 = 1.05 cu". This should be equal to the volume of free air in the sample i.e. 0.99. The difference, however, is very small.

SHEET II

Typical Calculation for Correcting "B" Test Results

Moisture Content = optimum + 0.38%

Dry density γ_d = 134.55 lb/cu.inch

Degree of Saturation = 88.7%

Volume of Water = 17.7 cu. inch

Volume of Air :-

Free = 3.25

Dissolved in Water = 0.354

Total 3.604 cu.inch. = VA

Cell Pressure p.s.i	Compr-ession cu.inch ΔV	Pore Pressure p.s.i.	VA cu inch	VA_1 cu inch	$(VA_1 - VA) = V'$ cu inch
5	0.67	4.0	3.604	3.92	0.316
15	1.13	8.4	3.604	3.11	0.506
40	1.65	14.0	3.604	3.39	0.786
55	1.80	17.5	3.604	3.32	0.716
70	1.95	20.0	3.604	3.39	0.786
90	3.14	23.6	3.604	3.47	0.866
110	3.24	27.4	3.604	3.45	0.846

Average value of v = 0.8, Fig. 5:73

Compressibility in Drained and Undrained Conditions

Theoretically the consolidation is a function of the effective stress. It follows that a partially saturated soil element under identical systems of effective stresses will undergo almost the same amount of consolidation whether tested drained or sealed and that the effective stress, volume change relationship is almost identical (neglecting the effect of change of moisture in the drained conditions, which is small).

To investigate this principle experimentally, a special set of consolidation tests was carefully carried out in the triaxial machine where the all round pressure was added in increments, while complete drainage was allowed. A further purpose for performing these tests was to determine the initial volume changes of samples in the drained and consolidated undrained shear tests. The initial values of volume changes when added to those during shear gave in some cases high values of dry densities that exceeded those corresponding to 100% saturation, which is physically impossible. It was then realised that there existed an experimental source of error due to trapped air in the membrane as found in the "B" tests. (This error in the volume measured during initial consolidation for such tests will not affect the volume changes measured during subsequent shear).

Comparison between the results of such tests and those of the "B" tests (in terms of effective stresses) showed a very good agreement, Figs 5:72, 5:73 and 5:74. Therefore it is justifiable to correct these particular tests in the same way as the "B" tests by taking from the latter the value of "v" for each moisture content and then following the same procedure. ("v" is an experimental error, and as such can hardly be a constant for a particular moisture content. It is applied to consolidation tests with drainage only if the observed volume changes agree with those obtained from the corresponding "B" test; a result that is achievable only with carefully performing the tests).

To complete the corrected pressure, volume change relationship in the low load range where "v" is erratic an equation of the curve representing the corrected part will be necessary. When plotted logarithmically, a group of such curves gave straight lines (also obtained by Gould, 1953). This is in accordance with the equation suggested by Hilf (1948):

$$\triangle = K\,(\sigma')^{m} \qquad 5:1$$

where $\triangle$ is the consolidation in per cent of total volume

K and m are constants.

From this equation, the rest of the curve can be plotted after computing K and m.

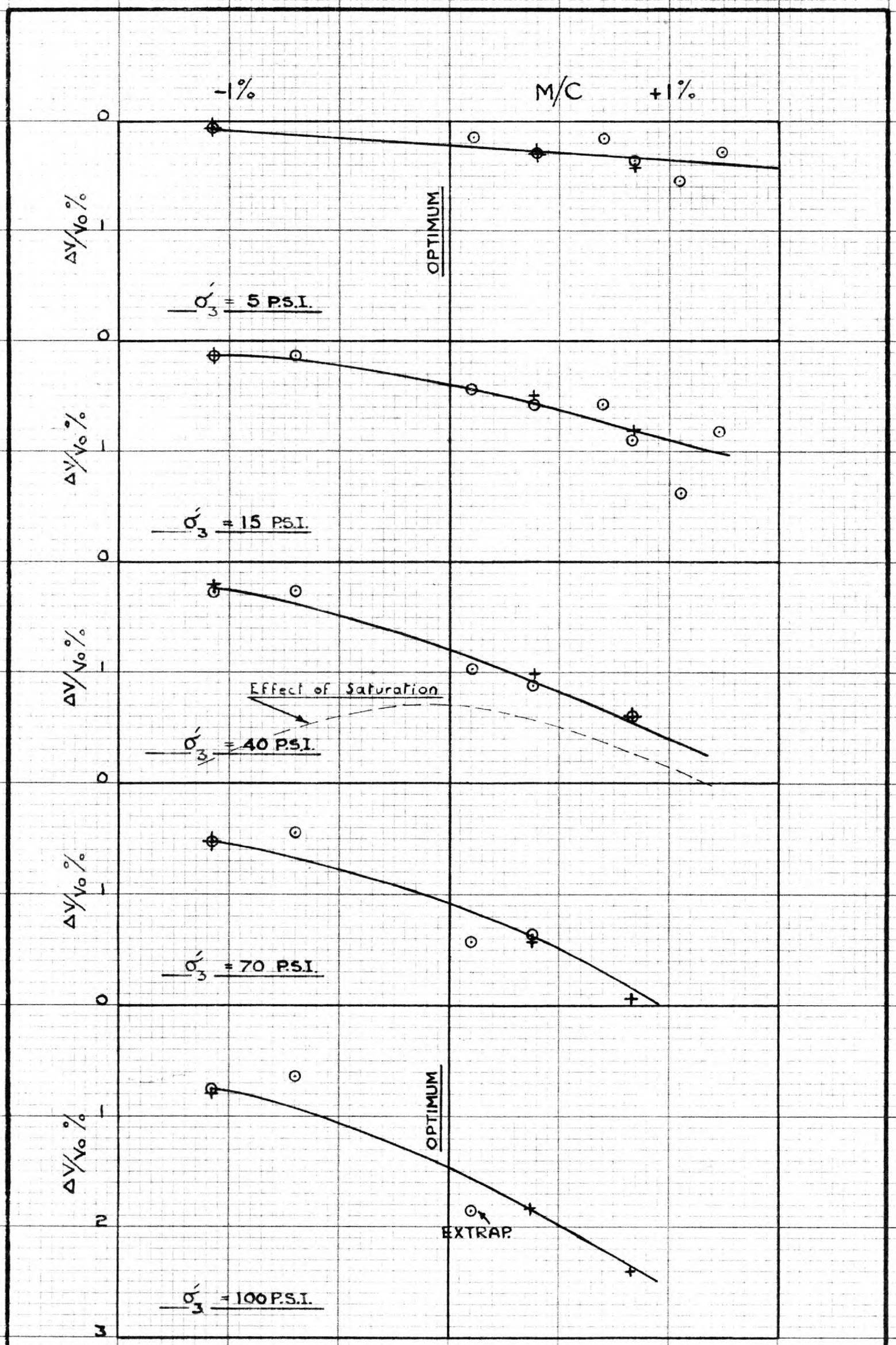
The following table gives values of m and K for different

moisture contents as computed for the "B" tests, and shows that while "m" can be considered to have an average value of 0.7, K varies considerably. More data is still needed to allow for a final conclusion to be drawn out.

M/C	m	K
Opt. - 1.08%	0.774	0.00031
Opt. + 0.1%	0.700	0.00072
Opt. + 0.38%	0.460	0.00186
Opt. + 0.7%	0.860	0.0006
Opt. + 0.85%	0.678	0.00135
Opt. + 1.03%	0.740	0.0018
Opt. + 1.23%	0.670	0.0013

Fig. 5:75 shows the corrected volume changes for all "B" tests and consolidation tests.

The validity of the above procedure has been proved by investigating the results of the consolidated undrained tests where the cell pressure during shear is higher than the consolidating pressure. The initial consolidation consisted of two terms; that before saturation and is obtained from the graphs in Fig. 5:75 and that during saturation is taken directly from the test in consideration. Since there is no moisture content change during subsequent shear, the degree



ALL ROUND CONSOLIDATION TESTS.

MOISTURE CONTENT; $\frac{\Delta V}{V_0}$ % RELATIONSHIP

FIG. 5:75

of saturation after consolidation can thus be determined.

The volume change $\Delta V\%$ due to the increment of cell pressure was introduced into equation 3:8 and the pore pressure computed checked fairly well with the excess pore pressure measured, as shown in the following table:-

Initial			After Consolidation		
M/C	S%	γ_d	M/C	S%	γ_d
Opt. 0.1	86.6	135.0	Opt.-0.5	86.75	136.9
Opt.	89.8	136.1	Opt.	93.75	137.2
Opt.	90.0	136.3	Opt.-0.5	93.0	138.4
Opt.-0.2	86.5	135.5	Opt.-0.2	89.0	136.9
Opt.+.35	93.0	136.0	Opt.	92.7	137.1

'initial' consolidation %	Consolidation Pressure p.s.i.	Cell Pressure p.s.i.	$\Delta V\%$	Pore Pressure Expt. p.s.i.	Pore Pressure Calculated. p.s.i.
I.27	40	70	0.21	1.5	1.2
0.8	15	40	0.26	2.86	3.15
I.22	40	120	0.338	7.3	7.6
I.05	70	120	0.36	5.2	6.5
0.8	15	70	0.97	7.2	17

Settlement due to Saturation

The Compression of a partially saturated soil element upon saturation depends on its placement condition. This extra amount of compression is generally large with dry soils while with wet soils it is comparatively small.

Gibbs, 1948; showed that with samples compacted at a moisture content which is slightly lower of optimu", the amount of extra compression is almost negligible, which leads to the conclusion that such a placement condition is the lowest limit to be used for a fill material if settlement, because of saturation, is to be avoided.

Fig. 5:75 shows that with the type of material used in the present series of tests, large volume changes will occur on saturation for dry samples. It is also noticed that a small amount of extra compression also takes place with wetter samples which may be attributed to secondary consolidation effects on saturation.

Pore Pressure under Decreasing Loads

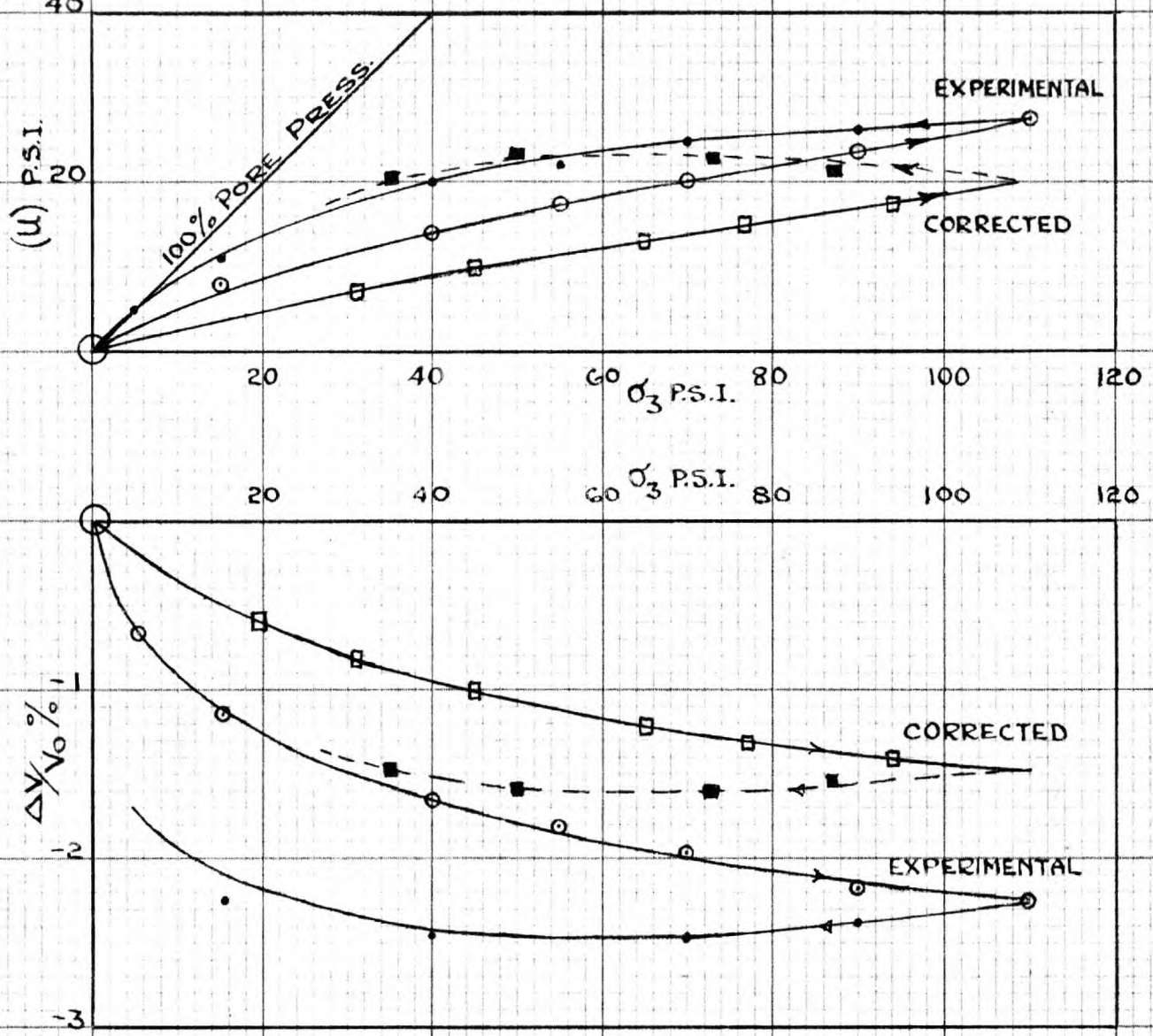
The expansibility of a soil element associated with a decrease in the acting loads is generally less than its compressibility. This results in higher values of excess pore pressure during an unloading run as already discussed in

Chapter 3 (equation 3:10); and consequently higher values of B. Fig. 5:70.

This is generally the case during rapid draw down where the total stresses decrease due to the lowering of the reservoir water at a rate allowing no dissipation to take place. This may result in giving a factor of safety for the rolled fill dam that may be less than that at the end of construction which is regarded in most cases as the governing factor in the design.

The test results can be corrected in the same way as those for the loading stage by using the average value of "v", already determined, to correct the effective stress volume change curve over a certain range of loads. The resulting curve does not represent a typical consolidation relationship and no attempt was made to complete its early part as for the loading stage. However, the corrected values of pore pressure are naturally higher than the corrected values under increasing load. Figs. 5:76 and 5:77 show typical results for two moisture contents.

Attempts were made to determine a value of "v" for decreasing loads in the same way outlined before, but were not successful due to large discrepancies in the values obtained that did not permit an average value to be considered. The solution presented in the preceding paragraph is only a tentative one and more study is thus needed.



LOADING.

UNLOADING.

M/C = OPT. + 0·38 %

S = 88.7 %

γ_d = 134.55

FIG. 5.76

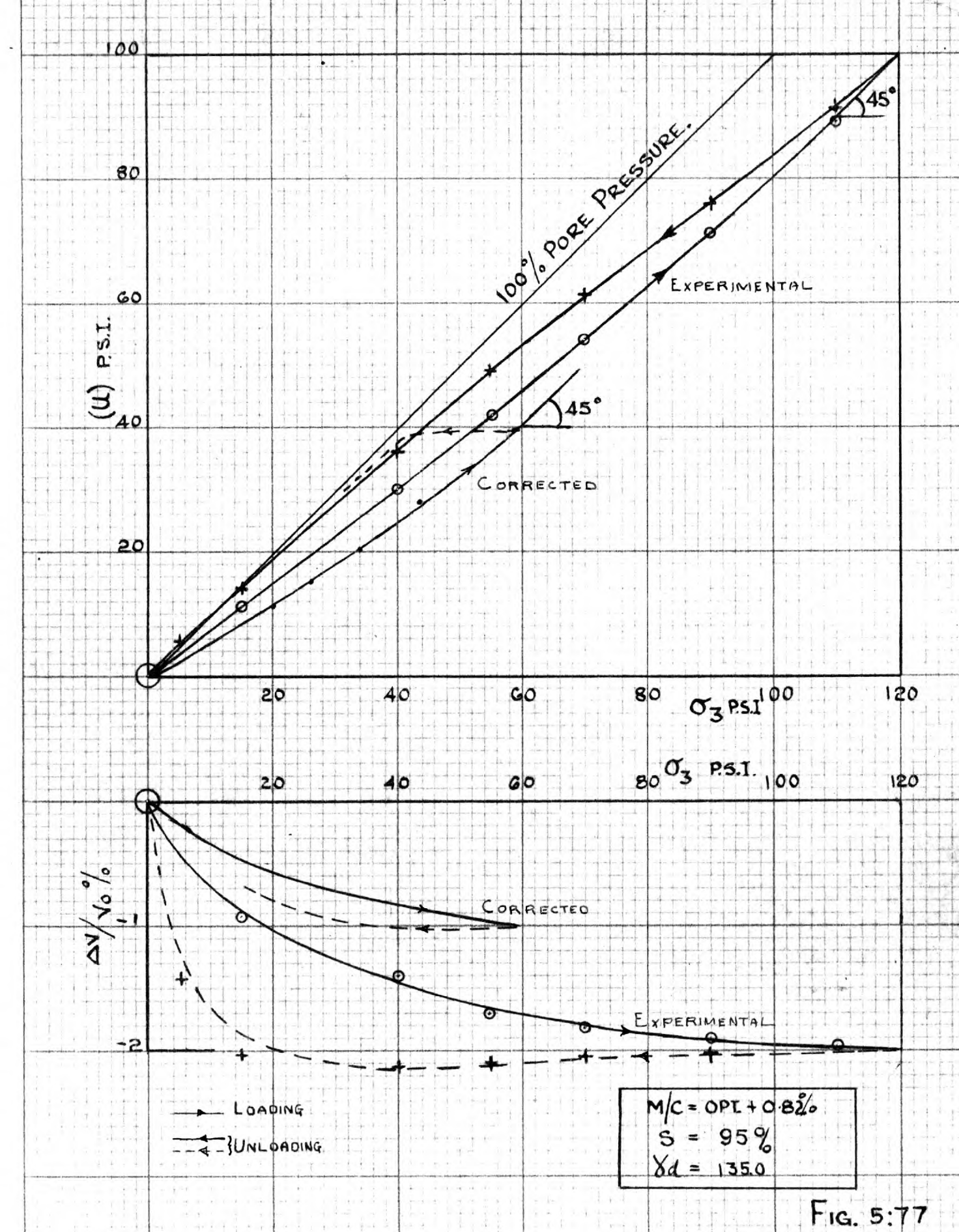

100
80
60
40
20
(u) P.S.I.
100% PORE PRESSURE.
45°
EXPERIMENTAL
45°
CORRECTED
20
40
60
80
100
120
σ3 P.S.I
20
40
60
80
σ3 P.S.I.
100
120
ΔV/Vo %
-1
-2
CORRECTED
EXPERIMENTAL
LOADING
UNLOADING
M/C = OPT. + 0.8%
S = 95%
γd = 135.0

FIG. 5:77

It is believed that the rate at which the air is freed from solution is less than that at which it is forced into solution in water, resulting, probably, in erratic volume changes with decreasing loads.

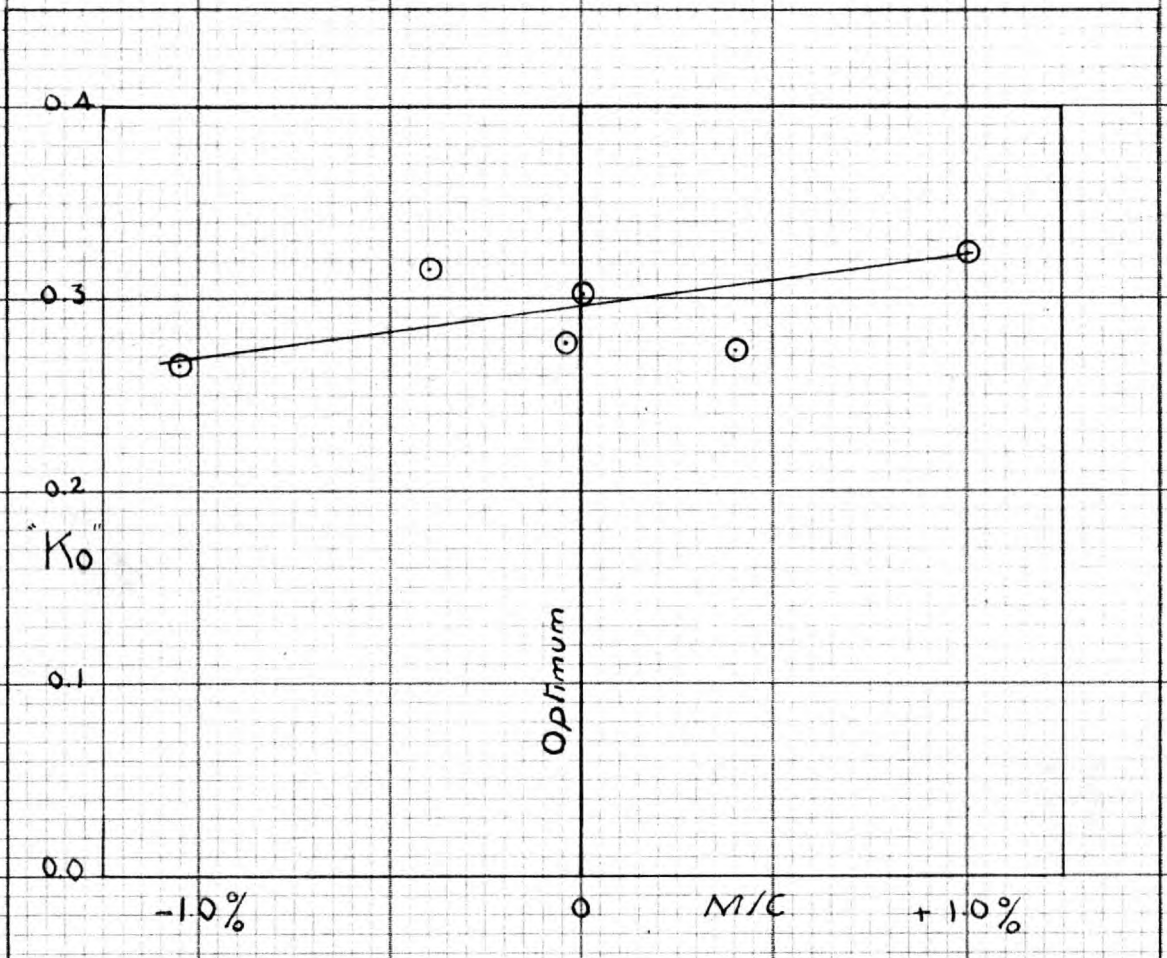
2. The K_o System $\frac{\bar{\sigma}_1'}{\bar{\sigma}_3'} = \frac{1}{K_o}$ $(K_o < 1)$

These tests represent a case of uniaxial consolidation (at constant moisture content) where lateral strains are prohibited, which is approximately the case of a soil element well inside a dam. Such tests furnish a relationship between the applied loads as represented by the total major principal stress $\bar{\sigma}_1$, the pore pressure and the volume changes for this condition of loading. Furthermore they provide an estimate of K_o, the coefficient of earth pressure at rest.

K_o was found to change only slightly with moisture content after a certain range of loads (at $\bar{\sigma}_1$ = 100 p.s.i. approximately). Test results, however, have shown that the dryer the sample, the greater is the shear strength and we would anticipate a smaller value of K_o * Fig. 55:78. The difference is not large, since the angle of shearing resistance ϕ' varies only slightly with moisture content and if

---

* In the case of water with no shear strength $K_o = 1$.



TYPICAL VALUES OF "Ko" AT σ_1 = 100 P.S.I

For Various Moisture Contents.

FIG. 5:78

the cohesion is neglected samples at different moisture contents would have almost the same strength.

Fig. 5:79 shows the results of K_o tests for samples compacted at approximately - 1%, Opt. and + 1% of optimum. In determining the relationship between the volume change and the load, the test results were corrected for the extra free air "v" in the same way as for the"B" tests. The value of "v" was of almost the order of magnitude as for the "B" tests. Fig. 5:80 gives the relationship between volume change and effective stresses for different moisture contents.

It may be argued, however, that the existence of this entrapped air will make the adjustment of the volumes during the test in conformity with the K_o condition (i.e. no lateral yield) rather inadequate. As already explained, this extra air will be incorporated into the sample under a small increment of cell pressure after which the K_o condition will be adequately fulfilled. This may explain the large discrepancies in the value of K_o at low pressures.

Regarding the value of the principal stress ratio, these tests represent an intermediate stage between the all round pressure and the failure conditions in an undrained test, either at maximum principal stress ratio or at maximum deviator stress, (principal stress ratio is 1 and about 5 respectively). The test results showed that the pore pressures and the volume changes followed this pattern for all moisture

	M/C	γ_d	S%
o – OPT. +1%		134·6	95·7
Δ – OPT.		136·0	89
□ – OPT.–1·08%		134·6	73

■ ● ▲ – POINTS FROM UNDRAINED TESTS AT EQUAL σ_1'/σ_3' (TO THOSE IN K_o TEST)

□ o Δ – K_o TESTS

100% PORE PRESSURE.

(u) P.S.I.

200
150
100
50

50 100 150 200 250 300 350

σ_1 P.S.I.

K_o

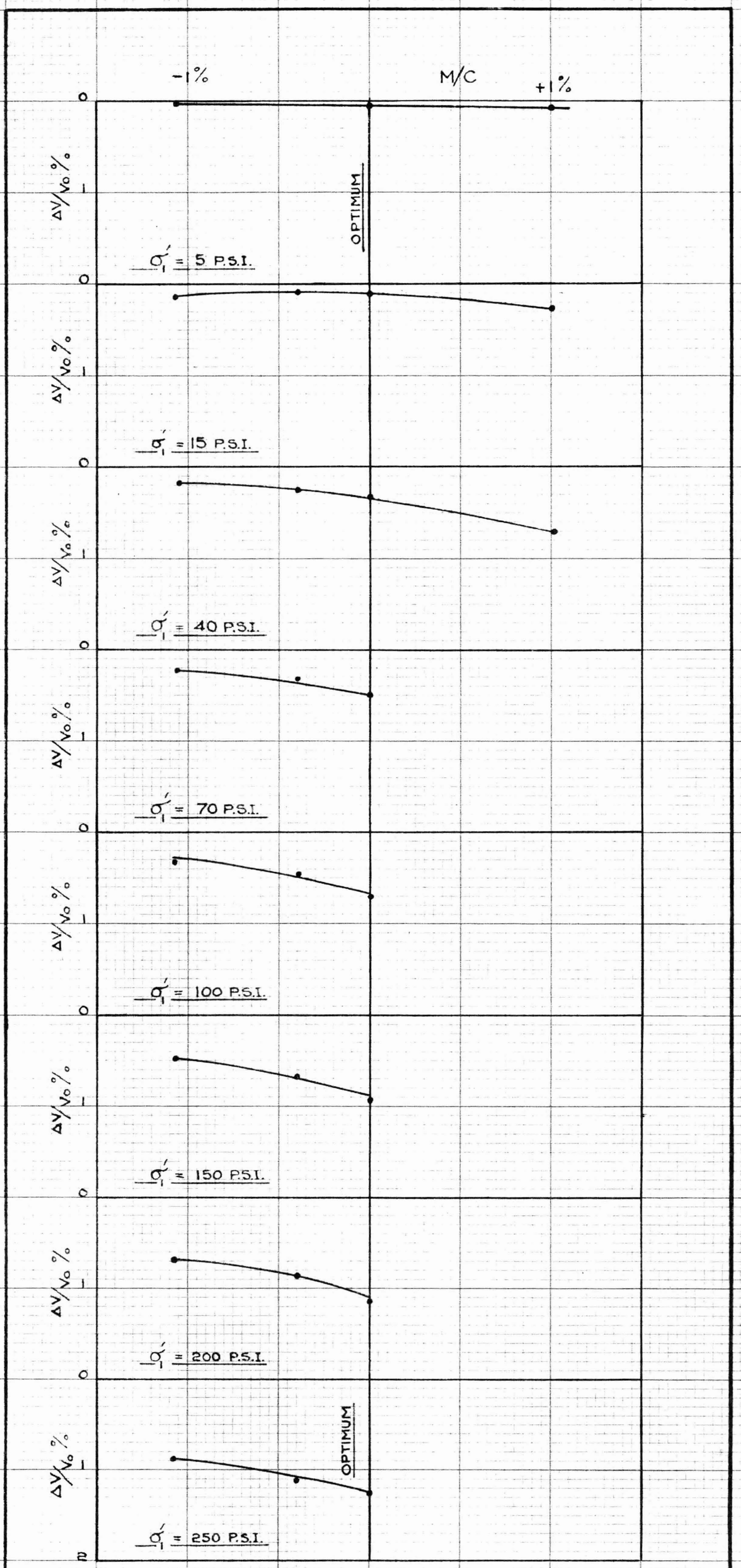
0·6
0·5
0·4
0·3
0·2
0·1

50 100 150 200 250 300 350

σ_1 P.S.I.

K_o TESTS.

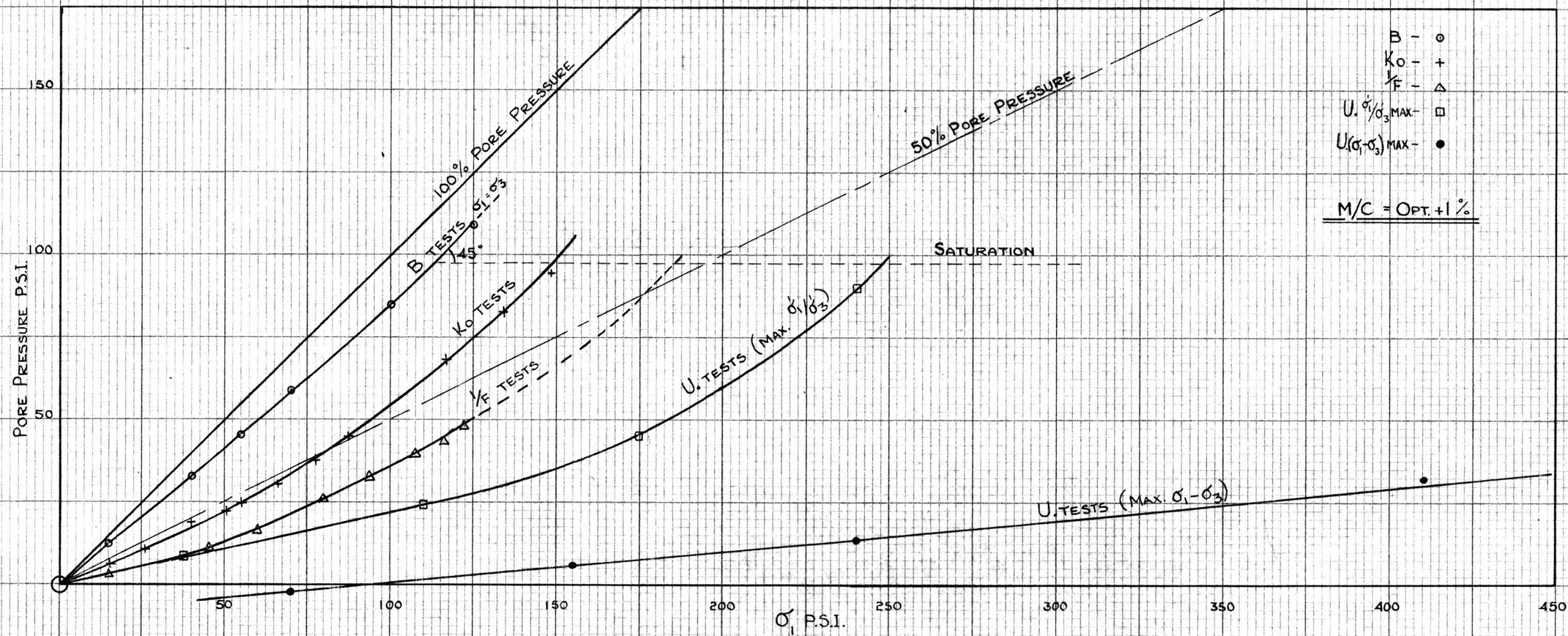
FIG. 5:79



K_o TESTS

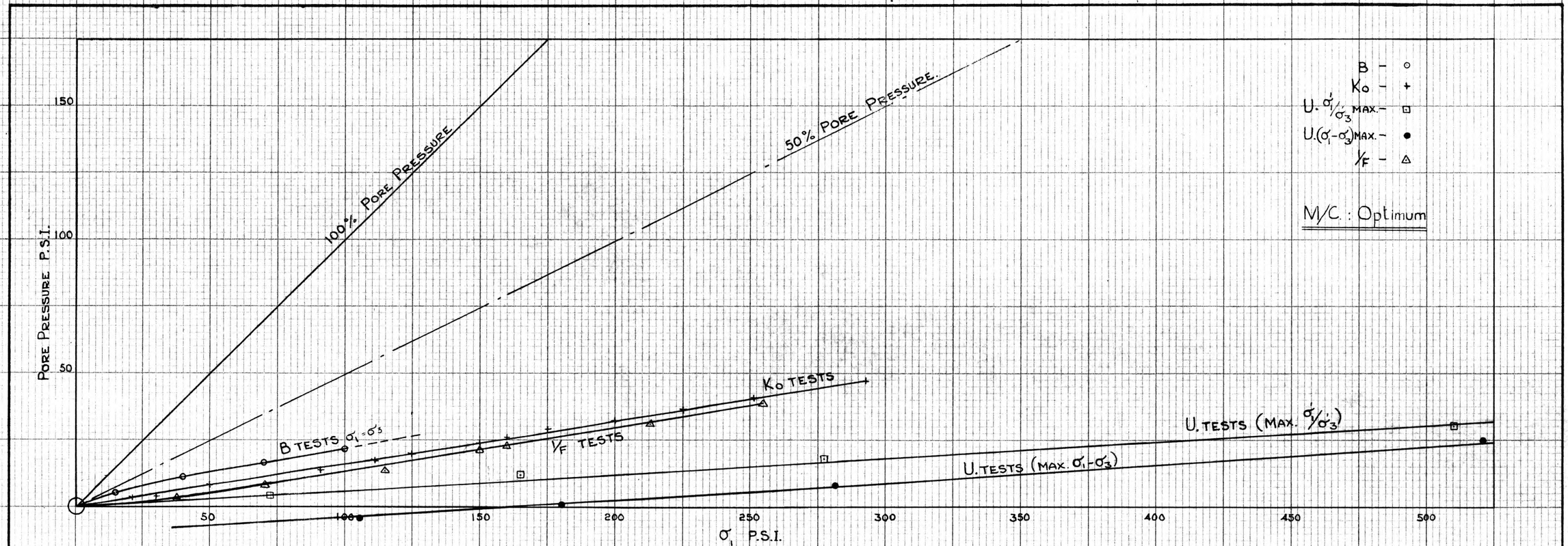
MOISTURE CONTENT – CONSOLIDATION RELATIONSHIP
FOR VARIOUS VALUES OF σ_1'

FIG. 5:8.0



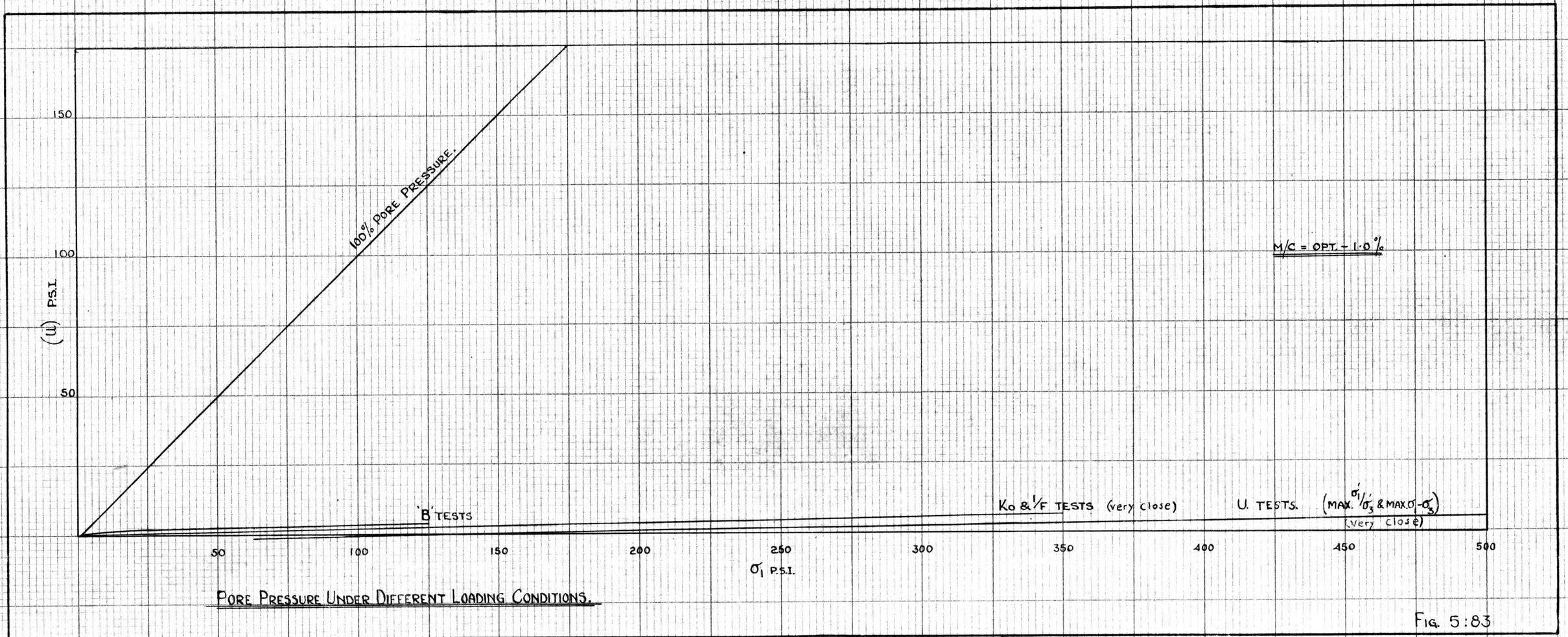
PORE PRESSURE UNDER DIFFERENT LOADING CONDITIONS.

FIG. 5:81



PORE PRESSURE UNDER DIFFERENT LOADING CONDITIONS

FIG. 5:82



PORE PRESSURE UNDER DIFFERENT LOADING CONDITIONS.

FIG. 5:83

contents investigated, Figs. 5:71, 5:81, 5:82, 5:83 and 5:84. The following table gives values of K_o for saturated soil as determined by several authors and is included here for comparison together with one result for a dry sand.

TABLE 3

	Soil	K_o
Gersevanoff (1936)	Clay	0.65
	Sand	0.41
Tschebotarioff (1948)	Plastic Clay	0.5
Eldin (1951)	Loose brasted sand (porosity 45%)	0.471
	Dense brasted sand (porosity 38%)	0.338
ElRamli (1949)	Medium dense dry sand (porosity 42%)	0.50

3. The $1/F$ Tests

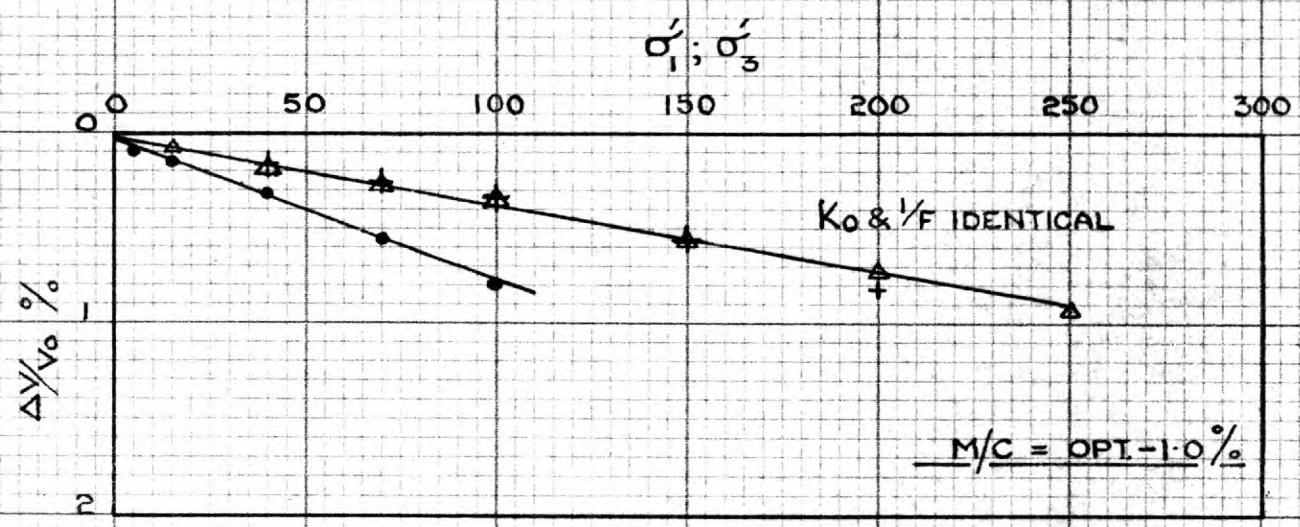
The object of these tests has already been outlined (Chapter 4). F is the factor of safety used in the design of an earth dam and is here chosen, in accordance with common practice as equal to 1.5. Experimentally, it is the factor

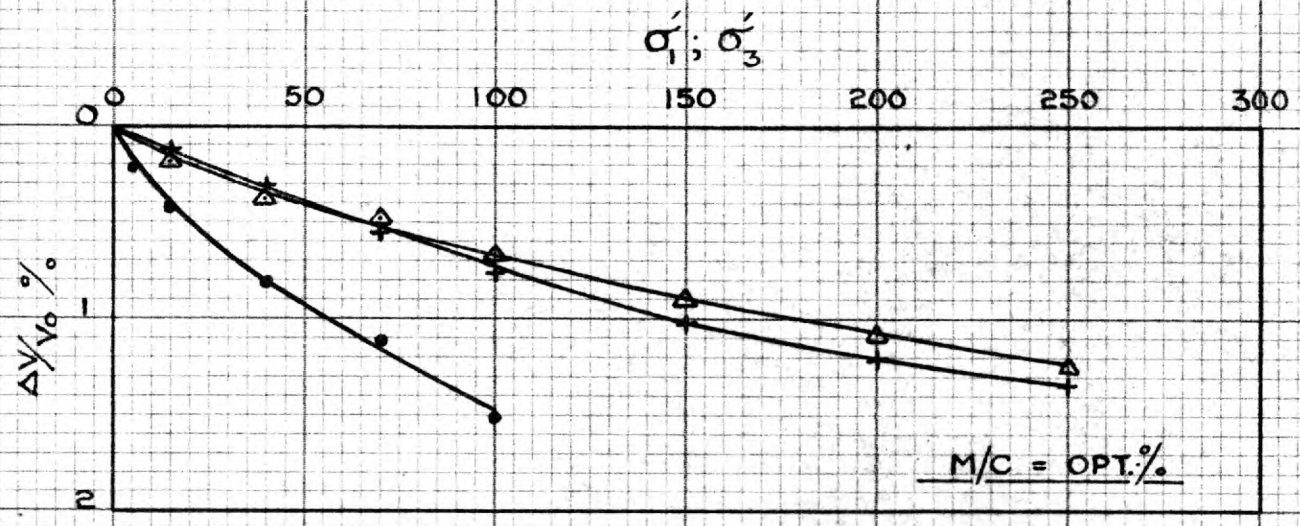
by which (C') and (tan $\emptyset'$) obtained from failure conditions in undrained tests are reduced. Consequently, no incipient failure will occur during such tests. But the main value of these tests is in establishing a relationship between loads, pore pressures and volume changes comparable to that in an actual dam.

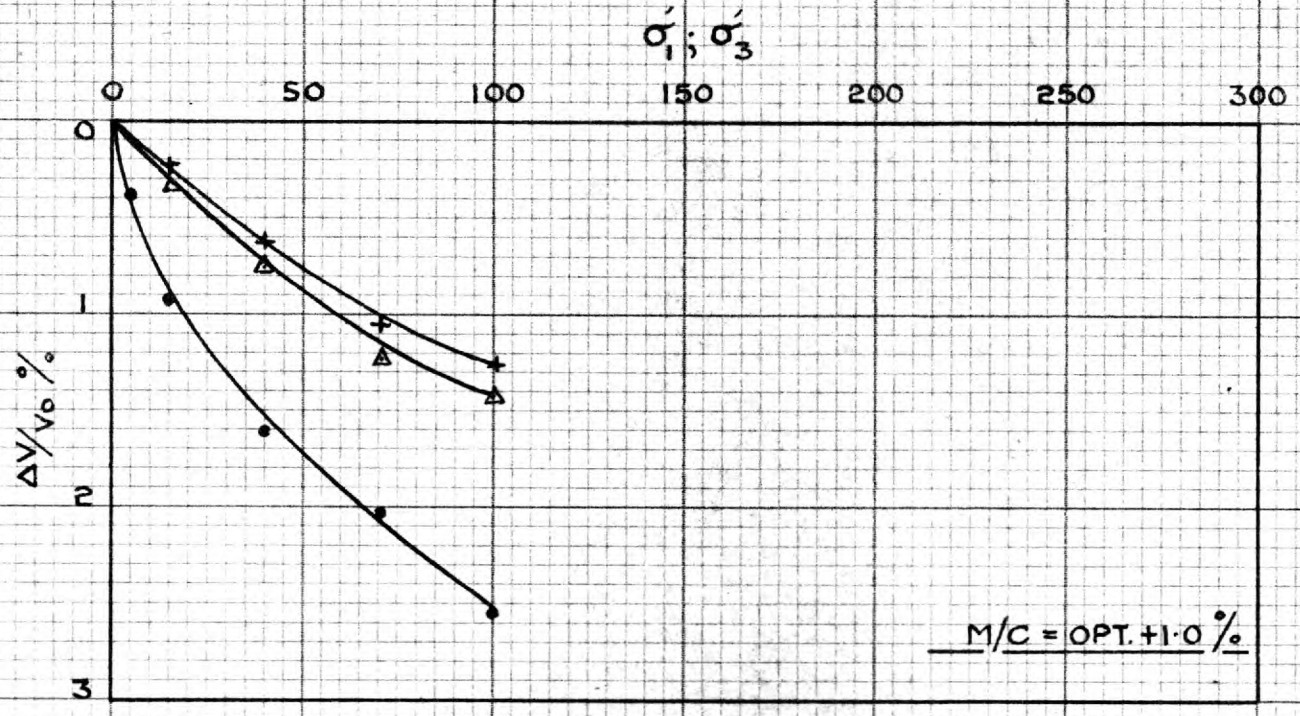
The results of these tests show that the pore pressure for both failure criteria in undrained shear tests is an underestimate, while those under all round load conditions are on the conservative side. This means that, while in a stability analysis we use C' and $\emptyset'$ as obtained from failure conditions, the corresponding pore pressures will not correspond to those in an actual dam.

Fig. 5:85 shows the results of $1/F$ tests for three moisture contents. Fig. 5:86 shows the corrected volume change, effective stress relationship.

The principal stress ratio at a given load does not vary considerably from those obtained for the K_o tests for F = 1.5. Comparison of results of the "B" tests, "K_o" tests and the "$1/F$" tests show clearly that the excess pore pressure, and the compressibility are a function of the principal stress ratio for any moisture content. Fig. 5:84 and Figs. 5:81, 5:82 and 5:83 show that the higher the value of σ'_1/σ'_3 the lower is the excess pore pressure and the compressibility. (σ'_1/σ'_3 = 1 in "B" tests, about 3 in K_o and "$1/F$" tests and about 5 is







TYPICAL VALUES OF σ'_1/σ'_3 — AT σ_1 = 150 P.S.I.

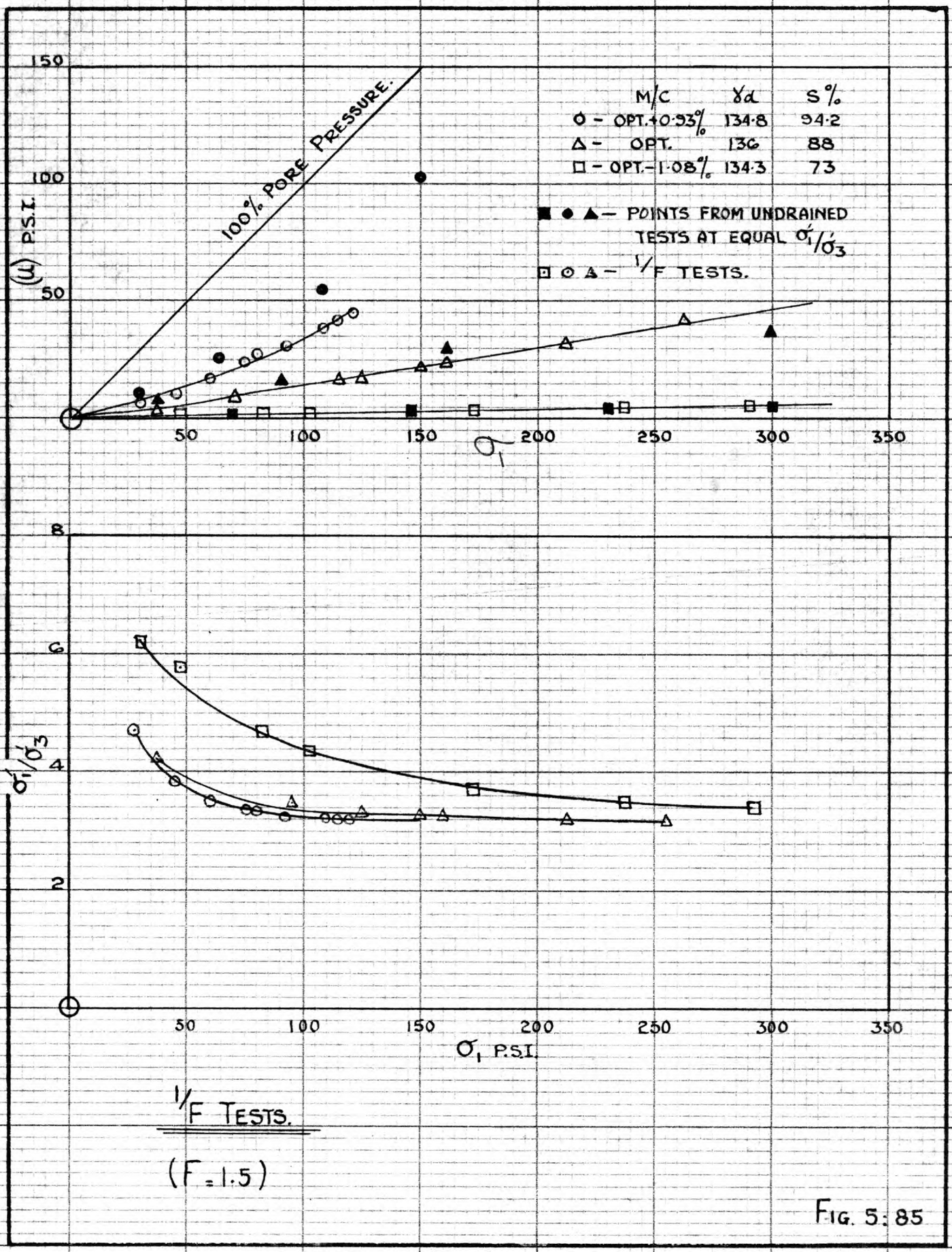
M/C	B	Ko	1/F
OPT. -1	1	4·0	4·0
OPT.	1	3·3	3·3
OPT. +1	1	3·1	3·22

● = ALL ROUND
△ = Ko CONDITION
\+ = 1/F CONDITION

SUMMARY OF CONSOLIDATION RESULTS.

RELATIONSHIP BETWEEN EFFECTIVE STRESS & CONSOLIDATION $\frac{\Delta V}{V_o}$ %
UNDER DIFFERENT LOAD CONDITIONS

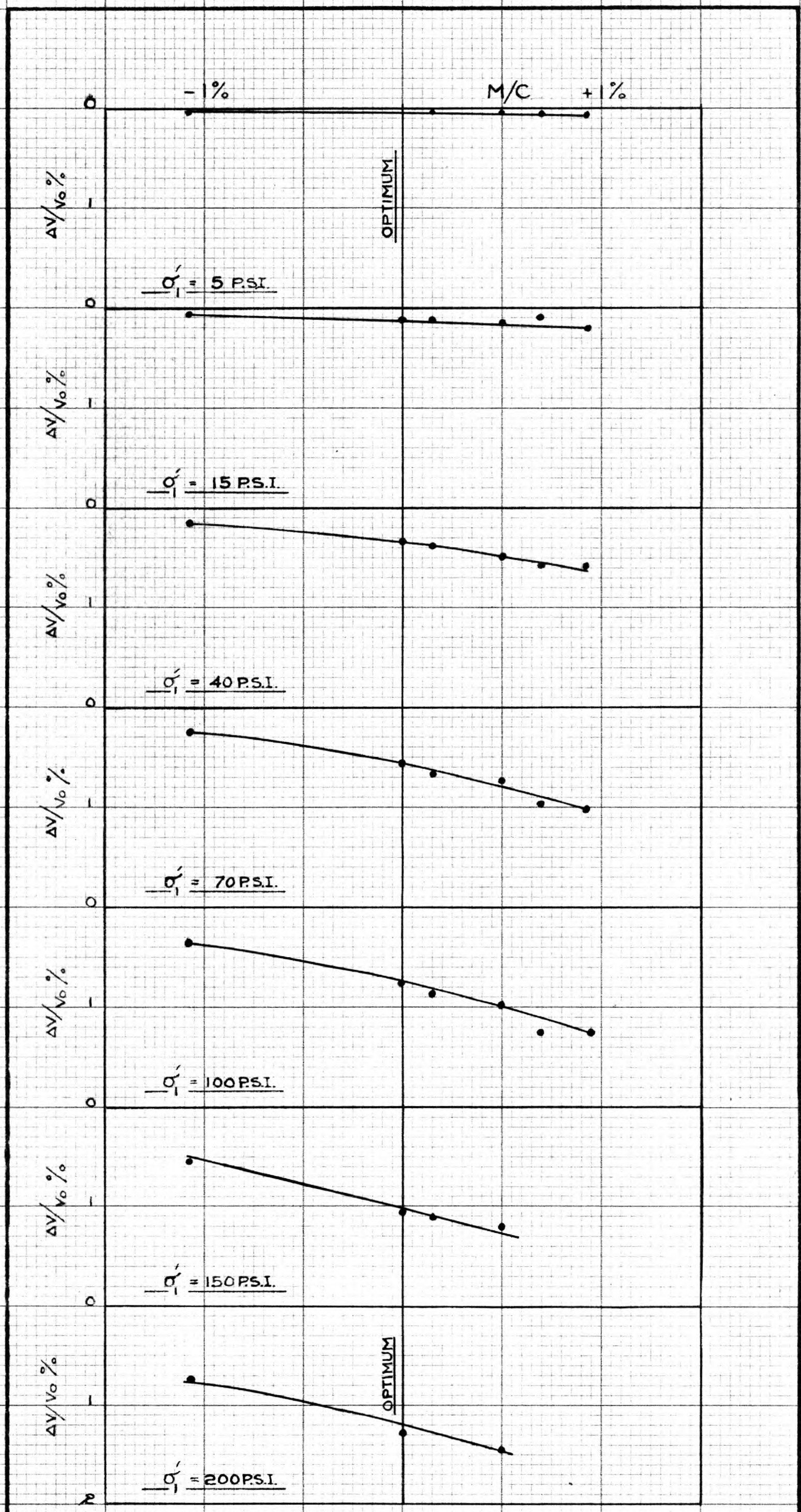
FIG. 5:84



1/F TESTS.

(F = 1.5)

FIG. 5:85



1/F TESTS

MOISTURE CONTENT - CONSOLIDATION RELATIONSHIP
FOR VARIOUS VALUES OF σ_1'

FIG. 5:86

its maximum value in undrained tests).

These findings, in fact, suggested the conclusion that, irrespective of the type of test, equal excess pore pressures or compressibility will correspond to equal values of the principal stress ratio at a given load, i.e. that the pore pressure ratio is similarly related to the principal stress ratio irrespective of the sequence of loading.

The results of the undrained tests offered a further chance of checking the validity of this conclusion, i.e. if at a certain load $(\bar{\sigma}_1)_1$ the principal stress ratio $\bar{\sigma}_1'/\bar{\sigma}_3'$ is the same in both the undrained test and the K_o test (or indeed any other test) the corresponding pore pressures will be approximately the same.

To determine $(\bar{\sigma}_1)_1$, a graphical method was devised. This consists in plotting for both the undrained test at a particular cell pressure and the K_o test at the same moisture content, the experimental relation between $\bar{\sigma}_1$ and $\bar{\sigma}_1'/\bar{\sigma}_3'$ which results in two curves that intersect at a point corresponding to $(\bar{\sigma}_1)_1$, Fig. 5:87. From the particular undrained test results the pore pressure corresponding to $(\bar{\sigma}_1)_1$ can be obtained. Four values of pore pressures corresponding to the four cell pressures in the undrained tests series were determined in this way and are shown in Fig. 5:79 and Fig.5:85

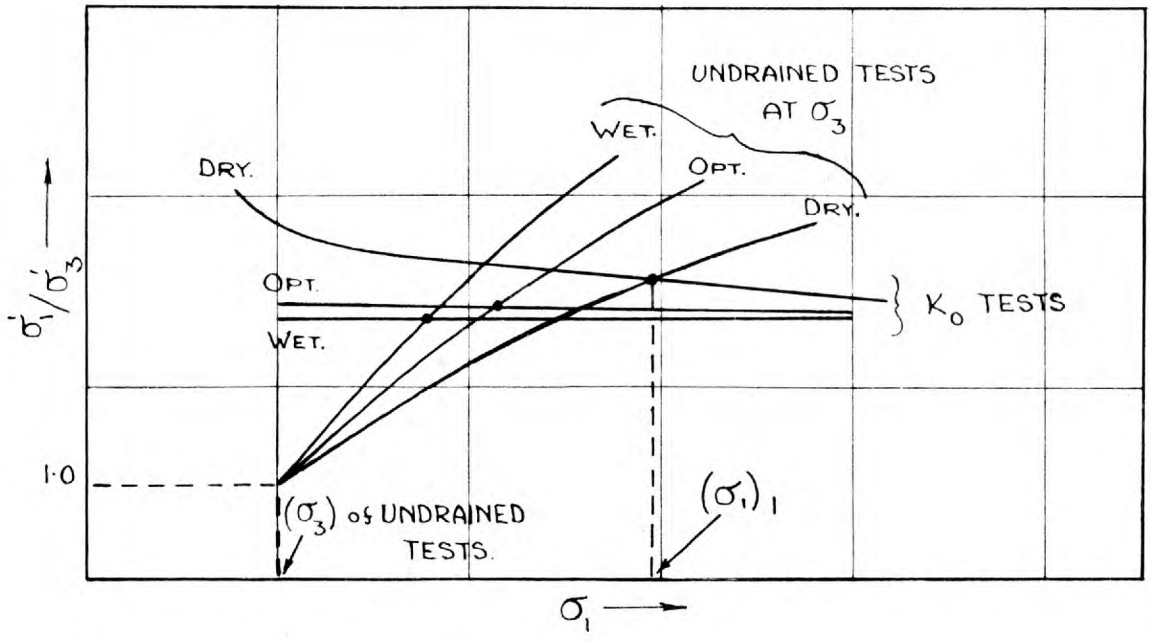


DIAGRAM SHOWING METHOD TO DETERMINE $(\sigma_1)_1$ CORRESPONDING TO IDENTICAL VALUES OF σ_1'/σ_3' IN K_0 & UNDRAINED TESTS.

FIG. 5:87

for the K_o and $1/F$ tests which show a fairly good agreement

Relationship between Pore Pressure Ratio and Effective Principal Stress Ratio

It was shown that for a partially saturated soil element the excess pore pressure Δu is given by the following equation:

$$\Delta u = B\Delta\sigma_3 + a \cdot (\Delta\sigma_1 - \Delta\sigma_3)$$

$$= B(\Delta\sigma_3' + \Delta u) + a \cdot (\Delta\sigma_1' - \Delta\sigma_3')$$

$$\therefore \Delta u (1 - B) = B\Delta\sigma_3' + a(\Delta\sigma_1' - \Delta\sigma_3')$$

$$\therefore \frac{\Delta u}{\Delta\sigma_1} = \frac{1}{(1-B)} \times \frac{1}{(\Delta\sigma_1' + \Delta u)} \cdot \left\{B\Delta\sigma_3' + a(\Delta\sigma_1' - \Delta\sigma_3')\right\}$$

or $$\frac{\Delta u}{\Delta\sigma_1'} = \frac{1}{1-B}\left(B \cdot \frac{1}{r} + a - a \cdot \frac{1}{r}\right) \quad \text{where } r = \sigma_1'/\sigma_3'$$

but $$\frac{\Delta\sigma_1}{\Delta u} = 1 + \frac{\Delta\sigma_1'}{\Delta u}$$

$$\therefore \frac{\Delta u}{\Delta\sigma_1} = \frac{(B - a) + ar}{(B - a) \cdot (1-r) + r} \qquad 5:2$$

Therefore if we assume that B for a given pressure is constant, it follows that, since "a" is in fact a function of $(\sigma_1 - \sigma_3)$ at any stage during shear, the pore pressure ratio is a function of the principal stress ratio as proved experimentally, Fig. 5:79 and 5:85.

To complete the picture experimentally, the results of two sets of undrained shear tests, each corresponding to a

particular moisture content under four different cell pressures are plotted as a relationship between the pore pressure ratio and the principal stress ratio, fig. 5:88 and 5:89. In these figures points obtained from K_o and $1/F$ tests are also shown.

Fig. 5:88 shows the relationship between $\frac{\Delta u}{\Delta \sigma_1}$ and σ'_1/σ'_3 from four undrained tests on samples compacted at approximately 1% above the optimum. Except for the cell pressure of 120 p.s.i. where the sample became fully saturated under loads, points corresponding to the other three cell pressures followed more or less the same course as long as the pore pressure was increasing. Afterwards each group of points followed a separate course. It is also noticed that points corresponding to the cell pressure of 120 p.s.i. joined the same pattern at this stage as the sample became no longer fully saturated due to dilatency.

Fig. 5:89 gives the results for a sample compacted at optimum. At the initial stage where the pore pressure is increasing we notice that there is a larger scatter of the points. The greatest deviation is for the points corresponding to a cell pressure of 15 p.s.i., where, with this moisture content, larger values of "B" are associated with low cell pressures, Fig. 5:70. If we consider the other cell pressures (especially 40 and 70 p.s.i.) as representing

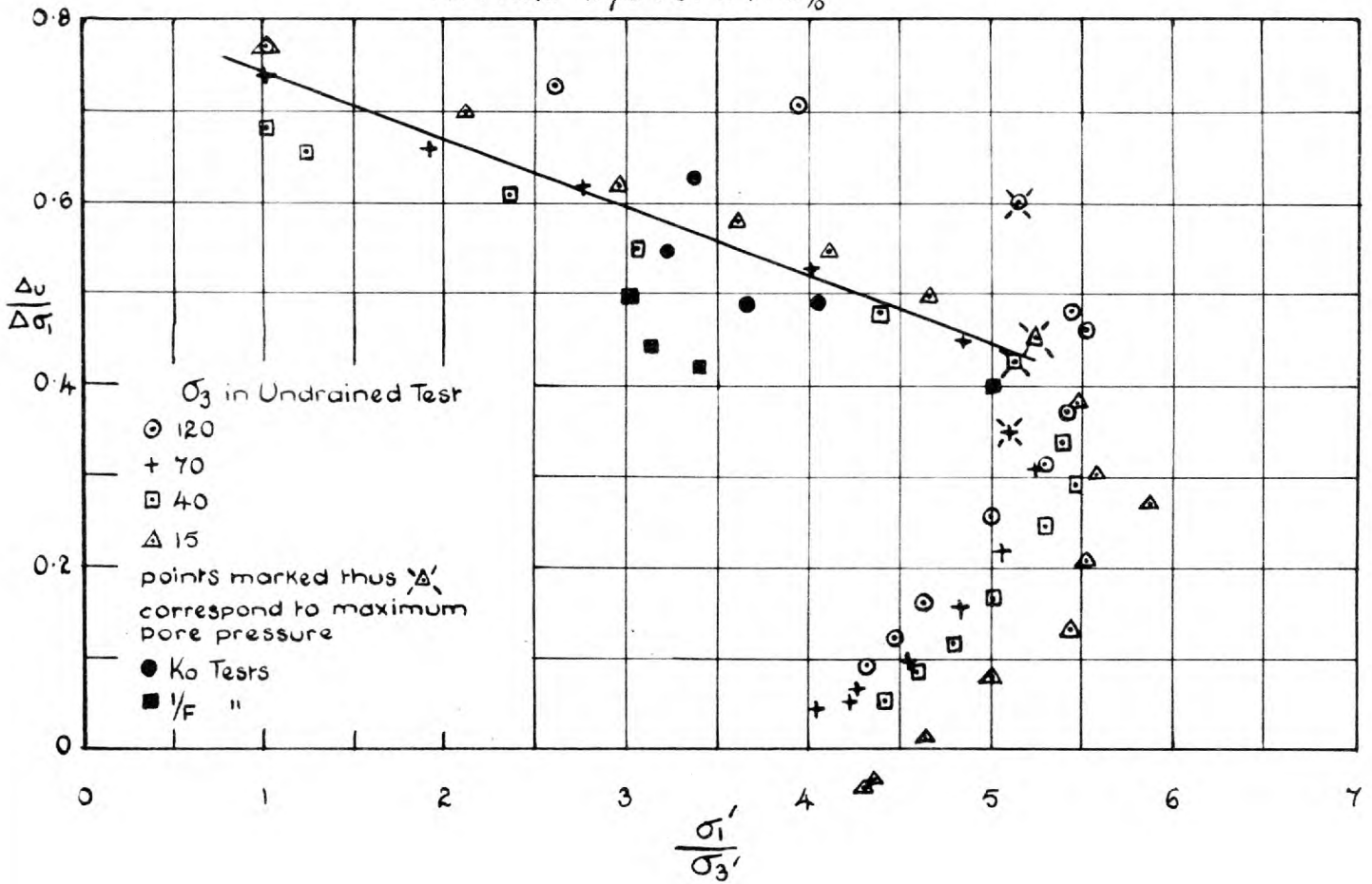
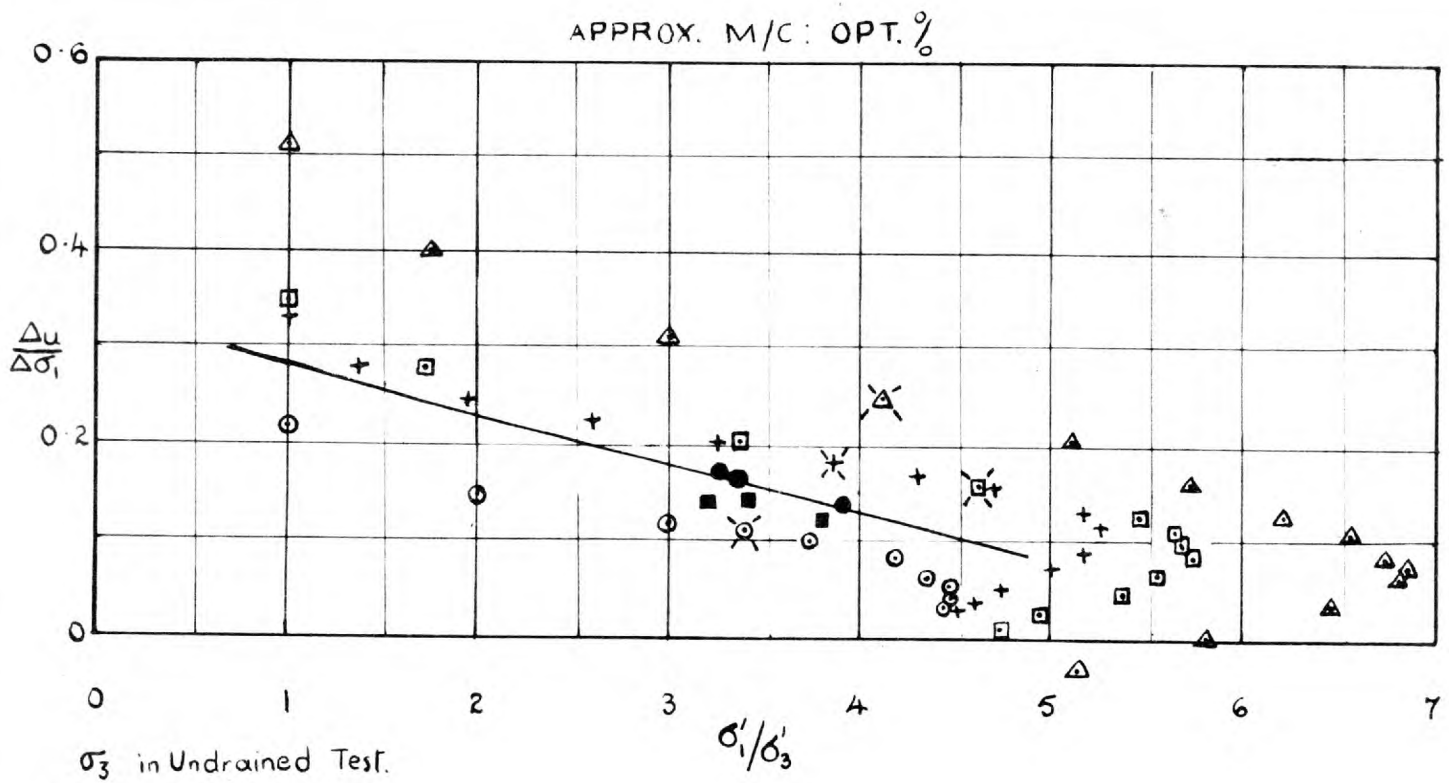

APPROX. M/C : OPT. +1·0 %
0·8
0·6
0·4
0·2
0
Δu/Δσ1
σ3 in Undrained Test
⊙ 120
+ 70
⊡ 40
△ 15
points marked thus '△' correspond to maximum pore pressure
● Ko Tests
■ 1/F "
0
1
2
3
4
5
6
7
σ1'/σ3'

FIG. 5:88



σ_3 in Undrained Test.

⊙ 120
\+ 70
⊡ 40
△ 15

points marked thus ⧋ correspond to maximum pore pressure

● K_0 Tests
■ $1/F$ "

FIG. 5:89

the average loads for practical purposes, it will follow that w.r.t. to the compression part of the $\frac{\Delta u}{\Delta \sigma_1}$ v $\frac{\sigma'_1}{\sigma'_3}$ relationship (i.e. increasing pore pressure) both samples possess similar characteristics.

Although equation 5:2 is not linear, the test results in Figs. 5:88 and 5:89, showed that within the range of loads used in practice, it can be approximated to an average straight line as long as the pore pressure increases. This provides for an approximate method to determine the pore pressure ratio for any value of σ'_1/σ'_3 (provided the sample does not become saturated) by only performing the series of undrained tests necessary to determine C' and ϕ' and avoiding the elaborate procedure followed in the K_o and $1/_F$ tests. The value of σ'_1/σ'_3 for the $1/_F$ condition is a function of that at failure, while that corresponding to the K_o condition is approximately the mean of unity (the B condition) and maximum σ'_1/σ'_3 in the undrained shear test for the range of loads met with in practice.

5. Pore Pressure at Failure in Undrained Shear Tests.

The relationship between the pore pressure at failure and the corresponding major principal stress has been studied w.r.t. the two failure criteria, i.e. the maximum principal stress ratio criterion and the maximum deviator stress, Fig. 5:81, 5:82, and 5:83.

For a certain range, this relationship was found to be approximately linear, which in fact is a direct evidence that over this range ϕ_u and ϕ' are constants. The excess pore pressure at failure (Δuf) can thus be determined in terms of ϕ_u and ϕ' by equation 3:6.

In terms of the pore pressure parameters B and a:-

$$\Delta uf = B\,\Delta\sigma_3 + (a)f\,.\,(\Delta\sigma_1 - \Delta\sigma_3)$$

(af) for triaxial tests is equal to $\dfrac{\Delta uf - B\Delta\sigma_3}{(\Delta\sigma_1 - \Delta\sigma_3)_f}$

It is a constant for all cell pressures in the case of saturated soils where B = 1. For partially saturated soils (af) varies with cell pressure since B also is not constant (S. and B. 1954)*. To prove this experimentally let us put equation 3:12 in the form:

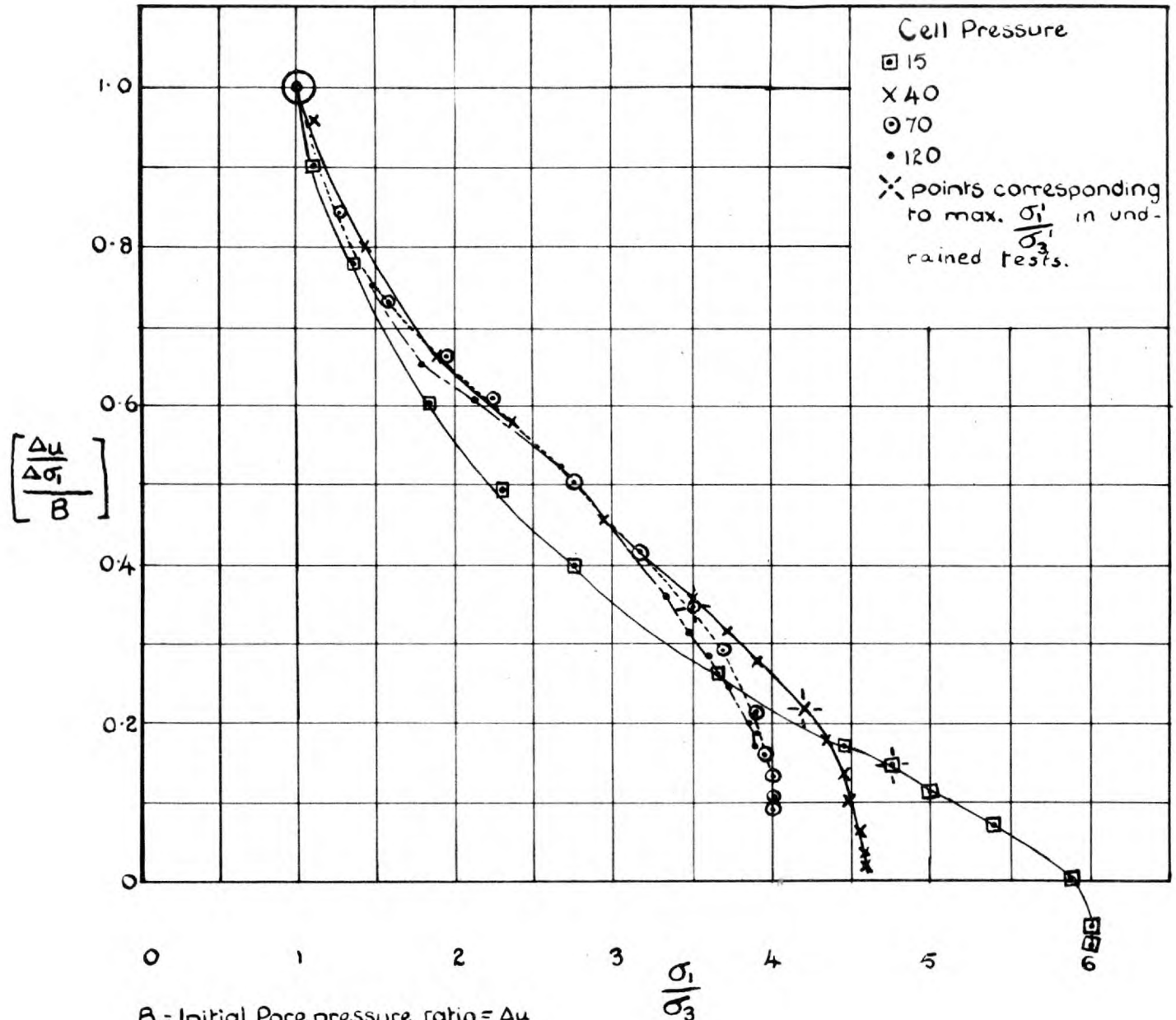
$$\frac{\Delta u}{B.\Delta\sigma_1} = 1 + \left(\frac{a}{B} - 1\right)\left(\frac{\Delta\sigma_1 - \Delta\sigma_3}{\Delta\sigma_1}\right)$$

$$= 1 + \left(\frac{a}{B} - 1\right)\left(1 - \frac{\Delta\sigma_3}{\Delta\sigma_1}\right) \qquad 5:3$$

$\dfrac{\Delta u}{B\Delta\sigma_1}$ is unity before shearing the sample.

If we plot $\dfrac{\Delta u}{B\Delta\sigma_1}$ vs $\dfrac{\sigma_1}{\sigma_3}$ from the results of undrained shear tests on samples compacted at the same moisture content but under different cell pressures we find that the resulting curves start at the same points (where $\dfrac{\Delta u}{B\Delta\sigma_1} = 1$) and then proceed independently which shows that "a" varies with cell pressure at failure. Fig. 5:90 shows the results of four samples at approximately optimum moisture content and

* Skempton & Bishop (1954)



B = Initial Pore pressure ratio = $\frac{\Delta u}{\Delta \sigma_3}$.

$\frac{\Delta u}{\Delta \sigma_1}$ = Pore pressure ratio at any stage during shear.

Aprox. M/C. : Opt. %

FIG. 5:90

tested in undrained shear under four cell pressures of 15, 40, 70 and 120 p.s.i. Fig. 5:91 gives typical values of af for different saturated and partially saturated soils, together with the results obtained from the present series of tests for the dry, optimum and wet samples.

In conclusion we note that the excess pore pressure is a direct function of the volume change a sealed partially saturated soil element undergoes. The pore pressure ratio $\frac{\Delta u}{\Delta \sigma_1}$ can also be expressed as a function of the principal stress ratio corresponding to the system of loads causing them. It was shown that the greater the principal stress ratio the lower is the value of $\frac{\Delta u}{\Delta \sigma 1}$ for a particular moisture content. The pore pressure ratio and the principal stress ratio can be considered approximately to possess a linear relationship.

Pore Pressure Parameter "a" At Failure.

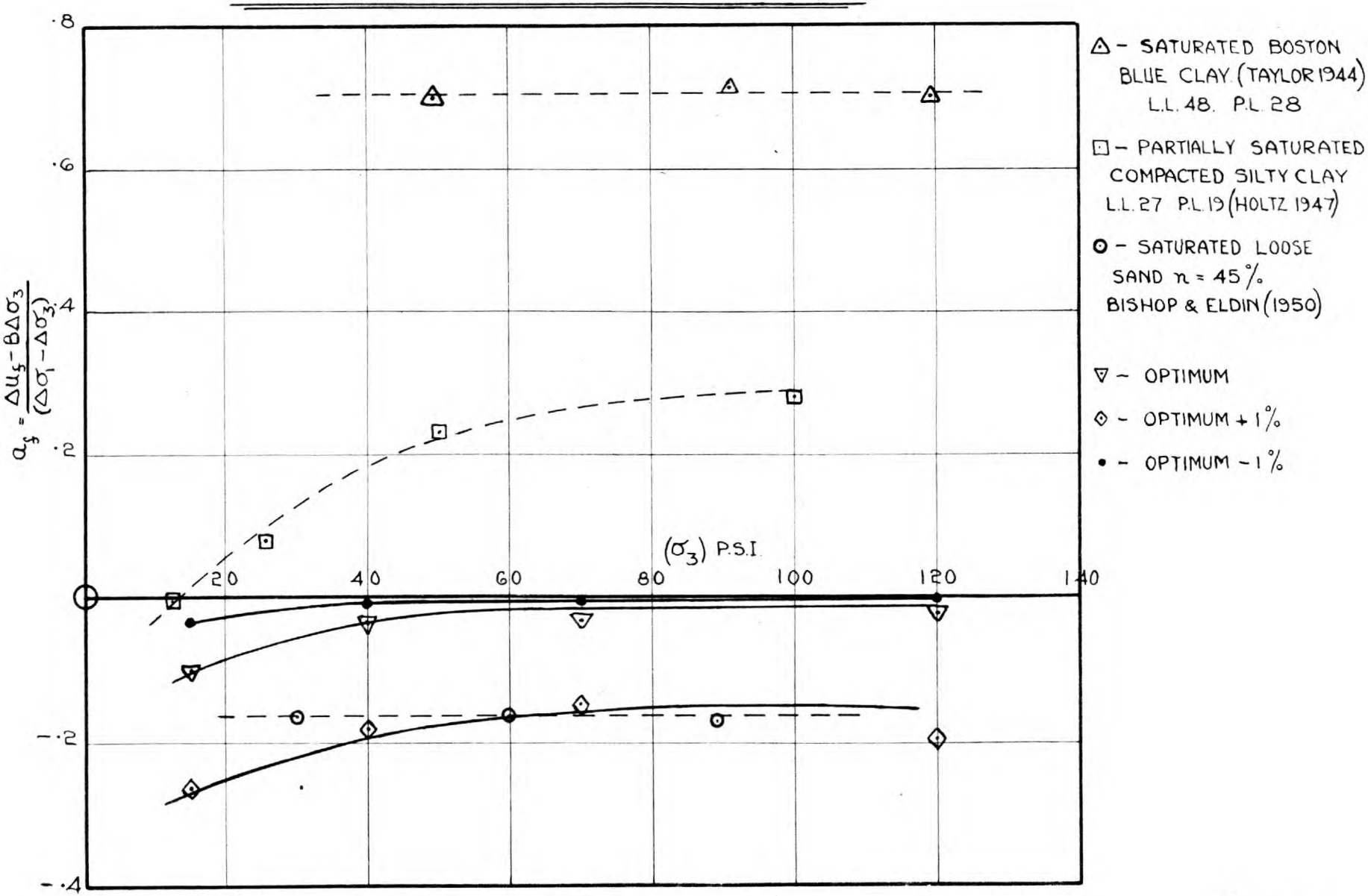


FIG. 5:91

Chapter 6

SUMMARY AND GENERAL CONCLUSIONS

A. The Shear Strength

The angle of shearing resistance ϕ' varies only slightly with moisture content and the degree of saturation. It is also slightly affected by the type of shear test provided the test results are corrected for the energy necessary to change the volume of the sample during shear. The results of undrained shear tests represent to a good deal of accuracy the average results obtained under different conditions of shear provided these results are in terms of the moisture content at failure.

The apparent cohesion C' varies only slightly with the type of tests, but is closely related to the moisture content at failure.

For a given initial moisture content we find that soils compacted at optimum show only little change in strength on saturation (as compared with the results of undrained tests)

while dry soils show a large decrease in strength. Soils placed on the wet side of the optimum show a gain in strength.

From the point of view of earth dam construction, the drop in strength on saturation of dry soils can be allowed for in the design, but the accompanying decrease in volume has in practice led to dangerous settlement cracks and even complete failure (Sherard, 1953). On the other hand, soils placed on the wet side of the optimum moisture content will be subject to very large pore pressures at the end of construction. Provided that these pore pressures are allowed for in the design (either by using a wider cross section or drainage layers), the settlement which occurs during the dissipation of such high pore pressures does not appear to affect the watertightness of the dam.

If field control of the moisture content is possible (climatic conditions and technical organisation favourable) it will be seen from the test results that the moisture content close to the optimum will to a large extent avoid the disadvantages of the two extremes.

B. The Pore Pressure and Compressibility

For any particular moisture content, the highest excess pore pressure occurs when an all round system of loads is applied. The minimum excess pore pressure occurs at undrained shear failure. The loading condition in which no lateral

yield is allowed (the K_o condition) together with the condition corresponding to a factor of safety F (the $1/F$ condition) represent two intermediate values of the pore pressure. Thus, while in a limit design stability calculation we use C' and ϕ' obtained from failure conditions, the pore pressure corresponding to undrained failure conditions would be much less than that measured in the actual dam.

The pore pressure ratio i.e. the ratio between the excess pore pressure Δu and the major principal stress $\Delta \sigma_1$ was found to be a function of the effective principal stress ratio σ'_1/σ'_3. This ratio varies from 1 for the all round system to an average maximum value of 5 in undrained tests (i.e. the maximum σ'_1/σ'_3 in undrained shear tests) while for the K_o and $1/F$ conditions σ'_1/σ'_3 has intermediate values and are both close to the mean of 1 and 5 for practical purposes (if F = 1.5). The relationship between $\frac{\Delta u}{\Delta \sigma_1}$ and σ'_1/σ'_3 can be approximated to a straight line for all types of tests as long as the pore pressure is increasing. This permits the use of an approximate method of determing the excess pore pressure for any value of the principal stress ratio, by only performing the series of undrained tests necessary in any case to obtain C' and ϕ' (initial pore pressure corresponds to $\sigma'_1/\sigma'_3 = 1$ and the other values are obtained as σ'_1/σ'_3 increases during the shear test).

The rate of variation of the excess pore pressure with moisture content is largest around the optimum. Therefore, fill materials placed at optimum will be sensitive to the slight changes in moisture contents w.r.t. pore pressure. This effect must be allowed for both in design and in field control during construction.

The volume change, which is a function of the effective stress, was also found to be controlled by the principal stress ratio in the same way as the excess pore pressure.

ACKNOWLEDGEMENTS

The work described in this thesis was carried out in the Soils Laboratory of Imperial College, University of London, under the supervision of Assistant Professor A. W. Skempton, D.Sc., A.M.I.C.E., to whom the author wishes to express his gratitude for kind help and encouragement throughout the research.

Thanks are also due to Dr. A. W. Bishop, A.M.I.C.E. for much valuable help and constant interest.

The author wishes to thank his colleagues, Miss U. Desai, and Mr. J. G. Lewis for assisting in carrying out some of the tests.

The research has been carried out during a study leave granted to the author by the Egyptian Government.

APPENDIX

EFFECT OF RUBBER MEMBRANE OF THE MEASURED STRENGTH OF 4" DIA. SAMPLES

Henkel and Gilbert (1952) showed that in the undrained triaxial tests on saturated clay samples ($1\frac{1}{2}$" Dia. x 3") the rubber membrane gives rise to an apparent increase in strength. Tests on identical saturated clay samples indicated that the unconfined compression test gives the lowest strength while a higher strength was obtained when the unconfined sample was surrounded by a membrane. Still a higher strength was obtained in the triaxial compression test. This experimental evidence gave rise to an approximate theoretical investigation into the effect of the rubber membrane.

By assuming that the membrance and the triaxial specimen deform as a unit, the rubber membrane acts as a compression shell and the total compression load P at any axial strain "e" will be given by the equation:

$$P = (\bar{\sigma}_1 - \bar{\sigma}_3)_1 \cdot Ae + \pi \cdot D_o \cdot M e$$

where $(\bar{\sigma}_1 - \bar{\sigma}_3)_1$ denotes deviator stress in specimen

Ae denotes corrected area of the sample at strain e

D_o denotes initial diameter of the sample

M denotes compression modulous of rubber member lb/inch

and the measured compression stress will be equal to:

$$(\bar{\sigma}_1 - \bar{\sigma}_3)_1 + \frac{\pi \cdot D_o \cdot e(1-e) \cdot M}{A_o}$$

where Ao is the initial area of the sample, and the second term is the rubber correction.

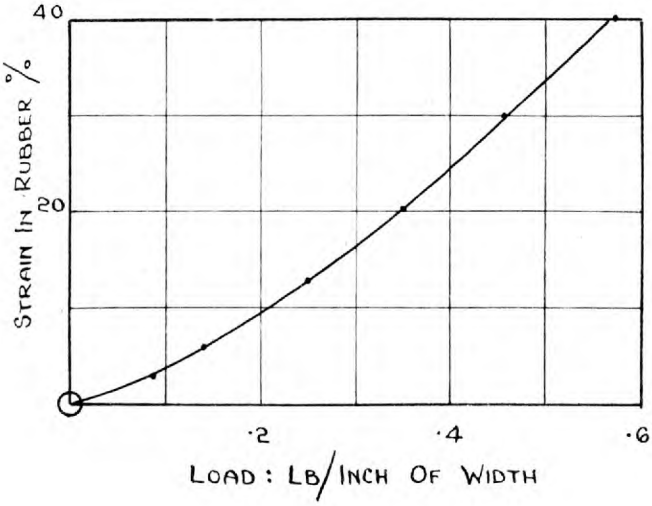
To determine the compression modulous M of the rubber membrane (9×10^{-3} inch thick)and 4 inch dia.) a load, strain relationship was established by performing extension tests on a one inch strip of the membrane as shown in Fig. A:1.

The following table gives the rubber corrections in lbs/square inch at four different strains for a 4inch diameter sample:

Strain %	M lb/inch	Rubber Correction p.s.i.
5	2.4	0.12
10	2.0	0.20
15	1.8	0.23
20	1.75	0.29

LOAD, STRAIN RELATIONSHIP

FOR A $\frac{9}{1,000}$ INCH RUBBER MEMBRANE.



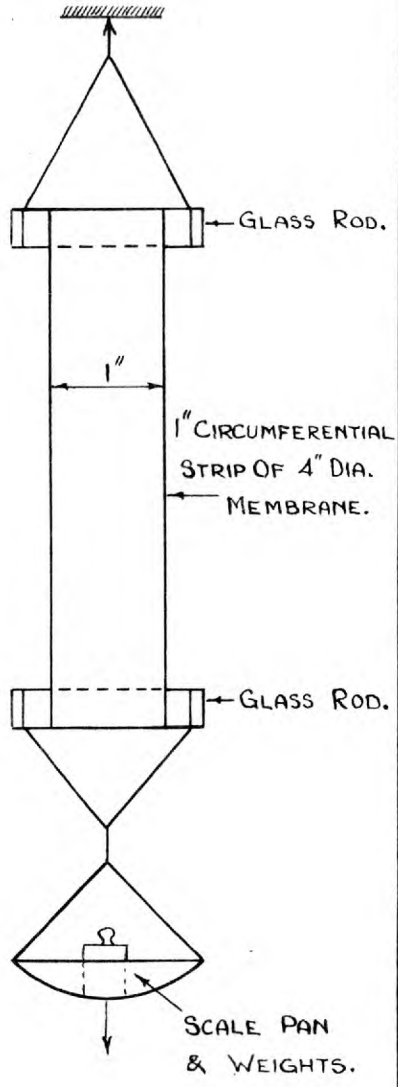


FIG. A:1.

It is noticed that the rubber correction is so small as compared with the strength of the samples. In the series of tests presented in this thesis, the effect of the rubber membrane was neglected.

BIBLIOGRAPHY

Bishop A. W. (1950)
"Summarised proceedings of a Conference on Stress Analysis". British JOURNAL OF APPLIED PHYSICS.

Bishop A. W. and Eldin G. (1950).
"Undrained triaxial tests on Saturated Sands and their Significance in the General Theory of Shear Strength". GEOTECHNIQUE, Vol. II No. 1.

Bishop A. W. (1952).
"The Stability of Earth Dams". A Thesis submitted to London University.

Bishop A. W. and Gamal A. K. (1953).
"The effect of the Stress History on the Relation between ϕ and the Porosity". Proceedings of the Third Int. Conf. Soil Mech. Vol. I. Zurich.

Bjerrum L. (1951).
"Results of some Triaxial Tests carried out for a Rolled Earth Dam". E. T. H. Zurich - a private report.

Bjerrum L. (1951).
"Kraftwerk Marmorera - Tinzen Stadt Zurich". Versuchsanstalt für Wasserbau und Erdbau an der E. T. H. Erdbaubteilung.

Brahtz J. H. A. with Bruggeman J. R. and Zangar C. N. (1939)
"Notes on Analytic Soil Mechanics".

Casagrande A. and Wilson S. D. (1951)
"Report to Waterways Experiment Station, Vicksburg U. S. A. on "Triaxial research performed during 1950 - 1951.

Eldin A. K. (1951)
"Fundamental factors controlling shear properties of Sands". A Thesis submitted to the University of London.

El Ramli A. H. (1949)
"Theoretical and Experimental Study on Sand Pressure on retaining L walls". A Thesis submitted to Cairo University.

Gersevanoff N. (1936).
"Improved methods of Consolidation Test and of the Determination of the Capillary pressure on Soils". Proc. Int. Conf. on Soil Mech., Harvard, Mass. U. S. A. Vol. 1.

Gibbs H. J. (1948).
"Placement Moisture Control Test". Proc. of Training Conferences on Earth and Concrete and Allied Subjects; Bureau of Reclamation U. S. A.
Also, Holtz. W. G., Proc. Amer. Soc. Test Mat. Vol. 48 (1948) P.1240.

Gibbs H. J. (1950).
"The Effect of Rock Content and Placement Density on Consolidation and Related Pore Pressures in Embankment Construction". Proc. Amer. Soc. Test Mat. 50.:1343.

Gibson R. F. (1951).
"An Investigation of the Fundamental Shear Strength Characteristics of Clays". A Thesis submitted to the University of London.

Gibson R. F. and Henkel D. J.
"Influence of Duration of Tests on Measured "Drained" Strength". A paper to be published in GEOTECHNIQUE in 1954.

Glynn D. F. (1948)
"Application of Triaxial Compression Tests to Stability Analysis of Rolled Fill Earth Dams". Proc. 2nd Int. Conf. Soil Mech. Rotterdam. Vol. III.

Gould J. P. (1953)
"The Compressibility of Rolled Fill Materials determined from Field Observations". Proc. of the Third Int. Conf. on Soil Mech., Zurich. Vol. II.

Gueze E. C. W. A. (1948)
"Critical Density of some Dutch Sands". Proc. 2nd Int. Conf. Soil Mech. Rotterdam. Vol. III.

Hamilton L. W. (1939)
"The Effects of Internal Hydrostatic Pressure on the Shearing Strength of Soils". Proc. Amer. Soc. Test Mat. Vol. 39, P.1100.

Hilf J. W. (1948)
"Estimating Construction Pore Pressures in Rolled Earth Dams". Proc. 2nd Int. Conf. Soil Mech., Rotterdam. Vol. III.

Holtz W. G. (1947)
"The Use of the Maximum Principal Stress Ratio as a Failure Criterion in Evaluating Triaxial Shear Tests on earth Materials." Proc. Amer. Soc. Test Mat. Vol. 47, P. 1067.

Hvorslev M. J. (1937)
"Uber die Festigkeitseigenschaften gestoerter bindiger Boeden". Ingeniorvidenskabelige Skrifter. A. No. 45. Copenhagen.

Reiner M (1954) See Skempton and Bishop (1954)

Rendulic L. (1937)
"Ein grundgesetz der Tonmechanik und sein experimenteller Beweis". Bauingenieur 18.

Sherard J. L. (1953)
"Influence of Soil Properties and Construction Methods on the Performance of Homogeneous Earth Dams". Tech. Memo. 645 Bureau of Reclamation, U. S. A.

Skempton A. W. (1948)
"The Effective Stresses in Saturated Clays Strained at Constant Volume". Proc. Int. Conf. on Applied Mechanics, London. P. 378.

Skempton A. W. and Golder H. Q. (1948)
"Practical Examples of the $\phi = 0$ Analysis of Stability of Clays". Proc. 2nd. Int. Conf. Soil Mech. Vol. II.

Skempton A. W. and Bishop A. W. (1950)
"The Measurement of the Shear Strength of Soils". GEOTECHNIQUE, Vol. II No. 3.

Skempton A. W. and Bishop A. W. (1954).
Contribution to "Rheology of Building and Road Making Materials". To be published by "North Holland Publishing Company, Editor - M. Reiner.

Taylor D. W. (1944)
"M.I.T. Tenth Progress Report on Shear Research".

Taylor D. W. (1948)
"Fundamentals of Soil Mechanics" John Wiley and Sons, New York.

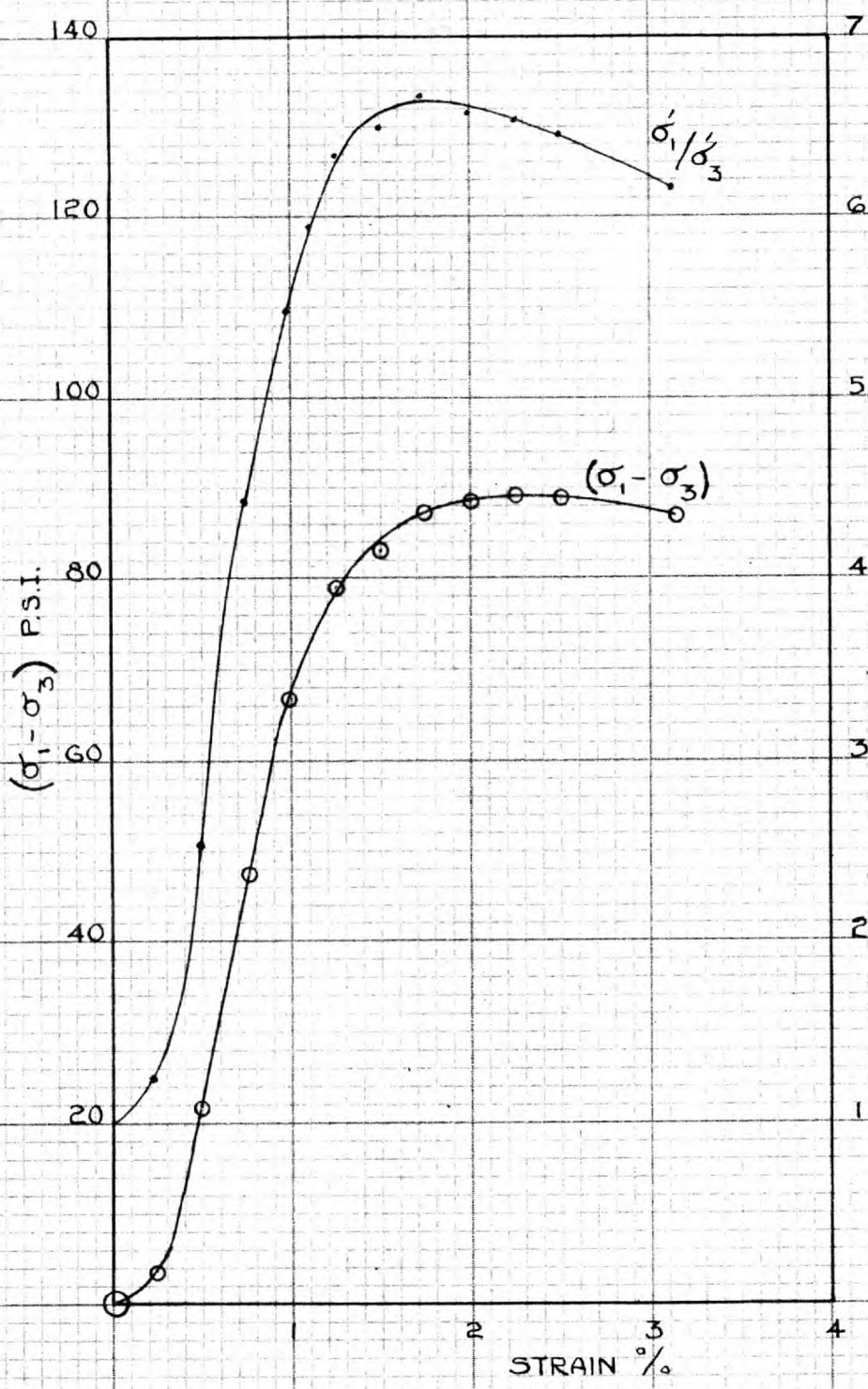
Terzaghi K. (1936).
"Simple Tests to Determine Hydrostatic Uplift". Eng. News Record. Vol. 113. No. 10. P.316.

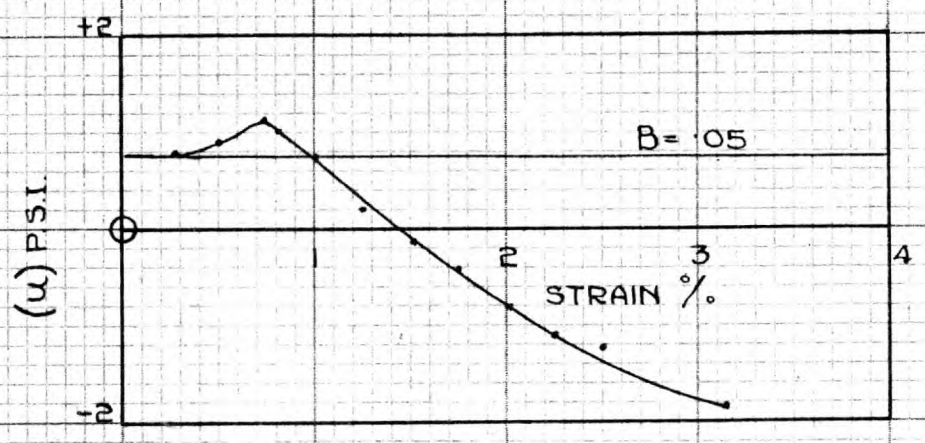
Terzaghi K. (1936).
"The Shearing Resistance of Saturated Soils and the Angle between the Planes of Shear". Proc. Int. Conf. Soil Mech. Harvard, Mass. U. S. A. Vol. I.

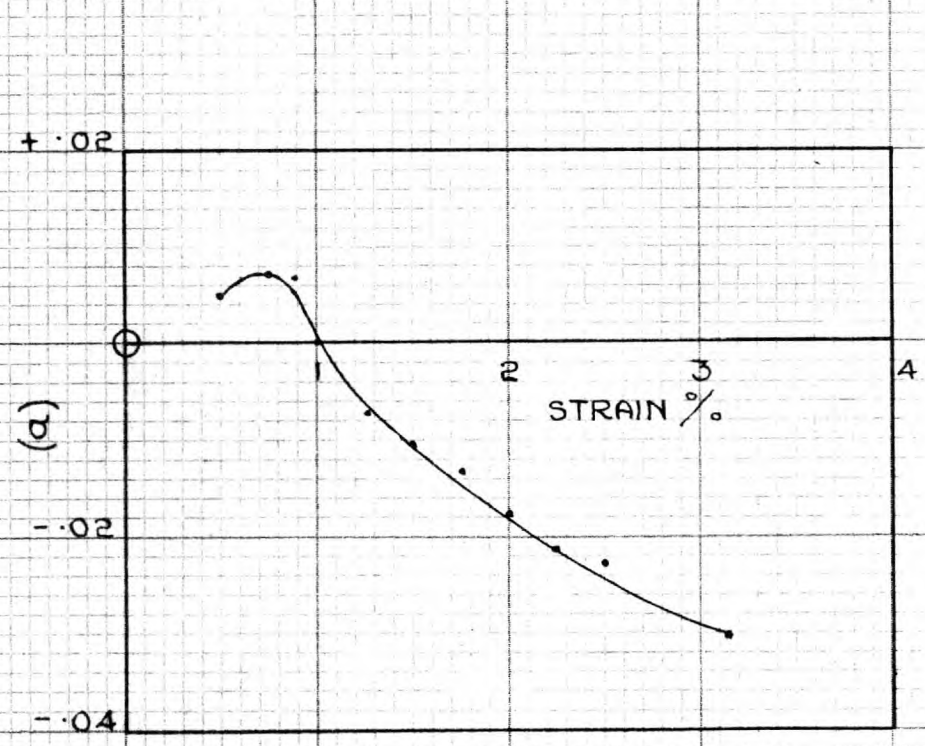
Terzaghi K. and Peck R. B. (1948)
"Soil Mechanics in Engineering Practice". John Wiley and Sons, New York.

Triaxial Shear Report (1947)
Waterways Experiment Station, Vicksburg, Mississippi U. S. A.

Tschebotarioff G. P. and Brown P. P. (1948)
"Lateral Earth Pressure as a Problem of Deformation or of Rupture". Proc. 2nd Int. Conf. Soil Mech. Rotterdam, Vol. II.





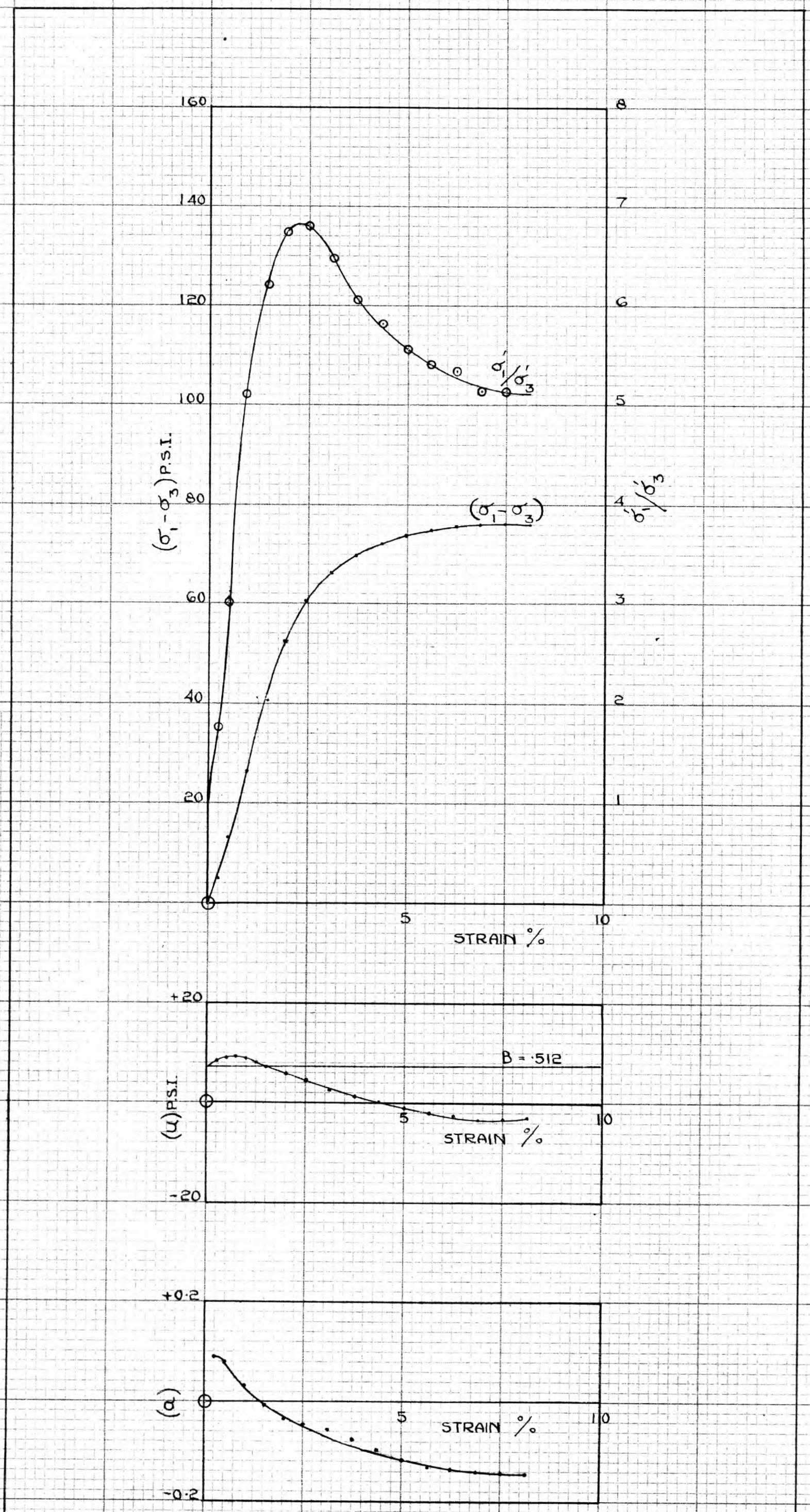


UNDRAINED TESTS.

CELL PRESSURE = 15 P.S.I.

M/C = Opt −1·0 %
S = 70 %
γ_d = 133·6 Lbs/Cu.Ft.

FIG. 5:8

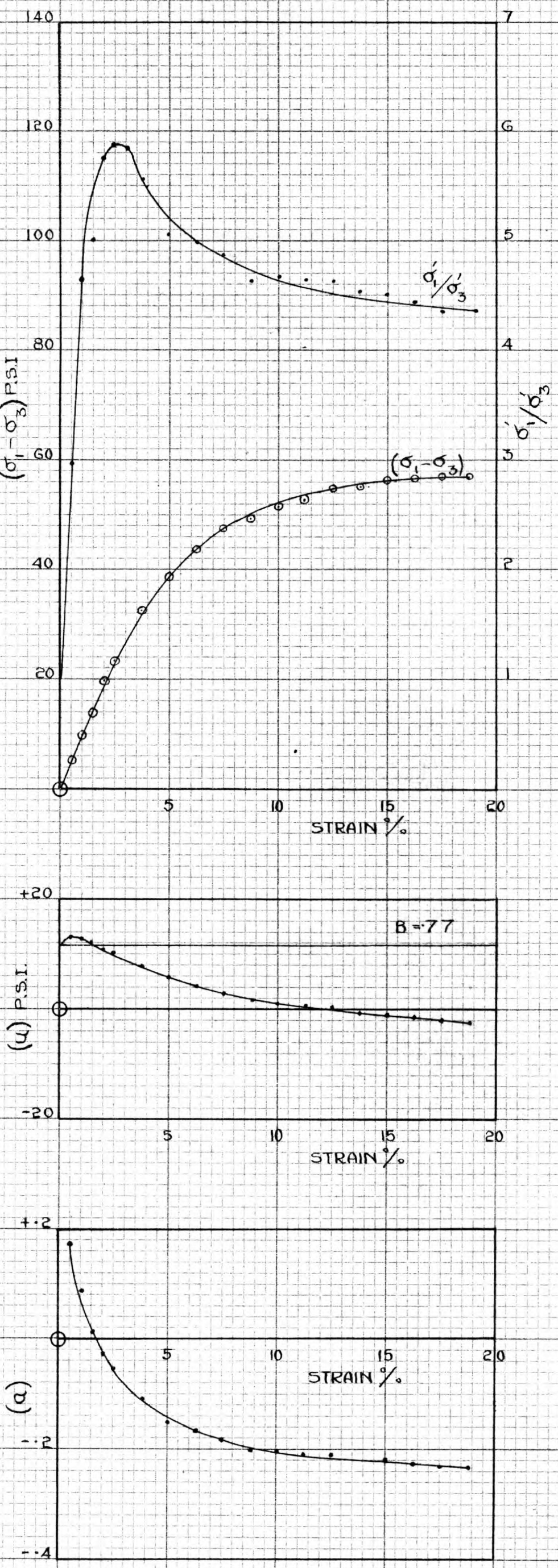


UNDRAINED TESTS.

CELL PRESSURE = 15 P.S.I

M/C = Opt
δ = 88 %
δ_d = 136 Lbs./Cu.Ft.

FIG. 5:9



UNDRAINED TESTS.

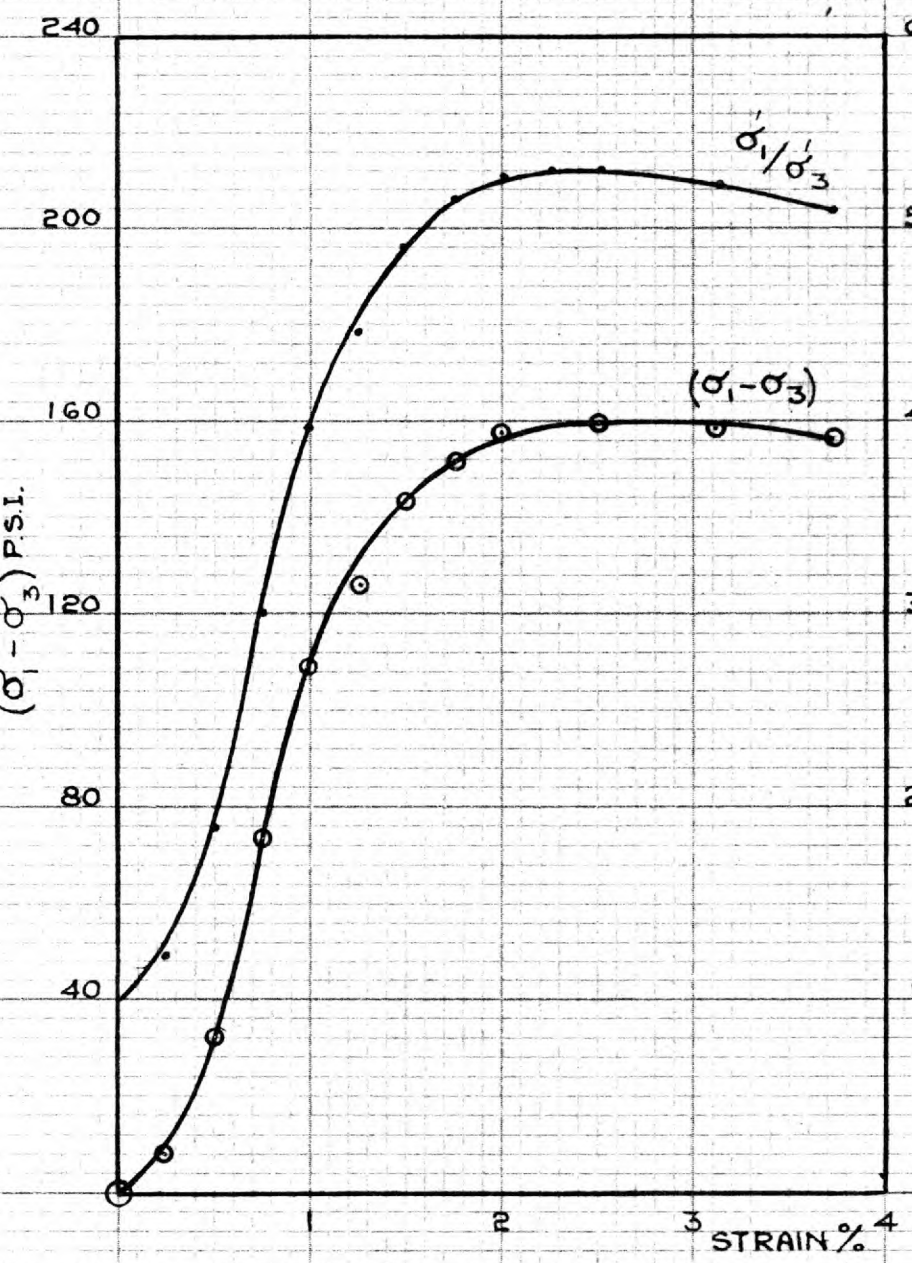
CELL PRESSURE = 15 P.S.I

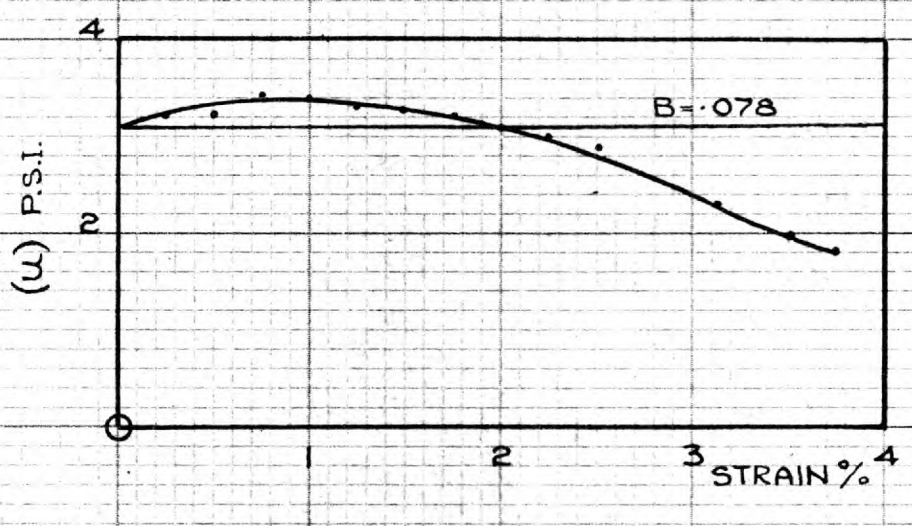
M/C = Opt + 1·15%

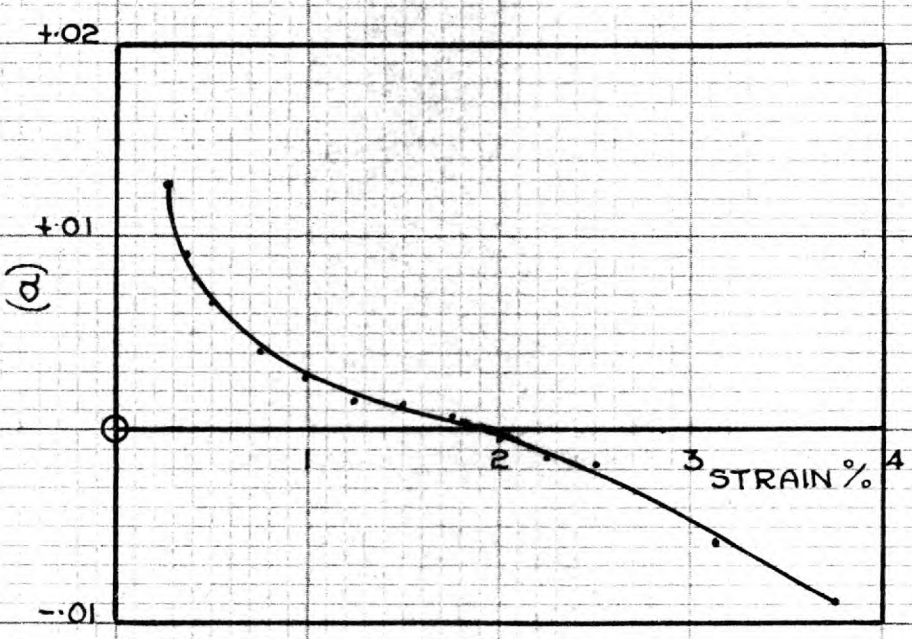
S = 93%

γ_d = 133·6 LBS/CU.FT.

FIG. 5:10





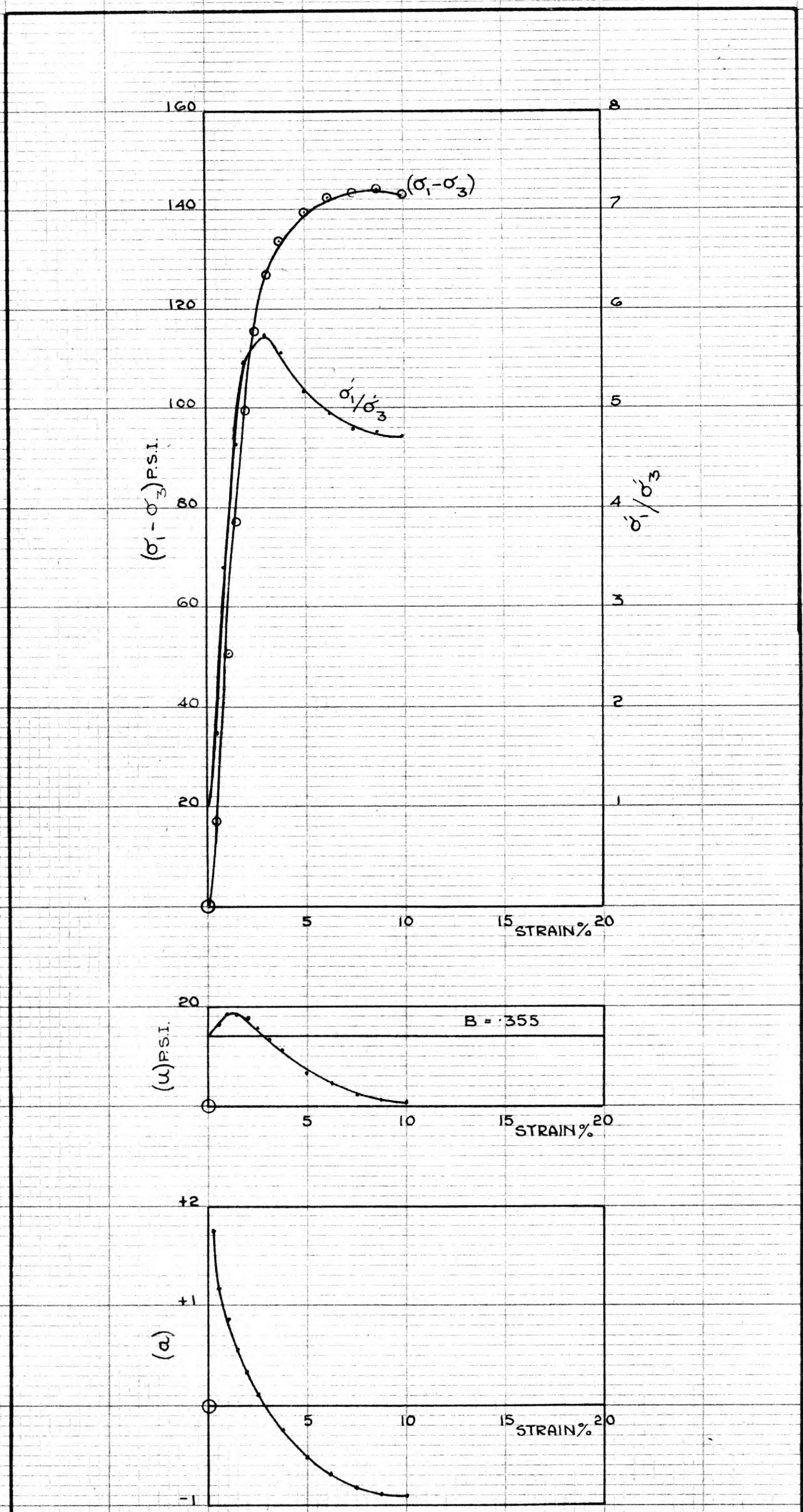


UNDRAINED TEST

CELL PRESSURE = 40 P.S.I.

M/C	= OPT. - 1·1%
S	= 70%
γ_d	= 133·0

FIG. 5:11

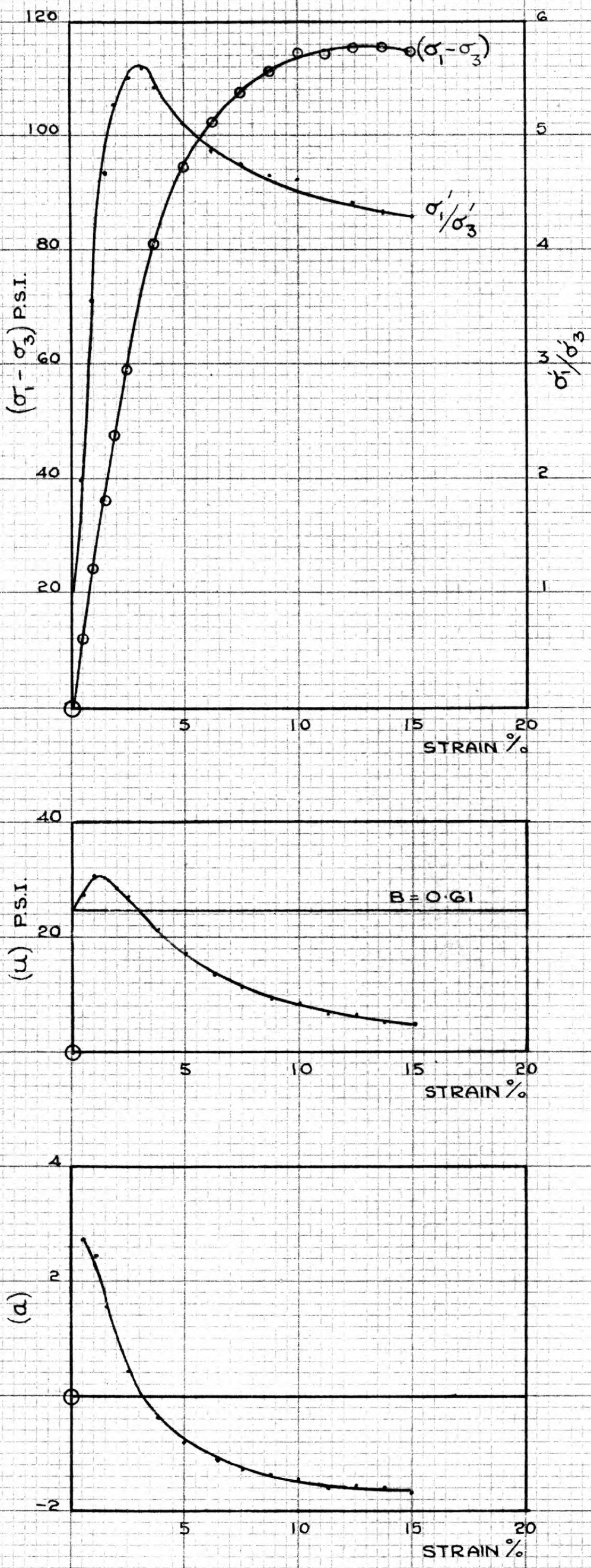


UNDRAINED TESTS.

CELL PRESSURE = 40 P.S.I.

M/C	= OPT.
S	= 87%
γ_d	= 135·5

FIG. 5:12

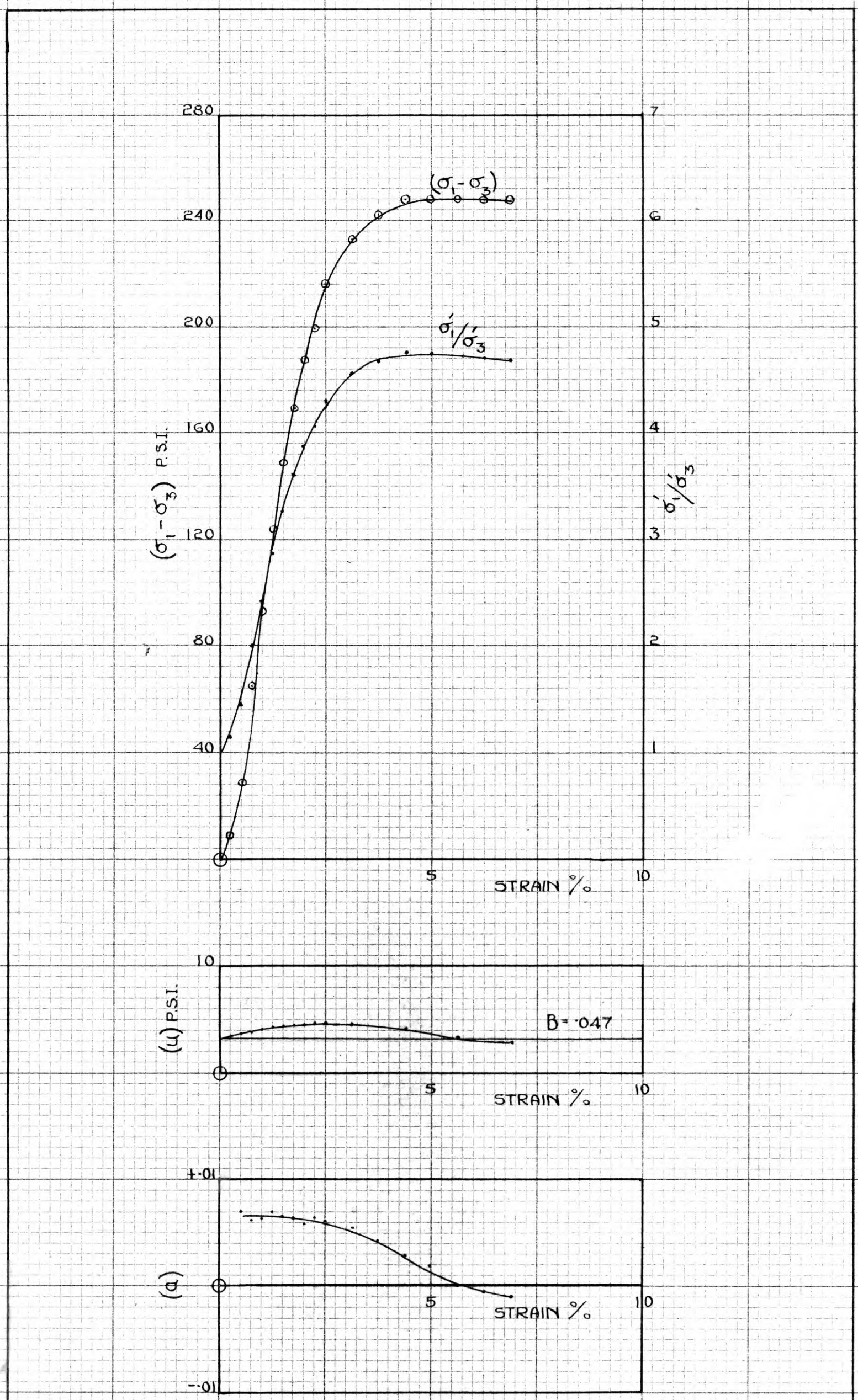


UNDRAINED TESTS.

CELL PRESSURE = 40 P.S.I.

M/C	= OPT. + 0·85%
S	≈ 92%
γ_d	= 134·4

FIG. 5:13

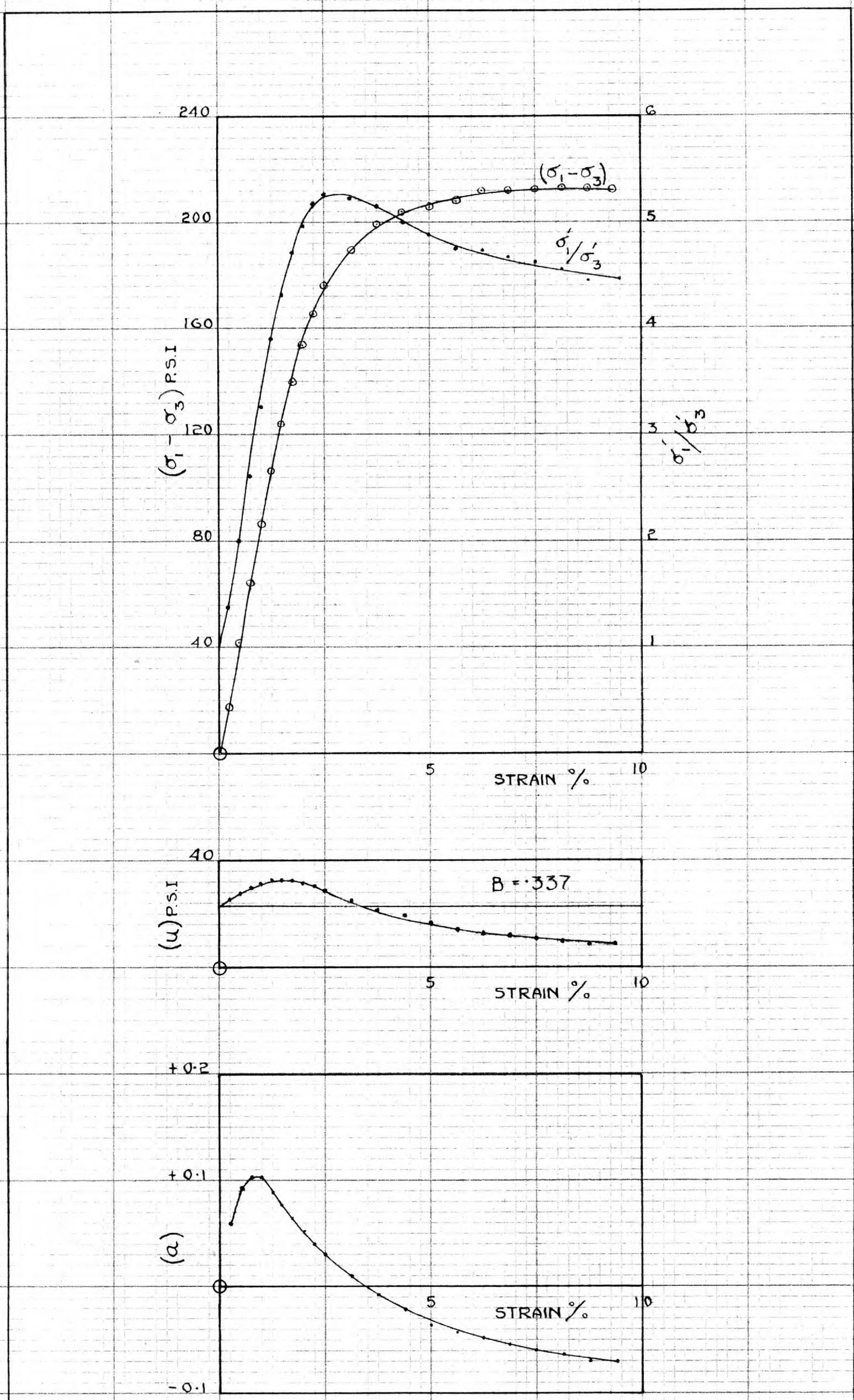


UNDRAINED TESTS.

CELL PRESSURE = 70 P.S.I.

M/C	=	Opt − 1·1%
S	=	69%
γ_d	=	133·5 Lbs/Cu.Ft

FIG. 5:14



UNDRAINED TESTS

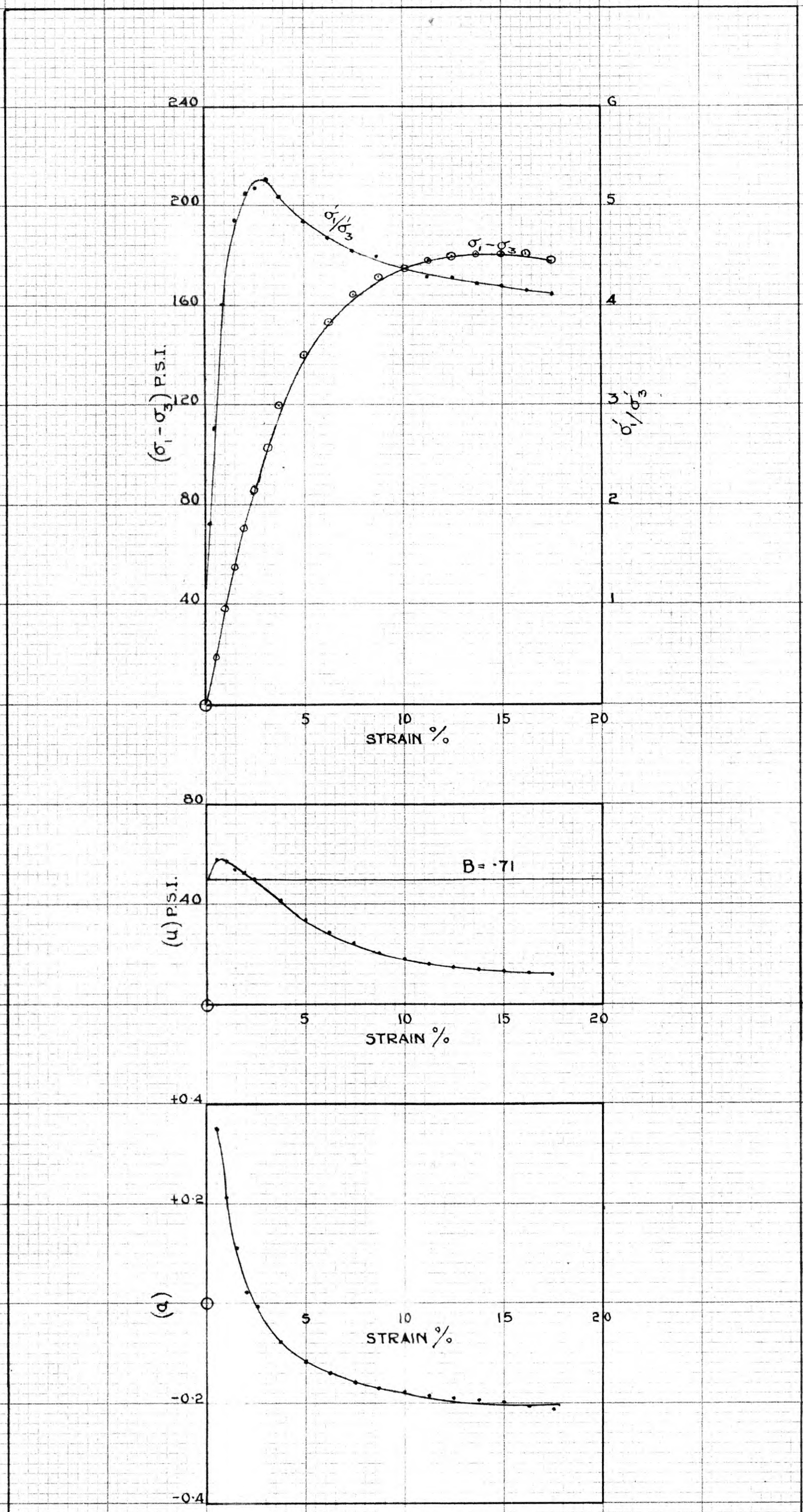
CELL PRESSURE = 70 P.S.I

M/C = Opt + 0·1 %

δ = 88 %

γ_d = 135·5 Lbs/Cu.Ft.

FIG. 5.15



UNDRAINED TESTS.

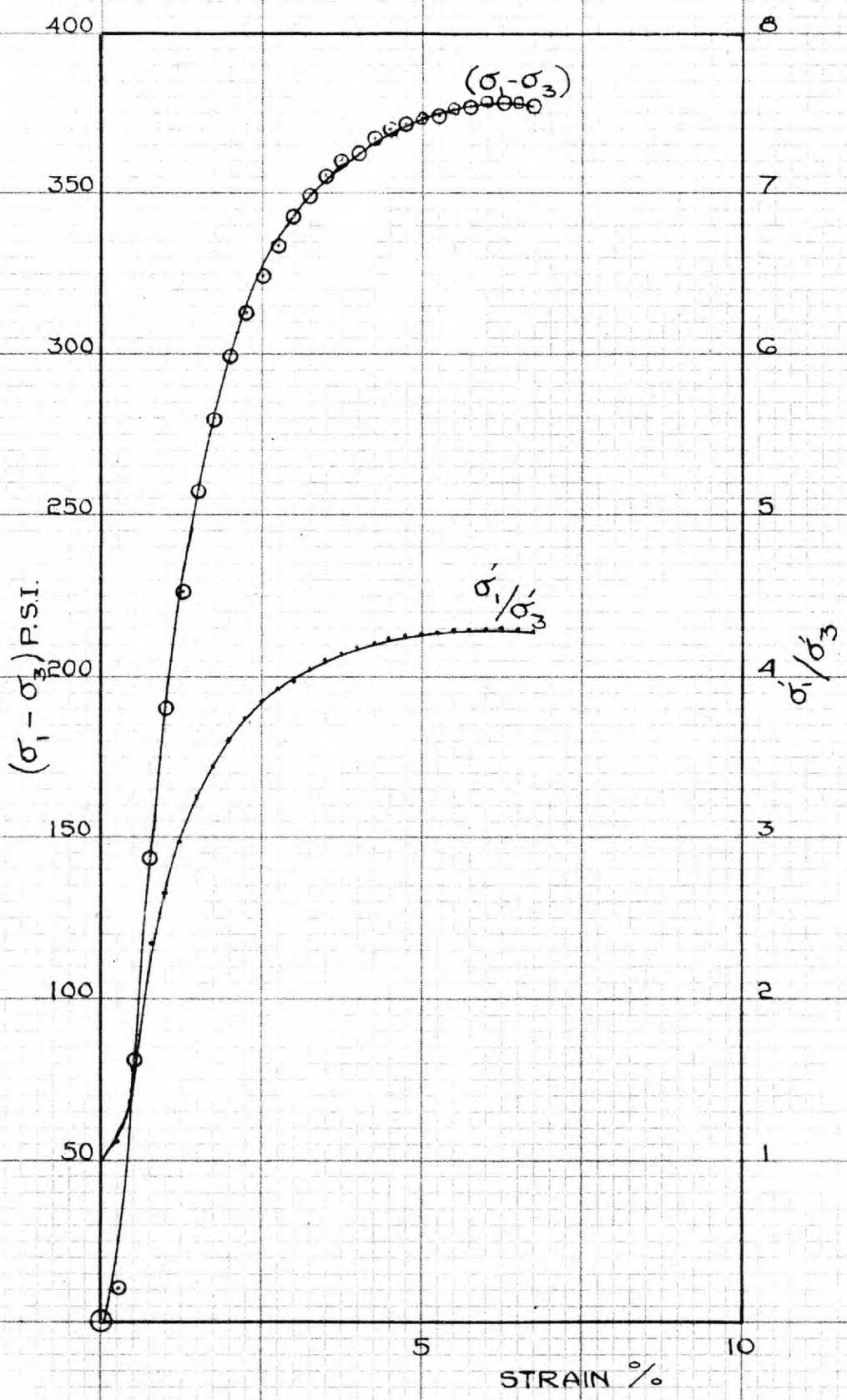
CELL PRESSURE = 70 P.S.I.

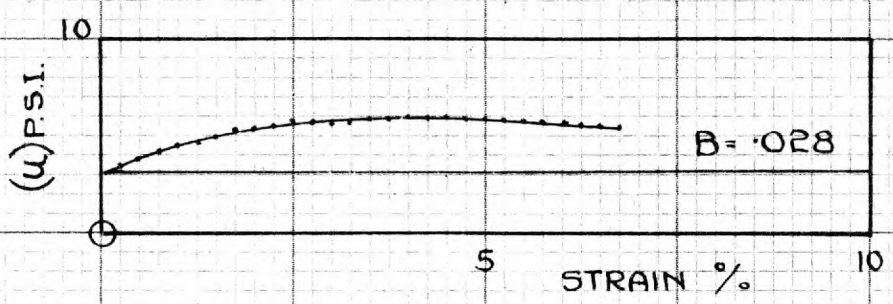
M/C = Opt + 1.0 %

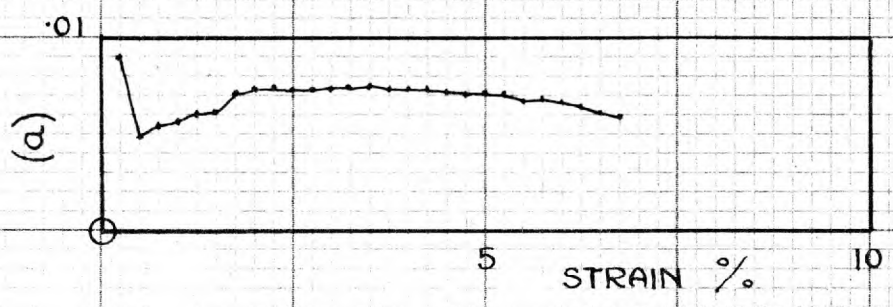
5% = 94

γ_d = 134·6 Lbs/Cu.Ft.

FIG. 5:16







UNDRAINED TESTS.

CELL PRESSURE = 120 P.S.I.

M/C = Opt − 1·15 %
S = 68 %
γ_d = 133·0 Lbs/Cu.Ft.

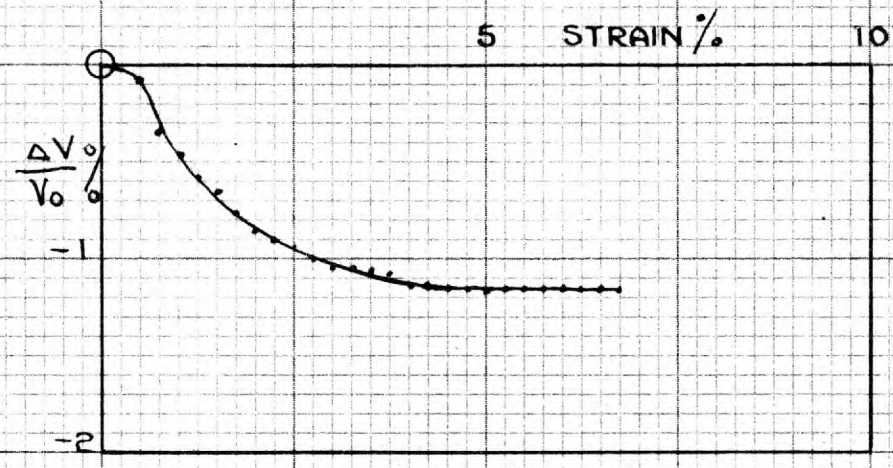
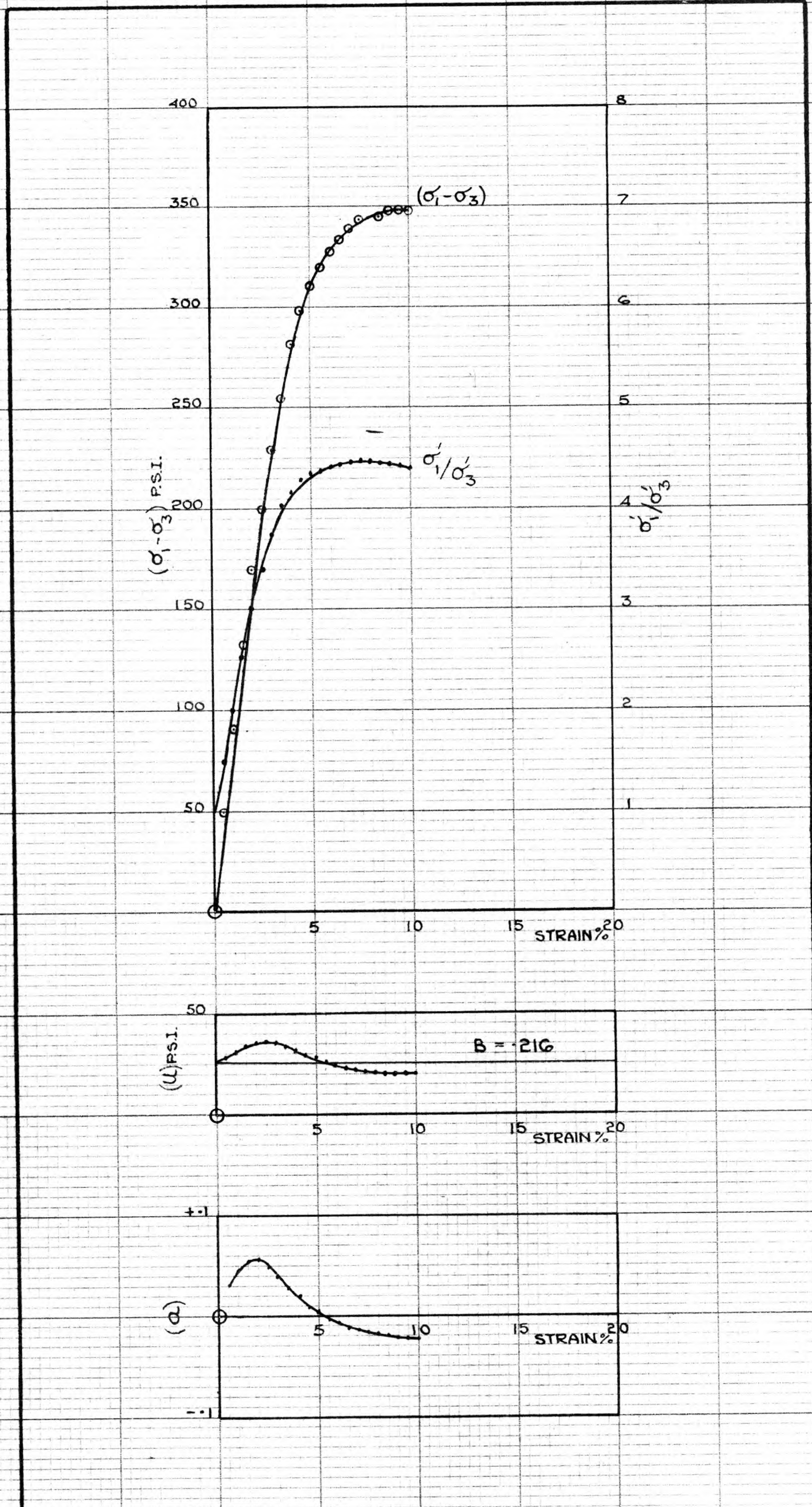


FIG. 5:17



UNDRAINED TESTS

CELL PRESSURE = 120 P.S.I.

M/C = OPT.
S = 89%
δ_d = 136

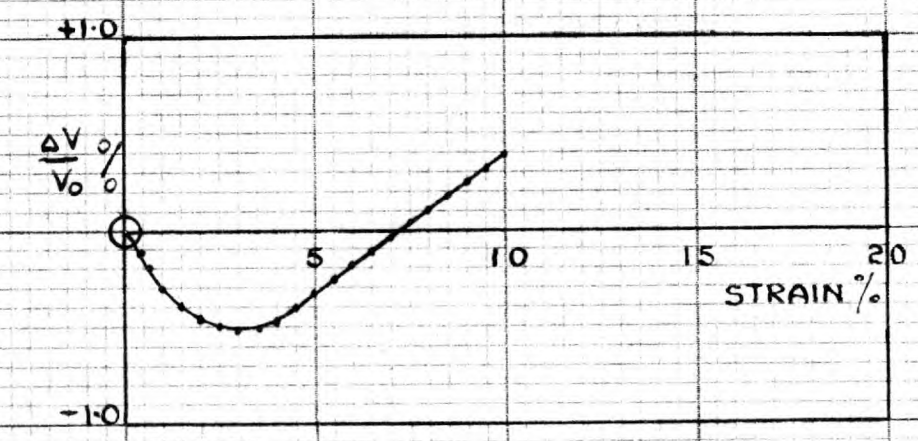
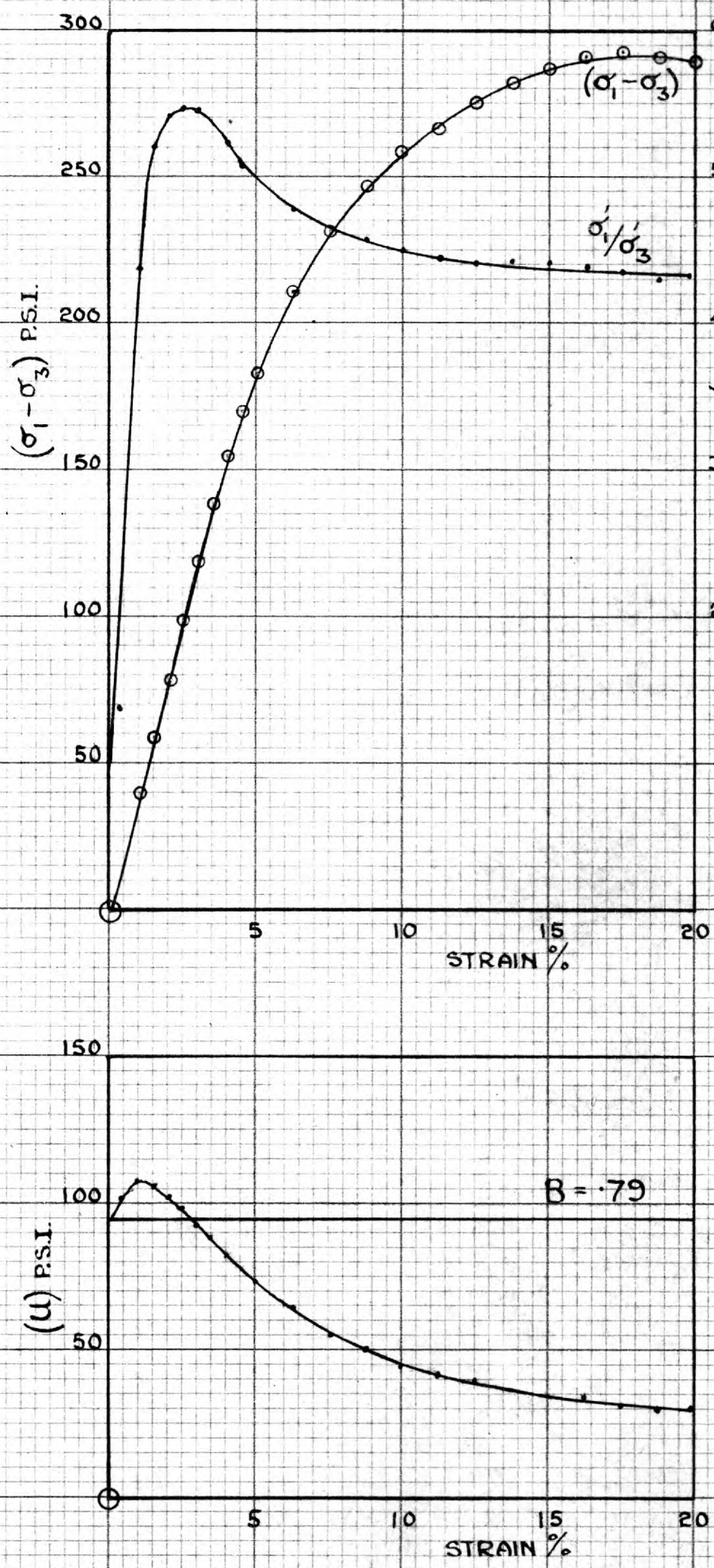
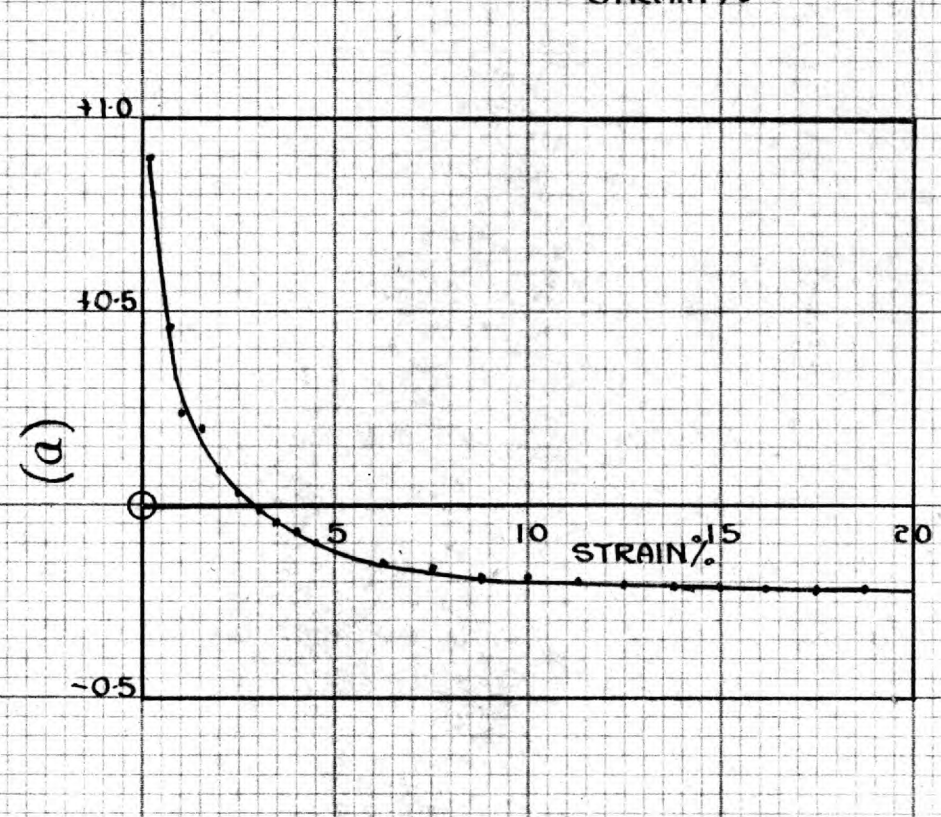
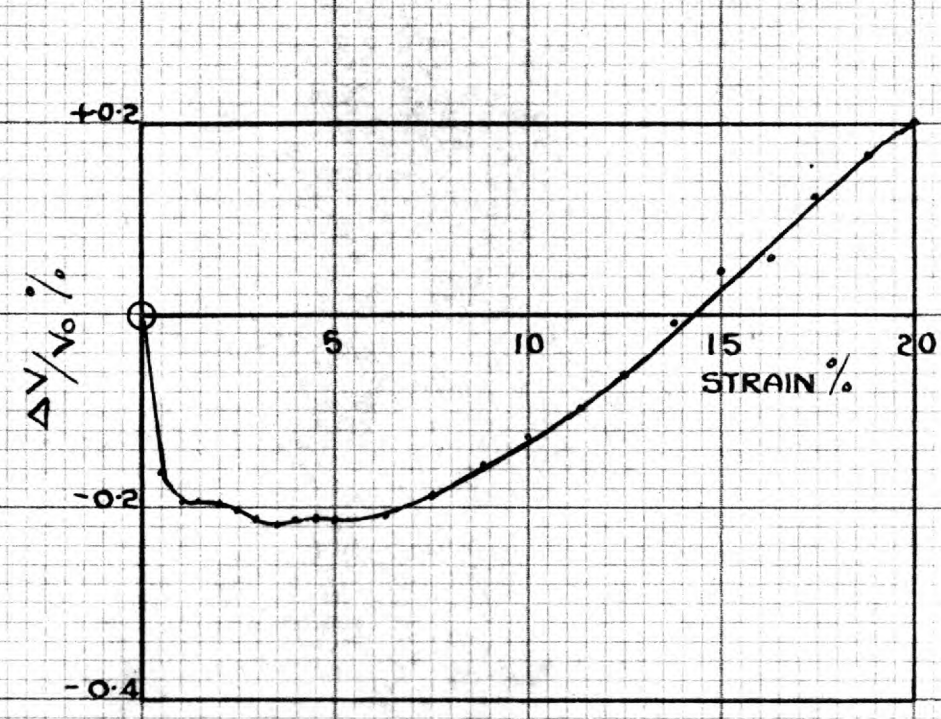


FIG. 5:18





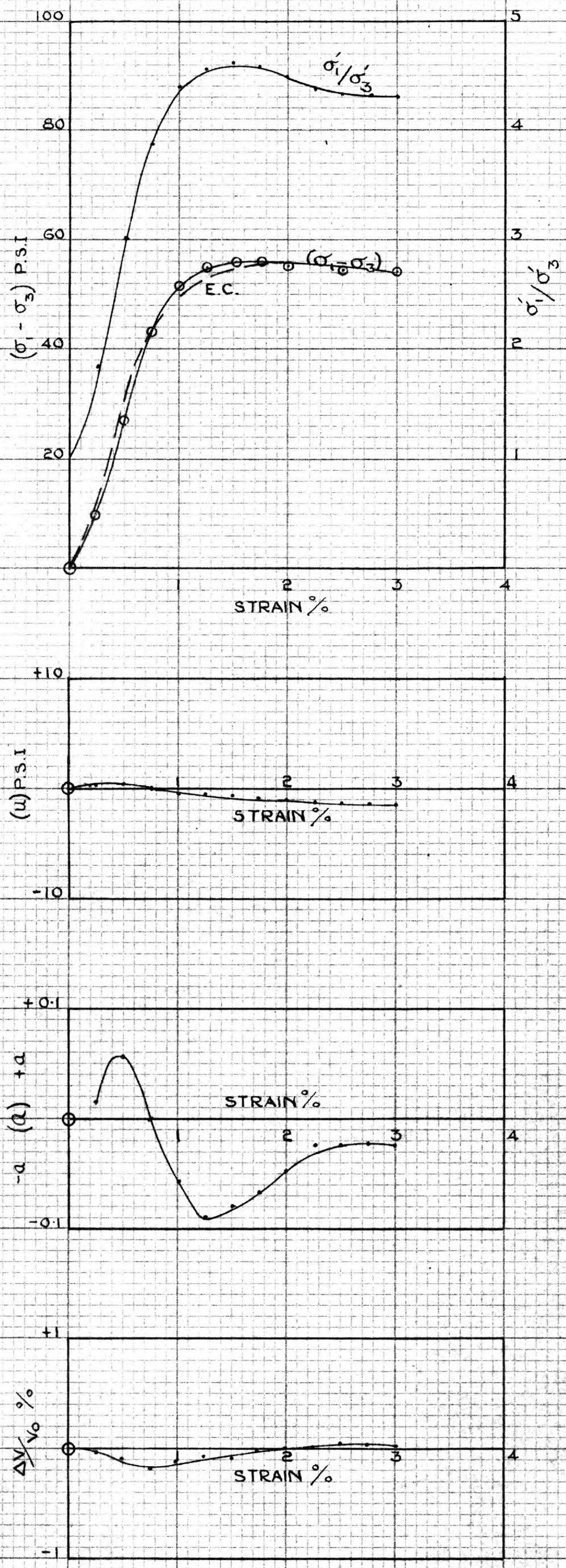


UNDRAINED TESTS.

CELL PRESSURE = 120 P.S.I.

M/C = OPT. + 0·9 %
S = 95·4 %
γ_d = 134·7 Lbs./Cu. Ft.

FIG. 5:19



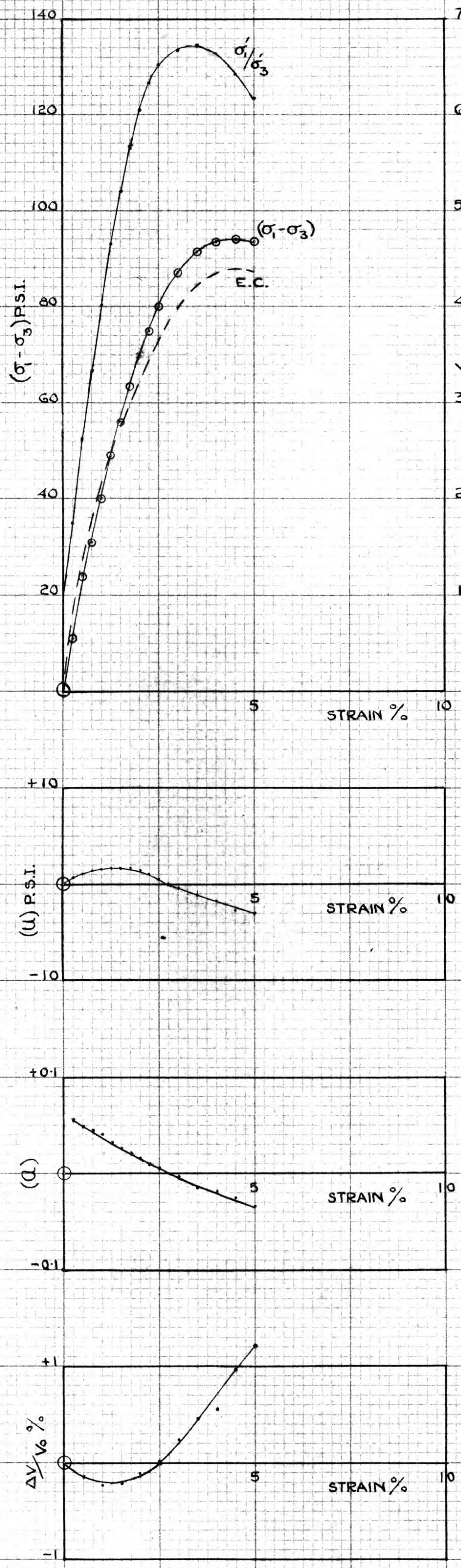
CONSOLIDATED UNDRAINED TESTS.

CELL PRESSURE = 15 P.S.I.

INITIAL CONSOLIDATION = 1·2%

	INITIAL	FINAL
M/C =	OPT.-0·65%	OPT.+0·85%
S =	69·0%	90·5%
γ_d =	132·0	133·6

FIG. 5:20



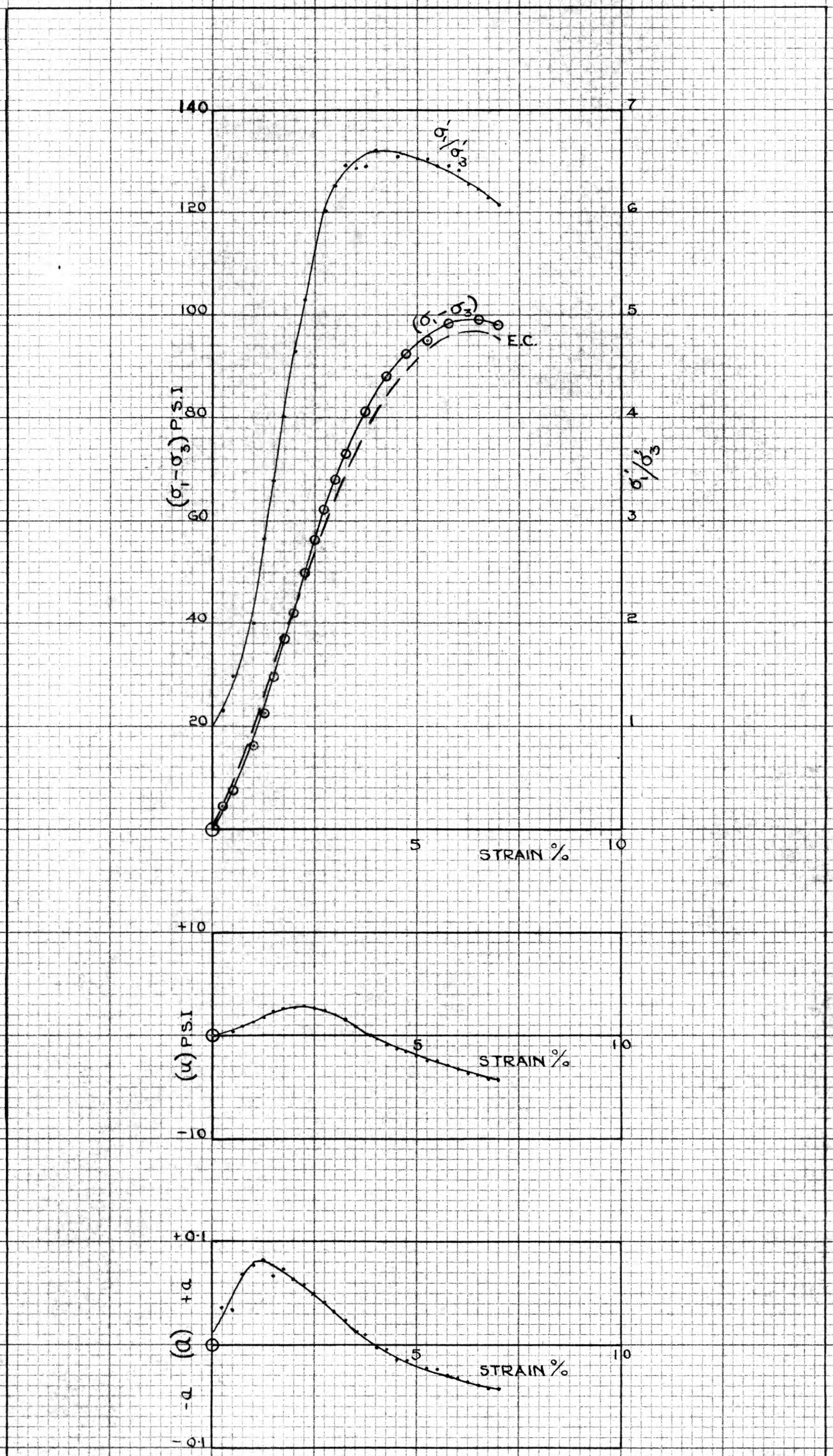
CONSOLIDATED UNDRAINED TESTS.

CELL PRESSURE = 15 P.S.I.

INITIAL CONSOLIDATION = 0·9%

	INITIAL	FINAL
M/C =	OPT. + 0·11 %	OPT. + 0·06 %
S	85·7 %	90·0 %
γ_d	134·7	136·0

FIG. 5:21



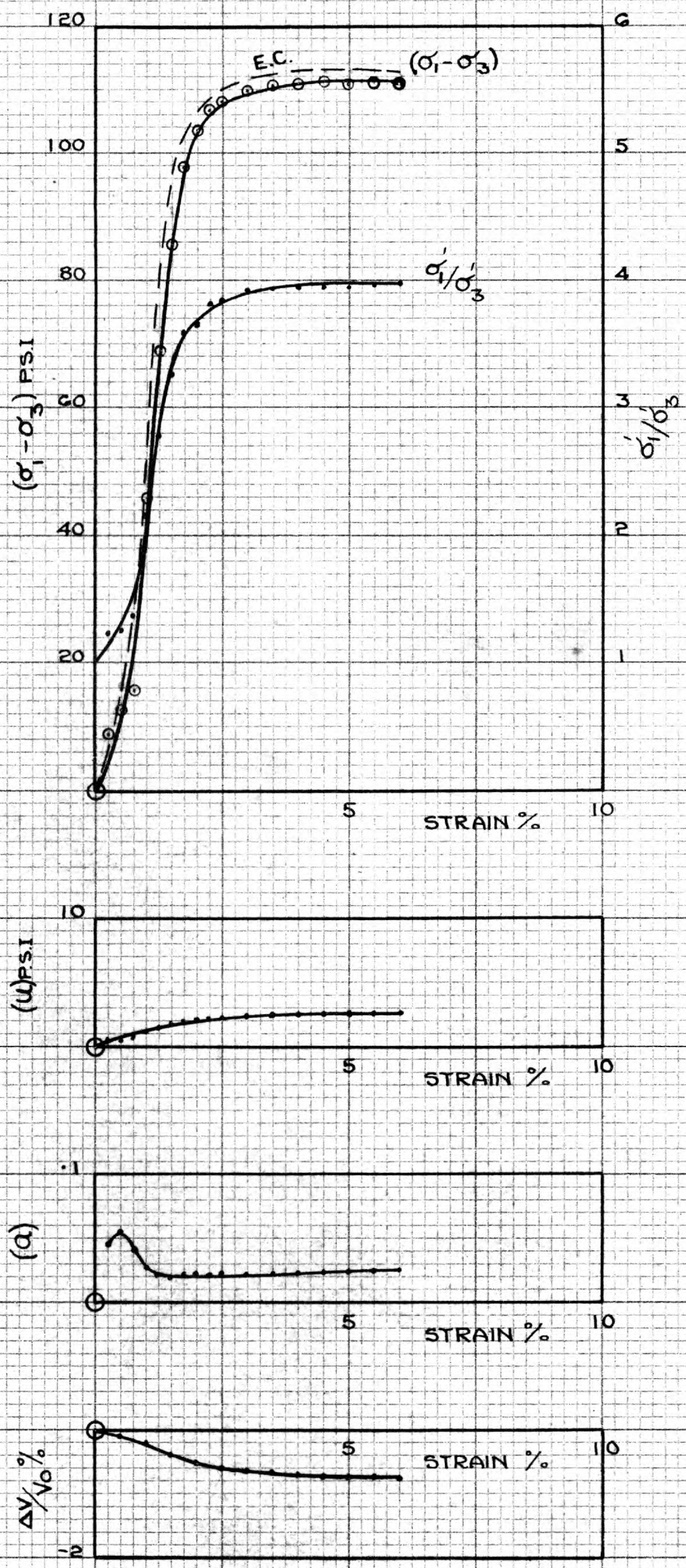
CONSOLIDATED UNDRAINED TESTS

CELL PRESSURE = 15 P.S.I

INITIAL CONSOLIDATION = 1·3%

	INITIAL	FINAL
M/C =	OPT. + 1·02 %	OPT. + 0·4 %
S =	94·5 %	94·2 %
γ_d =	134·3	136·0

FIG. 5:22



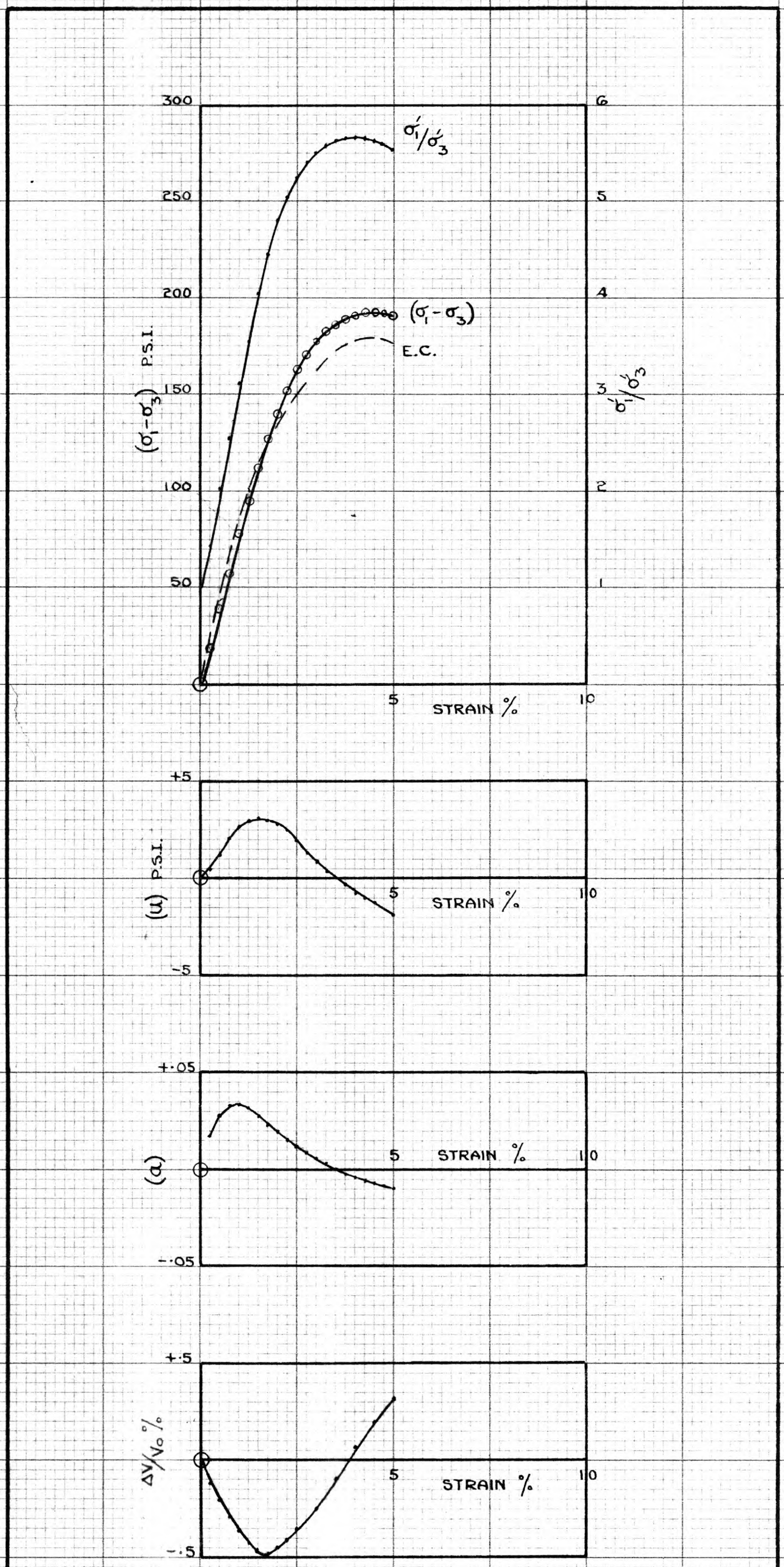
CONSOLIDATED UNDRAINED TESTS.

CELL PRESSURE = 40 P.S.I

INITIAL CONSOLIDATION = 1.9%

	INITIAL	FINAL
M/C	= OPT. − 1·1 %	OPT. + 0·67 %
S	= 67 %	89 %
γ_d	= 132	133·8

FIG. 5:23



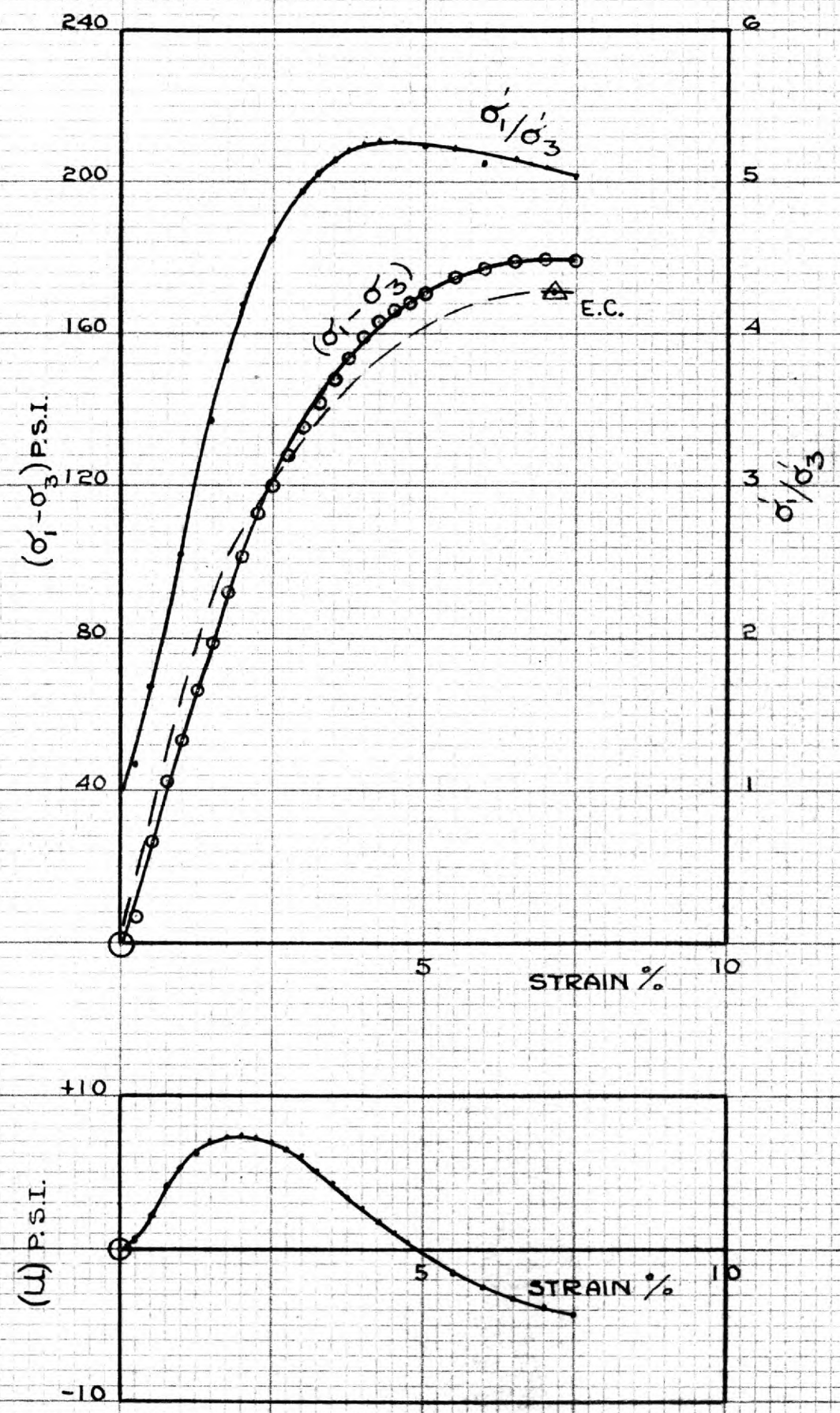
CONSOLIDATED UNDRAINED TEST

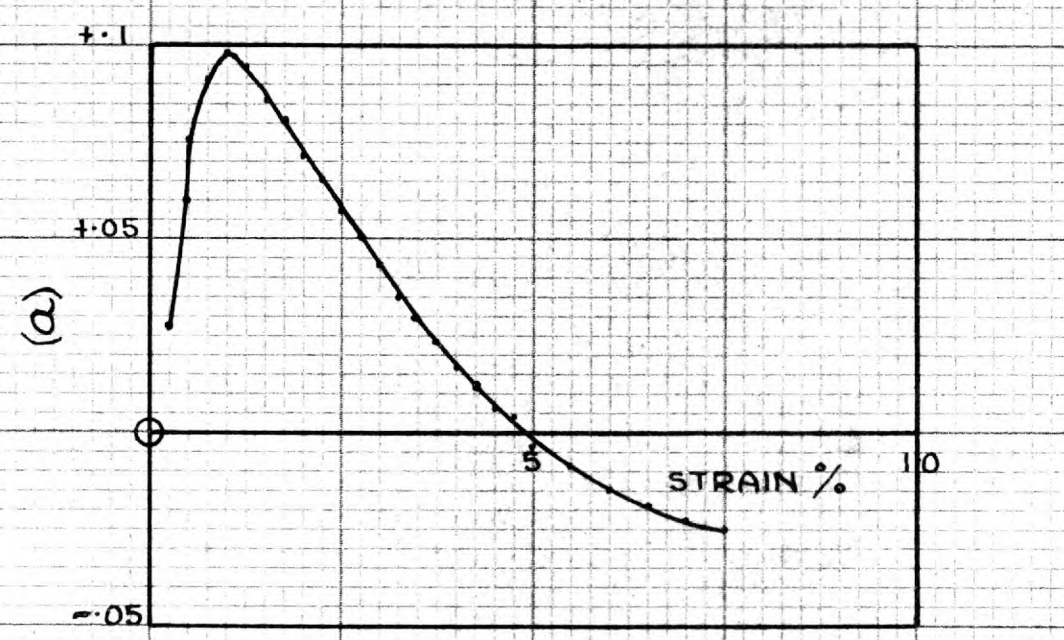
CELL PRESSURE = 40 P.S.I.

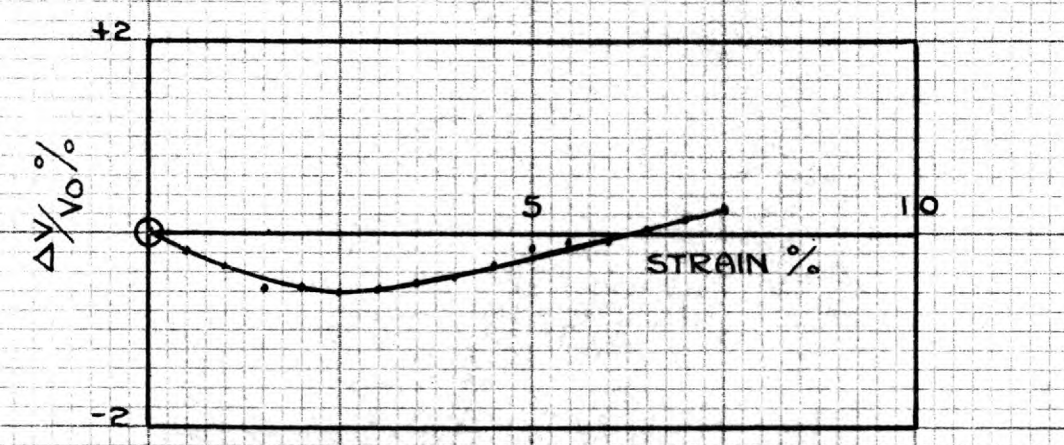
INITIAL CONSOLIDATION = 1·6%

	INITIAL	FINAL
M/C =	OPT. + 0·25%	OPT.- 0·4%
S =	86%	91·8%
γ_d =	135	138

FIG. 5:24







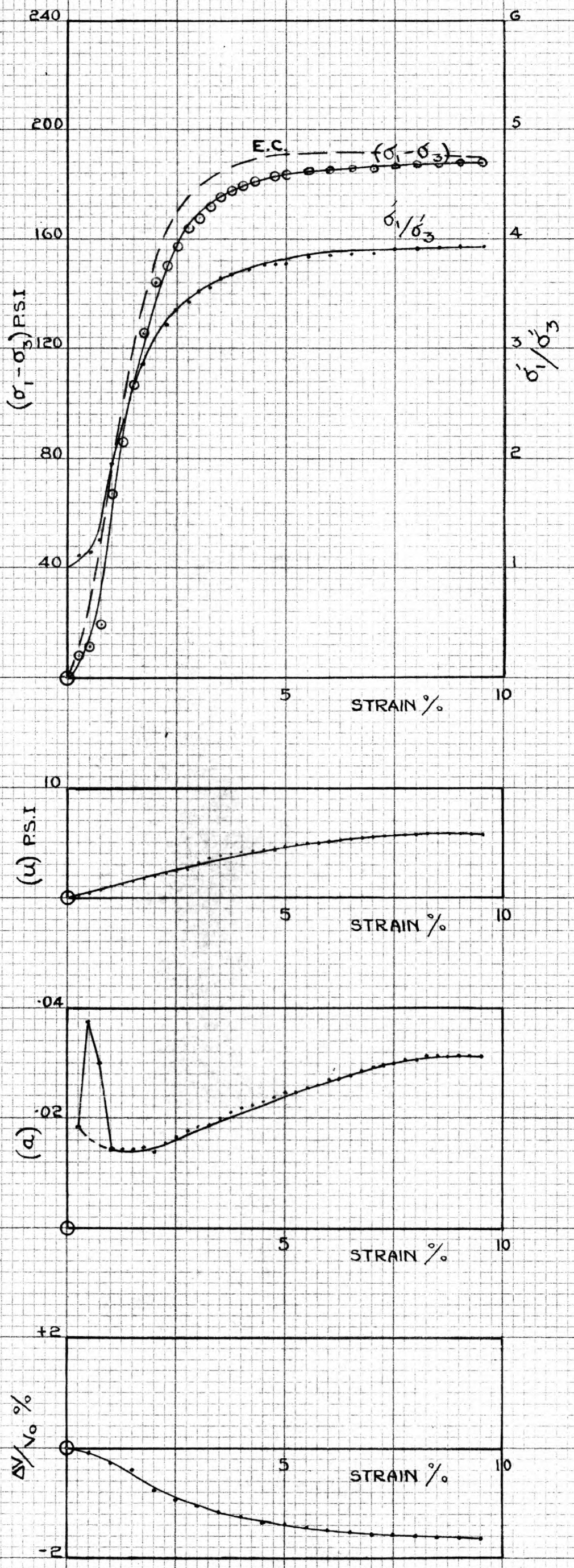
CONSOLIDATED UNDRAINED TESTS.

CELL PRESSURE = 40 P.S.I.

INITIAL CONSOLIDATION = 2·1 %

	INITIAL	FINAL
M/C =	OPT. + 1·2 %	OPT. + 0·12 %
S =	94 %	91·8 %
γ_d =	133·4	136·3

FIG. 5:25



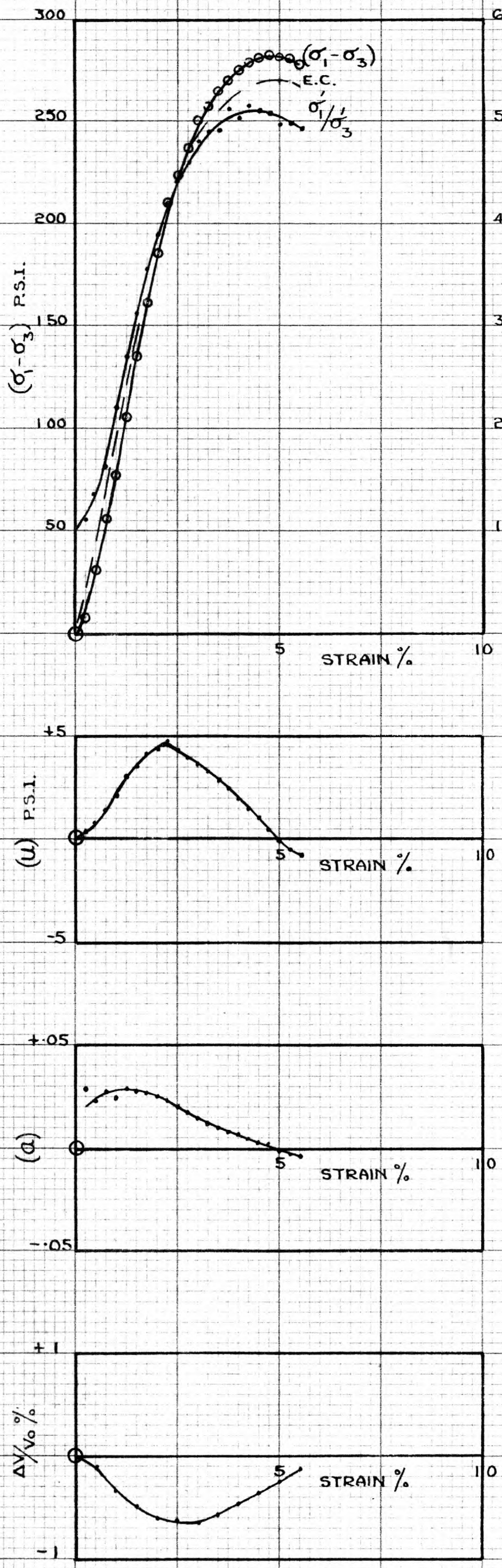
CONSOLIDATED UNDRAINED TESTS

CELL PRESSURE = 70 P.S.I.

INITIAL CONSOLIDATION = 2·6%

	INITIAL	FINAL
M/C =	OPT.- 1·12%	OPT. + 0·06%
S =	66·5%	91·5%
γ_d =	131·6	135·3

FIG. 5:26



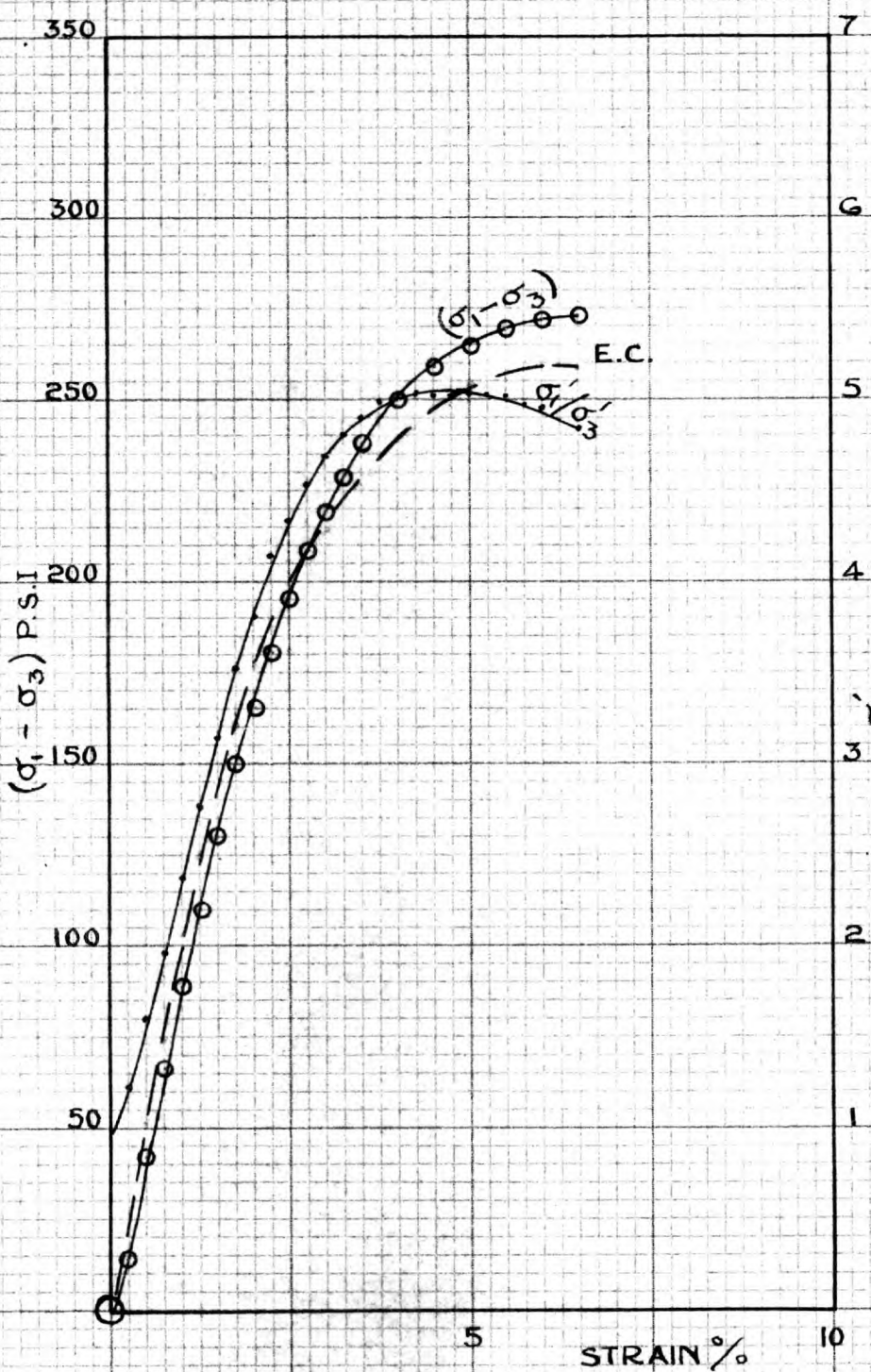
CONSOLIDATED UNDRAINED TEST.

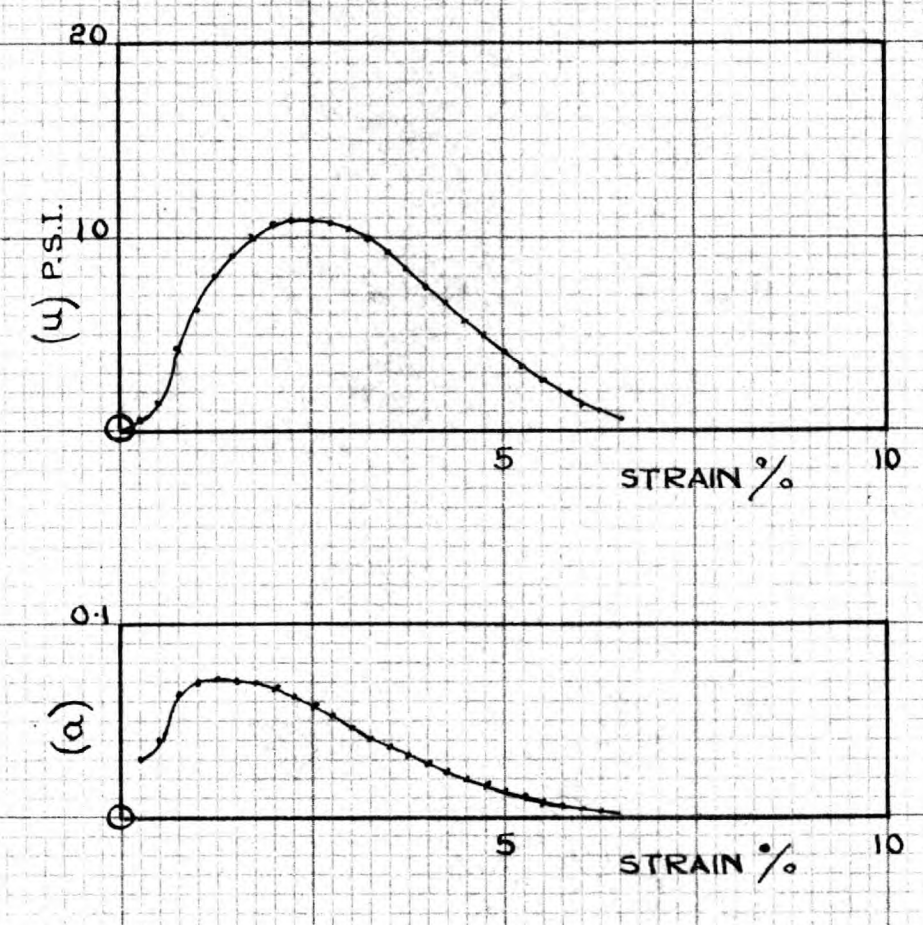
CELL PRESSURE = 70 P.S.I.

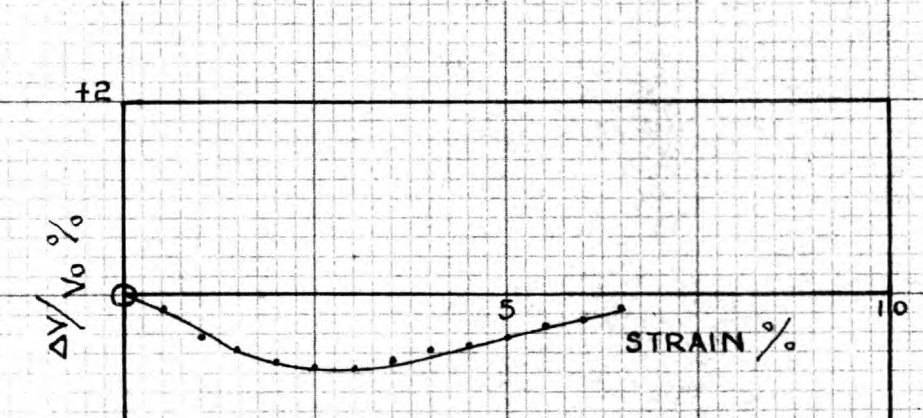
INITIAL CONSOLIDATION = 1·9 %

		INITIAL	FINAL
M/C	=	OPT. + 0·09 %	OPT. − 0·5 %
S	=	83·0 %	84·7 %
γ_d	=	133·9	136·3

FIG. 5:27







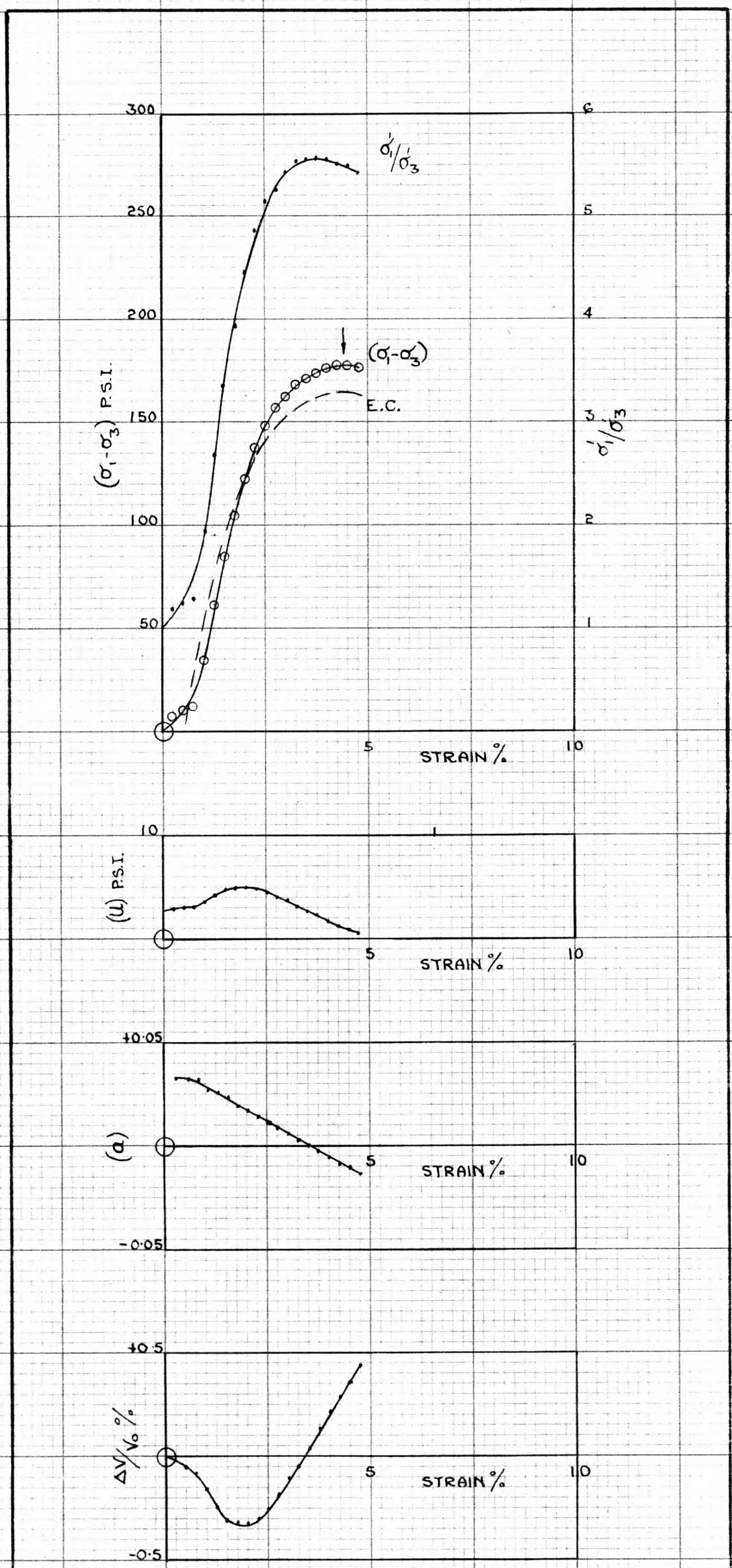
CONSOLIDATED UNDRAINED TESTS

CELL PRESSURE = 70 P.S.I.

INITIAL CONSOLIDATION = 2·65%

	INITIAL	FINAL
M/C =	OPT. +1·07%	OPT. -0·2%
S =	92·6%	90·3%
γ_d =	133·5	136·9

FIG. 5:28



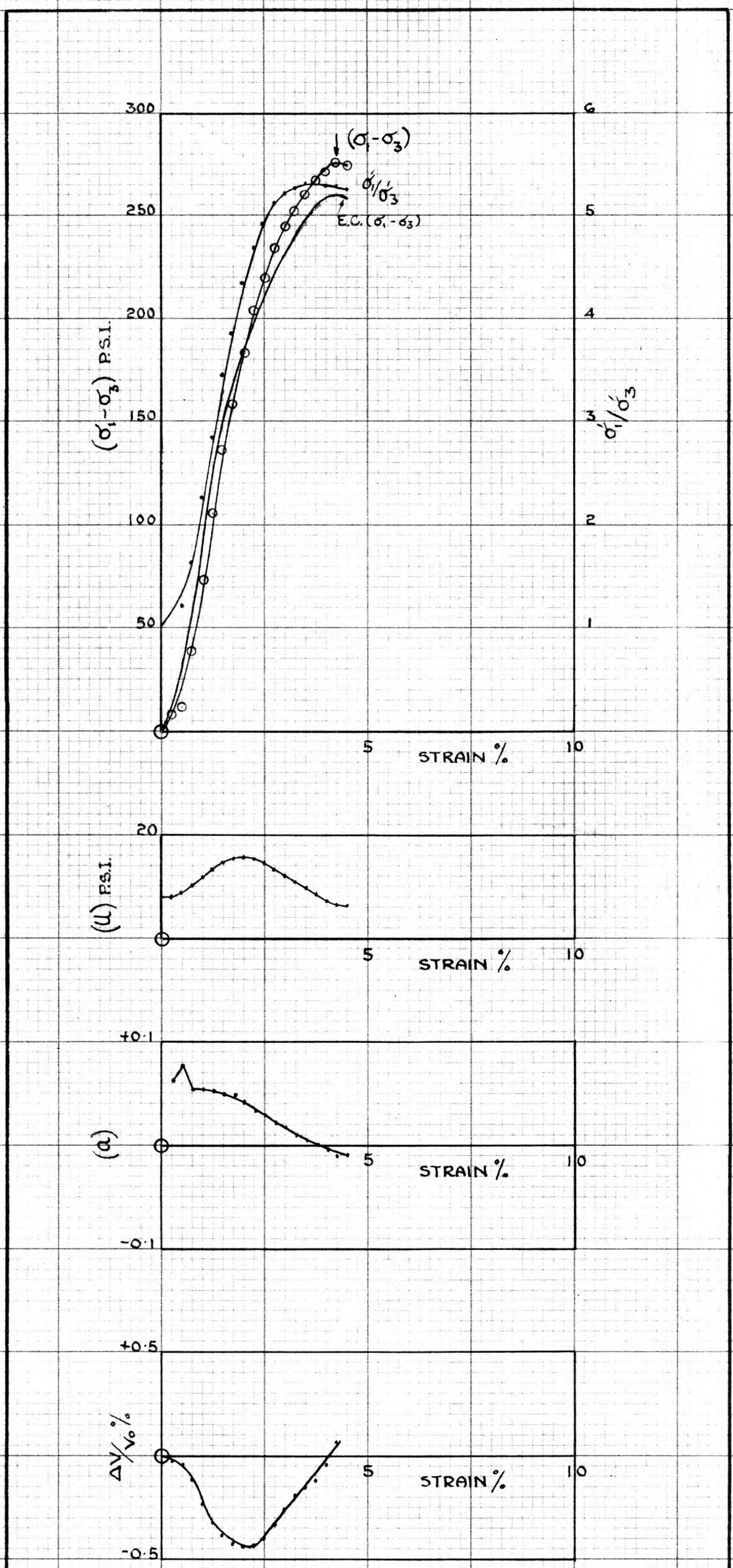
CONSOLIDATED UNDRAINED TEST. (Series b)

CONSOL.ᴺ PRESS. - 15 P.S.I. CONSOL.ᴺ - 0·8 %
CELL " -40 " " -0·26 %
1·06 %

PORE PRESS. AFTER CONSOLᴺ = 0·2 P.S.I.
" " BEFORE SHEAR = 2·4 " .

	INITIAL	FINAL
M/C =	OPT.	OPT.
S =	89·8 %	91·75 %
γ_d =	136·1	136·8

FIG. 5:29



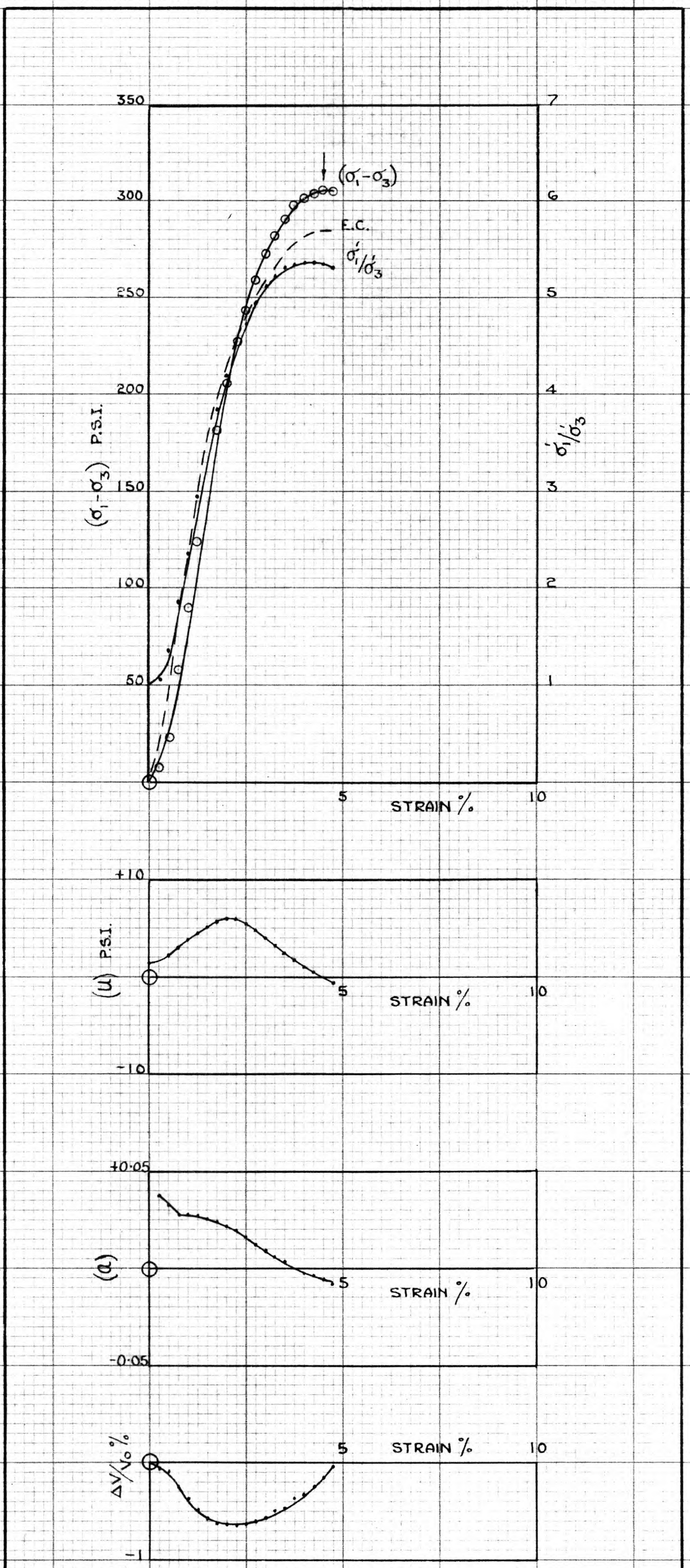
CONSOLIDATED UNDRAINED TEST. (Series b.)

CONSOL^N PRESS. - 15 P.S.I. CONSOL^N - 0·80 %
CELL PRESS. - 70 " " - 0·97 %
1·77 %

PORE PRESS. AFTER CONSOL^N - 0·3 P.S.I.
" " BEFORE SHEAR - 7·2 "

	INITIAL	FINAL
M/C =	OPT. +0·35 %	OPT.
S =	93 %	92·7 %
γ_d =	136.0	137.0

FIG. 5: 30



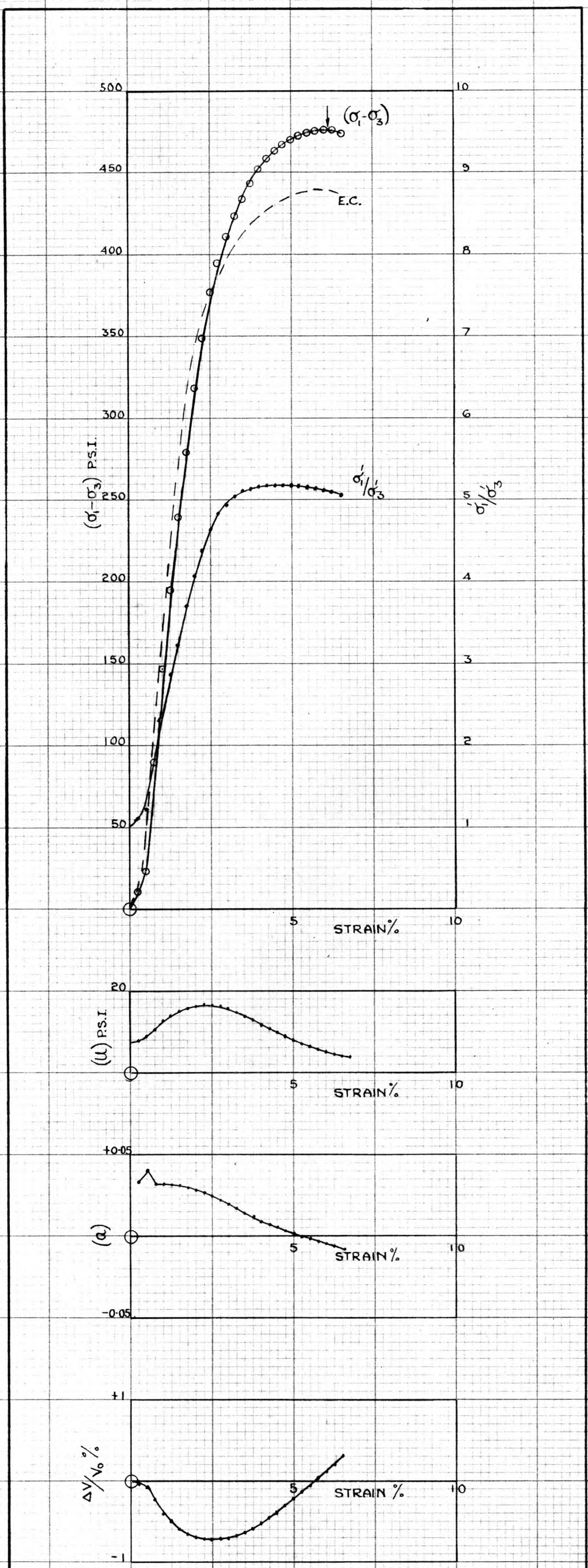
CONSOLIDATED UNDRAINED TEST. (Series b.)

CONSOL^{N} PRESS. 40 P.S.I. CONSOL^{N} - 1·27%
CELL " 70 " " ·21%
1·48%

PORE PRESS. AFTER CONSOL^{N} =-0·12 P.S.I.
" " BEFORE SHEAR =+1·5 P.S.I.

	INITIAL	FINAL
M/C =	OPT.+0·1%	OPT.-0·5%
S =	86·6%	86·75%
γ_d =	135	137

FIG. 5:31



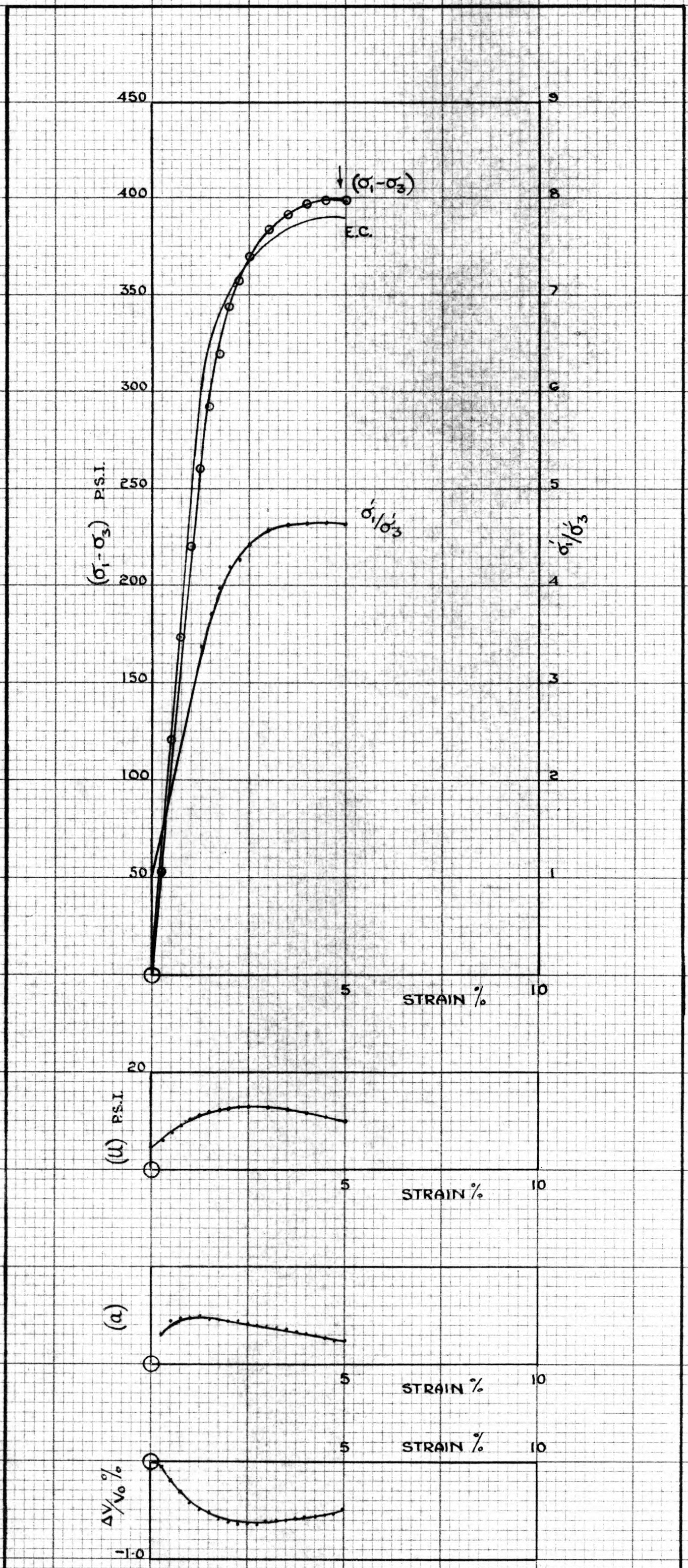
CONSOLIDATED UNDRAINED TEST. (Series 6)

CONSOL^N PRESS.- 40 P.S.I. CONSOLIDATION - 1·22 %
CELL PRESS.- 120 P.S.I " - ·338 %
1·558 %

PORE PRESS. AFTER CONSOL. = 1·8 P.S.I.
" " BEFORE SHEAR. = 7·6 P.S.I.

		INITIAL	FINAL
M/C	=	OPT.	OPT.- 0·5 %
S	=	90 %	92·5 %
γ_d	=	136·3	138·0

FIG. 5:32



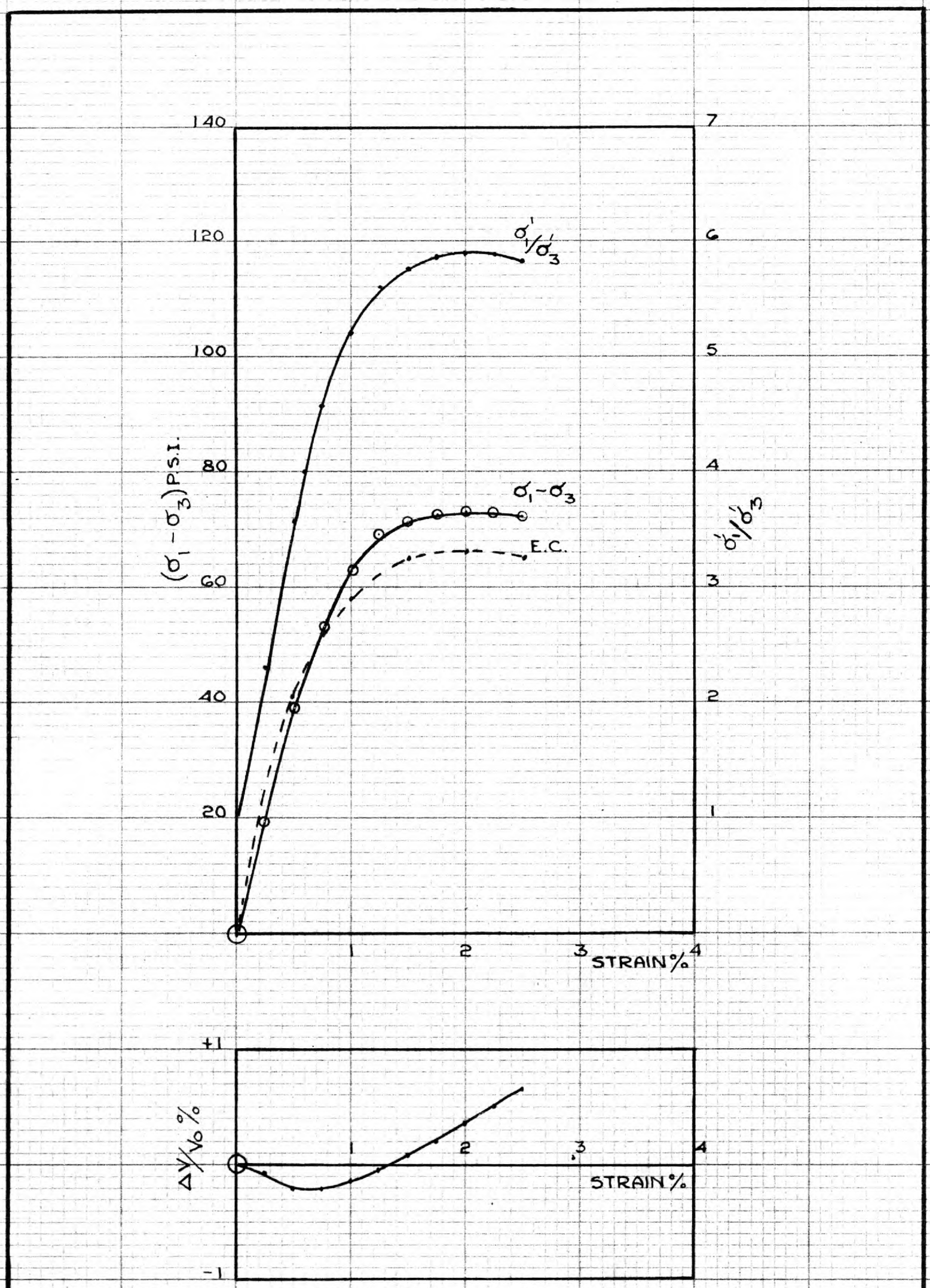
CONSOLIDATED UNDRAINED TEST. (Series b.)

CONSOLIDATION PRESS.-70 P.S.I. CONSOL.^{N}-1·05 %
CELL PRESS-120 " " -0·36 %
1·41 %

PORE PRESS. AFTER CONSOL.^{N} = 3·5 P.S.I.
" " BEFORE SHEAR. = 5·2 "

	INITIAL	FINAL
M/C =	OPT. - 0·2%	OPT. - 0·2%
S =	86·5%	93%
γ_d =	135·5	137·8

FIG. 5:33



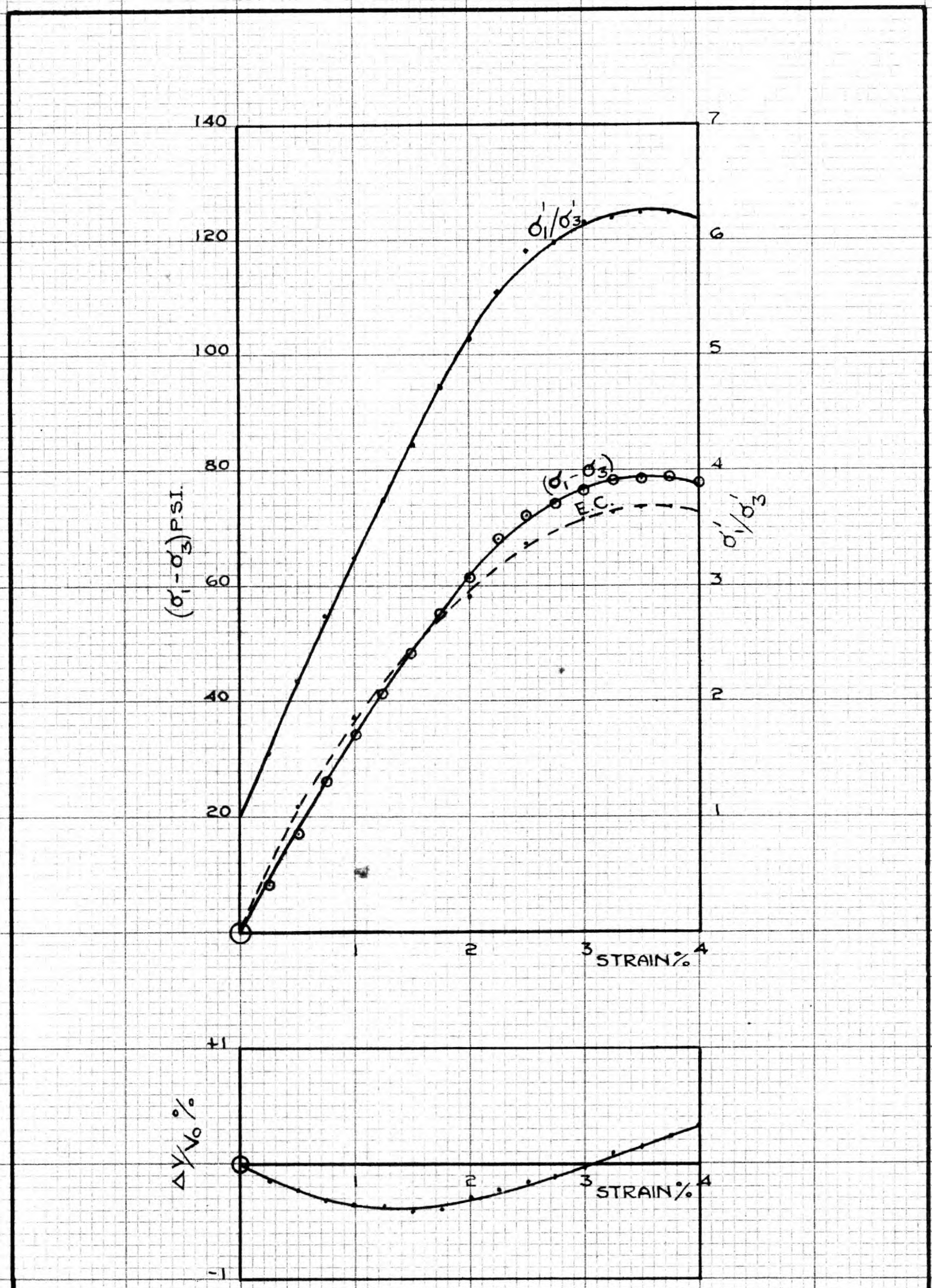
Drained Tests.

Cell Pressure = 15 P.S.I.

Initial Consolidation = 0·18 %

		Initial	Final
M/C	=	OPT.−0·76%	OPT.+0·00
S	=	74%	85%
γ_d	=	133·6	134·8

Fig. 5:34



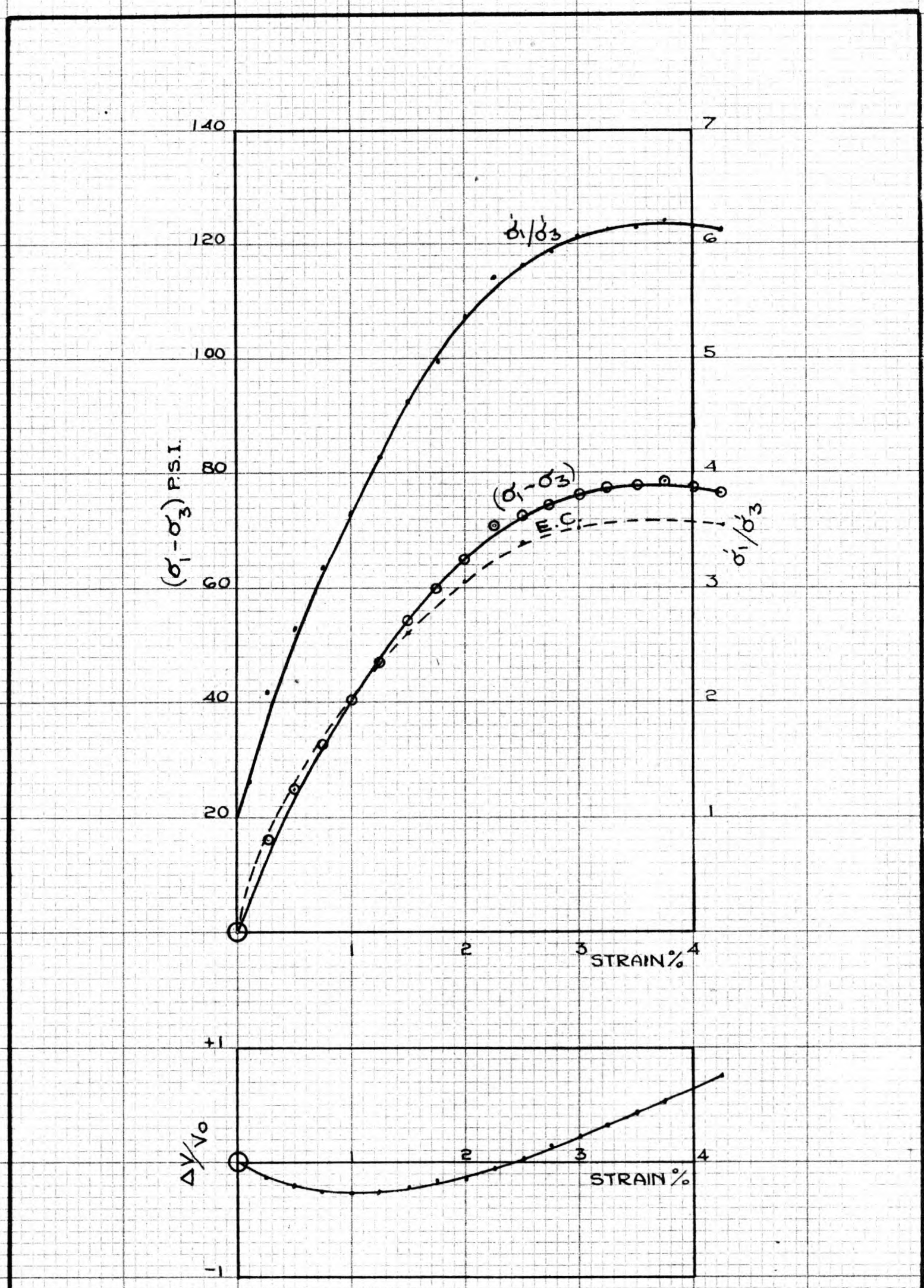
DRAINED TESTS.

CELL PRESSURE = 15 P.S.I.

INITIAL CONSOLIDATION = 0·6%

	INITIAL	FINAL
M/C =	OPT. + ·37%	OPT. + 0·00
S =	86·2%	84·0%
γ_d =	134	134·5

FIG. 5:35



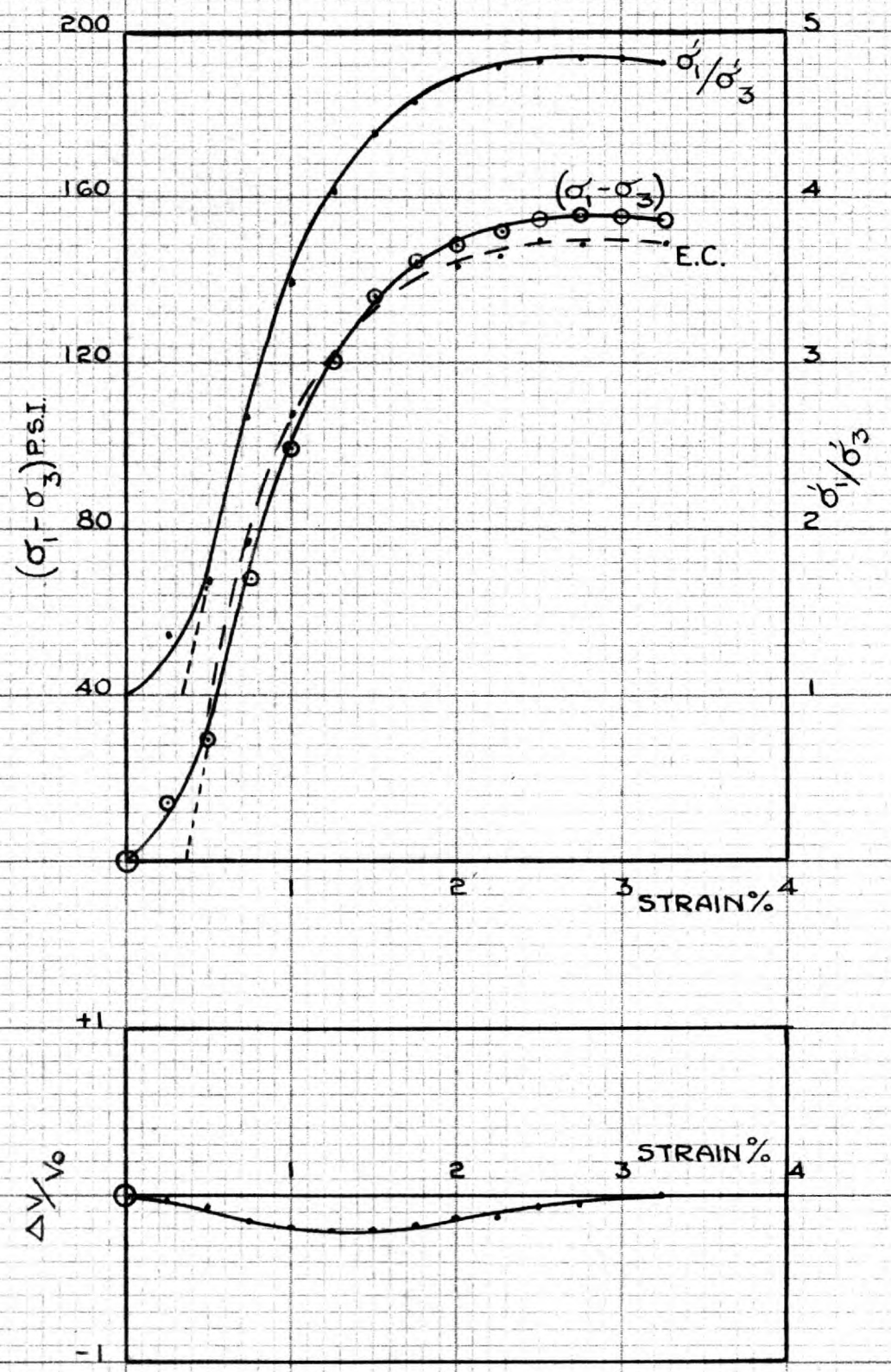
Drained Tests.

Cell Pressure = 15 P.S.I.

Initial Consolidation = 1·2%

	Initial	Final
M/C	= OPT. + 1·42%	OPT. + 0·82%
S	= 95·6%	91·5%
γ_d	= 133·5	134·1

Fig. 5:36



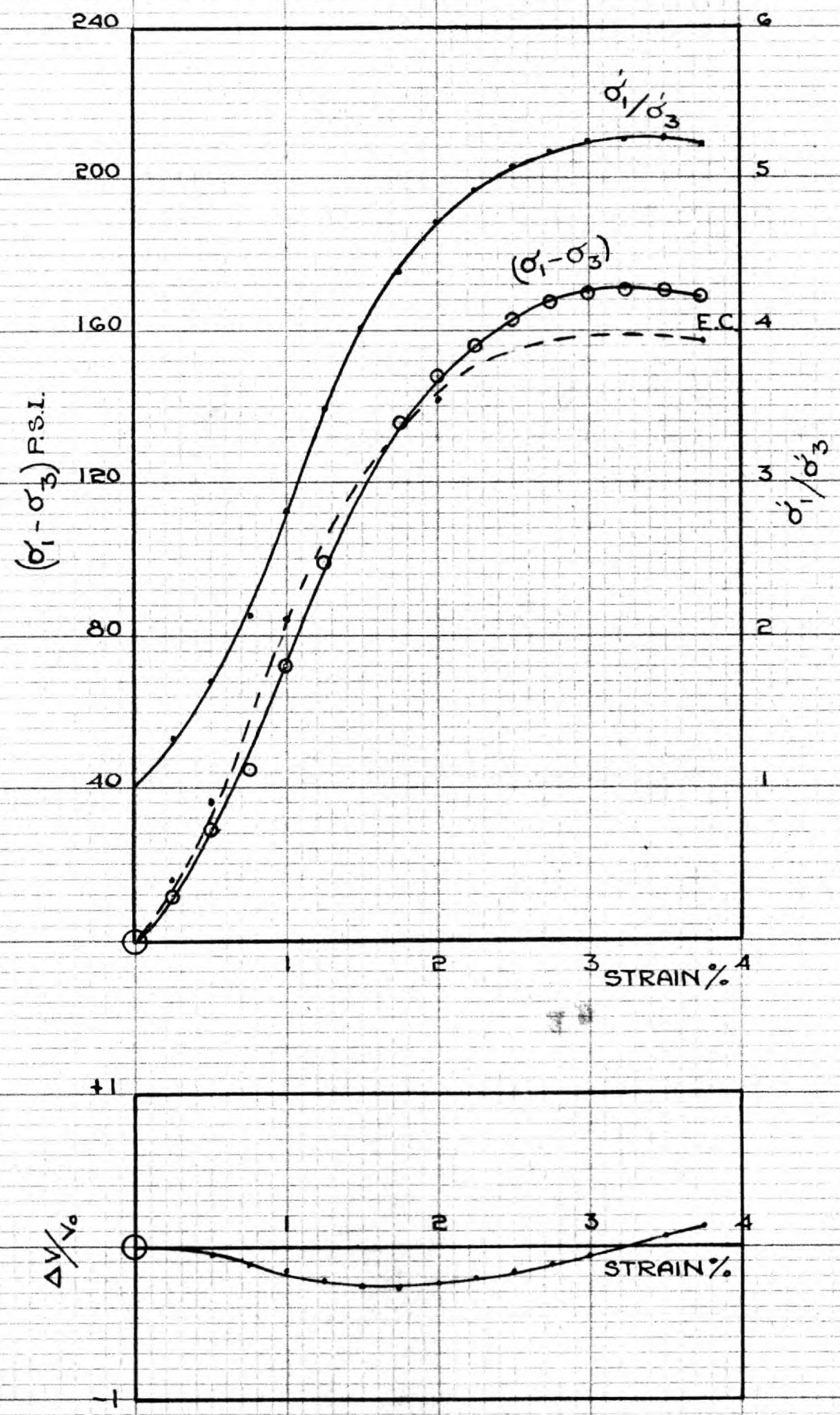
DRAINED TESTS

CELL PRESSURE = 40 P.S.I.

INITIAL CONSOLIDATION = 0·32%

	INITIAL	FINAL
M/C =	OPT.-0·9%	OPT.-0·45%
S =	73·5%	81·5%
γ_d =	134·0	135·1

FIG. 5:37



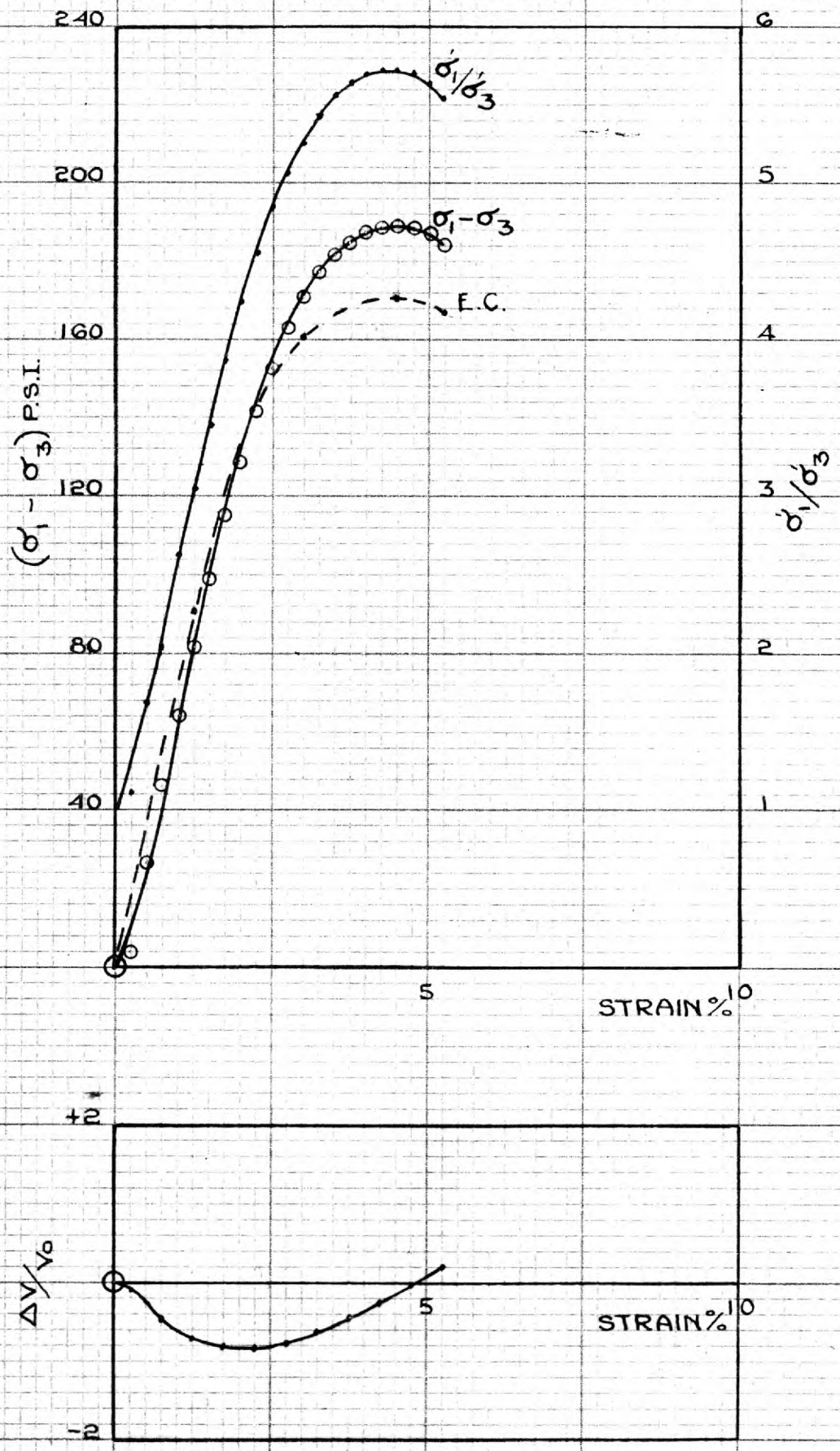
DRAINED TESTS.

CELL PRESSURE = 40 P.S.I.

INITIAL CONSOLIDATION = 0·7 %.

	INITIAL	FINAL
M/C =	OPT. − ·15 %	OPT. + 0·00
S =	85 %	90 %
γ_d =	135·3	136·2

FIG. 5:38



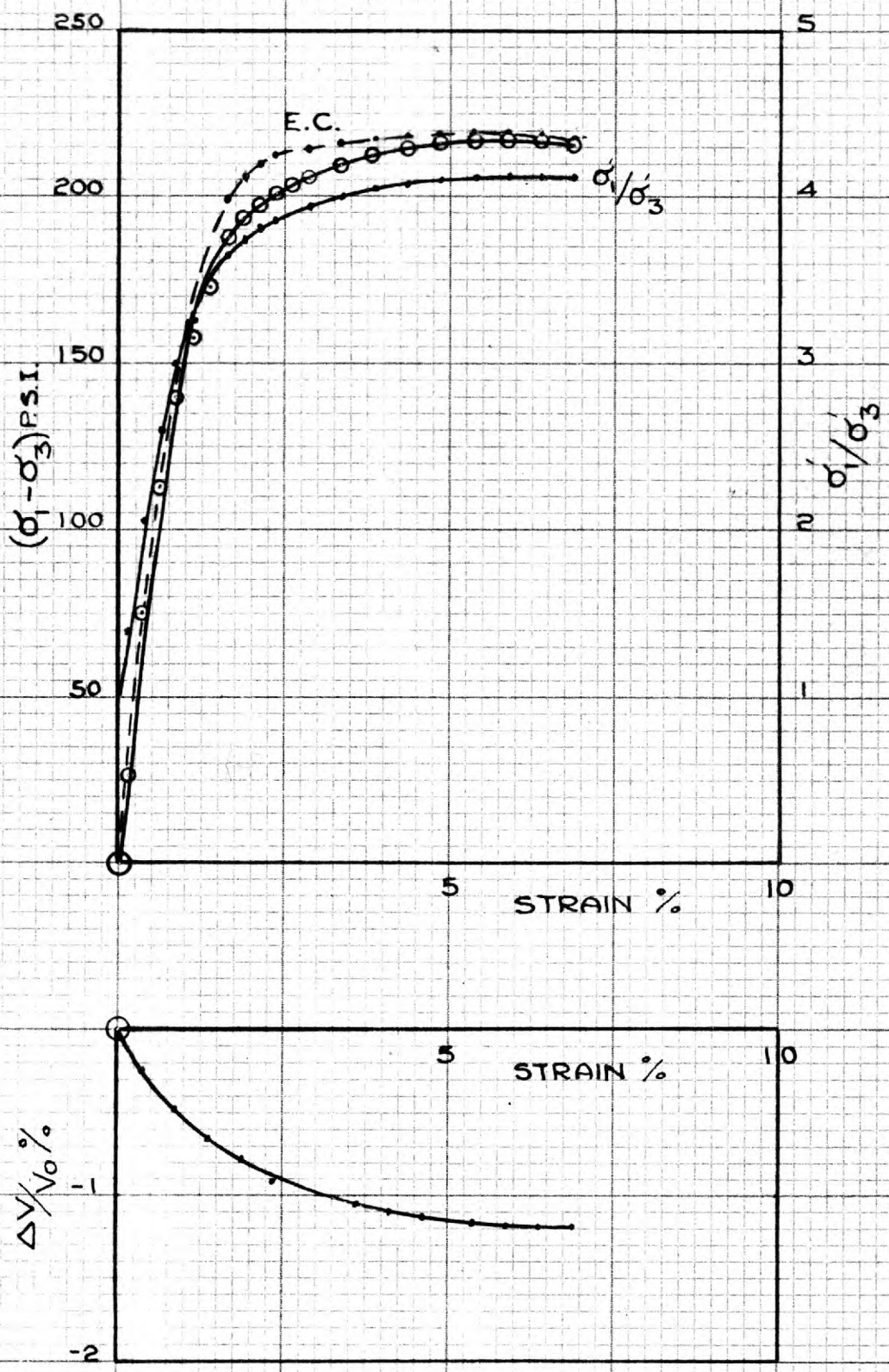
Drained Tests.

Cell Pressure = 40 P.S.I.

Initial Consolidation = 1·7 %

	Initial	Final
M/C	= Opt. + 1·12 %	Opt. + 0·45 %
S	= 92·7 %	94 %
γ_d	= 133·5	135·9

Fig. 5:39



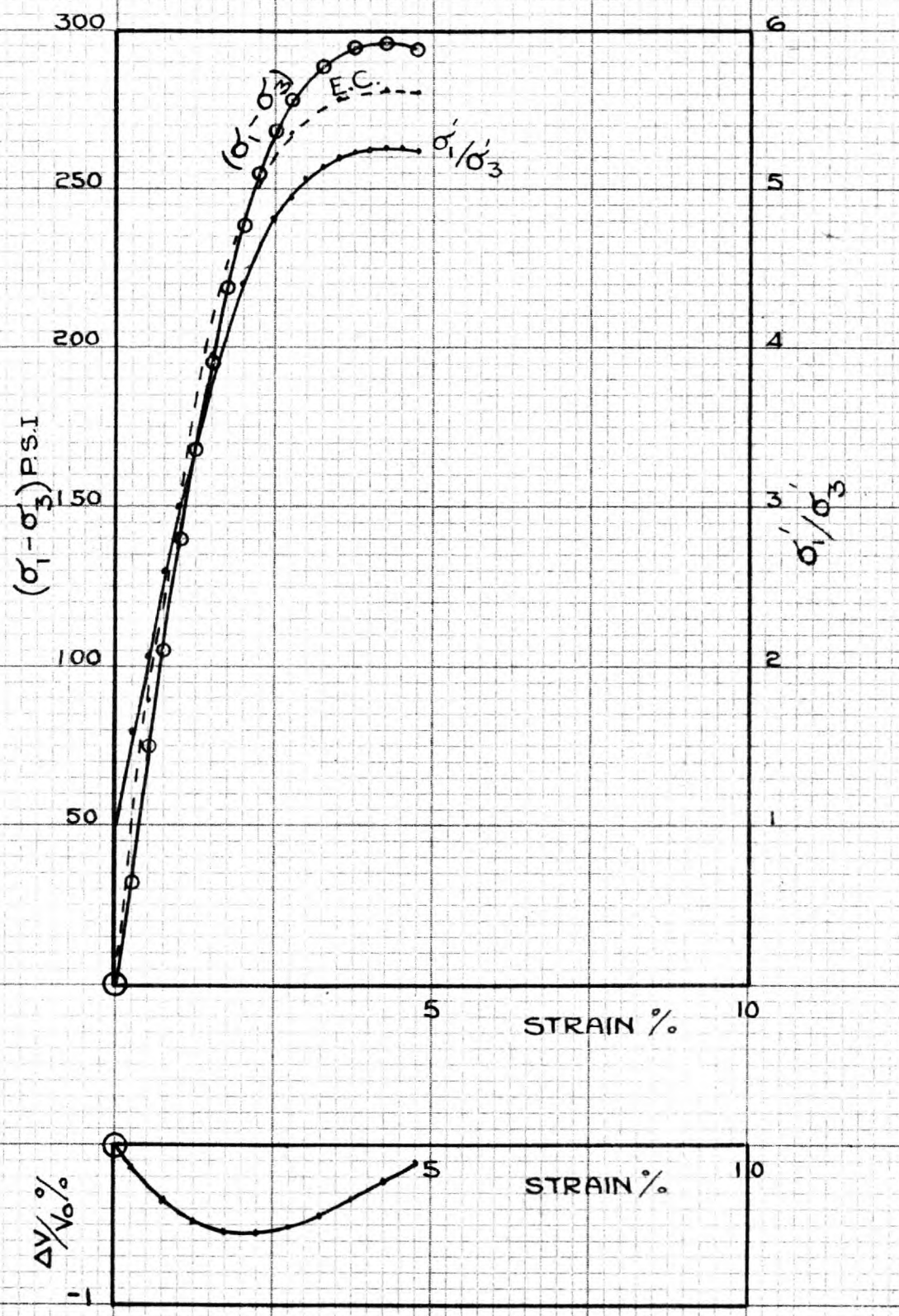
DRAINED TESTS

CELL PRESSURE = 70 P.S.I.

INITIAL CONSOLIDATION = 0·6%

	INITIAL	FINAL
M/C =	OPT. − 1·06%	OPT. + 0·00
S =	68·0%	84·1%
γ_d =	132·0	134·5

FIG. 5:40



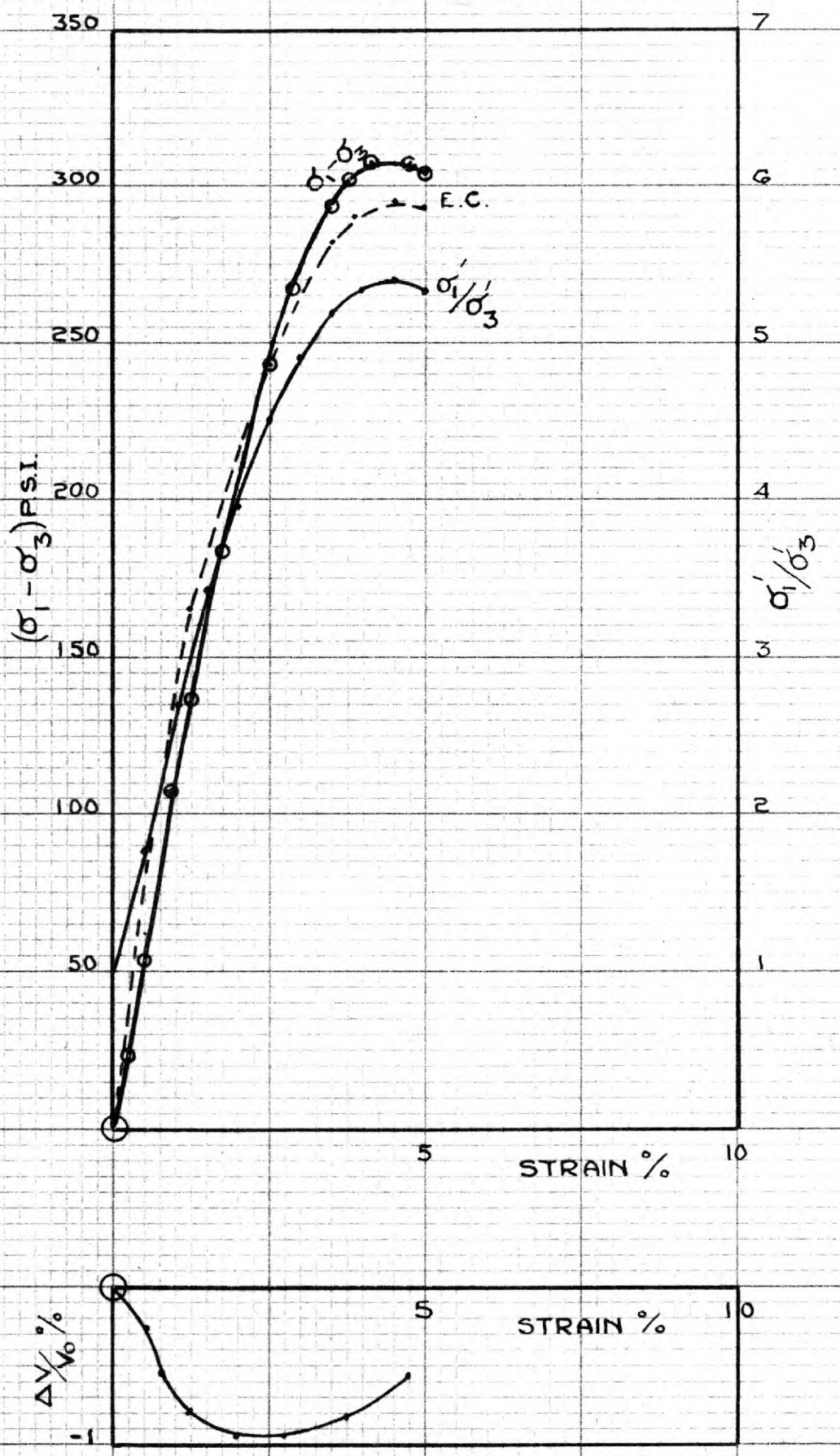
DRAINED TESTS

CELL PRESSURE = 70 P.S.I.

INITIAL CONSOLIDATION = 1·17%

	INITIAL	FINAL
M/C	= OPT. + 0·1%	OPT. - 0·68%
S	= 86%	82·5%
γ_d	= 134·7	136·2

FIG. 5:41



DRAINED TESTS.

CELL PRESSURE = 70 P.S.I.

INITIAL CONSOLIDATION = 2·1%

	INITIAL	FINAL
M/C =	OPT. + 1%	OPT. − 0·55%
S =	92·5%	89·5%
γ_d =	133·9	137·8

FIG. 5:42

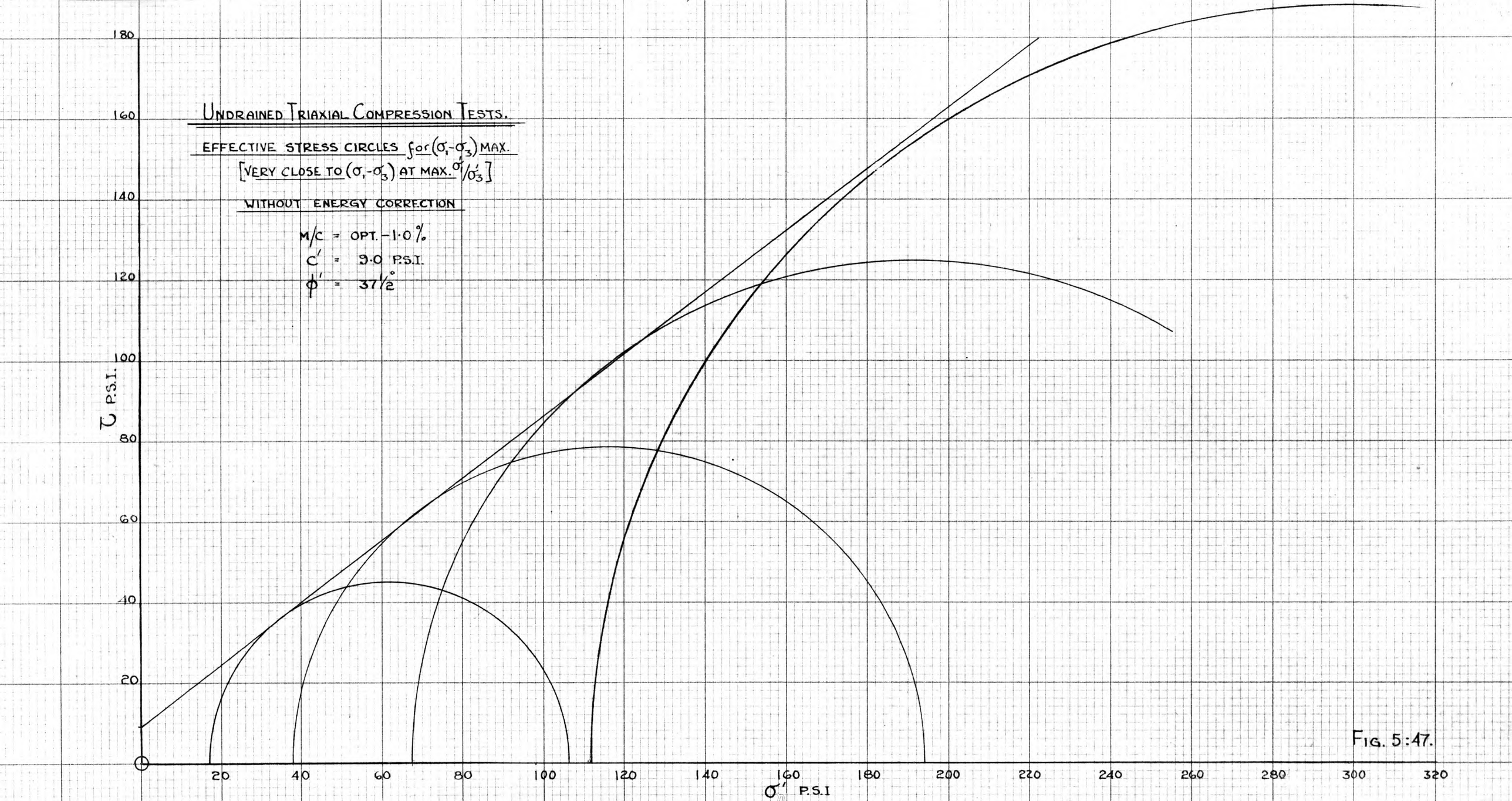

UNDRAINED TRIAXIAL COMPRESSION TESTS.
EFFECTIVE STRESS CIRCLES for $(\sigma_1-\sigma_3)$ MAX.
[VERY CLOSE TO $(\sigma_1-\sigma_3)$ AT MAX. σ_1'/σ_3']
WITHOUT ENERGY CORRECTION
M/C = OPT. −1·0 %
C′ = 9·0 P.S.I.
φ′ = 37½°
τ P.S.I.
σ′ P.S.I
180
160
140
120
100
80
60
40
20
20
40
60
80
100
120
140
160
180
200
220
240
260
280
300
320

FIG. 5:47.

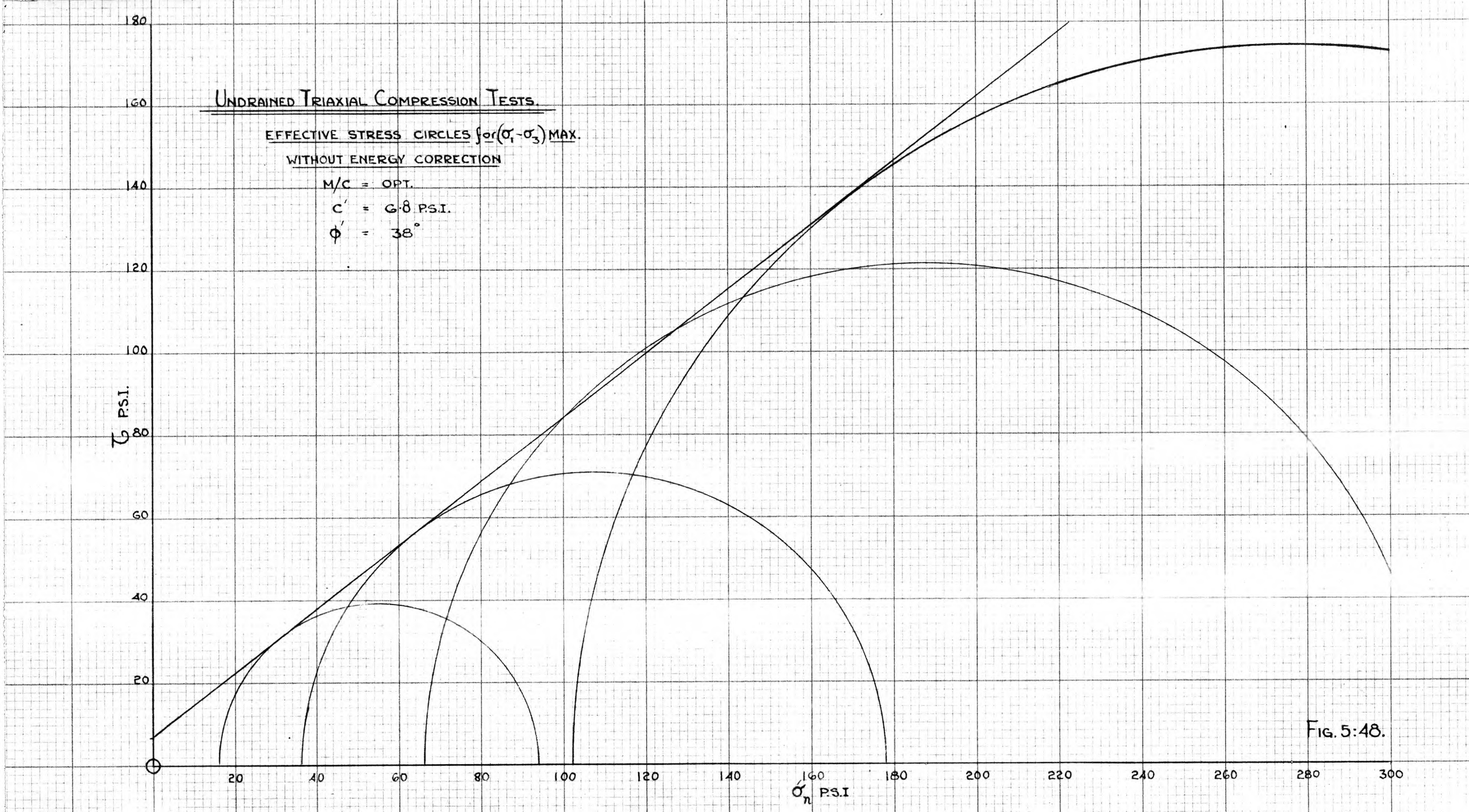

UNDRAINED TRIAXIAL COMPRESSION TESTS.
EFFECTIVE STRESS CIRCLES for $(\sigma_1 - \sigma_3)$ MAX.
WITHOUT ENERGY CORRECTION
M/C = OPT.
C' = 6·8 P.S.I.
ϕ' = 38°
τ P.S.I.
σ_n P.S.I
180
160
140
120
100
80
60
40
20
20
40
60
80
100
120
140
160
180
200
220
240
260
280
300

FIG. 5:48.

UNDRAINED TRIAXIAL COMPRESSION TESTS.

EFFECTIVE STRESS CIRCLES for $(\sigma_1 - \sigma_3)$ MAX.

WITHOUT ENERGY CORRECTION.

M/C = OPT. + 1·0 %

C' = 1·8 P.S.I.

ϕ' = 37°

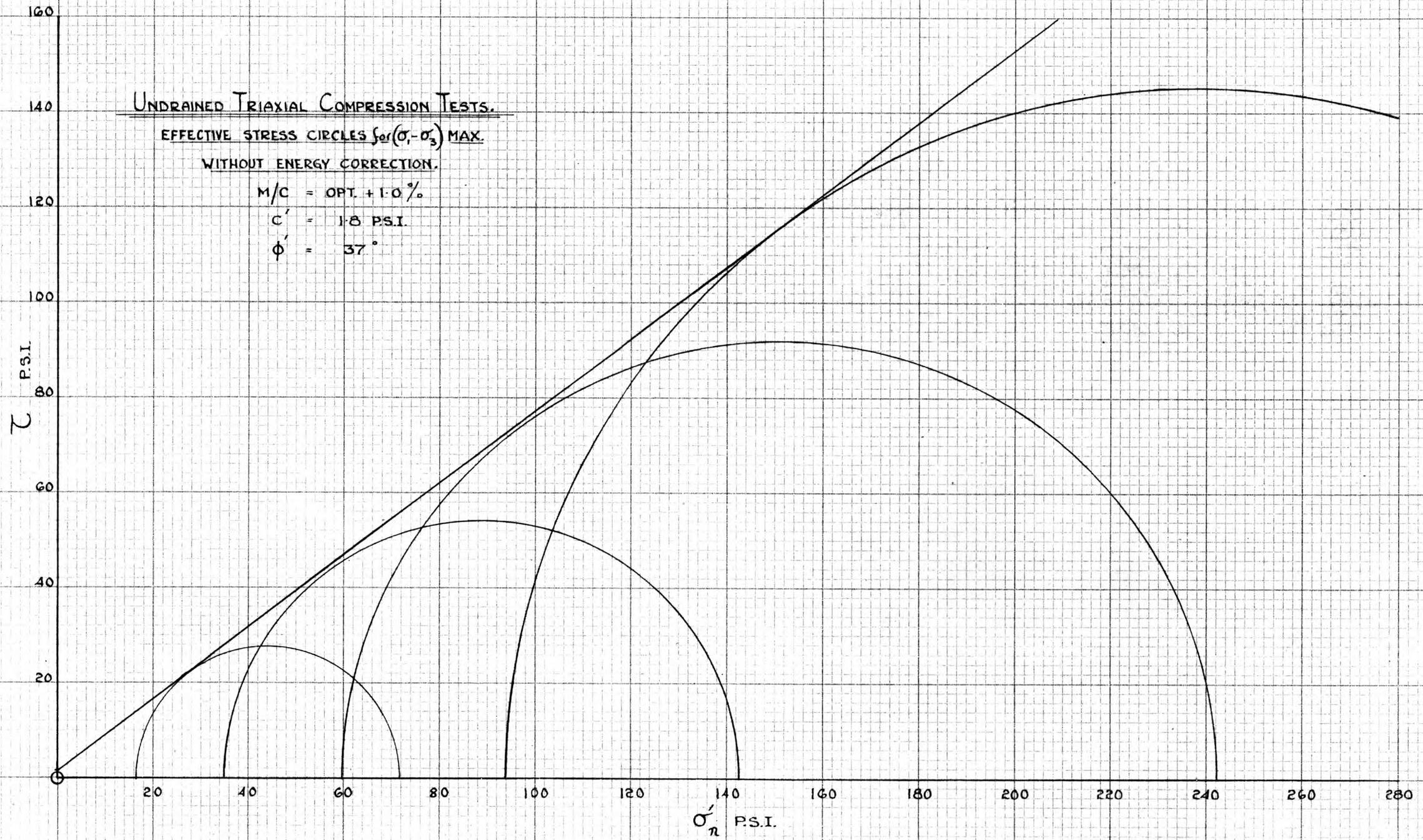


FIG. 5 : 49.

UNDRAINED TRIAXIAL COMPRESSION TESTS.

EFFECTIVE STRESS CIRCLES for $(\sigma_1 - \sigma_3)$ AT σ'_1/σ'_3 MAX.

M/C = OPT.

C' = 6·0 P.S.I.

ϕ' = 38·7°

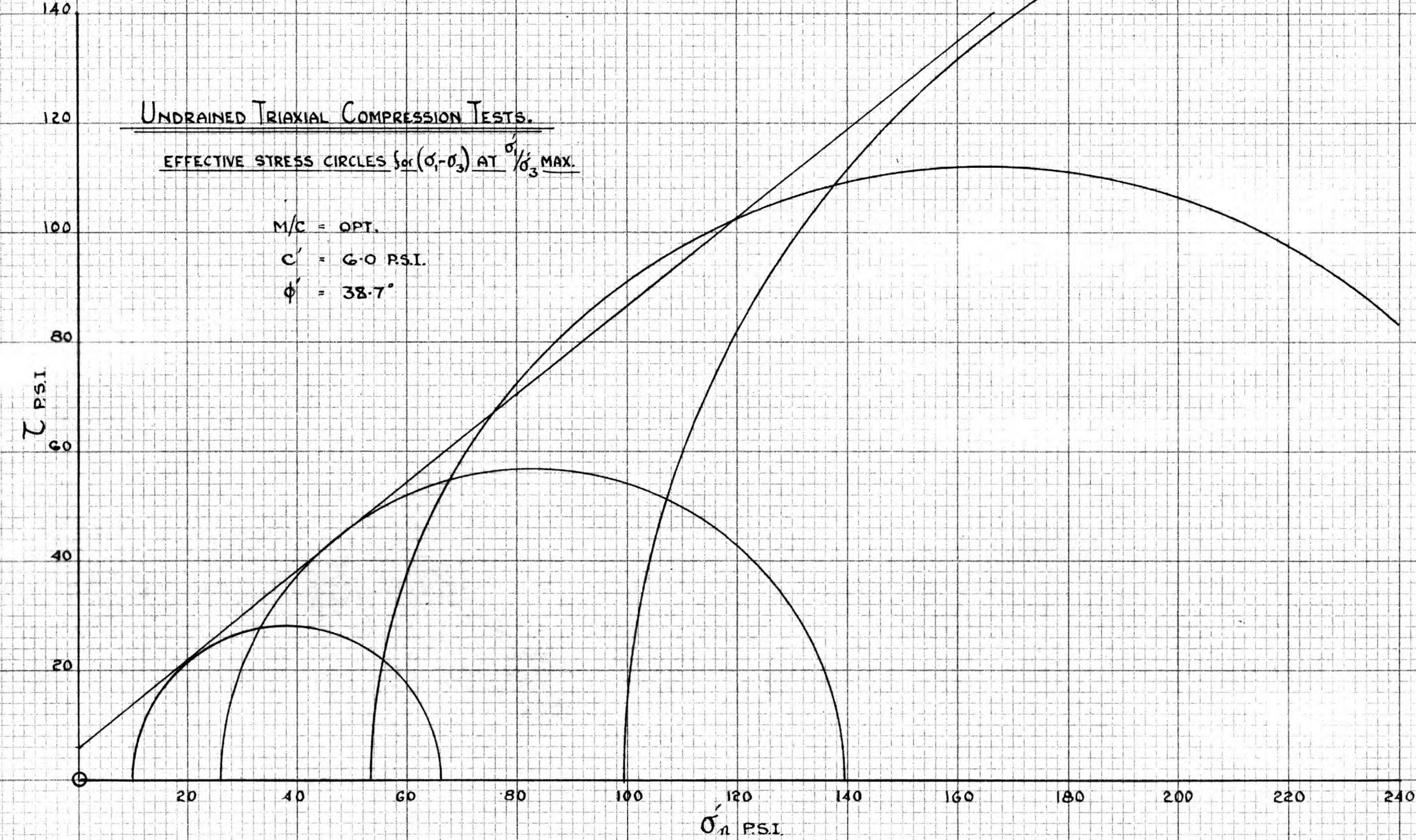


FIG. 5:50.

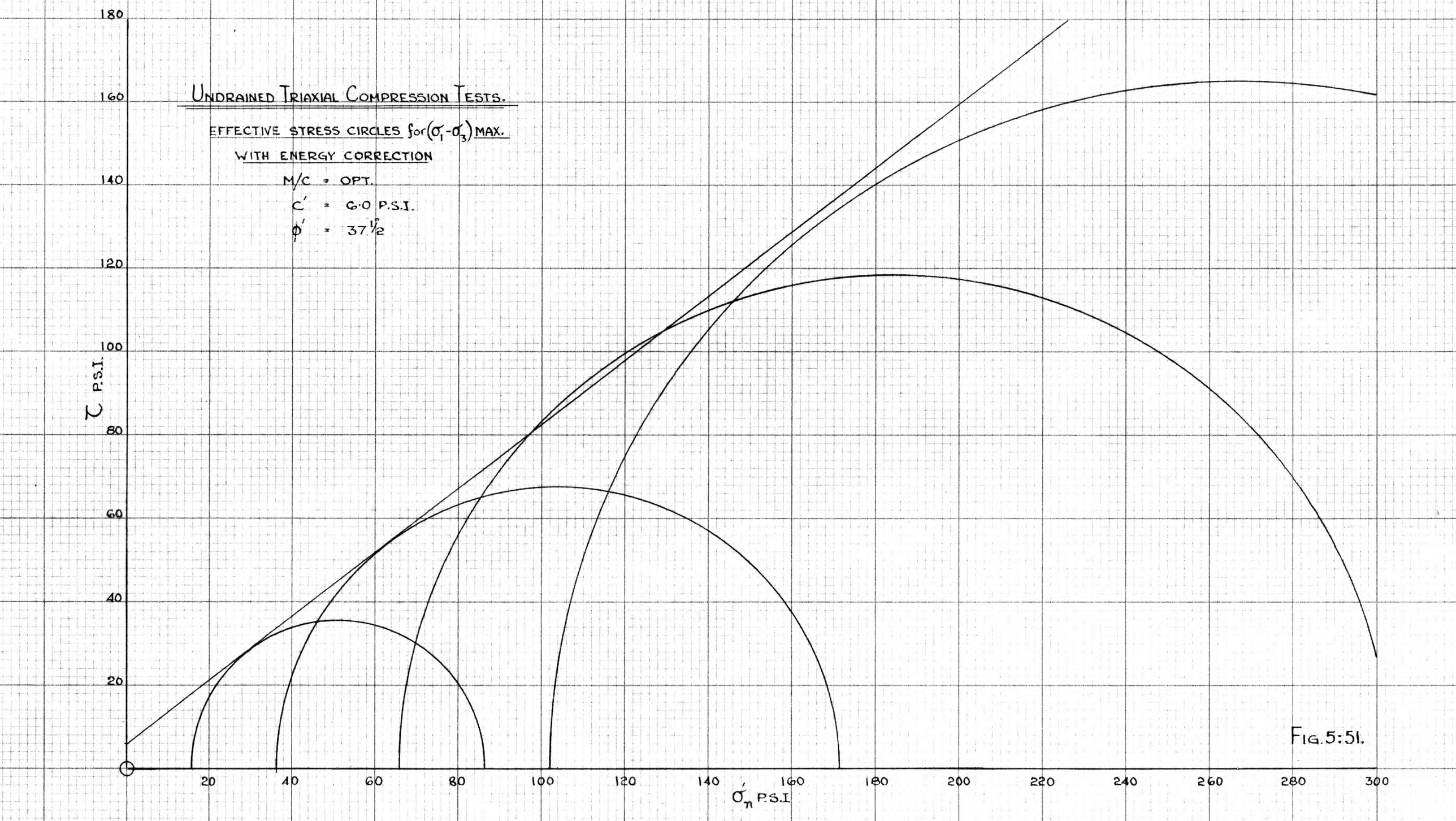

UNDRAINED TRIAXIAL COMPRESSION TESTS.
EFFECTIVE STRESS CIRCLES for $(\sigma_1 - \sigma_3)$ MAX.
WITH ENERGY CORRECTION
M/C = OPT.
C′ = 6·0 P.S.I.
φ′ = 37½
τ P.S.I.
σ_n' P.S.I.
180
160
140
120
100
80
60
40
20
20
40
60
80
100
120
140
160
180
200
220
240
260
280
300

FIG. 5:51.

UNDRAINED TRIAXIAL COMPRESSION TESTS.

EFFECTIVE STRESS CIRCLES for $(\sigma_1-\sigma_3)$ MAX.

WITH ENERGY CORRECTION

M/C = OPT. + 1%

c' = 1·3 P.S.I.

ϕ' = 37°

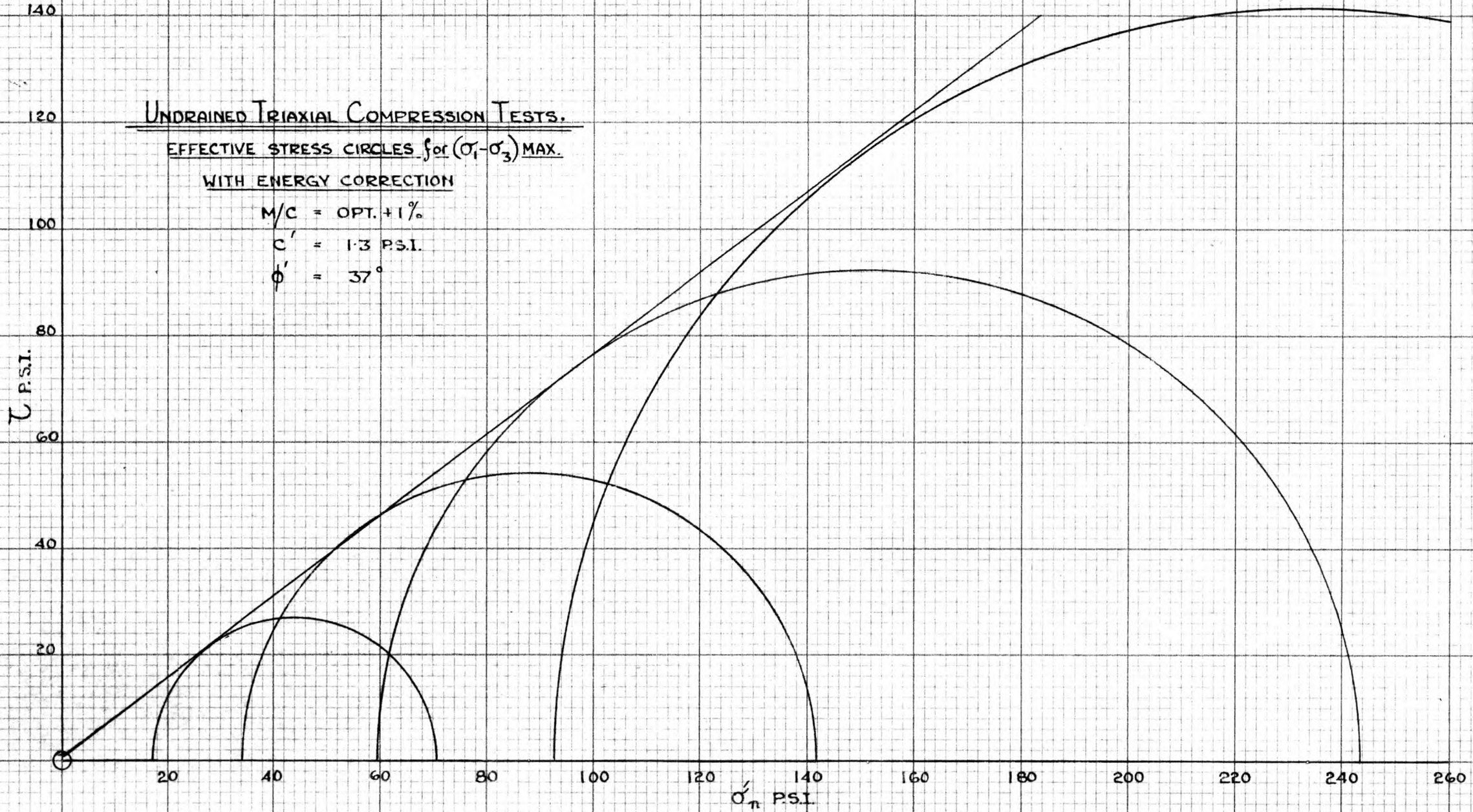


FIG. 5:52.

CONSOLIDATED UNDRAINED TRIAXIAL TESTS.

EFFECTIVE STRESS CIRCLES for $(\sigma_1-\sigma_3)$ MAX.

WITHOUT ENERGY CORRECTION.

FINAL M/C = OPT.

$C' = 11$ P.S.I.

$\phi' = 36.8°$

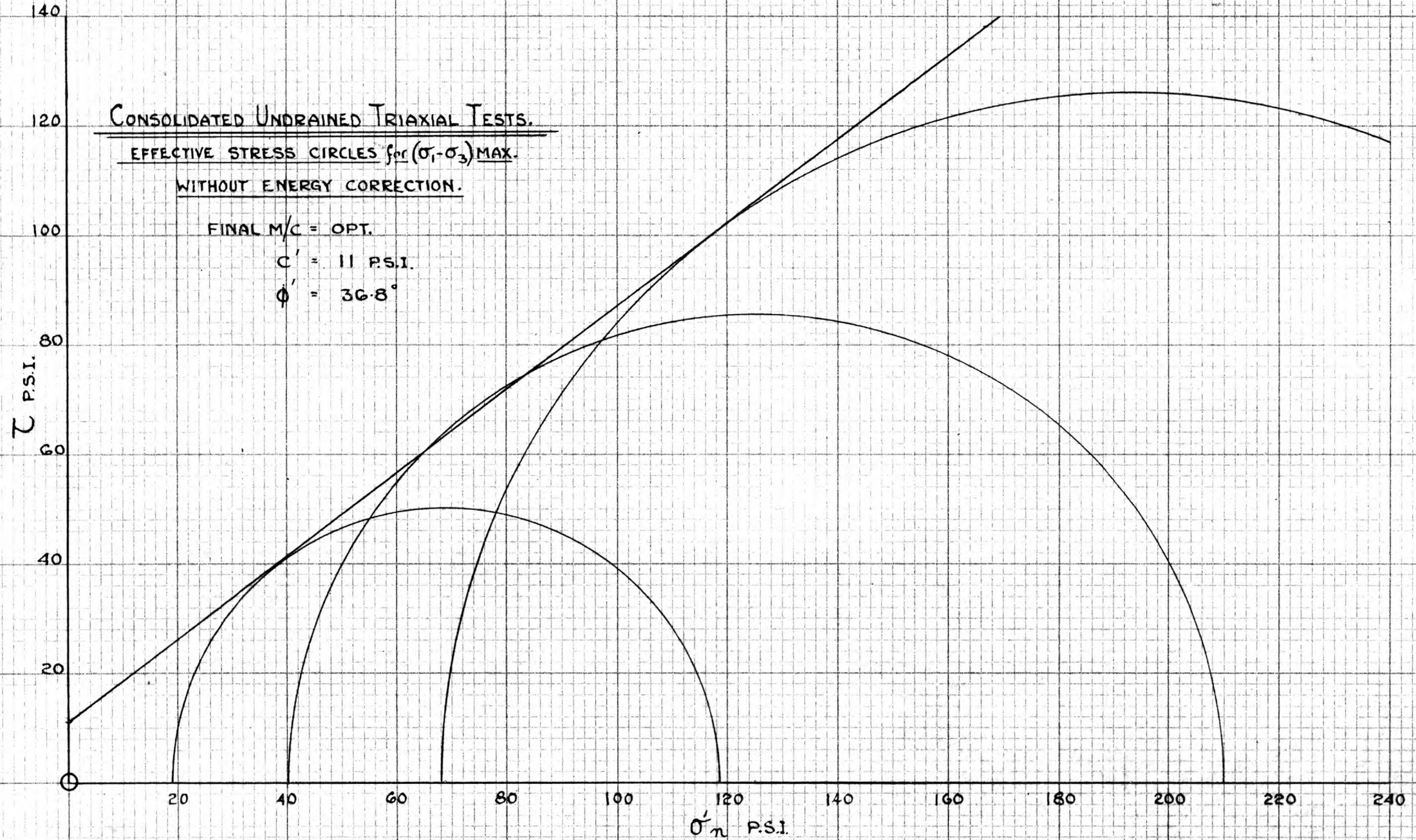


FIG. 5:53.

CONSOLIDATED UNDRAINED TRIAXIAL TESTS.

EFFECTIVE STRESS CIRCLES for $(\sigma_1 - \sigma_3)$ MAX.

WITHOUT ENERGY CORRECTION

FINAL M/C = OPT. + 1%

$c' = 3.8$ P.S.I.

$\phi' = 35°$

DATA FOR $\sigma_3 = 70$ P.S.I. NOT AVAILABLE.

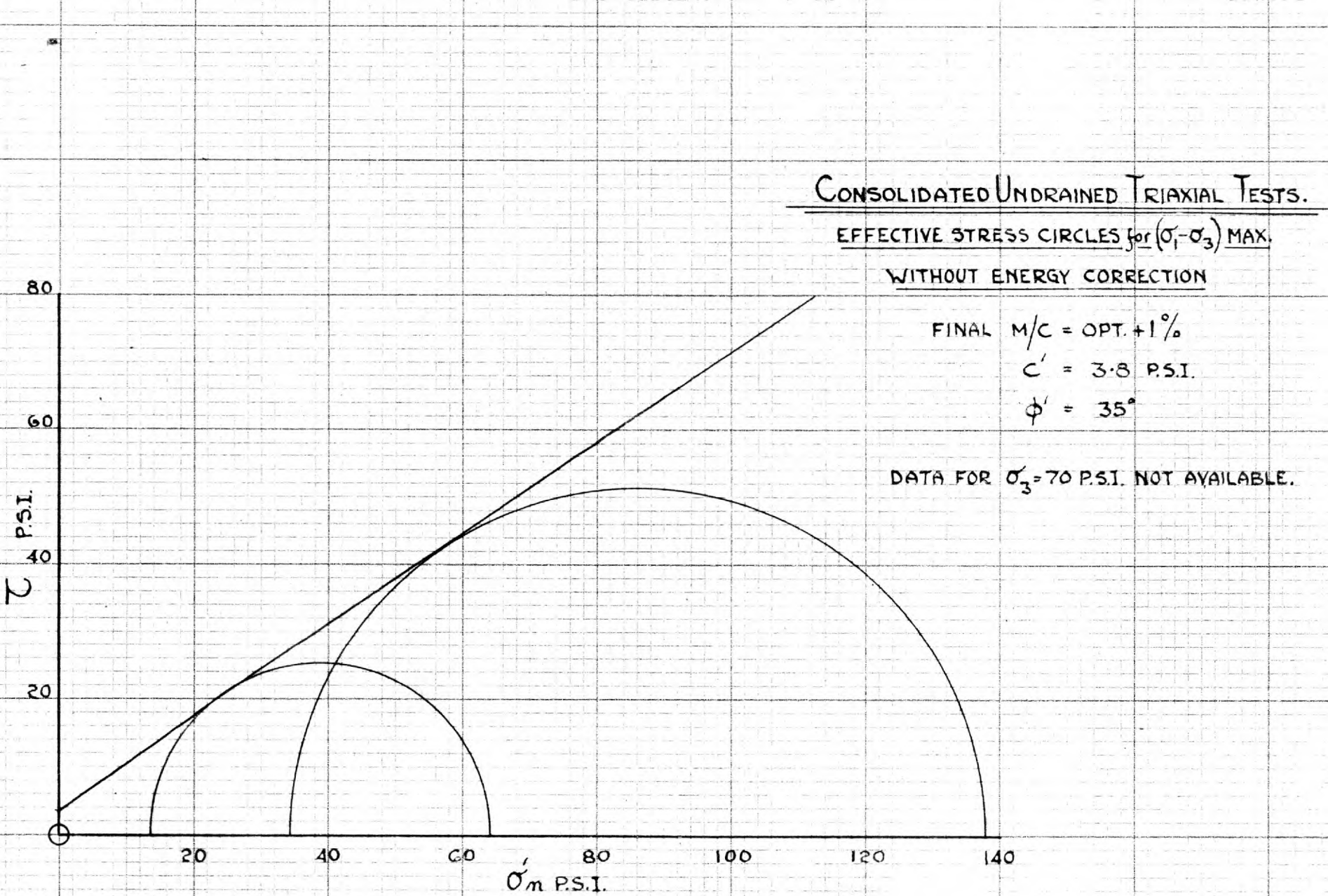


FIG. 5:54.

GREAT BRITAIN

Consolidated Undrained Triaxial Tests.

Effective stress circles for $(\sigma_1-\sigma_3)$ max.

With energy correction

Final M/C = Opt.

$c' = 7$ P.S.I.

$\phi' = 38°$

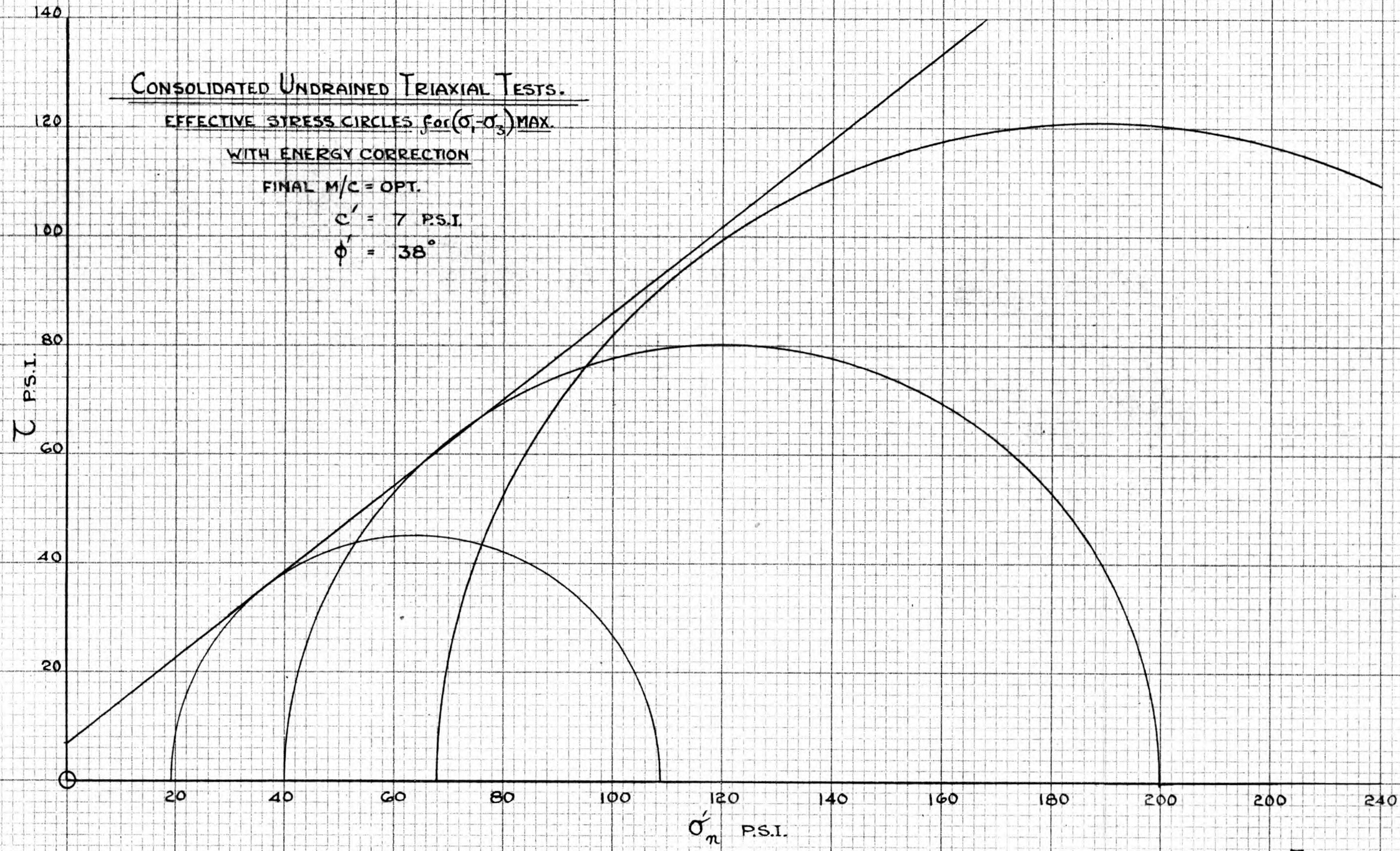


Fig. 5:55.

CONSOLIDATED UNDRAINED TRIAXIAL TESTS.

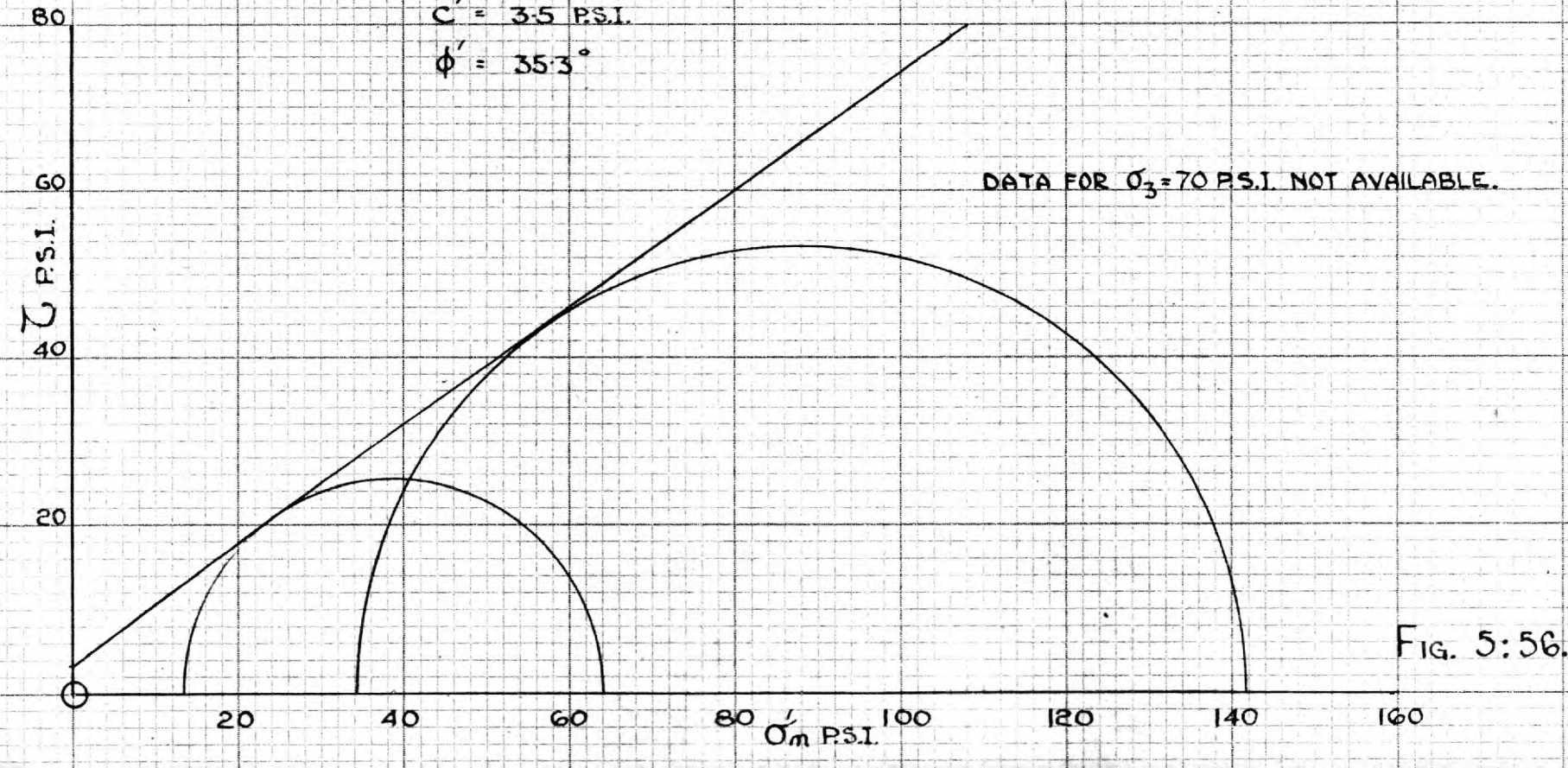
EFFECTIVE STRESS CIRCLES for $(\sigma_1 - \sigma_3)$ MAX.

WITH ENERGY CORRECTION

M/C = OPT. + 1 %

$C' = 3.5$ P.S.I.

$\phi' = 35.3°$



DATA FOR $\sigma_3 = 70$ P.S.I. NOT AVAILABLE.

FIG. 5:56.

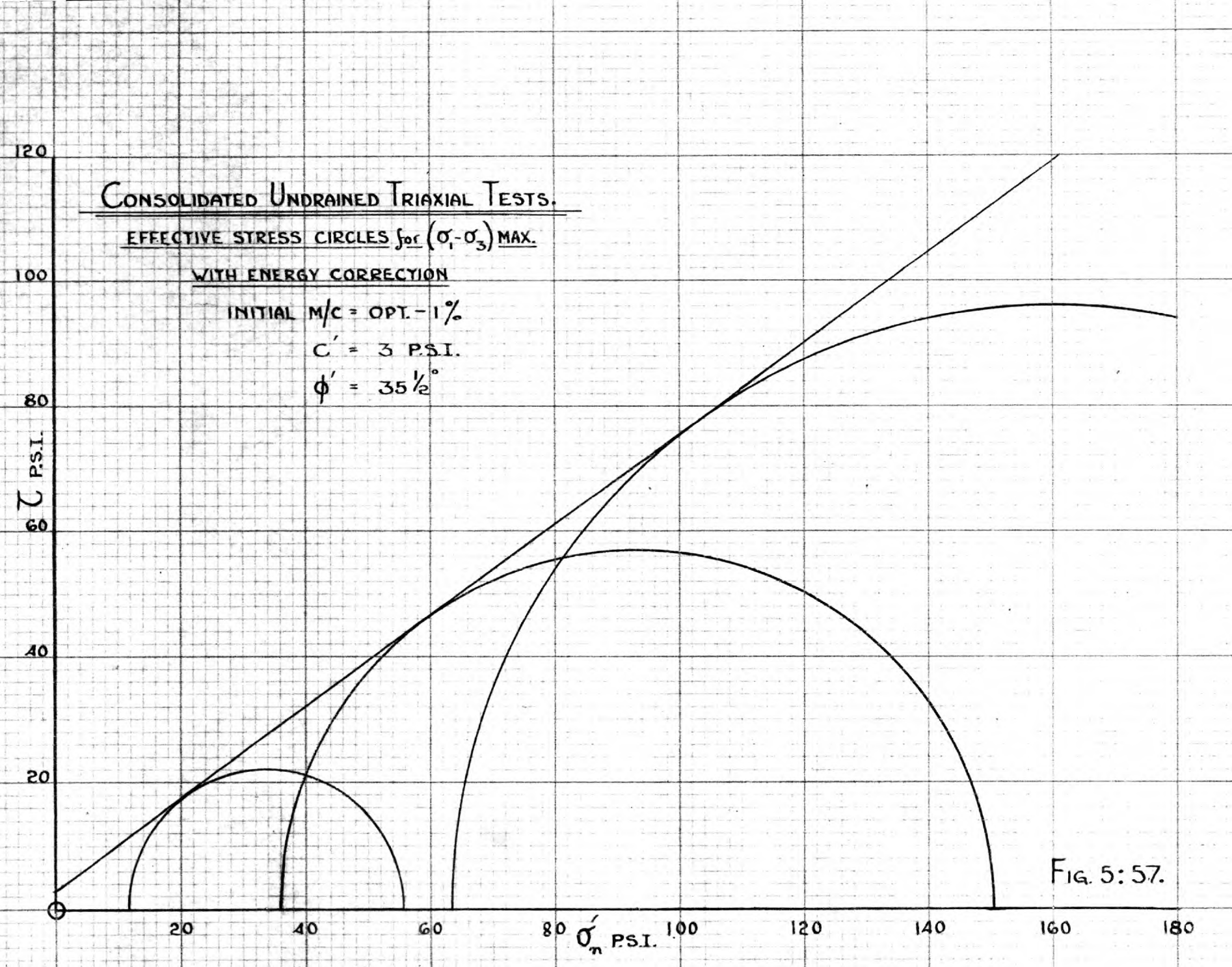

CONSOLIDATED UNDRAINED TRIAXIAL TESTS.
EFFECTIVE STRESS CIRCLES for $(\sigma_1-\sigma_3)$ MAX.
WITH ENERGY CORRECTION
INITIAL M/C = OPT. - 1%
C' = 3 P.S.I.
ϕ' = 35½°
120
100
80
60
40
20
τ P.S.I.
20
40
60
80
100
120
140
160
180
σ'_n P.S.I.

FIG. 5: 57.

CONSOLIDATED UNDRAINED TRIAXIAL TESTS.

EFFECTIVE STRESS CIRCLES for $(\sigma_1-\sigma_3)$ MAX.

WITH ENERGY CORRECTION.

INITIAL M/C = OPT.

$c' = 7{\cdot}0$ P.S.I.

$\phi' = 39\frac{1}{2}°$

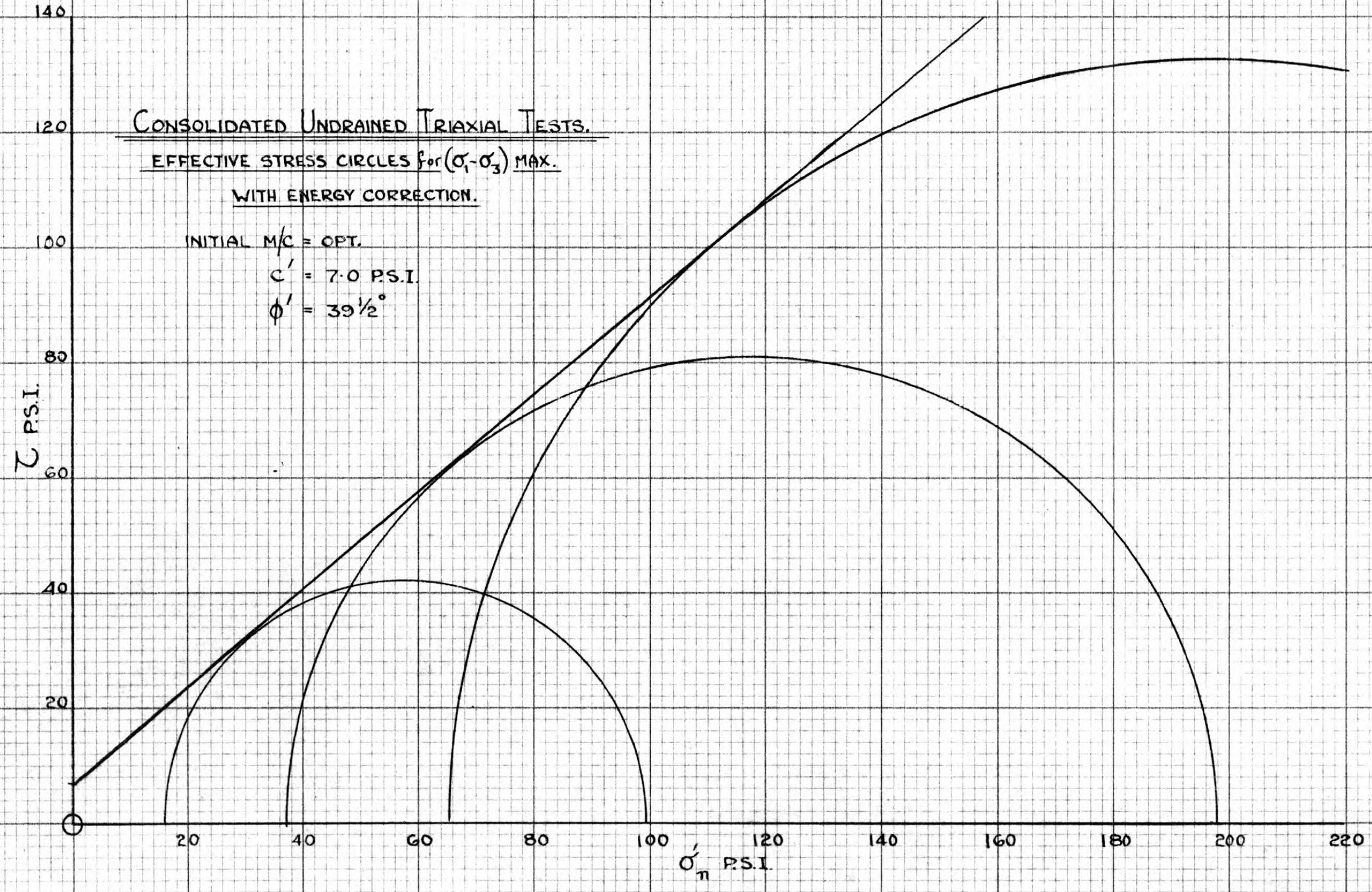


FIG. 5:58.

CONSOLIDATED UNDRAINED TRIAXIAL TESTS.

EFFECTIVE STRESS CIRCLES for $(\sigma_1 - \sigma_3)$ MAX.
WITH ENERGY CORRECTION

INITIAL M/C = OPT. + 1%

$c' = 7.2$ P.S.I.

$\phi' = 39\frac{1}{2}°$

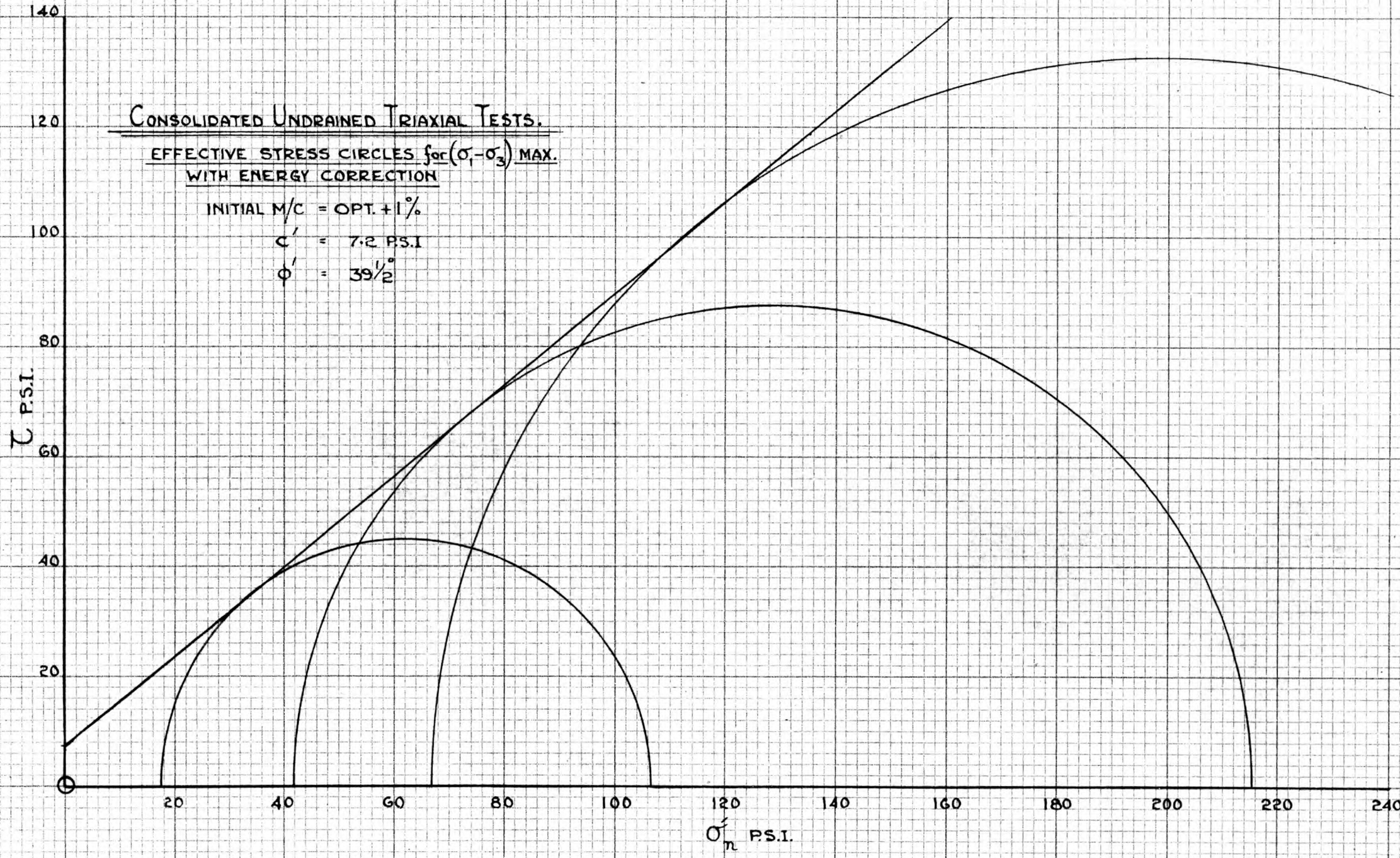


FIG. 5:59.

DRAINED TRIAXIAL COMPRESSION TESTS.

WITHOUT ENERGY CORRECTION

FINAL M/C = OPT.

$c' = 8$ P.S.I.

$\phi' = 37\frac{1}{2}°$

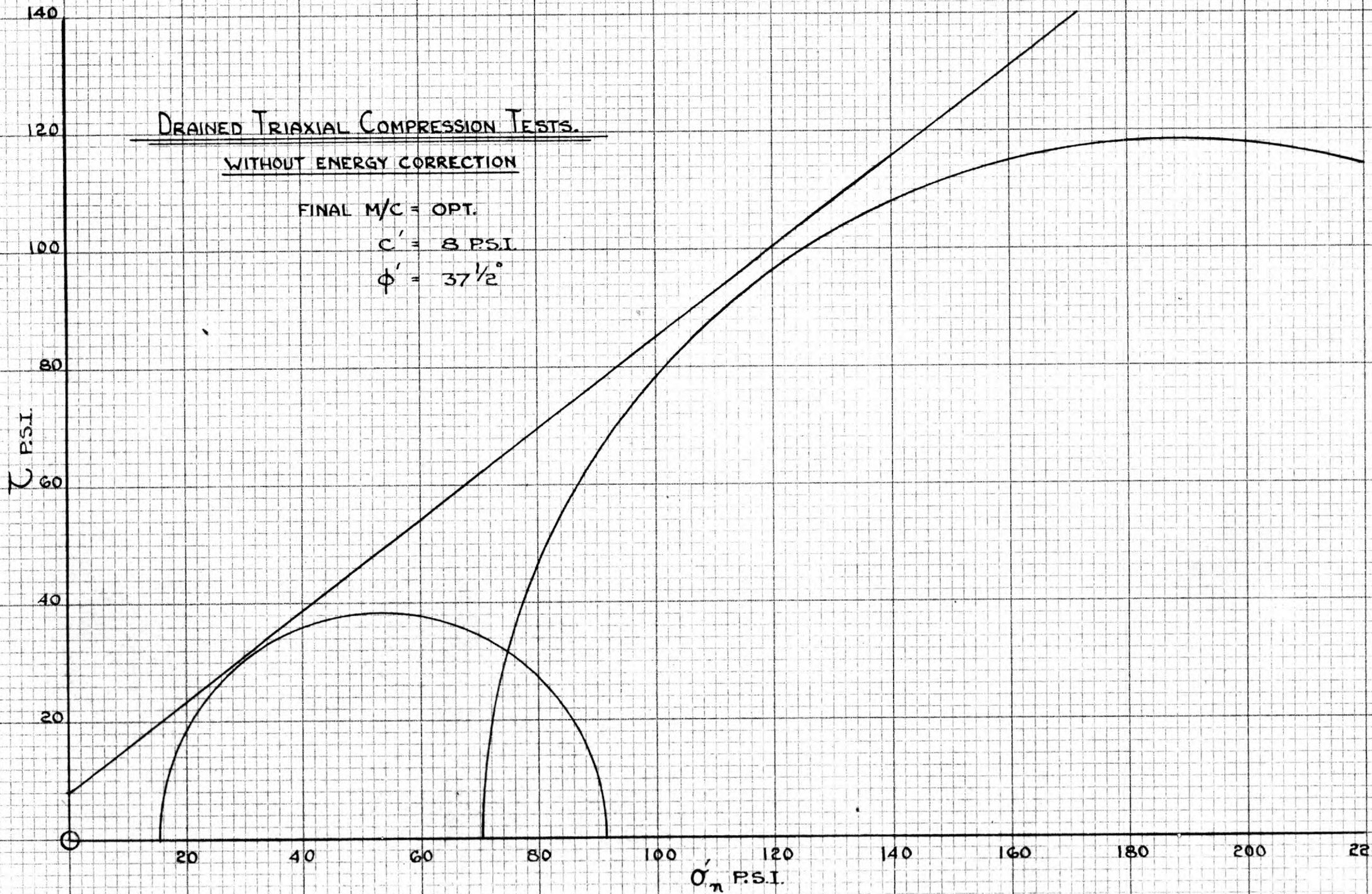


FIG. 5:60.

DRAINED TRIAXIAL COMPRESSION TESTS.

WITHOUT ENERGY CORRECTION.

FINAL M/C = OPT. + 1·0 %

$C' = 4$ P.S.I.

$\phi' = 39\frac{1}{2}^{\circ}$

DATA FOR $\sigma_3 = 70$ P.S.I. NOT AVAILABLE.

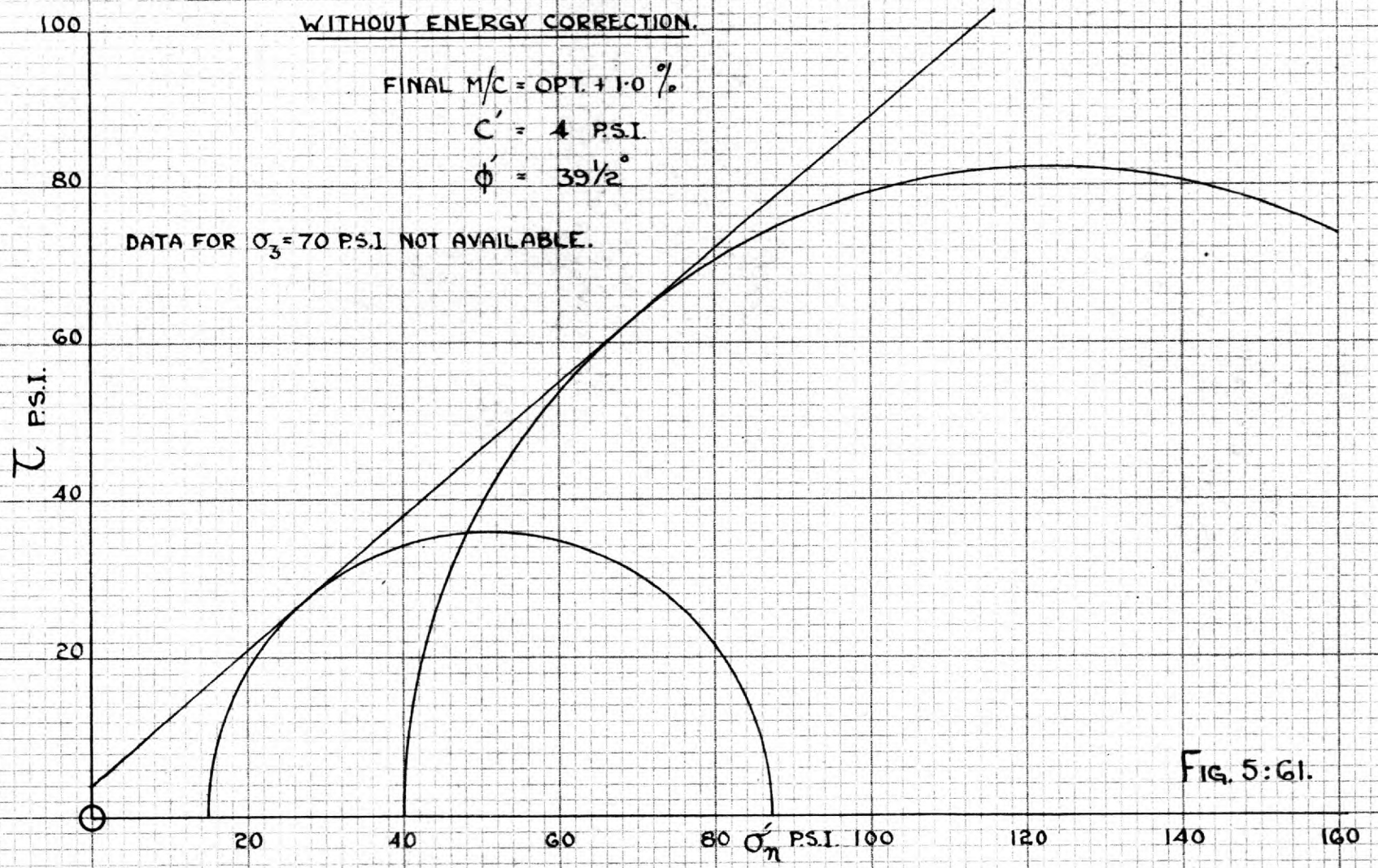


FIG. 5:61.

DRAINED TRIAXIAL COMPRESSION TESTS.

WITH ENERGY CORRECTION.

FINAL M/C = OPT.

$C' = 6.5$ P.S.I.

$\phi' = 38°$

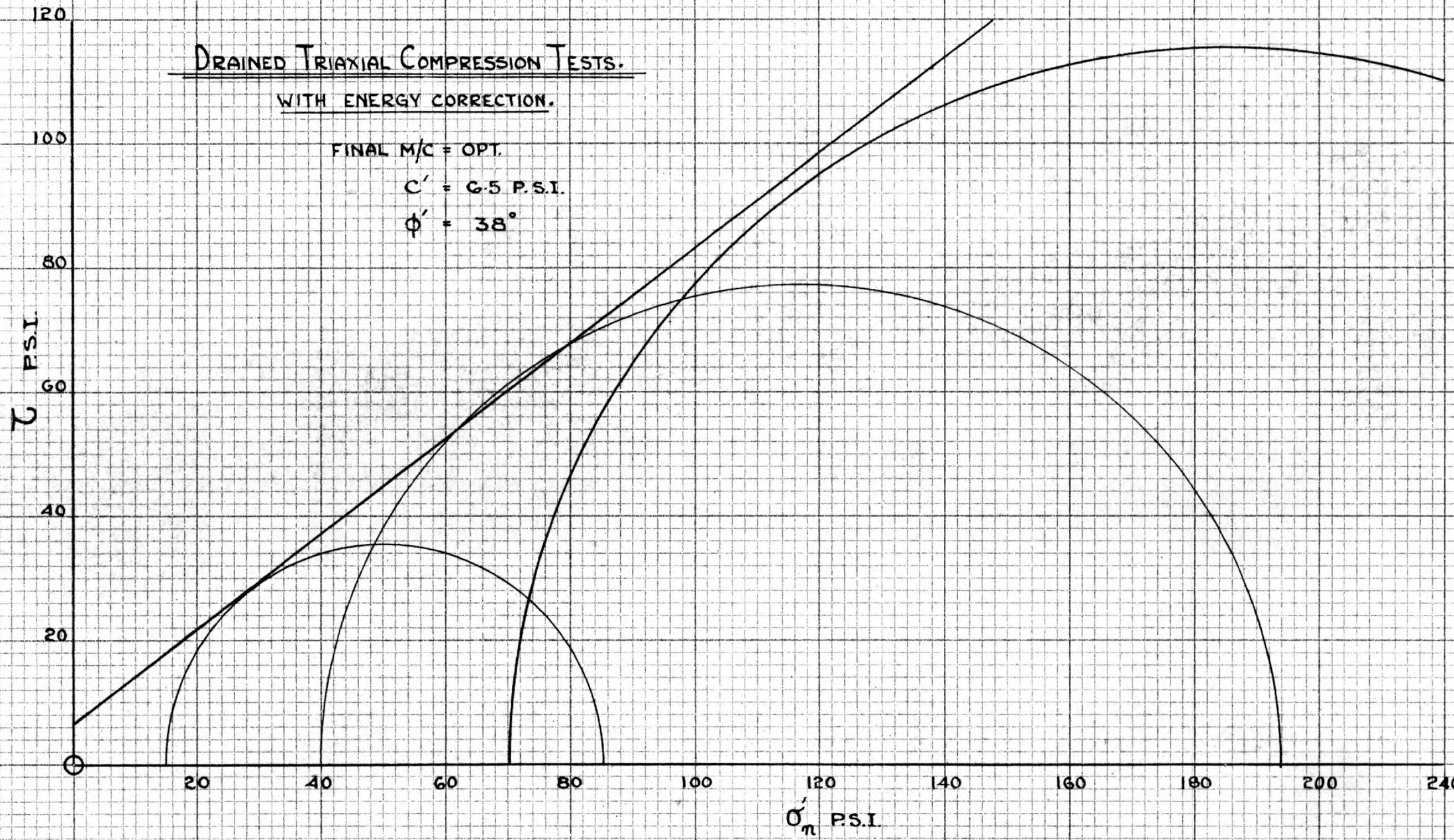


FIG. 5:62.

DRAINED TRIAXIAL COMPRESSION TESTS.

WITH ENERGY CORRECTION.

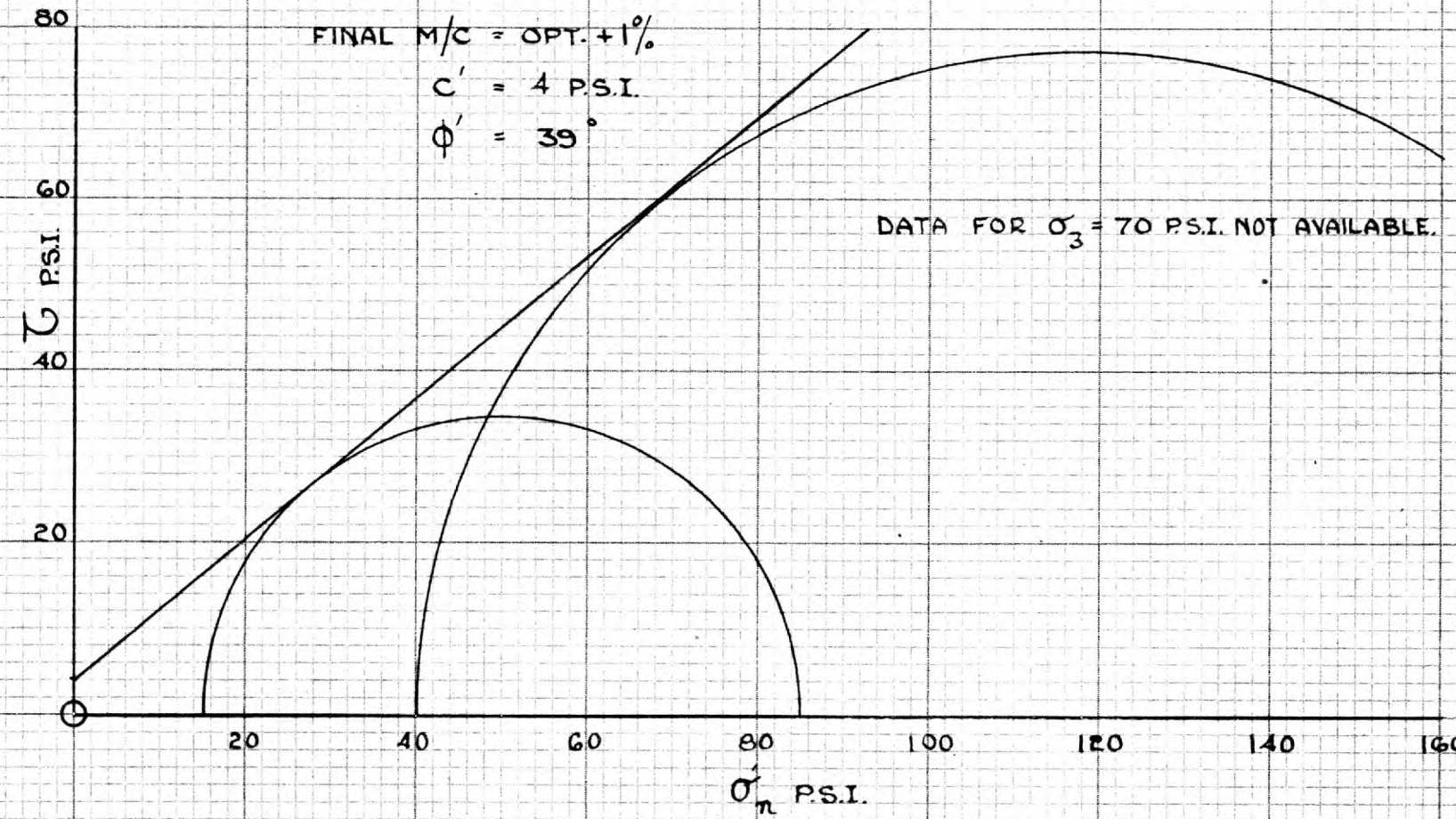


FIG. 5:63.

DRAINED TRIAXIAL COMPRESSION TESTS.

WITH ENERGY CORRECTION.

INITIAL M/C = OPT. −1%

$C' = 5$ P.S.I.

$\phi' = 35\frac{1}{2}°$

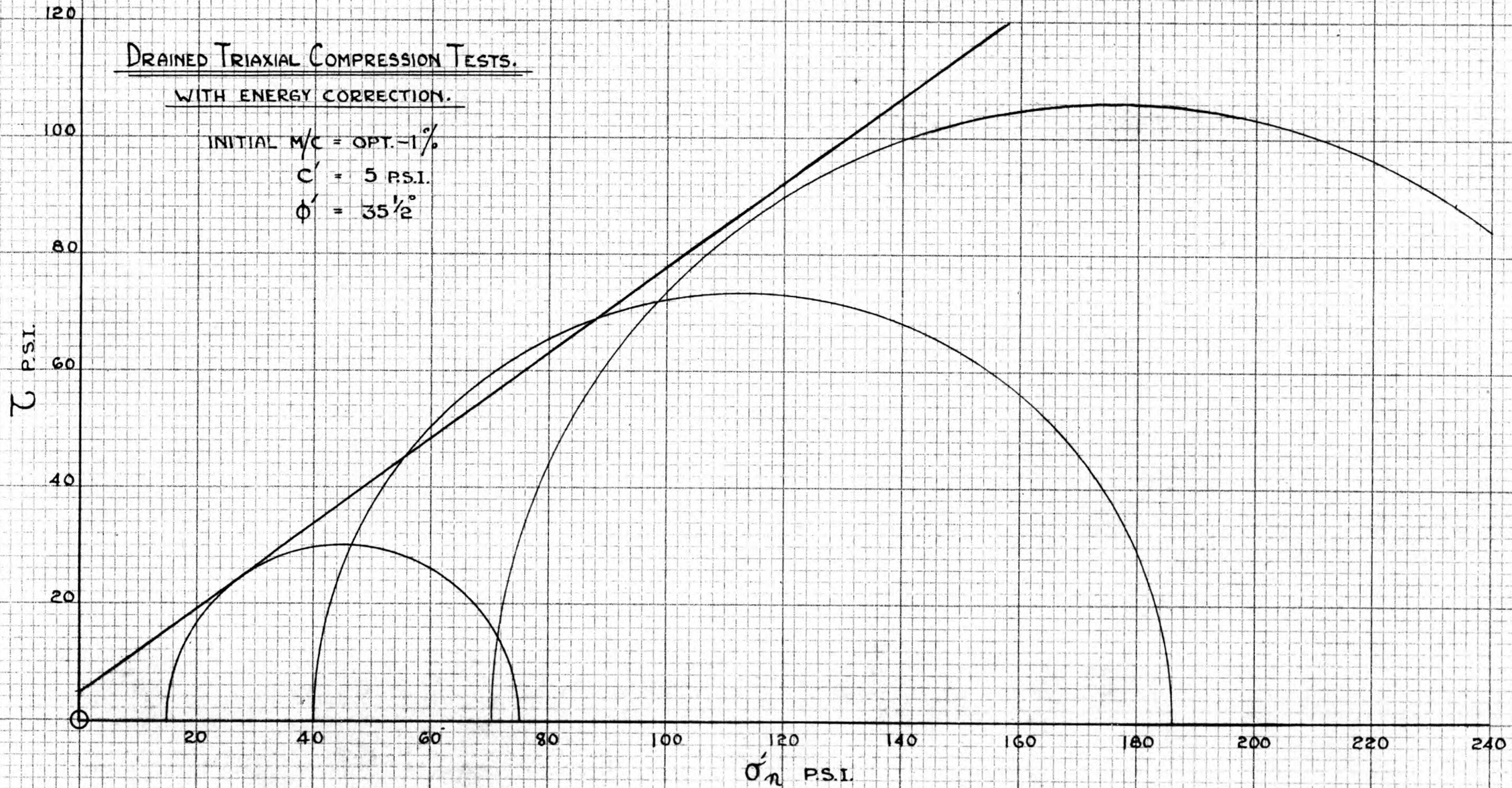


FIG. 5:64.

DRAINED TRIAXIAL COMPRESSION TESTS.

WITH ENERGY CORRECTION

INITIAL M/C = OPT.

$C' = 6$ P.S.I.

$\phi' = 38°$

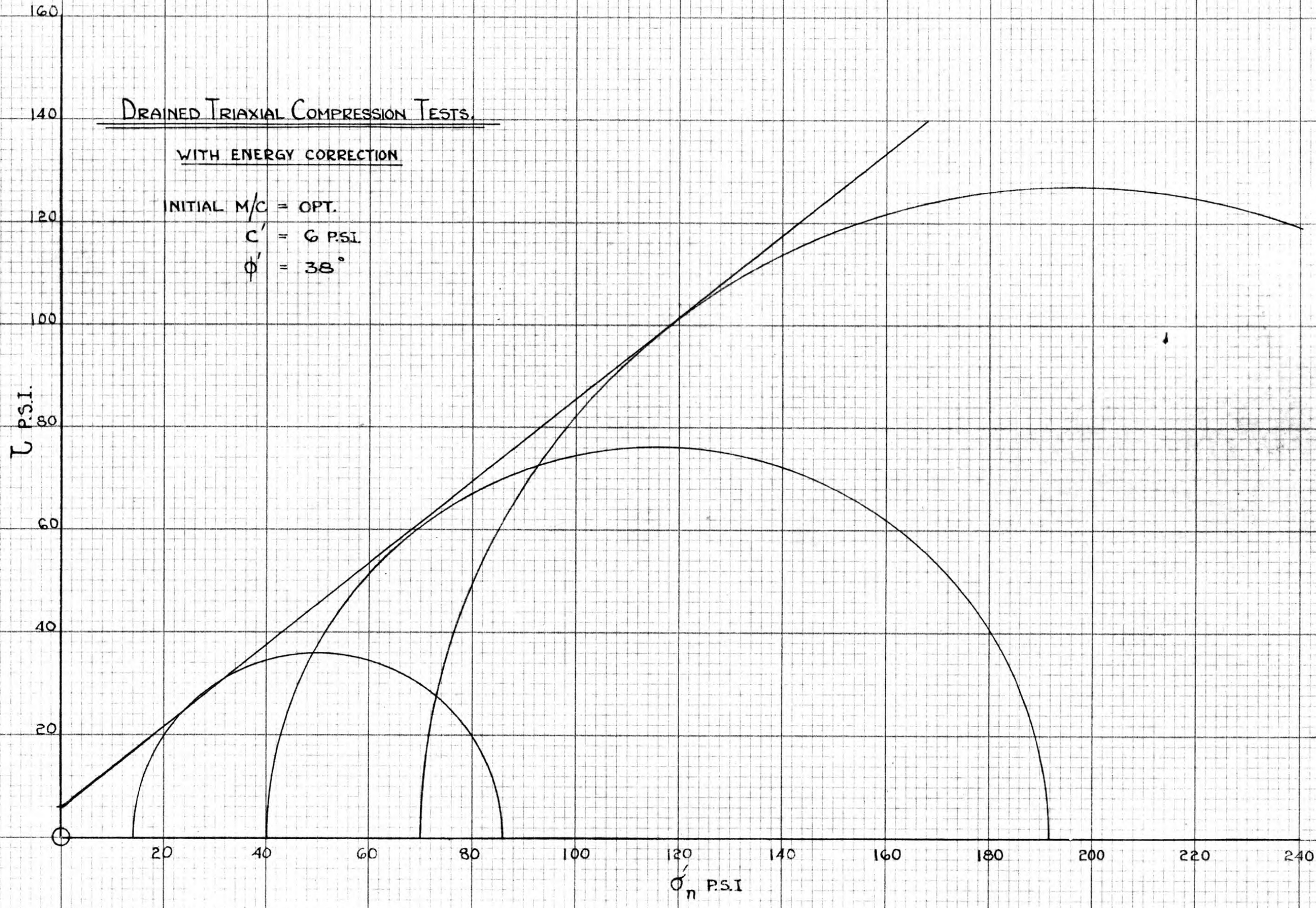


FIG. 5:65.

DRAINED TRIAXIAL COMPRESSION TESTS.

WITH ENERGY CORRECTION.

INITIAL M/C = OPT. + 1%

$C' = 5$ P.S.I.

$\phi' = 41°$

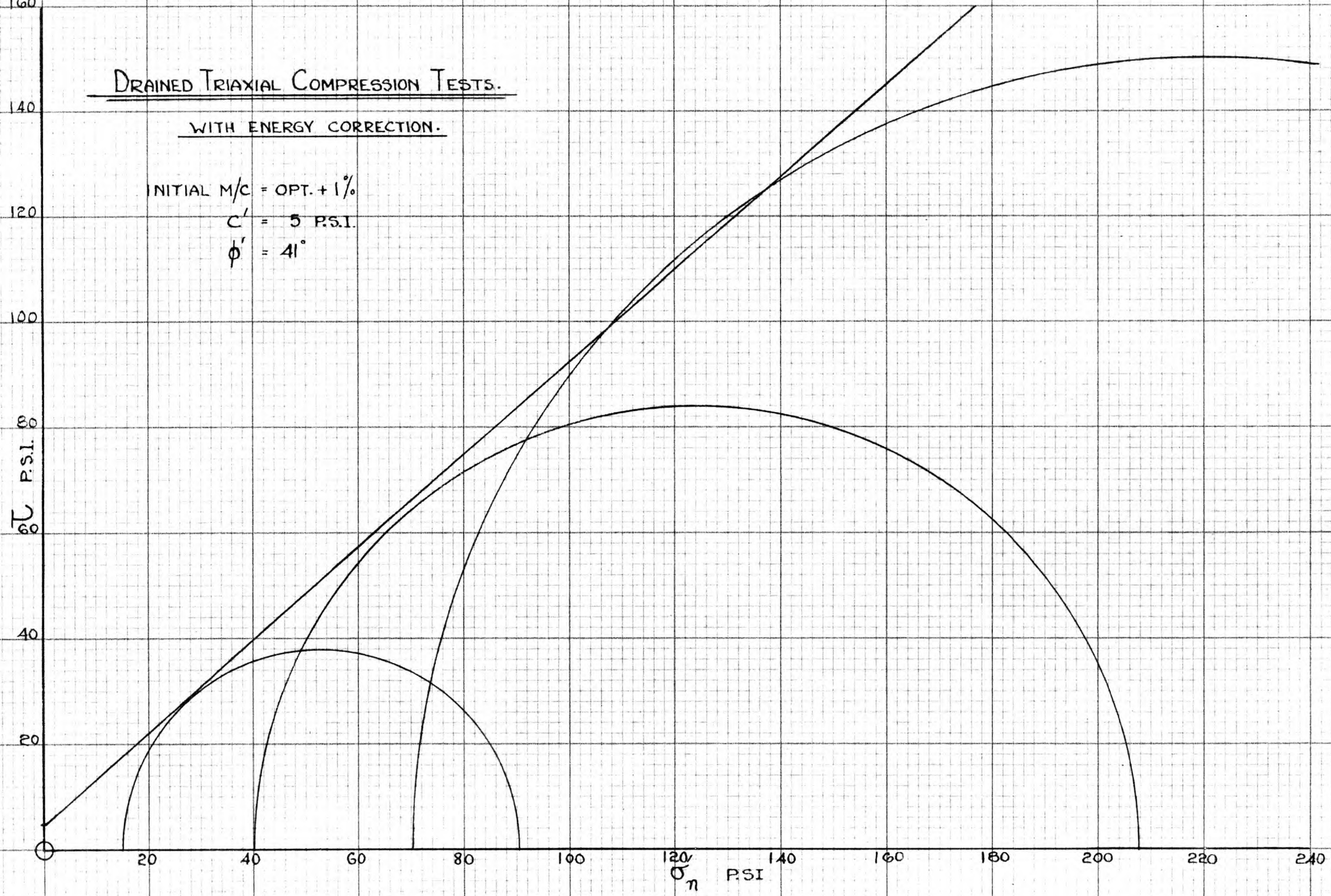


FIG. 5:66.